
Electronic Thesis and Dissertation Repository

8-8-2024 10:00 AM

Innovative Techniques for Partially Upgrading Oil Sand Bitumen to Pipeline Transportable Crude

Moataz Abdrabou, *Western University*

Supervisor: Zheng, Ying, *The University of Western Ontario*

Co-Supervisor: Zeng, Yimin, *CanmetMATERIALS, Natural Resources Canada (NRCan)*

A thesis submitted in partial fulfillment of the requirements for the Doctor of Philosophy degree in Chemical and Biochemical Engineering

© Moataz Abdrabou 2024

Follow this and additional works at: <https://ir.lib.uwo.ca/etd>

 Part of the [Catalysis and Reaction Engineering Commons](#), and the [Petroleum Engineering Commons](#)

Recommended Citation

Abdrabou, Moataz, "Innovative Techniques for Partially Upgrading Oil Sand Bitumen to Pipeline Transportable Crude" (2024). *Electronic Thesis and Dissertation Repository*. 10277.
<https://ir.lib.uwo.ca/etd/10277>

This Dissertation/Thesis is brought to you for free and open access by Scholarship@Western. It has been accepted for inclusion in Electronic Thesis and Dissertation Repository by an authorized administrator of Scholarship@Western. For more information, please contact wlsadmin@uwo.ca.

Abstract

Optimizing the use of unconventional oil resources, like oil sand bitumen, is crucial for meeting the global energy demand in an environmentally sustainable and economically viable way. Unconventional oils, including extra-heavy oil and oil sand bitumen, make up over 55% of the world's oil reserves. Therefore, this research focuses on innovative partial upgrading techniques that significantly reduce bitumen's viscosity and improve its quality for pipeline transportation and refining. The work presented in this thesis examines various potential routes for effectively partially upgrading bitumen through a series of experimental studies. The first investigation starts with using ionic surfactants to enhance the thermal cracking reactions and the dispersion of asphaltenes, which greatly reduces bitumen viscosity by up to 60% and improves the quality of the upgraded bitumen. Then, the research continues to investigate the use of iron-based catalysts for further conversion, focusing on how their oxidation state, particle size, and concentration affect the upgrading efficiency. The results highlight the great potential of Fe_3O_4 nanoparticles as a cheap, robust, and sustainable catalyst and its effectiveness in promoting hydrogenation and cracking reactions resulting in up to 59% vacuum residue conversion. The research goes further to introduce a novel approach through the utilization of waste fly ash cenospheres which are coated with a layer of Fe_3O_4 . These new innovative catalysts are then used to catalyze bitumen upgrading with the help of various organic H-donor solutions, with SEM, EDX, XRD, and XPS characterizing the catalysts' properties and their impact on the upgrading process. Additionally, an Artificial Neural Network (ANN) model was developed and fine-tuned to predict the physical properties of the upgraded bitumen with high accuracy, showcasing the potential of machine learning in optimizing the upgrading processes. Finally, the thesis investigates the use an alternative form of heating using microwave irradiation assisted by carbon-based microwave susceptors, which significantly lowers viscosity and enhances bitumen quality at reduced temperatures with minimal environmental impact. These findings not only demonstrate the feasibility of various partial upgrading techniques but also offer insights into optimizing catalyst properties, contributing significantly to the development of sustainable and economically viable solutions for bitumen partial upgrading.

Keywords

Bitumen Partial Upgrading, Catalytic Upgrading, Sustainable Catalysts, Artificial Neural Networks in Energy, Microwave-assisted Upgrading.

Summary for Lay Audience

Meeting the world's growing energy needs in a way that's both environmentally friendly and affordable is a big challenge, especially when it comes to using uncommon oil resources that aren't easy to extract, like oil sand bitumen. This kind of oil makes up more than half of the world's oil reserves and is known for its high viscosity and density. This research explores several innovative techniques to make the oil less viscous and with higher quality for pipeline transportation and use. The study explores several innovative methods to improve the properties of the bitumen. One approach uses special chemicals known as surfactants to enhance the break down and dispersion of the heavy components within bitumen, making it less viscous and easier to transport and refine. Another method involves using iron-based catalysts—substances that speed up chemical reactions without being consumed themselves. These catalysts are particularly exciting because they are cheap, effective, and environmentally friendly. The research further tests a creative technique that uses small sand-like spheres coated with iron, derived from waste material, to help in further upgrading the bitumen. In addition to that, a computer model that uses artificial intelligence was developed to predict how well the oil upgrading process will work. This tool can help optimize the process, saving time and resources. Lastly, the study examines the use of microwave technology, with the help of carbon materials, to make these processes more efficient and less harmful to the environment. The findings show that these new methods could significantly reduce the environmental impact of processing bitumen, cut down on energy use, and open up new ways to use bitumen beyond just burning it for fuel. This is good news for the environment and for meeting global energy needs in more sustainable ways. The research is a step forward in making the oil industry eco-friendlier and more efficient, aligning with global goals for a cleaner and more sustainable energy future.

Co-Authorship Statement

This thesis includes several publications co-authored by myself and other researchers. The contributions of each co-author and the nature and extent of their involvement are stated below.

List of Publications:

1. M. K. Abdrabou, X. Han, Y. Zheng, Y. Zeng, and S. Rohani, “The effect of cationic surfactants on bitumen’s viscosity and asphaltene nanostructure under thermal partial upgrading,” *Energy Sci. Eng.*, Volume 10, issue 7, pp. 2540–2560, **2022**. <https://doi.org/10.1002/ese3.1137>.
2. M. K. Abdrabou, X. Han, Y. Zheng, Y. Zeng, “Harnessing the Power of Microwave Irradiation: A Novel Approach to Bitumen Partial Upgrading,” *Molecules*, 28, 7769, **2023**. <https://doi.org/10.3390/molecules28237769>.
3. M. K. Abdrabou, X. Han, Y. Zheng, Y. Zeng, “Optimization of iron-based catalyst for partial upgrading of Athabasca Bitumen: The role of Fe oxidation state, particle size, and concentration”, *Fuel*, vol. 357, Feb. **2024**. <https://doi.org/10.1016/j.fuel.2023.129941>.
4. M. K. Abdrabou, X. Han, Y. Zheng, Y. Zeng, “Recent Developments in the Utilization of Unconventional Resources: A Focus on Partial Upgrading Techniques and Sustainability of Canadian Oil Sand Bitumen,” submitted to *Resources Chemicals and Materials* on July **2024**.
5. M. K. Abdrabou, X. Han, Y. Zheng, Y. Zeng, “Enhancing Bitumen Processing with Fe₃O₄ Coated Cenospheres and ANN-Driven Process Optimization: A Novel Approach to Sustainable Partial Upgrading,” submitted to *Energy and Fuel* on July **2024**.

The contributions to these publications are distributed as follows:

- **Moataz K. Abdrabou**: Experimental work, data analysis, data interpretation, and manuscript preparation.
- **Xue Han (NRCan)**: Validation, resources, and funding acquisition.
- **Yimin Zeng (NRCan)**: Resources, project administration, funding acquisition and reviewing and editing.
- **Ying Zheng**: Writing – review & editing, supervision, funding acquisition, and conceptualization.

Acknowledgments

I wish to express my deepest gratitude to my supervisor, Professor Ying Zheng, for her unwavering guidance and support throughout my Ph.D. journey. I am equally thankful to Dr. Yimin Zeng, my co-supervisor, for his invaluable feedback and insights, which have been instrumental in my academic development.

A special acknowledgment goes to my teammates at Dr. Ying Zheng's lab in TEB 417—Reem, Vahid, Nan, Joshua, Rasoul, Zoe, Chun Li, and Wei. Your collaboration and support have been a cornerstone of my research experience.

My heartfelt thanks are extended to my parents (Dr. Khaled Abdrabou and Mrs. Manal Metwali) and my dear siblings (Hossam and Nadeen), who set me on this path and continuously aided me throughout my journey. Being away from them has left a void in my life that only their presence can fill. Every day without them is a reminder of their enduring love and sacrifice.

I am profoundly grateful to my new family and my new parents, Dr. Mahmoud El-Sakka and Ms. Hiba Al-Ghazali, for embracing me and considering me as their own son from day one, they have showed me nothing but love and support since our first encounter. And also, my sisters-in-law, Nada and Salma, who have been always there for us whenever we needed them the most, for which I am eternally thankful.

To my beloved wife, Yomna El-Sakka, my foremost supporter throughout this journey, my gratitude knows no bounds. Your love, patience, and encouragement have been my guiding light. I am blessed to share my life with you, and I look forward to our future, filled with peace, love, and harmony. Lastly, I cannot conclude without mentioning my daughter, Lujain, our glow of silver, and the most precious gift I have had during my entire Ph.D. journey. May God protect you and bless you, always.

To all of you who have been part of my journey, directly or indirectly, my heartfelt thanks for your invaluable support and encouragement, so thank you so much!

Table of Contents

Abstract.....	ii
Summary for Lay Audience.....	iii
Co-Authorship Statement	iv
Acknowledgments	v
Table of Contents	vi
List of Tables	xi
List of Figures.....	xiii
Chapter 1 - Introduction	1
1.1 Background and Motivation	1
1.2 The Nature of Bitumen.....	5
1.3 Economic and Environmental Implications for Utilizing Bitumen.....	9
1.4 Thesis Objectives.....	10
1.5 Thesis Organization/Outline	11
Chapter 2 – Literature Review	14
2.1 Overview of the Upgrading Technologies.....	14
2.2 Thermal Cracking.....	15
2.2.1 Process Thermodynamics and Kinetics	15
2.2.2 Mild Thermal Cracking.....	17
2.2.3 Coking.....	19
2.3 Catalytic Cracking.....	21
2.4 Hydro-Cracking	23
2.4.1 Direct Use of Hydrogen Gas.....	23
2.4.2 Methane as a H Donor	24
2.4.3 Water as a Hydrogen Donor	25

2.4.4	Organic Liquids as Hydrogen Donor	25
2.5	Asphaltene Removal	26
2.6	Emerging technologies.....	27
Chapter 3 – Challenges and Opportunities in Bitumen Upgrading.....		35
3.1	Environmental and Economic Aspects of Bitumen Upgrading.....	35
3.2	The Potential of Partial Upgrading.....	37
3.3	Industrial Examples and Case Studies for Partial Upgrading	39
3.4	Comparative Analysis of Current Partial Upgrading Technologies.....	42
3.5	Economic Implications of the Partial Upgrading Techniques.....	47
Chapter 4 - The effect of cationic surfactants on bitumen’s viscosity and asphaltene nanostructure under thermal partial upgrading		48
4	Abstract.....	48
4.1	Introduction.....	49
4.2	Experimental Methodology	53
4.2.1	Materials	53
4.2.2	Sample Processing Method.....	55
4.2.3	Characterization Tests.....	55
4.3	Results and Discussion	56
4.3.1	Surfactant Effect on bitumen’s Physical Properties.....	56
4.3.2	Thermogravimetric analysis (TGA) of upgraded oil:	64
4.3.3	XRD of Product’s Asphaltene:	70
4.3.4	HRTEM of Product’s Asphaltene:.....	74
4.4	Conclusion	79
Chapter 5 - Optimization of Iron-Based Catalyst for Partial Upgrading of Athabasca Bitumen: The Role of Fe Oxidation State, Particle Size, and Concentration		80
5	Abstract.....	80
5.1	Introduction.....	81
5.2	Experimental Methodology	84
5.2.1	Materials	84

5.2.2	Product analysis and Characterization	85
5.2.3	Uncertainties in analysis	87
5.3	Results and Discussion	88
5.3.1	Catalyst Morphology	88
5.3.2	Catalytic Effect of Fe-based Nano-Catalysts	89
	The effect of iron oxidation state	89
	The Effect of Catalyst Particle Size	99
	The Effect of Catalyst Concentration.....	100
5.3.3	Screening for the Best Catalyst.....	102
5.3.4	Catalyst Characterization	103
	Magnetic properties Via VSM	103
	Catalyst characterization Via SEM	104
	Catalyst characterization Via XRD	105
	Catalyst characterization Via XPS	106
5.3.5	Proposed Mechanism for Bitumen Partial Upgrading Using Fe-based catalyst.....	107
5.3.6	Comparison of Fe ₃ O ₄ nanoparticles with metallic alloys	108
5.4	Conclusion	110
Chapter 6 - Enhancing Bitumen Processing with Fe₃O₄ Coated Cenospheres and ANN-Driven Process Optimization: A Novel Approach to Sustainable Partial Upgrading.....		112
6	Abstract.....	112
6.1	Introduction.....	113
6.2	Experimental Methodology	116
6.2.1	Synthesis of Fe ₃ O ₄ Coated Cenospheres.....	116
6.2.2	Characterization of the Catalyst:.....	118
6.2.3	Upgrading of Oil Sand Bitumen:	118
6.2.4	Analysis of the Upgraded Bitumen.....	119
6.3	Results and discussion	120
6.3.1	FESEM.....	120
6.3.2	EDX analysis:	121
6.3.3	VSM analysis	123
6.3.4	XRD analysis	124
6.3.5	XPS analysis	125

6.3.6	Catalytic effect of Fe-coated cenospheres in bitumen upgrading	126
6.3.7	Artificial Neural Network (ANN) Model:	131
	Description of the ANN Model	131
	Fine-Tuning of the ANN Model.....	133
	Validation of the ANN Model with experimental data	135
	Limitations of the ANN Model	137
6.4	Conclusion	138
Chapter 7 - Harnessing the Power of Microwave Irradiation: A Novel Approach to Bitumen Partial Upgrading.....		140
7	Abstract.....	140
7.1	Introduction.....	140
7.2	Experimental Methodology	143
7.2.1	Materials	143
7.2.2	Experimental Design.....	143
7.2.3	Sample Processing Method.....	145
7.2.4	Characterization Methods	145
7.3	Results and Discussion	146
7.3.1	Effects of Carbon Susceptors on Bitumen Upgrading	146
	The Role of Carbon Susceptors in Microwave Absorption and Heating Rates.....	146
	The Effect of Carbon Susceptors on Bitumen’s Viscosity	147
	The Effect of Carbon Susceptors on Bitumen’s SARA Fractions.....	149
	The Role of Carbon Susceptors on Desulfurization of Bitumen	150
7.3.2	Surface Properties of Carbon Susceptors and their Effect on Microwave Absorption	151
	Effect of Trace Metal Content.....	151
	Impact of Surface Area and Porosity	152
7.3.3	Evaluation of Microwave Irradiation Operational Parameters on Upgrading Bitumen	154
	Effect of Microwave Irradiation Time	154
	Effect of Maximum Microwaving Temperature	156
	Impact of the Stirring Rate.....	159
7.3.4	Discussion of the key results.....	160
7.4	Conclusion	163

Chapter 8 – Comparative Analysis, Conclusion, and Recommendations	164
8 Comparison of the Partial Upgrading Techniques	164
Environmental Analysis	168
8.2 Best Practices and Recommendations	169
Future Research Directions	170
8.3 Thesis Overall Conclusions	171
8.4 Significance and Novelty of the Research	172
References	174
Appendices	187
Curriculum Vitae	202

List of Tables

Table 1.1: Canadian Pipeline specifications adapted from Gray [13].	3
Table 3.1: Comparison between Full and Partial Upgrading approaches.	38
Table 3.2: Comparison of the upgrading technologies based on their operation principles.	43
Table 3.3: Comparison of the upgrading technologies based on their process viability.	45
Table 4.1: Canadian Pipeline specifications adapted from Gray [13].	49
Table 4.2: Physical properties of the original bitumen of interest.	53
Table 4.3: List of surfactants of interest.	54
Table 4.4: SARA analysis for the upgraded bitumen at various temperatures.	57
Table 4.5: Viscosity and density measurements for the upgraded bitumen at various temperatures.	57
Table 4.6: The effect of surfactants on the physical properties of bitumen before thermal upgrading.	58
Table 4.7: Viscosity measurements of upgraded bitumen with differently charged surfactants.	59
Table 4.8: Viscosity measurements of bitumen upgraded at various temperatures with and without surfactants.	61
Table 4.9: SARA analysis for the upgraded bitumen at various temperatures with surfactants.	62
Table 4.10: Diluent concentrations required for bitumen to reach 300 cP.	63
Table 4.11: Measurements of the total acid number (TAN) of the upgraded bitumen products.	63
Table 4.12: Activation energies for upgraded oil samples.	68
Table 4.13: Asphaltene parameters calculated from XRD plots.	71
Table 4.14: Asphaltene parameters calculated from XRD plots.	73
Table 4.15: The calculated nanostructure parameters from HRTEM.	77
Table 5.1: Measured properties of the original bitumen of interest.	84
Table 5.2: Specifications of the iron particles used as catalysts.	85

Table 5.3: Property measurements for the upgraded oil with and without 0.5wt% of Fe-based nanocatalysts upgraded at 400°C for 120 minutes.....	89
Table 5.4: Reaction interval and mass loss for each reaction zone for the upgraded oil with Fe-based catalyst.	94
Table 5.5: Concentrations and average molecular mass of gas products using different Fe catalyst– Ave. values (values are recorded as mass fractions per gram of gas released per gram of bitumen reacted).....	98
Table 5.6: Property measurements for the upgraded oil using 0.5wt% of Fe-based nano and micro-catalysts at 400°C.....	100
Table 5.7: Chemical composition of the Catalyst alloys in (wt%).	109
Table 5.8: Property measurements for the upgraded oil using synthesized catalyst alloys at 400°C.	110
Table 6.1: Comparison between the physical properties of bitumen under various treatment conditions with the Canadian pipeline specifications.	113
Table 6.2: Chemical composition of cenospheres (wt%) as determined by XRF.	117
Table 6.3: The chemical compositions of cenospheres before and after coating with Fe ₃ O ₄ (EDX Analysis).	122
Table 6.4: Elemental Composition of Fe ₃ O ₄ Coated Cenospheres at Selected Sites (EDX Analysis).	123
Table 6.5: Measured properties of the upgraded oil at various conditions.	128
Table 6.6: Comparing the accuracy of different multilayered ANN models.....	135
Table 6.7: Predicted vs. Experimental Viscosity Values for Upgraded Oil Using Various H Donors.....	136
Table 7.1: SARA composition of oil samples before and after 10 min microwave heating at 150°C.	150
Table 7.2: The sulfur content of microwaved bitumen measured by XRF.....	151
Table 7.3: BET results of the four carbon susceptors.	153
Table 7.4: The maximum temperature reached by carbon susceptors via direct microwave heating.....	154
Table 7.5: Sulfur content of upgraded bitumen at various microwave temperatures and times.	158

List of Figures

Figure 1.1: Distribution of World Oil Resources adapted from SLB [1].	1
Figure 2.1: General flow diagram of the visbreaking process based on the process description from Speight [44].	18
Figure 3.1: GHG emissions from the pipeline transportation of feed to the upgrader and refinery [86].	36
Figure 3.2: Block flow diagrams for bitumen A) Full Upgrading Plant and B) Partial Upgrading Plant.	39
Figure 4.1: Viscosity measurements for bitumen upgraded at 360°C versus surfactant concentrations.	60
Figure 4.2: TGA and DTG curves for upgraded oil at various temperatures.	65
Figure 4.3: TGA and DTG curves for upgraded oil at 360°C with differently charged surfactants.	65
Figure 4.4: TGA and DTG curves for upgraded oil with different concentrations of DTAB.	67
Figure 4.5: Activation energy lines from TGA plots of bitumen samples.	69
Figure 4.6: XRD pattern of asphaltene samples derived from upgraded bitumen.	70
Figure 4.7: XRD pattern of asphaltene samples from cracked bitumen at 360°C with and without DTAB.	72
Figure 4.8: HRTEM images of the original bitumen asphaltene at different magnifications (20, 10, and 5 nm scale).	74
Figure 4.9: HRTEM images of the asphaltene of the partially upgraded bitumen at 360, 380, and 400°C at different magnifications (20, 10, and 5 nm scale) without surfactant.	74
Figure 4.10: HRTEM images of the asphaltene of the partially upgraded bitumen with 0.25wt% DTAB at 360°C at different magnifications (20, 10, and 5 nm scale).	75
Figure 4.11: Matlab images, fringe length, and tortuosity index of asphaltene particles, for (A) bitumen upgraded with no surfactant and (B) bitumen upgraded with 0.25wt% DTAB.	77
Figure 5.1: SEM images of Fe ₃ O ₄ A) Nano-particles and B) Micro-particles used as catalysts.	88
Figure 5.2: A) TGA and B) DTG plots for liquid oil samples upgraded with 0.5wt% Fe-based catalysts.	93

Figure 5.3: Conversion (α) vs Temp curves of different oxidation zones of upgraded oil + 0.5 wt% Fe-based nanocatalysts.	95
Figure 5.4: Variation of activation energy with conversion during (a) LTO, (b) FD, and (c) HTO reaction zones of upgraded bitumen with 0.5 wt% of Fe-based nanocatalysts.	96
Figure 5.5: Viscosity of the upgraded bitumen at various catalyst concentrations.	101
Figure 5.6: A) Pareto chart for the effects of various catalyst parameters B) Minitab optimized results for max liquid yield, viscosity reduction, and minimum asphaltene content.	103
Figure 5.7: Magnetization saturation measurements for fresh and spent Fe ₃ O ₄ nanocatalyst....	104
Figure 5.8: SEM images of A) fresh Fe ₃ O ₄ nanocatalyst and B) spent Fe ₃ O ₄ nanocatalyst.....	104
Figure 5.9: XRD for the fresh and spent Fe ₃ O ₄ nanocatalyst.	105
Figure 5.10: XPS plot for the Fe 2p peak for the A) fresh Fe ₃ O ₄ nanocatalyst and B) spent Fe ₃ O ₄ nanocatalyst.....	106
Figure 6.1: SEM images of cenospheres A&B) Before and C&D) After coating with Fe ₃ O ₄	120
Figure 6.2: EDX survey spectra of cenospheres A) before and B) after coating with Fe ₃ O ₄	121
Figure 6.3: Locations of the 4 selected sites for EDX comparison.	123
Figure 6.4: Magnetization saturation measurements of Fe-Ceno as compared with pure Fe ₃ O ₄ nanoparticles.	124
Figure 6.5: XRD patterns for coated and uncoated cenospheres.	125
Figure 6.6: XPS plot for the Fe 2p peak coated cenosphere catalyst (Fe-Ceno).	126
Figure 6.7: Oil product viscosity and density after upgrading at 400°C in the presence of Fe-Ceno using various H donors.....	127
Figure 6.8: H NMR spectra of the upgraded bitumen with and without the use of H donors.	129
Figure 6.9: Microscopic images of upgraded oil diluted with toluene at A) 5 ml B) 10 ml) C) at complete dilution.	130
Figure 6.10: Schematic of the architecture of the ANN model proposed.....	133
Figure 6.11: Comparison of the ANN predicted viscosity and density values for the upgraded oil with Fe-Ceno catalyst with different H donors to the experimental values.....	136
Figure 7.1: Schematic for the microwave heating of bitumen.....	141
Figure 7.2: Pictures of the experimental setup used for microwave upgrading.....	144

Figure 7.3: A) Recorded temperatures with carbon susceptors at different concentrations. B) The effect of different carbon susceptor concentrations on the heating rates..... 147

Figure 7.4: The effect of carbon susceptor concentrations on bitumen’s viscosity after microwaving at 150°C for 10 minutes..... 148

Figure 7.5: The effect of microwave irradiation time at the fixed temperature of 150°C on the viscosity reduction and SARA components of upgraded oil with 0.1wt% AC..... 156

Figure 7.6: The effect of microwave (MW) reaction temperature at the fixed time of 10 mins on the viscosity reduction and SARA components of upgraded oil with 0.1wt% AC. 157

Figure 7.7: Summary of the combined effect of microwave reaction time and temperature on the viscosity reduction of upgraded oil with 0.1wt% AC..... 158

Figure 7.8: Real-time illustration of the hot-spots at various stirring rates a) at 0 rpm, b) at 100 rpm, and c) at 600 rpm..... 159

Figure 7.9: The effect of the stirring rate on the viscosity and heating rates..... 160

Chapter 1 - Introduction

1 Background and Motivation

As the world faces an ever-growing need for energy, the current situation unfolds with a pressing realization: our traditional oil resources are no longer enough on their own. The demand for lighter crude oils has significantly increased, rapidly depleting what was once thought to be abundant. It's clear that we need to turn the page and look toward more unconventional sources of energy to bridge this gap. Almost 55% of the world's oil reserves consist of unconventional oil, which includes extra-heavy oil and oil sand bitumen [1] as represented in Figure 1.1. Historically, global efforts predominantly targeted light and conventional oil resources due to their ease of production and processing. However, as the demand for energy and resources significantly rises, the world might be overlooking a treasure in the form of unconventional oil, lying just beneath our feet. This realization prompts a re-evaluation of the current energy strategies, acknowledging that an increase in oil utilization doesn't necessarily equate to an increase in greenhouse gas (GHG) emissions or a departure from environmentally friendly practices. Utilizing unconventional oil resources while adhering to net-zero carbon emission goals presents a formidable challenge. Indeed, these unconventional oil resources generally necessitate more energy-intensive extraction and processing methods than their conventional counterparts, inherently leading to increased carbon emissions [2]. Yet, this challenge isn't impossible as a range of strategies and technological innovations can be leveraged to mitigate these impacts significantly. Ongoing technological innovations continue to refine and improve the efficiency of unconventional oil production. Advances in drilling technology, energy efficiency, and renewable energy integration can significantly reduce the overall environmental impact especially when successfully coupled with technologies such as Carbon Capture and Storage (CCS) and Enhanced Oil Recovery (EOR) [3].

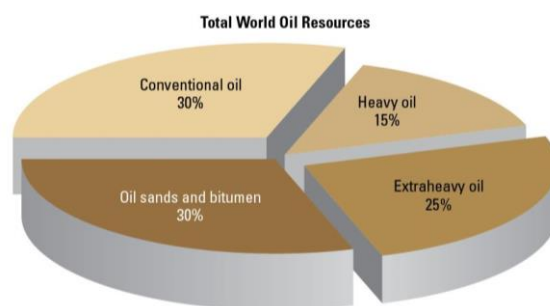


Figure 1.1: Distribution of World Oil Resources adapted from SLB [1].

In this evolving scenario, the path forward involves a balanced approach that recognizes the potential of unconventional oil while persistently committing to environmental stewardship and innovation. Let's take Canada for instance, a key contributor to this global energy story. Ranking as the fourth-largest oil producer and exporter [4], Canada is more than just an example in this case; it's a central figure with vast oil reserves. Yet, even a major exporter like Canada feels the pressure of the world's increasing energy demands, especially after the recent pandemic. A significant portion, over 30%, of its oil production comes from unconventional sources like oil sands [5]. According to the International Energy Agency (IEA) in 2022, Canada produced 9 million barrels of oil a day, with a notable 3.4 million coming from the unconventional oil sands [6]. In Alberta alone, the oil sands hold about 5,505 billion barrels of oil in place [7]. These resources represent a huge potential, yet they remain under-utilized due to their challenging nature. Furthermore, in its 2021 report, the IEA Stated Policies Scenario projected that the total global energy demand is set to increase by 21% by 2040, which includes an increase in demand for both natural gas and crude oil by 28% and 17% respectively by the year 2050 [8]. Moreover, the government of Alberta projects that bitumen production will continue to rise, as its production capacity is estimated to reach a massive 4.3 M bbl/day by the end of 2029, and then it will further increase by another 1.5 M bbl/day by the end of 2040 [9] in both the upgraded and nonupgraded forms of bitumen as represented by the projections shown in Figure 1.2.

ENERGY PRODUCTION FORECAST

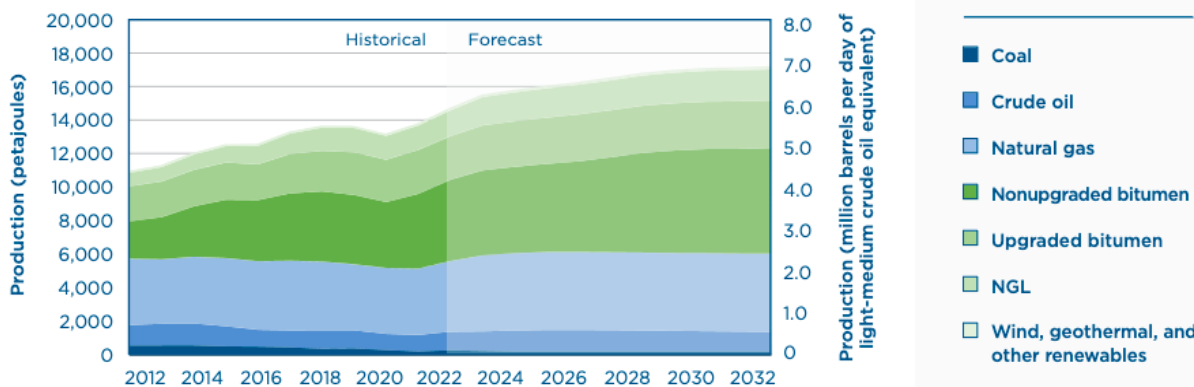


Figure 1.2: Alberta's Energy production levels between 2012-2032 adapted from Alberta Energy Outlook, 2023 [8].

However, with this increase in production comes the challenge of the oil's transportation. Bitumen is a complex material that is made up of a highly complex mixture of large hydrocarbon molecules infused with up to 5% sulfur compounds by weight, and some minor heteroatom impurities such as oxygen and nitrogen and metals (including vanadium, and nickel) [10]. Bitumen has a dynamic viscosity somewhere between $2 \times 10^5 - 2 \times 10^6$ (mPa.s) or (cP) and a density of more than $1,000 \text{ kg/m}^3$ at atmospheric conditions [11]. As a result, traditional methods of transporting this viscous material are proving inadequate as we strive to meet the increasing demand for oil.

The Canadian pipelines have strict standards for viscosity and density, and bitumen doesn't naturally meet these requirements. The Canadian pipeline specifications require the oil to have a dynamic viscosity of 300 cp (or equivalently, the kinematic viscosity of 350 cSt) or less and a density of $< 940 \text{ kg/m}^3$ at the reference temperature of 7.5°C for winter and 15°C for the summer [12]. Table 1.1 below shows a comparison between the different types of treated oil with respect to the required Canadian pipeline specifications.

Table 1.1: Canadian Pipeline specifications adapted from Gray [13].

Property	Pipeline specs	Athabasca bitumen	Diluted bitumen	Fully upgraded synthetic crude oil
VISCOSITY (cSt)	< 350	1×10^6 (Average)	200-300	10
DENSITY (kg/m^3)	< 940	>1000	920	850
API ($^\circ$)	> 19	> 8	> 20	> 30
OLEFIN CONTENT (wt%)	< 1	~0	~0	~0
T.A.N (mgKOH/g)	< 1	4.32	4.32	0.3
P-VALUE	> 1.1	3.4	3.4	~0

To tackle this issue, two main strategies are currently employed by the Canadian producers to meet the pipeline specifications. The first strategy involves diluting the bitumen with a light diluent to make it flow better, but this approach is relatively expensive and reduces pipeline capacity. On the other hand, the alternative strategy is to upgrade bitumen to synthetic crude oil, but this is also costly and comes with its own environmental concerns [14]. For instance, when considering the former option, the diluents used to aid the transportation of bitumen to the US were reported to result in an extra production cost of \$14 per barrel of bitumen, which accounts for 20-30% of the

barrel's cost [15]. Also, about 33% of the pipeline capacity is lost due to the additional volume of the diluents being used. When considering the latter option, despite having four full upgraders currently operating in Alberta, the Canadian government has no intentions of investing in any additional full upgraders because the building of such plants is no longer cost-effective [16]. The full upgrading plants are usually facilitated with expensive catalysts and hydrogen gas resources, which allows them to highly improve the quality of the oil, reducing its viscosity, sulfur, nitrogen, and other heavy metal contents [17], [18]. However, the cost of operation is high, and yet the current four full upgraders can only treat 35% of Alberta's bitumen before being sold to market. Another drawback of the full upgraders is that they lead to significant greenhouse gas (GHG) emissions during the refining process. The oil sands operations currently emit 70 Mega tones per year, accounting for about 8% of Canada's total GHG emissions [19]. Therefore, a new alternative must be implemented on an industrial scale to address the bitumen transportation demand and the older solutions' drawbacks.

In the quest to make oil sands more accessible and environmentally friendly, partial upgrading technique has emerged. This method is gaining attention as a smarter, more cost-effective route compared to the full-scale upgrading to synthetic crude oil (SCO) process. Its goal is straightforward: cut down or completely remove the need for diluents with the minimum cost possible. This change could significantly lighten the burden on the pipelines and shipping systems. Traditional upgrading methods focus on breaking down the heaviest parts of the oil, but partial upgrading is different. It specifically targets improving the oil's heavy fractions and how it flows, making it just right for its transportation to refineries [13]. While this sounds ideal, it's important to note that this process is still in the early development stages; no fully commercial technologies for partial upgrading are up and running just yet. Recognizing this potential, Canada has launched the National Partial Upgrading Program (NPUP) in 2015 [20]. This initiative is about encouraging fresh ideas and technologies to make partial upgrading a reality, focusing on reducing the need for diluents, enhancing oil quality, and doing it all with lower environmental impacts [20]. The goal of this program is not solely focusing on making the Canadian bitumen easier to handle but also making it more market-friendly and environmentally responsible source of energy that can adhere to the new policies and work towards achieving net-zero emissions by 2050.

1.2 The Nature of Bitumen

The two largest oil sands deposits in the world are situated in Venezuela and Canada [21]. While the Venezuelan deposits have slightly higher fluidity at reservoir conditions making their recovery possible using conventional drilling techniques that are adapted for heavy oil extraction, the Canadian oil sands, on the other hand, present a much greater challenge due to their low fluidity. Concentrated primarily in the province of Alberta, the Canadian oil sands are mainly found in three key regions: Athabasca Wabiskaw, Cold Lake, and Peace River. The unique composition of Canadian oil sands necessitates specialized extraction techniques such as surface mining or in-situ methods like steam-assisted gravity drainage (SAGD), underscoring the significance of understanding and managing these resources effectively.

Understanding bitumen and its place in the heavy oils category is vital due to its unique and challenging properties. Bitumen stands out with its high density and viscosity, key traits that define its behavior and use. Typically, it has density values greater than 1000 kg/m^3 , translating to a gravity of less than 10°API . This high density isn't just a number; it is an indicator that reflects the rich content of cyclic structures like aromatics and naphthenes in bitumen, along with substantial amounts of sulfur and nitrogen, which are present as heteroatoms. Diving deeper, the nature of bitumen is represented by its low hydrogen-to-carbon (H:C) ratio and high Conradson Carbon Residue (CCR) values. The average H:C molar ratio of oil sands bitumen is around 1.51 [22] whereas, the required acceptable fuel must have a H:C molar ratio within the range of 1.8–2.0 [23]. This low ratio in bitumen indicates a heavier and more complex composition. Moreover, a significant portion of bitumen's sulfur content, about 60%, is in the form of thiophenic sulfur, which is particularly difficult to remove compared to other sulfur forms [24]. The presence of nitrogen and oxygen in bitumen, although lower than sulfur, is still relatively high compared to conventional oils. These elements bring their own set of challenges during refining, affecting processes like acid catalyst inhibition and sulfur removal. The high total acid number (TAN) of bitumen further complicates refining, necessitating more sophisticated and extensive processes compared to conventional crude oils [24].

To illustrate these differences, Table 1.2 highlights the main differences between bitumen and conventional Brent oil in terms of density, viscosity, and elemental composition, underscoring why bitumen is in a league of its own when it comes to handling and refining. The average values

represented in the table indicate that both Athabasca and Cold Lake Bitumens exhibit significantly denser and more viscous properties compared to the Brent Blend, with densities about 20% higher and viscosities at least 11,500 times greater, reflecting the substantial handling and processing challenges that these oils are facing. Moreover, their Conradson Carbon Residue (CCR) is over 500% higher, and the Total Acid Number (TAN) is up to 3100% greater, indicating more complex refining needs due to higher residue production and acidity. Sulfur content in the bitumens exceeds Brent's by more than 10 times, necessitating advanced refining to meet the environmental standards. Finally, the distillation profiles reveal that bitumen lacks lighter naphtha fractions and has a vacuum residue content over 10 times higher than Brent, highlighting a predominance of heavy fractions that demand more intensive processing for valuable product yields. This makes us realize that the main challenge with bitumen lies within its significant vacuum residue fraction. Nearly half of bitumen doesn't distill even under extreme vacuum conditions, turning into a vacuum residue with very high boiling points [22]. Upon heating beyond 350°C, this residue tends to react and form solid coke. The tendency of bitumen to coke is measured using methods like the CCR or micro-carbon residue (MCR), shedding light on its behavior during processing. Furthermore, bitumen's residue contains a notable amount of asphaltenes which are complex molecular aggregates that play a significant role in its overall behavior, affecting traits like solubility and viscosity. Assessing the solubility and compatibility of asphaltenes is crucial for understanding and improving bitumen processing [25].

The link between bitumen's density and viscosity with the boiling point distribution is essential. Higher boiling points lead to increased density and viscosity, which in turn impact transportation and refining. The high density and viscosity of oil sands bitumen not only introduce its transport challenge but also affect how it's processed in refineries. These characteristics are also shared by other unconventional oils, indicating a broader relevance in understanding, and managing these complex substances.

Table 1.2: Typical compositions of Bitumen versus conventional Brent Oil retrieved from Klerk et al.[24].

Property	Athabasca Bitumen	Cold lake Bitumen	Brent Blend
Density (kg/m ³)	1000-1030	990-1000	833
Viscosity at 20°C (Pa.s)	80-12000	100	0.007
CCR (wt%)	13.5-16.5	12.6	2.1
TAN (mg KOH/g)	1.6-3.2	0.5-1.0	0.1
Elemental composition (wt%)			
Carbon	83.1-83.4	83.7	83-87
Hydrogen	10.1-10.6	10.5	11-14
Sulfur	4.8-5.1	4.7	0.4
Nitrogen	0.4-0.5	0.2	< 0.3
Oxygen	0.9-1.1	0.9	< 1.0
Distillation Fractions (vol%)			
<175°C (Naphtha)	0	0	34.9
(175 -343°C) Light Gas oil	8.6-14.4	18.2	35
(343-550°C) Heavy Gas oil	35.1-39.4	31.1	25.6
(>550°C) Vacuum Residue	46.2-56.4	50.7	4.5

When diving deeper into the chemistry of bitumen, it reveals that bitumen has an extremely complex chemistry that can be divided into four main classes of hydrocarbon fractions for simplicity, these fractions are referred to as "SARA": Saturates, Aromatics, Resins, and Asphaltenes. Each of these fractions contributes to bitumen's distinctive high viscosity and density, particularly the resins and asphaltenes found in the vacuum residue fraction. These components, due to their high boiling points, engage in strong physical interactions and form aggregated asphaltene species, significantly increasing bitumen's viscosity. For perspective, bitumen contains more than 15% asphaltenes by weight, a significant amount compared to the mere 0.6-0.7% found in the conventional Brent crude oil [20].

Asphaltenes, the heavyweights of bitumen chemistry, are defined as the fraction that is insoluble in lighter paraffin solvents like n-pentane or n-heptane but is soluble in aromatic solvents such as toluene [26]. These polycyclic aromatic hydrocarbons, linked by alkane chains, are notorious for their colloidal aggregate formations, substantially contributing to bitumen's high viscosity and density. Their behavior is crucial in determining the microstructure and mechanical properties of bitumen, making their study essential for understanding and managing bitumen effectively. In

addition to all that, asphaltenes pose significant challenges during oil production, upgrading, and refining due to their tendency to associate and precipitate, leading to blockages and issues with heavy-end processing [21]. On the other side, resins, the slightly lighter companions, help keep bitumen in a semi-liquid state, acting as solvents for asphaltenes. The other lighter fractions, aromatics and saturates, also play their part in influencing the fluidity and volatility of bitumen. It is important to note that the ratios of the SARA components play a crucial role in determining the overall colloidal stability of bitumen, with indices such as the asphaltene index (Ia) and colloidal instability index (Ic) serving as key indicators [27]. The asphaltene index (Ia), calculated as the ratio of asphaltenes plus resins to saturates plus aromatics, provides insight into the tendency of asphaltenes to precipitate from the mixture. On the other hand, the colloidal instability index (Ic), which is the ratio of asphaltenes plus saturates to resins plus aromatics, offers a measure of the bitumen's ability to maintain a stable dispersion of colloidal particles. A higher Ic value indicates a greater risk of phase separation, impacting the viscosity and flow properties of bitumen during extraction and transportation [28]. Additionally, the presence of heteroatoms like sulfur, nitrogen, and trace metals adds layers of complexity to bitumen's chemical composition, affecting its processing and behavior.

Bitumen's behavior under different operating conditions further adds to its complexity. Exhibiting non-Newtonian rheological characteristics, its viscosity isn't fixed but varies with shear rate and temperature. It can act both elastic and viscous, becoming more fluid with heat and less viscous at high shear rates—a property known as shear-thinning [13]. However, at lower temperatures, it can turn almost solid, posing challenges for pumping and transportation. While temporary viscosity changes due to temperature or composition are reversible, permanent reductions require altering the chemical composition or undergoing chemical reactions, such as hydrogenation or desulfurization [20]. Understanding these intricate details of bitumen chemistry is crucial for improving its processing and transportation.

1.3 Economic and Environmental Implications for Utilizing Bitumen

The Canadian crude oil is navigating through a warren of challenges and opportunities. Almost all Canadian crude oil finds its way to the United States, as highlighted by the Canadian National Energy Board [29]. While most of this oil is transported via pipeline, rail transportation could see an increase if new pipeline capacity isn't added. The Alberta Energy Regulator (AER) [30] forecasts a significant growth in both in situ and mined bitumen production by 2026, outpacing forecasts by the Canadian Association of Petroleum Producers (CAPP). This overwhelming dependence on a single market, combined with the limitations in pipeline capacity, sparks a crucial question: How can Canada manage and expand its bitumen production, especially when U.S. demand is becoming more uncertain and refining capacities are not growing as fast?

Given the limitations of the full upgrading plants and the diluent use as previously noted, partial upgrading of bitumen emerges as a compelling response to these challenges. It represents a balanced approach between diluting bitumen for easier transport and fully upgrading it into synthetic crude oil. This strategy could not only enhance the marketability of Canadian bitumen but also reduce the need for costly diluents and free up pipeline capacity. Moreover, the environmental and economic landscapes are shifting. As the U.S. looks towards increased fuel efficiency and alternative fuels, demand for traditional fuel is expected to decline. This makes the case for partial upgrading even stronger, offering a potentially more profitable and environmentally sustainable path forward [20]. The incentives for developing partial upgrading techniques are manifold. Environmentally, it presents an opportunity to reduce the sulfur content and density of bitumen, leading to lower emissions during refining. Economically, it could increase the value of bitumen, making it more attractive to refineries and end-users, thus boosting revenues. From an energy security perspective, it supports a more self-reliant supply of high-quality oil products, reducing dependence on imports. Technologically, it encourages the advancement of new methods and technologies, enhancing the efficiency and cost-effectiveness of bitumen processing [22]. Finally, it will support job creation in the industry and reinforce the global competitiveness of Canadian oil.

In the field of partial upgrading, any recent advancement will make a step in improving bitumen's quality, thus negating the need for diluents in pipeline transport. This includes innovations in

processes like thermal cracking and solvent deasphalting, each with its own set of benefits and challenges. Processes such as thermal treatment and desulfurization are being explored to achieve the desired quality for stable partially upgraded crude oil. However, these technologies are not without their limitations. Economic viability, energy intensity, and environmental impact are significant concerns that need careful consideration and continuous improvement. In this context, partial upgrading is an initiative that represents critical steps towards a more diversified, economically robust, and environmentally responsible energy future for the Canadian oil sands.

1.4 Thesis Objectives

The main objective of this project is to “Identify an efficient and sustainable process that can partially upgrade bitumen to pipeline transportable fuels while minimizing the overall cost and GHG emissions”. This objective can be summarized into 2 technical goals and 1 economic goal as follows:

- 1) Process the oil sand bitumen in a way to reduce its viscosity and density to satisfy the North American pipeline transportation.
- 2) Meet all pipeline transport specifications while maximizing liquid yield and minimizing both the gas and coke yields.
- 3) Reduce the cost of the partial upgrading process as compared to dilution and full upgrading strategies.

The objectives of this project complement and fulfill the contract requirements of NRCan CanmetMATERIALS Contract (3000702598) which aims to identify the optimal operating conditions of catalytic and non-catalytic thermal cracking of bitumen, and to determine the chemistry and toxicity of related Bitumen Partial Upgrading “BPU” processes. The major tasks requested by this contract include (1) optimization of the operating conditions of catalytic and non-catalytic thermal cracking techniques for bitumen partial upgrading; (2) analyzing upgrading products (both gaseous and liquid phases) and identifying the process toxicity and chemistry; (3) conducting preliminary research on the BUP using relatively cheap liquid organic hydrogen donors other than the direct use of hydrogen gas.

1.5 Thesis Organization/Outline

The work presented in this thesis is divided into eight chapters. Five of these chapters are manuscripts that were prepared for publication in refereed journals.

Chapter 1: This chapter serves as an introductory section to the topic of heavy oil/bitumen processing and upgrading where the background information, chemistry of bitumen, and the economic incentives are briefly discussed. Also, this chapter introduces the thesis's overall motivation, objectives, outline, and ultimate goals.

Chapter 2: This chapter provides a comprehensive literature review, as it explores all the heavy oil upgrading techniques in the oil and gas industry from conventional to innovative. Some of the conventional upgrading technologies included thermal cracking, catalytic cracking, hydrocracking, and solvent deasphalting while some of the more modern techniques included cavitation, microwave irradiation, and the use of chemical additives.

Chapter 3: This chapter delves deeper into the economic and environmental challenges and opportunities in bitumen partial upgrading. This chapter also provides a detailed comparison between all the possible partial upgrading techniques and identifies some of their potential benefits and drawbacks. The outcome of both chapters 2 and 3 will be compiled into one manuscript titled “*Recent Developments in the Utilization of Unconventional Resources: A Focus on Partial Upgrading Techniques and Sustainability of Canadian Oil Sand Bitumen,*” that will be sent for publication.

Chapter 4: This chapter includes an experimental investigation of the effect of adding ionic surfactants on bitumen’s thermal upgrading process. As a result of this phase, a detailed understanding of the effect of surfactants on the upgrading process was achieved, and hence, the results were successfully published. In this part of the research, bitumen was partially upgraded within the temperature range of 360-400°C with surfactants of different charges and concentrations. The results of this chapter were compiled into a manuscript that was published on the 14th of March 2022 under the title “*The effect of ionic surfactants on bitumen’s viscosity and asphaltene nanostructure under thermal partial upgrading*” in the **Energy Science & Engineering journal** Volume10, Issue 7, **2022**. Below is the digital link to this publication:

<https://onlinelibrary.wiley.com/share/ZSDKQGB98EY72FSZAQIK?target=10.1002/ese3.1137>.

Chapter 5: This chapter includes the experimental investigation of the application of relatively cheap Fe-based nanocatalysts for catalyzing the partial upgrading of bitumen, aiming to develop an economically viable and environmentally sustainable process. The primary focus is to analyze the impact of the oxidation state of iron, catalyst particle size, and catalyst concentration on partial upgrading efficiency to optimize bitumen resource utilization without the need for an external source/supply of hydrogen gas using an autoclave reactor. The results of this chapter were compiled into a manuscript that was published on the 14th of September 2023 under the title “*Optimization of Iron-Based Catalyst for Partial Upgrading of Athabasca Bitumen: The Role of Fe Oxidation State, Particle Size, and Concentration*” in **Fuel** Volume 10, Issue 7, **2024**. Below is the digital link to this publication:

<https://www.sciencedirect.com/science/article/pii/S0016236123025553>.

Chapter 6: This chapter aims to investigate the synergic effect of coupling the best iron catalyst identified in chapter 4 with the relatively cheap liquid organic H donor (such as tetralin) and optimize them to produce a high liquid yield product that satisfies the Canadian pipeline specifications without the need for hydrogen gas or any traditional reducing species. The primary focus of this section is to synthesize a cheap catalyst from a waste material “cenospheres” and coat it with a layer of Fe₃O₄. The new catalyst is then dispersed in various commonly used liquid H donors and tested to identify their catalytic and hydrogenation effect on the upgrading of bitumen. The results were compared to Husky's industrial Diluent Reduction technology and very similar and promising results were obtained. These promising results motivated us to build an AI model using an Artificial Neural Network (ANN) to model the synergic catalytic effect of the catalyst and the H donors. Even though the AI models have not been validated using other research group's experimental data, it still shows the potential to be used as a useful tool in the future to help optimize the catalyst selection process and minimize the experimentation time. The novel results of this chapter were compiled into a manuscript that was sent for publication under the title “*Enhancing Bitumen Processing with Fe₃O₄ Coated Cenospheres and ANN-Driven Process Optimization: A Novel Approach to Sustainable Partial Upgrading*”.

Chapter 7: This chapter explores a new non-traditional method of heating the thermal upgrading reactions of bitumen via the use of microwave irradiation powered by electricity instead of conventional heating techniques. This phase of this project includes upgrading bitumen using microwave irradiation with the aid of multiple variations of carbon-based catalysts (activated carbon, biochar, coke, and graphite). These catalysts were tested for their ability to promote localized thermal cracking reactions within the highly polar constituents of bitumen at much lower temperatures than conventional heating. The results demonstrated that the addition of small quantities as low as 0.1wt% of the carbon additives, used as microwave susceptors/catalysts, can effectively reduce the viscosity of bitumen by up to 94%. This viscosity reduction takes place at the mild conditions of 10 mins of microwaving time at 150°C. The results of this chapter were compiled into a manuscript that was sent for publication on the 28th of November 2022 under the title “*Experimental investigation of the partial upgrading of oil sand bitumen using carbon-assisted microwave irradiation*” in the **Chemical Engineering Science** journal. Below is the digital link to this publication: <https://www.mdpi.com/1420-3049/28/23/7769>.

Chapter 8: Finally, this chapter includes a comparative analysis between the partial upgrading techniques discussed in the previous chapters and then finally states the thesis’ main conclusions and highlights the main takeaways from the various investigations conducted. Furthermore, this section suggests some future work and recommendations for further research in this area of concern.

Chapter 2 – Literature Review

2 Overview of the Upgrading Technologies

As previously noted in chapter 1, the inherent high viscosity of bitumen presents significant challenges for transportation and processing. This dense, sticky substance is typically less favoured in its raw form due to the lower yields of valuable distillate products it produces. Moreover, factors like its high total acid number (TAN) and the presence of olefins diminish both the market value and processability of bitumen [31]. Additionally, the often-overlooked nitrogen content plays a pivotal role, particularly impacting the efficiency of sulfur removal processes. Therefore, a comprehensive examination of the various upgrading techniques available is necessary.

Upgrading is defined as a transformative process that turns the heavy oil into a lighter, more marketable form, known as synthetic crude oil (SCO). This transformation is crucial for meeting the strict specifications of Canadian pipelines and ensuring that the oil can be readily processed at its final destination refineries. Through upgrading, the quality of the oil is significantly enhanced; its viscosity drops, and levels of sulfur, nitrogen, and heavy metals are reduced. Once upgraded, about 35% of Alberta's bitumen proceeds to downstream refineries for conversion into more useful products [32]. The technologies employed in upgrading heavy crude feedstock predominantly involve hydrogen addition and/or thermal carbon rejection processes. These methods essentially upgrade the crude through catalytic action or exposure to high temperatures, driving chemical reactions within the heavy petroleum fractions. The primary goal here is to break down the long carbon-carbon (C-C) chains typical in heavy crude and increase the hydrogen-to-carbon ratio, thereby converting the dense crude into lighter, more valuable products [33].

Experiments have shown that regardless of the specific upgrading route taken, the key objective is to maximize the liquid yield by minimizing the production of gas and coke while ensuring the resulting liquid is high-quality and stable. When temperatures exceed 350°C, a variety of reactions of commercial interest take place, including cracking, addition, and hydrogen transfer [34]. Thermal cracking, for instance, effectively reduces viscosity but may not adequately increase API gravity for pipeline transportation. Overdoing thermal cracking can lead to unstable products, which might not mix well with diluents or fit into refinery streams. The rate of thermal cracking is predominantly influenced by temperature, with pressure playing a secondary role, although it

can affect outcomes in continuous processes. Ultimately, the specific yields and products obtained from a given feedstock depend on the time-temperature history of the components, which in turn influences the formation of vapor phase or solid-phase coke.

In summary, the fundamental chemical reactions involved in upgrading can be categorized as follows [13]:

- Cracking or scission: This involves breaking C-C, C-S, and C=O bonds to produce liquid and gaseous products, along with reactive species such as olefins and diolefins.
- Addition reactions: These occur with reactive species in the liquid phase, leading to the formation of coke precursors.
- Hydrogen transfer reactions: These are prompted by the formation of unsaturated and aromatic species.

2.2 Thermal Cracking

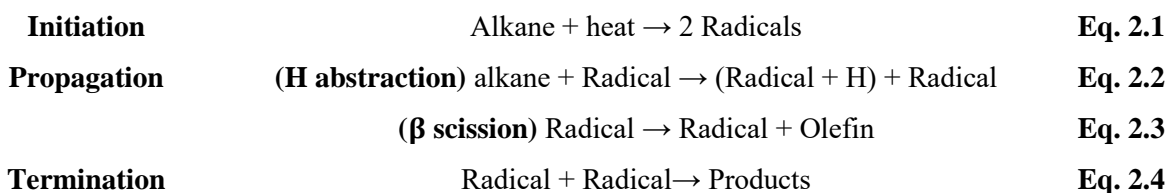
2.2.1 Process Thermodynamics and Kinetics

Thermal cracking, an essential technique in oil upgrading, operates on the intricate interplay of thermodynamics and kinetics. This process, particularly effective in removing sulfur, oxygen, and nitrogen, favors the cleavage of aliphatic carbon-carbon bonds over other types. Table 2.1 showcases the activation energies required to break various bonds in heavy petroleum and bitumen, providing a glimpse into the energy landscape of thermal cracking.

Table 2.2: Estimated activation energy for breaking bonds retrieved from Gray [35].

Chemical Bond	Energy required (KJ/mol)
C-C (aliphatic)	344 ± 4
C-H (Primary)	411 ± 4
C-H (Secondary)	398 ± 4
C-H (Aliphatic)	464 ± 8
C-S	307 ± 8
C-N	342 ± 8
C-O	344 ± 4

Thermal cracking is a non-catalytic and hydrogen-deficient process and radical mechanism predominates the cracking [35]. This mechanism unfolds in three stages: initiation, where heat generates radicals; propagation, where these radicals engage in hydrogen abstraction and β -scission to generate more radicals and olefins; and termination, where radicals recombine to form stable products. A summary of these stages is represented in Equations 2.1- 2.4.



The operating conditions for thermal cracking can vary, leading to different process intensities: mild, moderate, or severe. In the petroleum industry, this manifests as pyrolysis (severe, with temperatures exceeding 900°C at low pressures), visbreaking (mild, operating at 400–450°C with relatively higher pressure), and coking (intermediate, with conditions varying between delayed coking and fluid coking) [36]. The essence of thermal cracking lies in its thermodynamic principles. The process begins with heating bitumen to high temperatures, typically between 400 and 600°C. This induces pyrolysis, breaking down heavy hydrocarbons into lighter fractions. As the bitumen heats, heavy hydrocarbons vaporize and are swept away by hot gases, later cooling to separate lighter from heavier fractions. This depolymerization reduces the molecular weight of the heavy hydrocarbons, enhancing their value. The resulting lighter fractions then condense back into liquids as the temperature drops [37].

Thermally cracking bitumen is an endothermic reaction, demanding energy to break down complex hydrocarbons into simpler, more volatile compounds. This transformation increases the system's entropy, reflecting the greater diversity of microstates as larger molecules are converted into smaller ones. The thermodynamic driving force behind this process is the difference in Gibbs free energy between the reactants and products; the reaction proceeds favorably when the products have lower Gibbs free energy, indicating a spontaneous process under given conditions [38]. Typically, the heat required for this endothermic reaction is supplied by burning natural gas, a common practice that aligns with the industry's energy requirements while considering efficiency and environmental impact. To enhance the reaction's feasibility and efficiency, economical catalysts such as zeolites or metal oxides/sulfides may be employed. Zeolites, with their porous

structure, provide a large surface area for the reaction, facilitating the breakdown of complex hydrocarbon chains through acid-catalyzed mechanisms [39]. Metal oxides or metal sulfides, on the other hand, serve as inexpensive yet effective catalysts that can promote the dissociation of carbon-carbon bonds in heavy hydrocarbons, contributing to a more cost-effective process. The kinetics of thermal cracking usually follow first-order reaction kinetics, indicative of the reaction rate being proportional to the concentration of the reactant. In this context, pressure plays a minimal role in liquid-phase reactions, as the primary factor influencing the rate is the thermal energy supplied to the system [40]. However, in continuous processes, combined with reactor design, higher pressures can suppress vapor formation and increase liquid residence time, affecting the outcome. Recent studies, like that of Alade et al. [41], have explored the impact of reaction pressure on the thermal conversion of bitumen. Their findings suggest that lower pressure conditions, particularly atmospheric pressures, are more favorable for effective thermal conversion.

2.2.2 Mild Thermal Cracking

The application of thermal cracking in bitumen processing not only aims at reducing the viscosity of the heavy oil by breaking down larger molecules but also at enhancing the quality of the final product. The strategic control of reaction conditions can lead to the selective production of valuable lighter hydrocarbons, such as diesel and gasoline fractions, thereby increasing the economic value of the processed bitumen. Visbreaking, for instance, a form of mild thermal cracking, emerged in the early 20th century as a technology to reduce the viscosity of fuel oil. Today, it stands as a significant residue upgrading technology, processing about one-third of the global residue production [21]. The simplicity of the process—requiring only a tube furnace that serves both as a heater and reactor, and operating without a catalyst—is one of its appealing features. A process flow diagram of how the visbreaking process works is shown in Figure 2.1. Operating typically at temperatures between 450-510°C and pressures of 50-300 psi, visbreaking effectively converts heavy crude into lighter products by "cracking" or breaking molecular bonds. This reaction is inherently spontaneous at elevated temperatures and is characterized as endothermic, with activation energy varying based on the specific bonds being broken. The core objective of visbreaking is to improve bitumen's viscosity, making it more amenable to transport, particularly through pipelines. Castillo and De Klerk's experiments [42] illustrate this point; as

they pointed out that only thermal cracking reactions between 360 and 400°C resulted in significant conversion and a viscosity reduction conducive for pipeline transport. However, it's important to note that temperatures beyond 400°C often lead to an undesirable increase in coke formation, which in turn significantly diminishes the liquid yield. Despite its effectiveness in reducing viscosity, visbreaking on its own typically is not enough to meet pipeline transport requirements, especially concerning density reduction. Even after visbreaking, the product's density usually remains between range 980-1000 kg/m³. Hence, additional processing steps, like combining visbreaking with solvent de-asphalting, are often required to achieve an acceptable density range for pipeline specifications [13].

The stability of the heavy oil product, as assessed by the peptizing value (P-value) test, is a critical factor in this case [43]. Adjusting cracking conditions, such as lowering furnace temperature and prolonging residence time, can yield higher naphtha but lower conversion of heavier residues. Despite these challenges, visbreaking's basic principle of mild thermal conversion is attractive and often discussed as a component in proposed partial upgrading processes. However, it's crucial to understand that much of the data on bitumen reactions come from laboratory conditions with uniform temperatures, which may not reflect large-scale operations' realities. In pilot or demonstration plants, localized heating can cause wall temperatures to significantly exceed the bulk liquid temperature, leading to localized coke formation and fouling—a serious issue that might not be evident in batch laboratory reactors but could terminate a continuous process within hours [33].

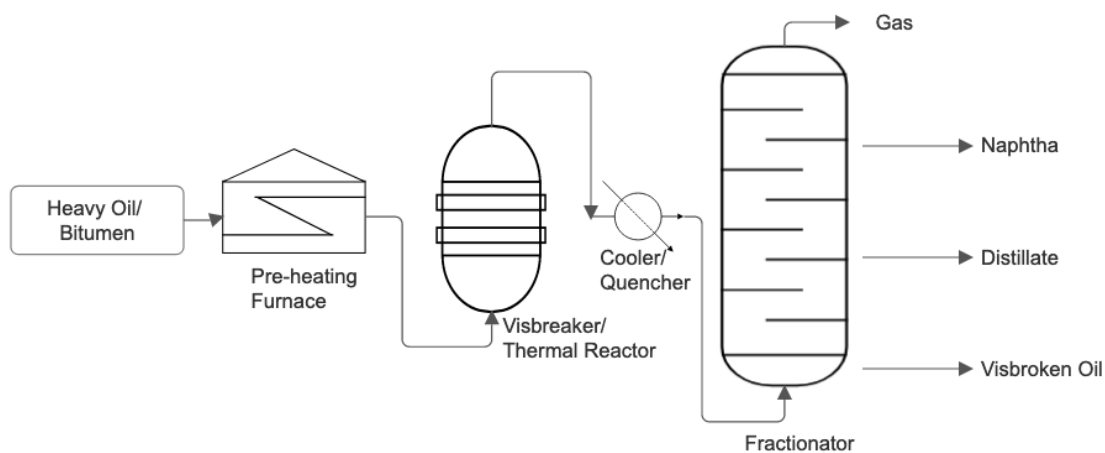


Figure 2.2.1: General flow diagram of the visbreaking process recreated based on the process description from Speight [44].

2.2.3 Coking

Coking has been a cornerstone in the upgrading of bitumen for decades, with a history tracing back to Suncor's implementation of delayed coking in 1968 and Syncrude's adoption of Fluid Cokers in 1978 [15]. As a robust carbon-rejection process, coking is particularly effective for handling residues rich in asphaltene cores, dividing these dense cores into a low-value byproduct (coke) and thus enabling the remaining resins to undergo further upgrading. Often favored over catalytic cracking, coking avoids issues related to catalyst poisoning by heteroatoms like metals and nitrogen, as well as clogging by high molecular weight compounds such as asphaltenes and resins. There are two classes of coking technology employed industrially, namely, delayed coking and fluid coking [13], [31].

Delayed Coking operates semi-batch coke drums in pairs, typically with cycles ranging from 12-20 hours. The process setup resembles that of visbreaking but with a more severe operational regime, employing slightly higher temperatures and significantly longer residence times. Here, the feed is heated to cracking temperatures (485-505°C) before being introduced into the coking drum, where thermal cracking reactions unfold over several hours, producing coke and volatile lighter products. This process is catalyst-free, relying on a free-radical mechanism for the thermal cracking and coking reactions. The lighter products are subsequently fractionated, while the coke, a solid material, is periodically removed. Operating two coking drums in parallel allows for alternating between coking and cleaning, maintaining a continuous operation [45].

On the other hand, Fluid Coking is a dynamic alternative that was Licensed by ExxonMobil and utilized in Alberta's Syncrude Upgrader [15]. This technology integrates thermal cracking with coke burning in a self-sustaining system that negates the need for an external fuel supply. While the reaction chemistry is similar to that of delayed coking, coke forms continuously in a fluidized bed reactor, not in a drum. Operating at higher temperatures of around 500-540°C, Fluid Coking is a continuous process, both in coking and product separation. This method allows for substantial upgrading of light products while transforming part of the material into coke, which is rich in carbon but poor in hydrogen, effectively decreasing the metal and heteroatom content of the lighter products [44]. Figure 2.2 below represents the typical process flow diagrams for both of the coking processes.

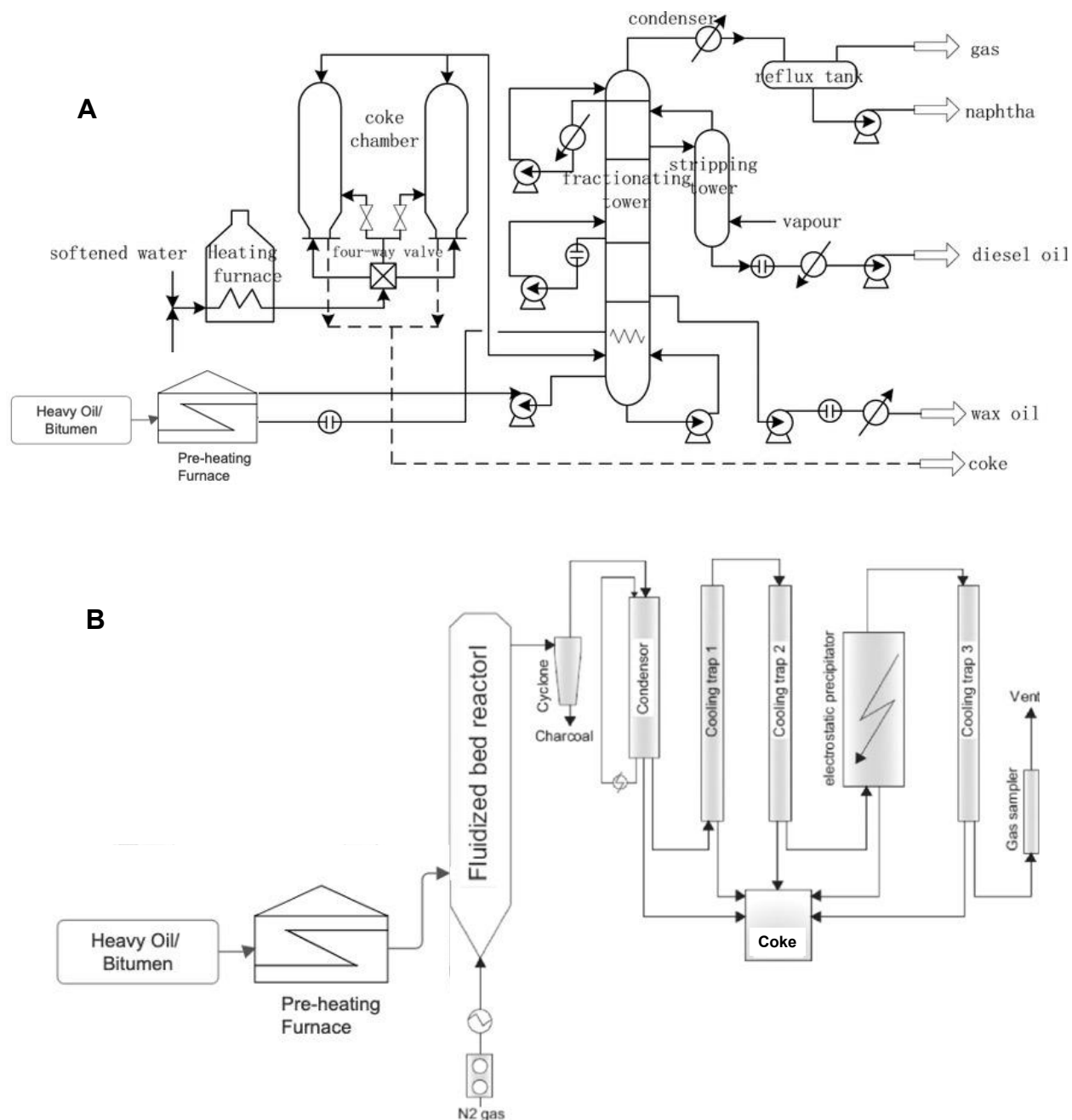


Figure 2.2: Comparison between the process flow diagram of A) Delayed Coking and B) Fluid Coking processes. Diagram recreated based on the description from EIA [45].

It is important to note that irrespective of the coking technique, providing ample residence time for thermal cracking reactions is crucial for substantial upgrading. As lighter products like distillate, naphtha, and gas are produced, the remaining material converts into coke—a solid, carbon-rich substance loaded with metals and heteroatoms. This process leads to hydrogen disproportionation, enhancing the H:C ratio in lighter products while the coke becomes more

aromatic with a lower H:C ratio. Essentially, coking tackles the upgrading challenge by rejecting carbon (in the form of coke) rather than necessitating the addition of hydrogen to the feed. Coking, whether delayed or fluid, is a fundamental process in bitumen upgrading. By effectively separating heavy asphaltenes and rejecting carbon, coking technologies transform dense, heavy feedstock into lighter, more valuable products. This process not only improves the marketability of the resulting oil but also addresses some of the most persistent challenges in bitumen processing, making it a key player in the ongoing story of energy production and resource utilization.

2.3 Catalytic Cracking

Catalytic cracking is a process that utilizes a catalyst to break down larger hydrocarbon molecules into smaller ones. Their role in upgrading is particularly effective in converting heavy bitumen into lighter, more valuable fractions like gasoline and diesel [46]. Figure 2.3 shows a typical process flow diagram of a catalytic cracking process that can be used for bitumen upgrading. Catalysts can be incorporated into the oil system in various forms, predominantly as water-soluble, oil-soluble, or in a solid dispersed state. The introduction of catalysts in heavy oil upgrading started in 1990 when scientists like Clark et al. [47] discovered the benefits of using water-soluble catalysts in cracking crude oil. Since then a series of studies confirmed the potential of such catalysts, for instance, a study conducted by Maity et al. [48] which employed water-soluble transition metals like ruthenium (Ru) and iron (Fe) as catalysts in asphaltene upgrading experiments conducted at temperatures ranging from 375–415°C. These catalysts yielded desulfurization efficiencies of 21% and 18%, respectively. Furthermore, despite an increase in asphaltene content from 14.6 to 19.7 wt%, the study observed a significant reduction in crude oil viscosity from 2140 to 520 cP. The authors attributed this to the high catalytic activity of first-row transition metals (mainly Cr, Mn, Fe, Co, Ni, Cu, Zn, and Al ions) particularly in breaking C–S bonds in thiophene and tetrahydrothiophene molecules. Another comprehensive analysis performed by Fan et al. [49] corroborated these findings, revealing that a variety of metal ions, including Fe^{2+} , Co^{2+} , Ni^{2+} , Cu^{2+} , Zn^{2+} , Mo^{2+} , Al^{3+} , and Mn^{2+} , all contributed to viscosity reduction in Liaohe heavy oil under hydrothermal cracking conditions. Notably, Fe^{2+} emerged as a cost-effective and efficient catalyst, achieving a viscosity reduction of up to 60% at 240°C over 72 hours. It was later confirmed by a recent study by Abdrabou et al. [50] that lower valency states of Fe were more effective in transforming heavier fractions into lighter ones opening the gate

towards a better understanding of ways to optimize the oxidation states of the transition metals catalysts used.

On the other hand, oil-soluble catalysts have gathered considerable attention for their efficiency in heavy oil upgrading, primarily due to their excellent solubility and dispersion within oil [51]. Work by Zhao et al. [52] reported a 90% reduction in the viscosity of Liaohe heavy oil through the utilization of nickel and cobalt-based catalysts, coupled with petroleum sulfonates as emulsifiers, at low reaction temperatures. This finding was supported by Chen et al. [53], who employed aromatic iron sulfonate catalysts to achieve a similar viscosity reduction at 280°C. Several iron-based compounds, including iron (II) naphthenate, ferric (III) acetylacetonate, and iron (III) dodecyl benzenesulfonate, have been also successfully employed in cracking reactions. Notably, Li et al. [54] designed an oil-soluble, iron-based catalyst using toluene sulfonic acid as a ligand, achieving a 90% viscosity reduction across multiple heavy oil samples at a relatively low temperature.

Among the numerous types of catalysts investigated, solid dispersed acidic catalysts have also been a cornerstone for nearly a century. Provided that they can properly be dispersed within the oil system [55], these catalysts find applications in a diverse array of organic reactions, including esterification, ring-opening, hydrogenation, and desulfurization. According to Zhao et al. [51], solid acid catalysts can be categorized into nine distinct types, such as metal oxides, metal sulfides, metal phosphates and sulfates, zeolite molecular sieves, heteropoly acids, and solid superacids. CoMo and NiMo catalysts, supported on alumina or silica-alumina matrices, excel in the removal of heteroatoms like sulfur, nitrogen, and metals. Zeolite-based hydrocracking catalysts, on the other hand, facilitate the conversion of larger hydrocarbon molecules into lighter products while simultaneously conducting hydrogenation [46]. Furthermore, metal sulfide catalysts, especially blends of molybdenum and nickel, have been identified as effective agents for hydrogenating sulfur, nitrogen, and metal-bearing compounds. Their application, in conjunction with high-pressure hydrogen, enables substantial conversion of vacuum residue components, thereby paving the way for partial bitumen upgrading. Also, bifunctional catalysts, which possess both acidic and metallic sites, are garnering attention for their versatility in facilitating both cracking and hydrogenation reactions [56]. However, it's crucial to address the limitations of these catalysts. Acidic catalysts, while effective in cracking carbon-carbon bonds, are susceptible to rapid deactivation due to the high nitrogen content in bitumen. This compromises their economic

viability for large-scale operations. Furthermore, catalyst deactivation due to coking, sintering, or poisoning by metals remains a significant challenge. Ongoing research is focused on the development of more robust catalysts that can operate under milder conditions and are resistant to deactivation. Such innovations are anticipated to significantly reduce the energy consumption and overall cost of the bitumen upgrading process.

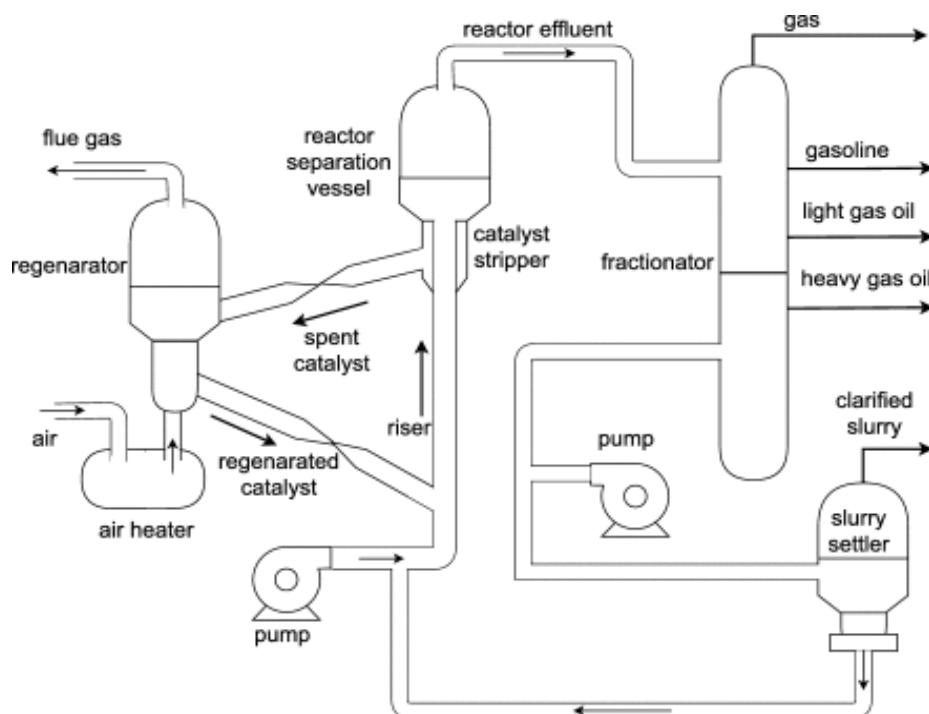


Figure 2.3: Process Flow Diagram of a typical industrial Catalytic Cracking Unit, recreated from Zhao et al. [51].

2.4 Hydro-Cracking

2.4.1 Direct Use of Hydrogen Gas

Hydrocracking is a process that uses hydrogen molecules (whether directly or indirectly) to break down heavy bitumen into lighter, more valuable fractions. The process combines heat, pressure, and hydrogen gas in the presence of a catalyst to increase the hydrogen-to-carbon ratio, reducing the viscosity and sulfur content of bitumen. Typically metal-catalyzed, hydrogen addition can be integrated with thermal or acid-catalyzed cracking to decrease the boiling point distribution of the feed [33]. The conversion is predominantly due to the thermal cracking of large molecules in the

feed, supplemented by sulfur removal and hydrogenation of aromatic rings. Despite its efficiency, the cost of using pure H₂ in the gas form is not justified, and at the same time, it is not feasible to produce H₂ gas in large quantities at the bitumen production sites which are normally remote. Alternatively, some indirect sources of hydrogen molecules are proposed, for instance, the utilization of H-donating species such as methane gas or an organic liquid H donor such as Tetralin-like compounds. Novel catalysts are actively studied in literature to be able to produce H free radicals from the methane gas and make it react with bitumen to generate an enhanced upgraded oil [13].

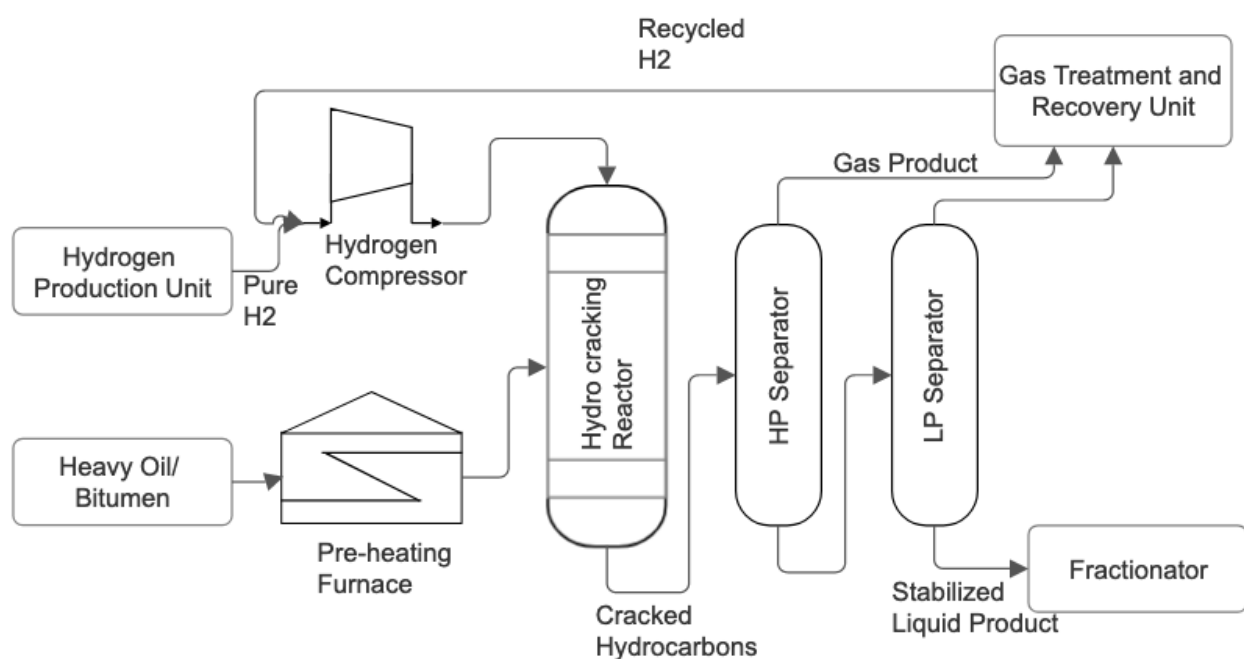


Figure 2.4: Process Flow Diagram of a typical Hydrocracking Unit, recreated by thesis Author.

2.4.2 Methane as a H Donor

Methane presents a viable alternative to pure hydrogen gas in hydrocracking. Effective utilization of methane as a hydrogen donor depends on developing catalyst systems capable of breaking the C-H bond of methane molecules, thereby generating reactive methyl radicals. This process, known as methano-treating, necessitates catalysts that can lower the activation energy for methane and facilitate C-H bond cleavage under less severe conditions [57]. However, challenges like the high

cost and complex regeneration of catalysts, including rare metals and zeolites, pose significant hurdles.

2.4.3 Water as a Hydrogen Donor

Water has emerged as a potential hydrogen source in hydrocracking, primarily through high-temperature gasification reactions. This approach, sometimes termed “aqua-conversion”, represents an advanced form of visbreaking aimed at significantly reducing the viscosity and density of viscous feedstocks [58]. Catalytic systems play a crucial role in enabling hydrogen transfer from water to the residue under visbreaking conditions. While this method offers environmental benefits and potential cost-effectiveness, it demands specific catalyst properties and often requires high temperatures and pressures, making the process energy-intensive [56], [59].

2.4.4 Organic Liquids as Hydrogen Donor

Tetralin, a hydrogen-rich cyclic compound, has gained much attention as an effective hydrogen donor in hydrocracking. Its advantages include high hydrogen content, stability, and compatibility with various catalysts. Several studies have shown that hydrogen donors can significantly reduce the molecular weight of heavy oil macromolecules [60]–[62]. In catalytic upgrading reactions, they play a vital role in transferring hydrogen to these structures, enhancing the quality of the resultant crude oil and reducing coking risk [63]. Moreover, tetralin has been found to improve the catalyst performance, resulting in a significant increase in the API gravity of the upgraded oil over that achieved with conventional heating methods [64]. Despite these benefits, challenges such as catalyst deactivation and the high cost of tetralin remain significant considerations.

However, hydrocracking remains a critical process in bitumen upgrading, offering a path to transform dense and heavy feedstocks into lighter, more valuable products. Whether employing hydrogen gas, methane, water, or organic liquids as hydrogen donors, each approach comes with its own set of advantages and challenges. The choice of method depends on a myriad of factors including cost, availability, environmental impact, and logistical considerations. As the industry continues to evolve, these hydrocracking techniques stand at the forefront of innovation, promising to enhance the efficiency, sustainability, and economic viability of bitumen processing.

2.5 Asphaltene Removal

Solvent deasphalting (SDA) is a process that uses light paraffinic solvents for liquid extraction while rejecting the heavier asphaltene fraction, offering an alternative approach to bitumen upgrading without creating unwanted olefins [65]. The low-asphaltene product exhibits reduced density, viscosity, and contaminants, making it a cleaner output, while the high-asphaltene product concentrates the feed's impurities and is often used as a cheap fuel or as a feed for asphalt production. Solvents like propane, butane, pentane, and light naphtha are employed in SDA, and the choice of solvent is crucial for determining the purity and yield of deasphalted oil (DAO). Higher molecular weight solvents give a better yield but also introduce more contaminants. SDA operates under less severe conditions compared to coking, resulting in less conversion of refractory carbon but at lower operational costs. The degree of this extraction is primarily dictated by the solvent-to-bitumen ratio [65]. Figure 2.5 represents a process flow diagram of the solvent deasphalting process. While this method has the advantage of not producing olefins, it poses a trade-off between yield and product quality. Specifically, higher yields of deasphalted oil result in less selective removal of heteroatoms like sulfur. However, there is a crucial limitation of SDA: it can only meet pipeline specifications if a large fraction of bitumen is rejected. The yield and purity trade-off in SDA is clear, showing that an increase in DAO yield is accompanied by a rise in contaminant levels. SDA could theoretically be coupled with thermal cracking for partial upgrading, the technology is deemed attractive especially if the byproduct of the process (asphaltenes) is used as a feedstock for carbon fiber synthesis. Zachariah and De Klerk's study [12] on combining SDA and visbreaking showed that both SDA-Vis and Vis-SDA sequences improve bitumen fluidity for pipeline transport. The SDA-Vis sequence had a slightly higher liquid yield, while Vis-SDA produced oil with a higher H/C ratio.

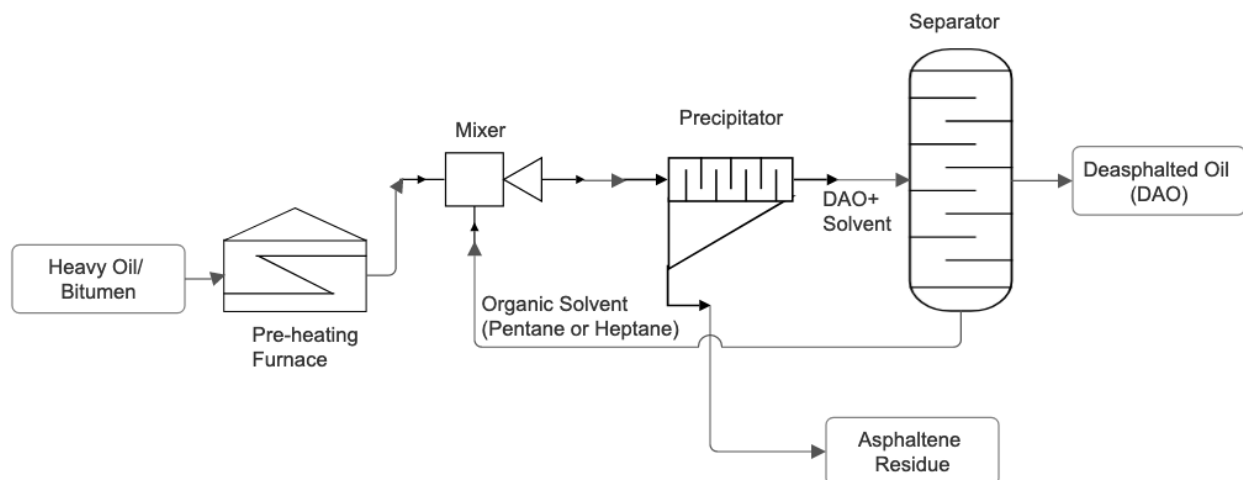


Figure 2.5: Process flow diagram of a typical Solvent Deasphalting unit, recreated by thesis Author.

2.6 Emerging technologies

Recent advancements in the field of bitumen and heavy oil upgrading are focusing on improving process efficiency, reducing environmental impact, and enhancing product quality. Some of these emerging technologies are:

a) Cavitation:

Among the emerging innovations in the field of bitumen upgrading, cavitation processing is gaining attention as an environmentally friendly and unique method for treating viscous oils like bitumen. Cavitation is the process where bubbles form, grow, and then collapse or implode in a liquid, a phenomenon that can be initiated by pressure changes either through ultrasound waves (acoustic cavitation) or through changes in the fluid velocity (hydrodynamic cavitation) [66]. When these bubbles collapse, they create small hot spots with extremely high temperatures and pressures, suitable for initiating chemical reactions without the need for external heating [44]. Figure 2.6 represents the main differences in setup between the hydrodynamic and acoustic cavitation processes.

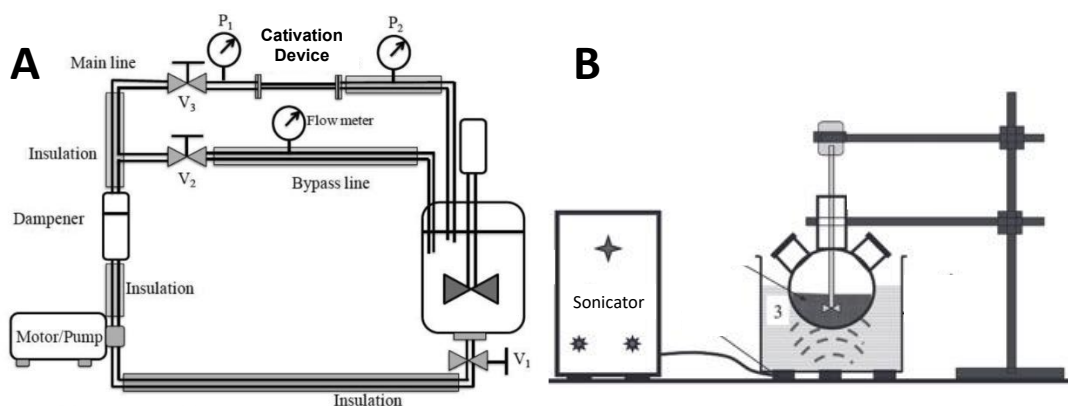


Figure 2.6: Schematic diagram of the process of A) hydrodynamic cavitation and B) acoustic cavitation adapted from Sawarkar [66].

The effectiveness of cavitation in altering the structural properties of heavy bitumen fractions has sparked considerable interest. For instance, a study by Askarian et al. [67] tested the upgrading of heavy fuel oil from an Iranian refinery using a hydrodynamic cavitation setup, with experiments conducted at 80°C, atmospheric pressure, and within 10–15 minutes. The findings revealed that adding 2% volume of gasoline as a hydrogen donor into the heavy oil cavitation upgrading process (HCUP) could reduce the oil's viscosity by about 33%. Furthermore, through several stages of HCUP, there was a 6.5% volume increase in diesel cuts and a 2.9° increase in API gravity, while extra heavy cuts and viscosity decreased by 20% volume and 84%, respectively. On the other hand, acoustic cavitation was also proven effective, as the study by Mohapatra and Kirpalani [68] has shown that the optimal conditions for the acoustic cavitation were at a sonication frequency of 574 kHz with a 50% power input, which was able to effectively reducing both the asphaltene content and viscosity of the treated material by up to 30%, thereby enhancing its fluidity and transportability [44]. A summary of the results of all the conditions investigated in this study is shown in Figure 2.7.

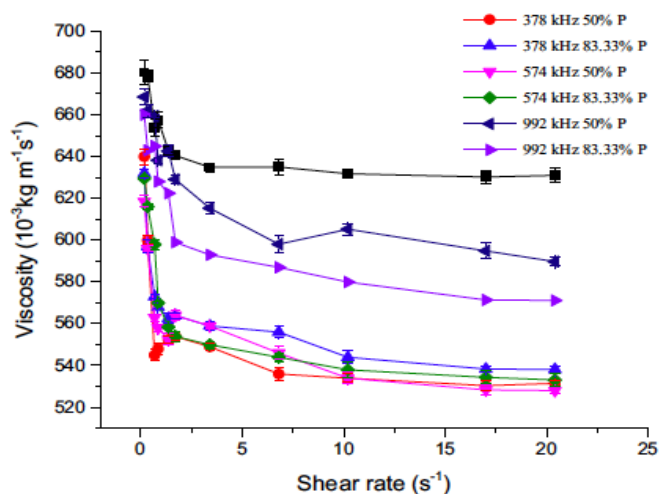


Figure 2.6: The changes in the viscosity of the upgraded oil at various power and sonication frequencies obtained from Mohapatra and Kirpalani [68].

Further studies have delved deeper into the impact of varying sonication conditions on the characteristics of bitumen, particularly focusing on its elemental composition and metal content. A notable finding from these studies is the decrease in the hydrogen-to-carbon (H/C) ratio in sonicated bitumen, which indicates a shift towards a higher proportion of aromatic hydrogen. This shift suggests a structural change in the bitumen, with a reduction in aliphatic hydrocarbons and an increase in aromatic compounds. Additionally, sonication has been associated with a reduction in metal content within the bitumen, which is beneficial for refining processes, as metals can catalyze undesirable reactions and wear out processing equipment [68]. The decrease in metal content, particularly vanadium and nickel, which are common in heavy oils and bitumen, could potentially reduce the need for extensive metal removal processes in refineries, further underscoring the environmental and economic advantages of cavitation processing. Moreover, the changes in asphaltene and resin fractions due to cavitation have implications for the downstream processing of bitumen, including improved catalytic cracking efficiency and reduced fouling in heat exchangers and pipelines [69]. Recent advancements in cavitation technology have explored the synergistic effects of combining cavitation with chemical additives or catalysts to enhance bitumen upgrading further. These studies suggest that the presence of certain catalysts during sonication can facilitate more targeted chemical reactions, leading to an even greater reduction in viscosity and an increase in the yield of more valuable hydrocarbon fractions [70]. These findings

highlight the potential of cavitation processing as an eco-friendly and effective approach for upgrading viscous feedstocks.

b) Chemical Surfactants

An alternative strategy for upgrading bitumen and heavy oil involves the use of chemical additives, such as surfactants, to improve the upgrading and the separation processes' efficiency. Surfactants are particularly noteworthy because they can reduce interfacial tension and enhance oil mobility [71]. This makes the upgrading process not only more efficient but also environmentally friendly, an increasingly important consideration given rising environmental regulations and societal expectations. Surfactants offer a customizable solution, tailored to address specific challenges encountered in bitumen and heavy oil upgrading like emulsion stability, viscosity reduction, and desulfurization. For example, anionic surfactants have proven effective in breaking water-in-oil emulsions, a recurring issue in bitumen extraction [72]. Another advantage is that surfactants can be synthesized from renewable resources, adding a sustainability dimension to this approach. Their versatility also allows for application in both in-situ and ex-situ upgrading processes, providing broad operational flexibility.

Numerous studies have shown that surfactants can enhance the performance of fluids injected for heavy oil and bitumen extraction. Molecular dynamics simulations have indicated that ionic surfactants can effectively disperse most of the asphaltene molecules within bitumen [72]. Cationic surfactants have also been found to notably influence bitumen's viscosity and asphaltene nanostructure, particularly under conditions of thermal partial upgrading [73]. Recent research has explored the synergistic effects of using surfactants in combination with other upgrading techniques like microwave irradiation or catalytic cracking. These hybrid approaches have shown significant improvements in upgrading efficiency, yield, and product quality. For instance, combining surfactants with activated carbon-assisted microwave irradiation significantly reduces the viscosity of Canadian bitumen by up to 60% while maintaining high yields of valuable fractions [74]. Despite these promising findings, the commercial implementation of surfactant-assisted upgrading is still in its early stages. This is mainly due to the limited scope of studies addressing the economic feasibility, long-term stability, and environmental impact of these surfactant

formulations. Therefore, there is a pressing need for multidisciplinary research that goes beyond understanding the basic mechanisms of surfactants to assess their scalability and sustainability.

c) Microwave-Assisted Upgrading

Microwave-assisted upgrading is a process that utilizes microwave radiation for selective heating and decomposition of heavy hydrocarbons, this process offers benefits such as lower energy consumption and reduced by-product formation. It efficiently initiates the breakdown of heavy hydrocarbons and reduces asphaltene and metal content. When used with catalysts like silicon carbide or nickel nanoparticles, microwave-assisted upgrading shows potential for efficient treatment of viscous feedstocks [75]. However, its scalability and economic viability still need further research optimization. A recent study by our group [76] investigated a method to partially upgrade bitumen using microwave irradiation in conjunction with carbon-based susceptors. This technique marks a significant departure from traditional methods, achieving a remarkable 96% reduction in viscosity at considerably lower temperatures (150-200 °C) and with minimal carbon additive (0.1 wt%). Notably, the process enhances the bitumen quality by increasing lighter components and reducing heavy hydrocarbons, as revealed by SARA analysis. Furthermore, microwave heating has been explored for hydrodesulfurization (HDS) reactions, often utilizing transition metals and molecular hydrogen, in a similar manner to conventional HDS processes. In literature, it was proven that significant sulfur removal from the hydrocracked pitch of Athabasca bitumen using microwave energy with metal hydride catalysts, notably achieving a 69% reduction with a magnesium-nickel hydride catalyst under specific conditions [77]. Further experimentation revealed iron and copper as effective catalysts for sulfur removal. For instance, Jackson and Soveran [78] investigated the desulfurization of heavy crude oil using microwave energy, achieving a 65% sulfur reduction under optimal conditions by incorporating activated carbon to enhance the dielectric properties, aligning the product with pipeline standards without dilution.

In addition to that, a couple of studies conducted by Nasri [75][79] investigated the upgrading of vacuum distillation residue from Tehran Oil Refinery, Iran, using microwave technology, focusing on how various parameters affect temperature, viscosity, API gravity, and asphaltene content. The key findings of these studies revealed that iron was the most effective catalyst. Key factors positively influencing the upgrading process were power level, activated carbon, iron catalyst, and

process time. An optimal 3 wt% NaBH₄ was identified, while the desulfurization agent did not positively affect the upgrade. Under optimal conditions (100% power level, 20 wt% Fe catalyst, 20 wt% activated carbon, 3 wt% NaBH₄, and 1-hour process time), there was a significant reduction in asphaltene content by 94.22%, a decrease in viscosity by 99.53%, and an increase in API gravity by 88.56%. Moreover, another similar study conducted by Gharibshahi et al. [80] explored how different forms of Fe₃O₄ nanocatalysts impact in-situ heavy oil upgrading when exposed to microwave radiation. The concentration of nanoparticles at 0.5 wt% had the most significant influence on lowering oil viscosity and increasing API gravity. Enhancing microwave power from 400 W to 1200 W improved all three system responses (viscosity, API gravity, and oil temperature). The optimal conditions for the most substantial reduction in crude oil viscosity were identified as 0.5 wt% Fe₃O₄-carbon nanotube catalyst exposure for 8 min at 400 W. The study concluded that microwave radiation not only lightened the oil but also decreased its sulfur content by 16.6%. A summary of the main findings of this study is shown in Figure 2.8.

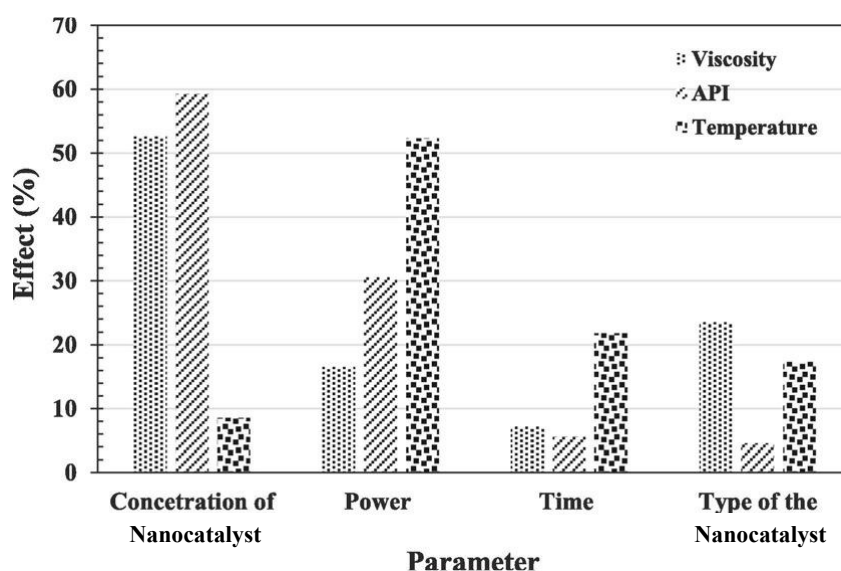


Figure 2.6: The effect of the microwave upgrading process parameters on the viscosity and density reduction efficiency adapted from Gharibshahi et al. [80].

The integration of microwave technology in bitumen upgrading not only promises substantial energy savings and environmental benefits due to its lower operating temperatures and efficiency but also paves the way for cost reductions in bitumen transportation by decreasing the need for diluents. The literature's findings offer a compelling, eco-friendly alternative for bitumen

upgrading, potentially revolutionizing practices in the oil and gas industry with its practicality and efficiency.

d) Ionic Liquids

There is a new approach that involves using ionic liquids for more efficient and environmentally friendly extraction and upgrading processes. The main advantage of this process is the reduced use of harsh chemicals and lower temperatures required as compared with other conventional processes. A representation of how the ionic liquids are implemented in an upgrading facility is shown in Figure 2.9. Ionic liquids, particularly imidazolium-based variants, demonstrate high selectivity in removing sulfur-containing molecules [81]. They are suitable for polishing steps in low-sulfur distillates but face challenges in bulk desulfurization due to sensitivity to air and moisture and variability in effectiveness based on anion size. They are more suitable for polishing steps in low-sulfur distillates rather than bulk desulfurization of high-density materials like bitumen [13].

Traditionally, asphaltene deposition is managed using aromatic solvents or surfactants; however, their effectiveness is limited when it comes to higher molecular weight asphaltenes. This is where ionic liquids come into play, emerging as a more effective and eco-friendly option for dispersing asphaltenes in crude oil. Studies by Atta et al. [82] have shown that synthesized ionic liquids, such as 1-allyl-3-methylimidazolium abetate and others, act actively as asphaltene dispersants. They work through ionic interaction and charge transfer, demonstrating a more active interaction with asphaltenes compared to other components in the ionic liquids. Boukherissa et al. [83] further explored the nature of ionic liquids as asphaltene dispersants. The study found that the boronic acid moiety and alkyl chain in the ionic liquids play a key role in controlling asphaltene deposition and aggregation. Similarly, Zheng et al.'s [84] research on 16 different ionic liquids provided insights into their ability to solubilize asphaltenes, with changes observed in the elemental composition and physical properties of the recovered asphaltenes. For controlling asphaltene precipitation, imidazolium-based ionic liquids like 1-butyl-3-methylimidazolium chloride have been tested, showing promising results in dispersing asphaltenes in solutions [85]. This finding underscores the potential for ionic liquids to be used in bitumen upgrading applications.

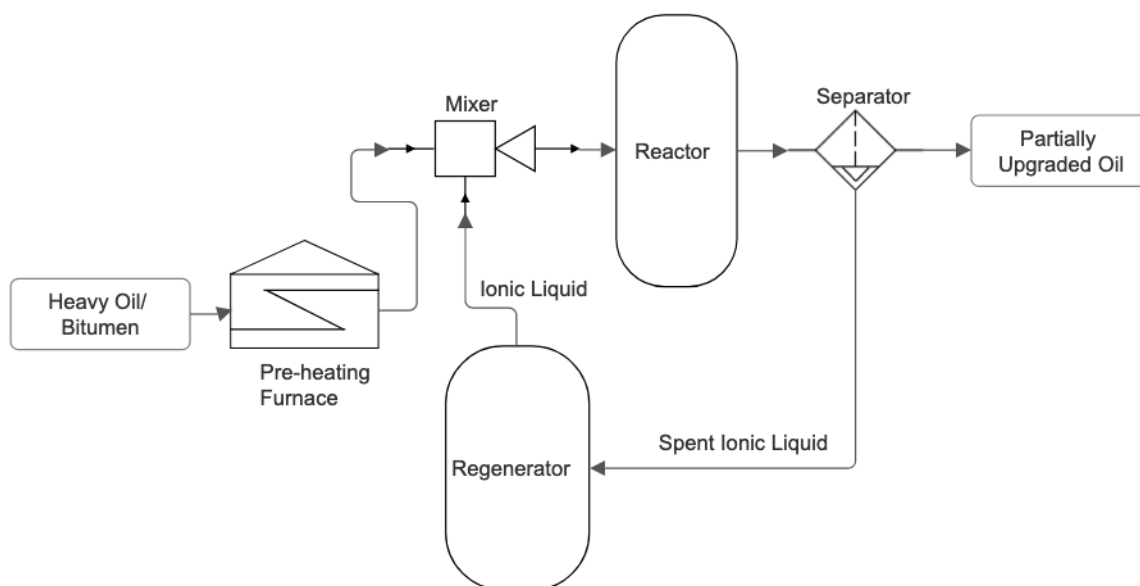


Figure 2.6: Process Flow Diagram of a typical ionic liquids upgrading unit, recreated by thesis Author.

Chapter 3 – Challenges and Opportunities in Bitumen Upgrading

3 Environmental and Economic Aspects of Bitumen Upgrading

In this intricate world of bitumen upgrading, we find ourselves navigating a delicate balance between environmental sustainability and the escalating global demand for energy. The current routes employed in Canada prior to bitumen transportation to the refineries are either done through fully upgrading bitumen to SCO or by diluting it to dilbit with significant amounts of diluents. The process of fully upgrading bitumen is inherently energy-intensive, and with this comes a significant increase in greenhouse gas emissions, a matter that casts a long shadow over ecological and environmental concerns. The main environmental challenge lies in the high energy demands of the upgrading processes, which not only lead to increased carbon emissions but also necessitate substantial water usage and complex waste management strategies. To combat these environmental impacts, there's a growing shift towards exploring more energy-efficient technologies and integrating carbon capture and storage methods. In a recent study, it was found that refining raw bitumen that was directly extracted in a typical refinery consumes significantly more energy (68.5% more) than refining synthetic crude oil (SCO) [86].

On the other hand, Life Cycle Assessment (LCA) studies such as the one conducted by Soiket et al. [86] assessed the GHG emissions from transporting bitumen and upgraded oil, as well as returning diluent to the extraction site. The study found that returning diluent alone is the most emissions-intensive part that can result in almost six times the CO₂ emissions as compared to the upgraded oil due to the smaller pipeline size, causing more friction and energy loss. Transporting dilbit also was identified as more energy- and emissions-intensive than transporting the upgraded oil because of its higher viscosity and density. The study also confirms that as distance increases, so do energy consumption and emissions. A summary of this study's results is represented in Figure 3.1.

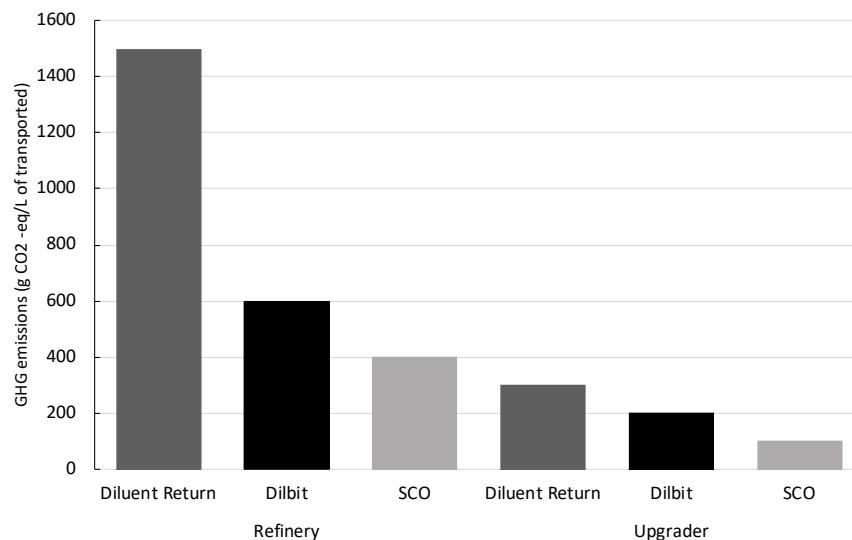


Figure 3.1: GHG emissions from the pipeline transportation of feed to the upgrader and refinery [86].

Similarly, the economic aspects of bitumen upgrading are just as complex and pivotal. The process of refining bitumen to produce synthetic crude oil (SCO) is both energy and emissions-intensive, escalating the overall greenhouse gas emissions. This aspect, coupled with the high costs associated with the purchase of diluents and transportation logistics, adds a significant financial burden to the supply chain. For instance, it was found that the diluent and transportation costs contribute to about 30% of the supply cost. This cost includes the purchase of diluent and the pipeline tariffs to transport the dilbit from Alberta to the US [87]. Moreover, the operational costs of the full upgraders, heavily influenced by the high cost of hydrogen production – a technology still in its nascent stage – represent a substantial part of the total expenses. In a simulation by the GAMS modeling system, it was proven in a recent study that hydrogen consumption represents roughly 47% of the total annual cost; which denotes the heavy burden of the hydrogen production unit over the upgrading process cost [88]. Adding to this complexity is the dynamic nature of global oil prices, which significantly impacts the economic viability of upgrading technologies. For instance, the Canadian Energy Research Institute (CERI) conducted a cost-benefit analysis revealing the projected economics of the greenfield refinery projects, underscoring their net social benefits against the backdrop of fluctuating oil prices. The cost-benefit analysis results suggested that a greenfield commercial refinery project might be net socially beneficial across a typical discount rate range (13-15%) for the refinery given that if and only if the average West Texas

Intermediate (WTI) price does not drop below \$85 over the life of the project [89]. However, the current West Texas Intermediate (WTI) price in early 2024 is around \$74-75 [90], which means that constructing a full upgrading unit might not be economically feasible. In the face of these environmental and economic challenges, the bitumen industry is pressed to innovate and adapt. This involves not only addressing the complexities in extraction and upgrading processes, particularly for heavy and extra-heavy oils but also aligning economic gains with sustainability goals.

3.2 The Potential of Partial Upgrading

Partial upgrading is an emerging technology that transforms bitumen into a substance that resembles medium-heavy crude, which is more easily transportable and incurs lower costs than fully upgraded products. Crucially, it also produces significantly lower greenhouse gas (GHG) emissions. This method is not just economically viable but also expected to yield substantial benefits in terms of employment, labor income, exports, and government revenue. Partial upgrading is defined as a process that combines various bitumen processing steps with reduced diluent addition to meet pipeline transport specifications [22]. The key goal is to reduce the viscosity and density of the oil, thus diminishing the need for diluents and creating an intermediate transportable fuel at a lower cost than dilution or full upgrading.

Economically, partial upgrading is attractive because its capital costs are estimated to be nearly half of those required for a full upgrading plant [22]. Additionally, operational costs are considerably lower, primarily due to the exclusion of hydrogen as a reactant, which removes significant costs and operational complexities associated with hydrogen production. Furthermore, hydrogen usage in full upgrading processes greatly impacts ancillary technologies, especially sulfur treatment, as hydrogenation releases sulfur in the form of hydrogen sulfide (H_2S). A complete comparison between the full upgrader and the partial upgrader is presented in Table 3.1.

Table 3.1: Comparison between Full and Partial Upgrading approaches.

Aspect	Partial Upgrading	Full Upgrading
Objective	Moderately improve quality for easier transport and limited refinery intake.	Convert to synthetic crude oil for wide refinery intake.
API Gravity	Increases but usually not to the same extent as full upgrading.	Significantly increases, often to levels similar to light crudes.
Sulfur & Nitrogen Content	May partially reduce.	Typically removes a high percentage.
Complexity	Generally simpler and less capital-intensive.	More complex and higher capital and operating expenditure.
Products	Partially upgraded bitumen may still require further processing.	Produces synthetic crude that is almost a finished product.
Technologies	Thermal cracking, solvent deasphalting, mild hydrotreating.	Delayed coking, hydrocracking, catalytic cracking.
Diluent Requirement	Reduces but may not eliminate the need for diluents.	Eliminates the need for diluents.

The concept of partial upgrading holds significant promise, but its practical implementation on an industrial scale remains a challenge that requires further research and demonstration. While the underlying principles are rooted in the established full upgrading techniques, adapting these methods for the sole purpose of enhancing bitumen properties for pipeline transportation is yet to be achieved at an industrial scale. Moreover, the implications of processing partially upgraded bitumen at refineries, as opposed to traditionally diluted bitumen, need thorough examination. A key focus of ongoing research is to analyze partial upgrading techniques in terms of liquid product yields, energy utilization, and greenhouse gas emissions, and to compare them with conventional full upgrading and diluent usage. Figure 3.2 presents a comparison of full and partial bitumen upgrading processes, outlining the distinct features and steps involved in each. While both processes start with bitumen blended with diluents, full upgrading is a comprehensive, multi-stage process conducted by specialized upgraders. It involves front-end separation (atmospheric and vacuum distillation units), cracking conversion, and hydroprocessing units to produce oil comparable to conventional crude. Additionally, supporting processes like sulfur treatment, hydrogen production, and water treatment add complexity and cost. Despite its challenges, full upgrading broadens the market for the upgraded product. Partial upgrading, in contrast, represents a balanced approach between dilution and full upgrading. Its primary goal is to meet pipeline specifications at a reduced cost, focusing on reducing oil viscosity and density to minimize diluent requirements. The process is generally less complex, avoiding the complexities of hydrogen production and sulfur treatment. Key technical strategies in partial upgrading include cracking

processes and possibly solvent deasphalting as a secondary unit. Gases produced during upgrading often require cleanup, including sulfur removal, and additional treatment might be needed to remove olefins and meet pipeline specifications. Ultimately, partial upgrading navigates a balance between technical feasibility and economic viability. It stands as a potentially cost-effective alternative to full upgrading, although with its set of challenges. The ongoing research aims to optimize this balance, rendering partial upgrading a feasible and sustainable option in bitumen processing.

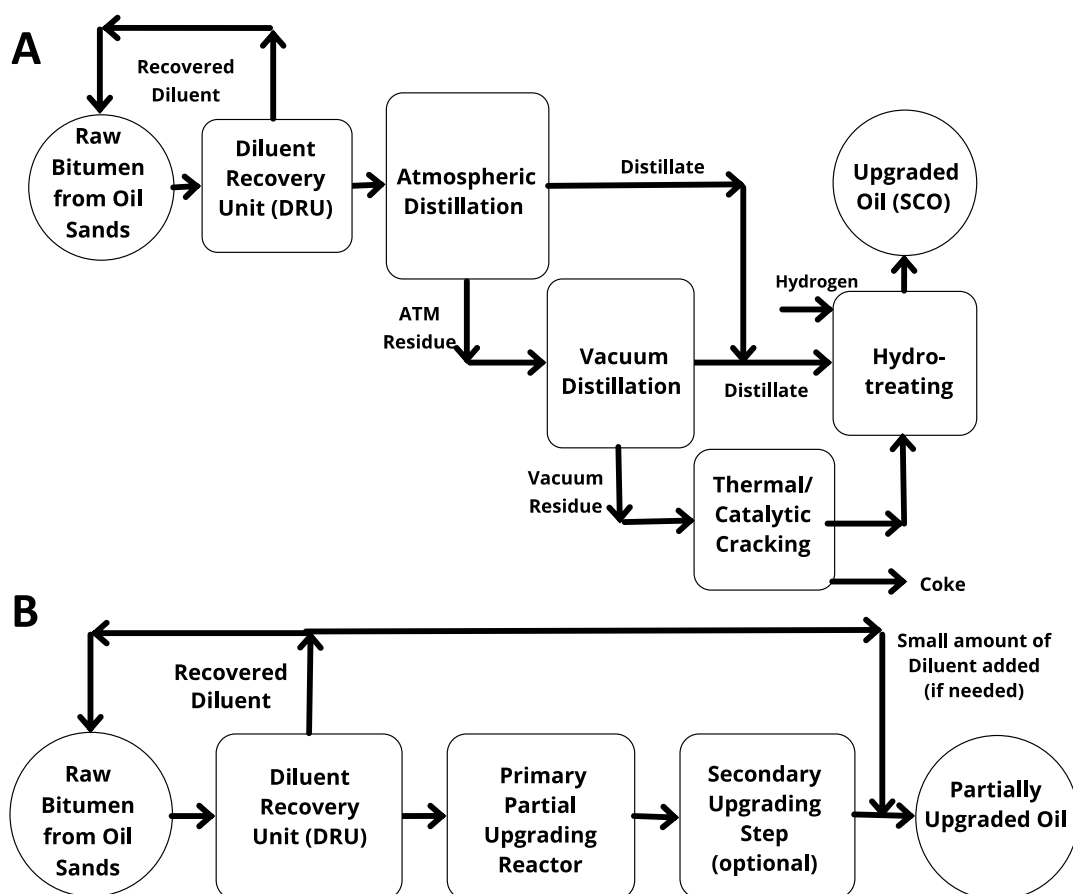


Figure 3.2: Block flow diagrams for bitumen A) Full Upgrading Plant and B) Partial Upgrading Plant.

3.3 Industrial Examples and Case Studies for Partial Upgrading

The exploration of partial upgrading technologies on the industrial level has led to a range of innovative case studies, each showcasing unique approaches and outcomes. These case studies of technologies that are currently being investigated and optimized by some oil companies exemplify

the technological strides being made in the sector, highlighting the potential benefits and challenges faced in the pursuit of more efficient and environmentally friendly processes for handling heavy crude oil and bitumen.

Case 1: FluidOil's Viscositor Heavy to Light (VHTL) Process:

FluidOil's VHTL process stands out as a novel implementation of thermal cracking. Using a fluidized bed with circulating sand as the heating medium, it rapidly and efficiently cracks heavy crude oil or bitumen at high temperatures [91]. The technology also offers operational flexibility, allowing for adjustments in parameters to yield different end-products based on market demand. Its scalability makes it suitable for both small and large-scale operations. Despite these advantages, VHTL faces challenges such as a high greenhouse gas (GHG) footprint, which makes it less attractive from an environmental standpoint.

Case 2. Bayshore Petroleum's Cold Catalytic Cracking (CCC):

Bayshore Petroleum introduces the Cold Catalytic Cracking “CCC” technology, which introduces an innovative approach to upgrading, functioning under ambient pressures and below 450°C temperatures [92]. The process employs a unique liquid catalyst crucial for cracking complex hydrocarbons, notably avoiding the use of water and hydrogen. CCC focuses on transforming asphaltene, resins, and aromatics into valuable mid-distillate products but also produces a substantial amount of coke as a by-product.

Case 3. Husky's Diluent Reduction (HDR) Technology:

Husky's HDR technology is a pioneering venture in hydrocracking, utilizing hydrogen donor solvents instead of external hydrogen. By employing Synthetic Crude Oil (SCO) as a hydrogen donor in a mild thermal cracking process, it significantly reduces the need for diluents in transport [93]. This process can potentially reduce up to 85% of the condensate-based diluent, increasing bitumen pipeline capacity by an impressive 60%. Upon commercialization, HDR could mitigate up to 5.1 million tonnes of CO₂ emissions annually per million barrels of processed bitumen [93]. A Greenhouse Gas (GHG) life cycle analysis has further validated the environmental potential of this technology, confirming a GHG reduction of 14 kg per barrel of oil as compared to the traditional hydrocracking technologies.

Case 4. MEG Energy's HI-Q Process:

Through integrating mild thermal cracking and solvent deasphalting, MEG Energy's HI-Q process aims to optimize liquid yield while selectively separating asphaltenes. Despite facing challenges in reactor control and process specialization, a 10 BPD pilot plant trial successfully demonstrated high liquid yields from Athabasca bitumen, producing a product low in asphaltenes, TAN, and MCR [94].

Case 5. Value Creation Inc. (VCI) Technologies:

VCI's Advanced Deasphalting Cracking (ADC) and Clean Oil Cracking (COC) technologies mark significant progress in upgrading methods. ADC focuses on solvent-based separation of asphaltenes and their subsequent cracking into lighter, more valuable fractions. COC uses catalytic cracking techniques to further upgrade deasphalted oil, maximizing yields of lighter hydrocarbons like diesel and naphtha while reducing sulfur and nitrogen compounds [95]. These technologies offer operational flexibility and can be used either independently or in combination.

Case 6. Fractal Systems' JetShear and Enhanced JetShear Technologies:

Fractal Systems' JetShear and Enhanced JetShear employ hydrodynamic cavitation and thermal energy, showing effectiveness in diluent displacement and Total Acid Number reduction. Enhanced JetShear goes beyond these benchmarks, improving product quality while also reducing diluent requirements by an impressive 50-60%. The upgraded product from Enhanced JetShear even achieves TAN levels below 1 mg KOH/g and maintains low olefinic content [96]. Despite these advances, both technologies encounter challenges related to product stability due to the remaining asphaltenes in the upgraded product. The market acceptance of JetShear and Enhanced JetShear will ultimately depend on their compatibility with existing refinery processing requirements. Preliminary data suggest that the greenhouse gas (GHG) emissions for these technologies are below industry baseline levels, adding to their environmental appeal.

3.4 Comparative Analysis of Current Partial Upgrading Technologies

This section offers a thorough framework for evaluating a range of technologies focused on the partial upgrading of bitumen. Technologies are evaluated according to Table 3.2, which categorizes them based on their current status and suitability for partial upgrading. This suitability is assessed as either "meets," "meets with diluent use," or "does not meet." The table also outlines the fundamental processing principles as well as whether olefin treatment is required. Table 3.3 goes further to assess the viability of these upgrading technologies. Criteria for this assessment include product liquid yield, the formation of coke as a byproduct, and the amount of diluent needed to meet pipeline specifications. Additionally, technologies are compared in terms of their cost, greenhouse gas (GHG) emissions, and potential drawbacks. All comparisons are made with reference to the delayed coking process, which serves as the baseline for evaluation. To estimate the amount of diluent required for the product of each compared process, the following equations are employed to meet pipeline specifications of 350 cSt and 940 kg/m³:

$$\log(\log(v_m + 0.7)) = w_1 * \log(\log(v_1 + 0.7)) + w_2 * \log(\log(v_2 + 0.7)) \dots \dots \dots (\text{Eq. 3.1})$$

$$\rho_m = \left[\frac{w_1}{\rho_1} + \frac{w_2}{\rho_2} \right]^{-1} \dots \dots \dots (\text{Eq. 3.2})$$

Here, v_1 is the viscosity of the upgraded bitumen, v_2 is the viscosity of the diluent, w_1 and w_2 are the weight fractions of bitumen and diluent respectively, v_m is the viscosity of the mixture (bitumen + diluent), and ρ_m is the density of the mixture. It should be noted that the density of the diluent is assumed to be 642 kg/m³, and its viscosity is taken to be 0.5 cP at 25°C, equivalent to 0.8 cSt.

Table 3.2: Comparison of the upgrading technologies based on their operation principles.

Upgrading Approach	Technology	Fit to Partial Upgrading of Bitumen (PUB)	Principles Behind Processing Technology	
			Primary Step with conditions	Olefin Treating Required
Thermal Cracking	Visbreaking	Meets - with diluent use	Mild thermal (400-450°C)	YES
	Delayed Coking	Exceeds	Coking (450-550°C+)	YES
	Fluid Coking	Exceeds	Coking (480-590°C+)	YES
Hydro Cracking	with Hydrogen gas	Meets	Mild thermal + Hydrogen + Catalyst	YES
	with Methane gas	Meets	Mild thermal + Methane + Catalyst	YES
	with water	Meets	Mild thermal using water in supercritical state	YES
	with Liquid H donor	Meets	Mild thermal + tetralin-like molecules + catalyst	YES
Catalytic Cracking	Water-soluble Catalysts	Meets	Mild thermal + Catalyst nanoparticles	YES
	Oil-soluble Catalysts			
	Acidic Catalysts			
Asphaltene Removal	Solvent Deasphalting	Meets - with diluent use	Mixing with additives/solvents	NO
Chemical Additives	Use of Surfactants	Meets - with diluent use	Mild thermal (400-450°C) + ionic Surfactants	YES
Mechanical Cavitation	Cavitation	Does not meet	Mechanical Cavitation	NO

Microwave Upgrading	Microwave Irradiation	Meets - with diluent use	Mild thermal with Activated Carbon	NO
Combination of Processes	Thermal + deasphalting	Meets	Mild thermal Cracking	YES
	Thermal + mechanical	Meets - with diluent use	Mild thermal Cracking	YES
	Thermal + catalyst solution	Meets	Thermal treatment in the presence of an organic H-donor and catalyst	YES

Efficiency metrics such as liquid yield, coke formation, and diluent requirements are key factors in assessing partial upgrading technologies as represented in Table 3.3. For instance, thermal cracking methods like visbreaking typically offer high liquid yields of around 90-95%, however, they do require diluents to satisfy both the pipeline viscosity and density requirements. On the other hand, hydrocracking technologies with hydrogen gas also yield high liquid returns, around 85%, without producing coke. Other methods like solvent deasphalting and surfactant-based approaches are promising in terms of yield but might still need some diluents to meet pipeline standards. Environmental considerations are also vital. Many technologies aim to function with greenhouse gas emissions below a given baseline, making them environmentally sound choices. Mechanical cavitation is noteworthy for its high liquid yield and low emissions. However, it still requires significant amounts of diluents which makes the process less economically favorable. Furthermore, hydrocracking with water is less environmentally friendly due to the high energy costs of maintaining water in a supercritical state.

On the economic front, visbreaking emerges as the most budget-friendly option in terms of capital costs, closely followed by solvent deasphalting. Delayed and fluid coking is at the other end of the spectrum, with the highest capital costs. Utility costs can rise with the severity of the visbreaking process, especially for additional sulfur recovery. In contrast, delayed coking has high utility costs but offsets this by eliminating the need for diluents. Costs for solvent deasphalting are influenced by design specifics, particularly the solvent-to-bitumen ratio. All these processes show a balance between capital costs, utility requirements, and yield loss, with coking methods being unique in their lack of diluent requirements. Finally, the technological complexity varies across these

methods. Thermal cracking methods are well-understood but bring their own set of challenges, such as high-temperature operations and coke handling. Hydrocracking involves catalysts and operates under high-pressure conditions, making it more complex yet scalable. Solvent deasphalting and surfactant-based methods are less complex but may need more research for scalability. Microwave-assisted and ionic liquid upgrading techniques are still in their early stages, requiring further study for scalability and process optimization.

Table 3.3: Comparison of the upgrading technologies based on their process viability.

Upgrading Approach	Technology	Liquid Yield (wt%)	Coke (wt%)	Viability of Technology			Process Drawbacks
				Approximate Diluent needed (vol %)	Cost	Environmental Basis (GHG)	
Thermal Cracking	Visbreaking	90-95%	~5%	13	Low	Low	Products may require hydrotreating, density of the product may still not satisfy the pipeline specs
	Delayed Coking	~70%	~10-15%	0	Medium	Moderate	Coke formation, olefinic products, and low liquid yields
	Fluid Coking	70-75%	~10-15%	0	Medium	High	Coke formation, olefinic products, and low liquid yields
Hydro Cracking	with Hydrogen	~85-90%	~5%	0	High	High	High costs to produce H ₂ and reactivation of catalysts which are usually expensive
	with Methane	~85-90%	~5%	0	High	High	
	with water	~85-90%	~5%	0	High	High	High energy cost to maintain water in supercritical form
	with Liquid H donor	~85-90%	~5%	0	Medium	Moderate	May require a significant amount of the H-donor liquids which may affect the bitumen yield and the overall cost
Catalytic Cracking	Water-soluble	~80-85%	~5-10%	0	Medium	Low	Catalyst separation and regeneration are required, also the required density for pipeline specs may not be met.
	Oil-soluble						

		Acidic Catalysts						
Asphaltene Removal	Solvent Deasphalting	~80%	0	14	Medium	Low	Cost of the additives and a good portion of the yield is lost as asphaltene	
Chemical Additives	Use of Surfactants	~90%	~5%	11	Low	Low	Like visbreaking drawback plus the cost of surfactants needs to be optimized	
Mechanical Cavitation	Cavitation	100%	0%	N/a	Low	Low	Cavitation on its own may not be sufficient as an upgrading method	
Microwave Upgrading	Microwave Irradiation	95%	~2-3%	20	Low	Low	Needs to be further investigated and optimized, still requires a significant amount of diluent	
Combination of Processes	Thermal + deasphalting	~85-95%	~2-5%	0	Medium-high	Moderate	Solvent recovery and management, complexity	
	Thermal + mechanical	~85-95%	~5-10%	10	Medium	Moderate	Mechanical wear and tear, olefinic products	
	(Thermal + catalyst solution)	~85-95%	~5%	0	Medium-high	Low	Catalyst management and regeneration may be an issue	

As a result of the detailed comparison in Tables 3.2 and 3.3, one can conclude that the ideal technologies for partial upgrading of bitumen are those that strike a balance. They should minimize overconversion, lower greenhouse gas (GHG) emissions, produce fewer low-value byproducts, and reduce the need for diluents to ultimately cut overall process costs. In light of these criteria, some technologies stand out. For instance, catalytic cracking processes that involve mild thermal cracking with dispersed catalysts show promise. These catalysts can be either water-soluble or oil-soluble, often forming part of an emulsion. Furthermore, hybrid approaches that combine two upgrading processes are particularly promising. One such approach is mild thermal cracking followed by fluid-mechanical manipulation to break down large molecules in bitumen. Another combines mild thermal cracking with partial asphaltene rejection, which produces a stable oil that can meet pipeline specifications with reduced or no need for diluents. A third approach involves mild thermal cracking paired with a renewable hydrogen donor in a catalyst solution, commonly

referred to as cold catalytic cracking. These technologies effectively address multiple challenges, making them strong contenders for efficient and sustainable partial upgrading of bitumen.

3.5 Economic Implications of the Partial Upgrading Techniques

Understanding the economic implications of bitumen upgrading techniques is crucial for evaluating their overall feasibility and potential for industry adoption. Therefore, in order to perform detailed economic analysis, the analysis should involve a thorough examination of both direct and indirect costs associated with various upgrading methods, alongside the potential return on investment (ROI) these technologies might offer.

Partial upgrading techniques entail expenses related to catalysts and additives, as well as operational costs primarily driven by energy consumption. Techniques that utilize catalysts like Fe-based nanocatalysts and/or Fe_3O_4 coated cenospheres require specialized materials, which can be expensive to produce or acquire. Similarly, microwave upgrading demands carbon-based susceptors, such as activated carbon or graphite, with costs varying significantly based on source and processing requirements. Furthermore, a significant indirect cost in bitumen upgrading is associated with the use of diluents, necessary to reduce the viscosity of bitumen to levels suitable for pipeline transportation. Methods that effectively reduce viscosity, like microwave upgrading and catalytic methods using Fe_3O_4 with hydrogen gas, can significantly decrease or even eliminate the need for these costly additives. This reduction not only offers potential savings on direct diluent costs but also on the expenses associated with blending and handling these additives. Moreover, by achieving viscosities near or below that of standard crude oil, these methods can substantially lower the energy required for pumping bitumen through pipelines.

As a result, the upcoming chapters of this thesis will be experimentally investigating innovative and novel techniques to attempt to fill some of the knowledge gaps in this field of research.

Chapter 4 - The effect of cationic surfactants on bitumen's viscosity and asphaltene nanostructure under thermal partial upgrading

4 Abstract

Bitumen extracted from oil sands is a highly viscous fluid; thus, its transportation via pipelines in its original form resembles a major challenge. Partial upgrading is a recently proposed approach that aims to reduce bitumen's viscosity to meet the pipeline specifications. To optimize the process and make it more cost-effective, a novel approach is proposed and researched in this work. Ionic surfactants were for the first time employed to promote thermal cracking reactions and dispersion of asphaltenes in bitumen at elevated upgrading temperatures. Three surfactants representing the cationic, non-ionic, and anionic charges were studied at the thermal upgrading conditions (360-400°C) at their optimal addition ratios to mimic the bitumen partial upgrading conditions. The results demonstrated that the cationic surfactant (DTAB) surpassed the other two surfactants and that with the addition of only 0.25wt% of it, it can effectively reduce the viscosity of bitumen by up to 60% more than the upgraded bitumen with no additives under the same upgrading temperature. The SARA analysis revealed that the contents of saturates and aromatics within the upgraded bitumen were also enhanced when DTAB was added. Moreover, the detailed asphaltene nano-structural analysis using XRD, HRTEM, and TGA revealed that the addition of the cationic surfactant (DTAB) resulted in an increased asphaltene nano-structural disorder, smaller polycyclic aromatic hydrocarbons size, and increased fringe curvature, as compared to the upgraded bitumen's asphaltene with no surfactants. Hence, the results have suggested that DTAB, a cheap and readily available ionic surfactant, can serve as a potential upgrading additive for designing partial upgrading procedures to produce upgraded bitumen with much less viscosity at lower upgrading temperatures. This upgrading technique will result in an upgraded bitumen that requires significantly reduced volumes of diluent for transportation.

4.1 Introduction

With the continuous increase in energy demand, the conventional oil resources will stand insufficient on their own to fuel the world and fill the energy gap. Hence, new unconventional resources of energy have to be exploited worldwide. Canada, for instance, has a vast amount of oil reserves, ranking it as the fourth-largest oil producer and exporter in the world [4]. Unconventional oil resources consist of heavy oil, extra-heavy oil, oil sand, tar sands, oil shale, and bitumen. Currently, more than half of the world's oil reserves (~53.3%) are in the form of unconventional oil reserves [105]. As a result, much attention has been directed towards the abundant yet inefficiently utilized petroleum resources such as oil sands and heavy “bitumen” oil. These unconventional resources present a much-under-utilized energy core, and with the expected increase in oil prices, their production and transportation present themselves as an increasingly economically viable solution. Oil sands are mainly defined as a mixture of sand, water, and bitumen that are known to be physically separable. Bitumen is made up of a highly complex mixture of large hydrocarbon molecules infused with up to 5% sulfur compounds by weight, and some minor heteroatoms impurities such as oxygen and nitrogen and metals (including vanadium, and nickel) [10], [19].

Bitumen is a highly viscous fluid, and its transportation resembles a significant challenge, especially since it has a dynamic viscosity somewhere between $2 \times 10^5 - 2 \times 10^6$ (mPa.s) or (cP) and a density of more than $1,000 \text{ kg/m}^3$ at atmospheric conditions [11]. Such high viscosities make transporting bitumen via pipelines to the refineries in their original state very difficult. The Canadian pipeline specifications require the oil to have a dynamic viscosity of 300 cP (or equivalently, the kinematic viscosity of 350 cSt) or less and a density of $\leq 940 \text{ kg/m}^3$ at the reference temperature of 7.5°C for winter [12]. Table 4.1 below shows a comparison between the different types of oil as compared with the required Canadian pipeline specifications.

Table 4.1: Canadian Pipeline specifications adapted from Gray [13].

Property	Pipeline specs	Athabasca bitumen	Diluted bitumen	Fully upgraded synthetic crude oil
Viscosity (cSt)	<350	1,000,000 (Average)	200-300	10
Density (kg/m³)	<940	>1000	920	850
API (°)	>19	>8	>20	>30

As a result of this limitation, there are currently two major strategies that are employed by producers to meet the pipeline specifications criteria to transport bitumen. These strategies are A) diluting bitumen with expensive diluents (condensate or light naphtha) or B) fully upgrading bitumen to synthetic crude oil using large upgrading and refining facilities [14]. However, both methods have revealed some major drawbacks in the past few years. For instance, when considering option A, the diluents used to transport bitumen to the US usually result in an extra production cost of \$14 per barrel of bitumen [15]. Also, about 33% of the pipeline capacity is lost due to the additional volume of the diluents [13]. Moreover, additional costs are needed for the final separation of the diluents from transported bitumen.

On the other hand, when considering option B, despite having four full upgraders currently operating in Alberta, the government has no intentions for any additional full upgraders because any investment in such plants is no longer cost-effective [16]. The full upgrading plants are usually facilitated with catalysts and hydrogen gas, which allows them to highly improve the quality of the oil, reducing its viscosity, sulfur and nitrogen contents, and any other heavy metal content [17], [18]. However, the cost of operation is high and yet the four full upgraders can only treat 35% of Alberta's bitumen before being sold to market. Another drawback of the full upgraders is that they lead to significant greenhouse gas (GHG) emissions during the refining process. The oil sands operations currently emit 70 Mega tonnes of GHG per year, accounting for about 8% of Canada's total GHG emissions [106]. Therefore, a new alternative must be implemented on an industrial scale to address the bitumen transportation demand and the older solutions' drawbacks. The new approach of bitumen partial upgrading manifests as a good alternative when compared to the full upgrading techniques. Partial upgrading seems to be a more efficient and cost-effective strategy that aims to reduce the intensity and cost of upgrading while producing bitumen that meets pipeline specifications. This technology not only will be more economically viable, but also will generate substantial gains in employment, labor income, exports, and government revenue. Partial upgrading brings bitumen to something resembling a medium-heavy crude that can be easily transportable at a lower cost per barrel than full upgrading while at the same time producing much lower GHG emissions [20].

While the idea of partial upgrading seems promising in principle, there is still a considerable need to demonstrate the viability of optimizing this technique. Against this background, the work

reported herein is to develop a new approach to partially upgrade bitumen to pipeline transportable crudes at a low cost and reduced GHG emissions.

One promising approach is to address bitumen's heaviest and most polar molecular fraction which is the asphaltene. Asphaltenes are defined as the fraction of oil that is insoluble in paraffin solvents (usually *n*-pentane or *n*-heptane) but soluble in aromatic solvents such as toluene or dichloromethane [26]. The asphaltene component is generally associated with forming a colloidal suspension of aggregates and this is one of the leading causes for the elevated viscosity of bitumen. As a result, the degree of association and dispersion of the aggregates is an important factor in the microstructure and mechanical behavior of bitumen. Asphaltenes are considered a major problem due to their tendency to associate and precipitate during oil production, upgrading, and refining. They reduce the oil flow and can even cause blockages during production and have severe drawbacks during the processing of heavy ends such as the tendency to form coke deposits in heat exchangers and reactors and to deactivate or poison catalysts [21].

Chemical surfactants are commonly used as dispersing agents for asphaltenes in crude oils to prevent their precipitation in pipelines during enhanced oil recovery (EOR). So, an interesting approach is proposed to investigate the effects of these surfactants at the operating conditions of bitumen partial upgrading. The strategy aims to modify the colloidal structure of bitumen to reduce the interactions between the asphaltene aggregates so that agglomeration is reduced. The addition of surfactants to oil for viscosity reduction purposes was recently reported in the literature [107], [108] but on a limited scope. In these studies, surfactants were tested for their abilities to de-asphalt or to promote asphaltene dispersion under atmospheric or mild conditions. It was noted that the surfactant molecules can progressively get attached to the available sites on asphaltene molecules/aggregates, occupying most of the available sites and sterically hindering the interactions between the asphaltene aggregates. The surfactant molecules can also cover some layers on asphaltene aggregates that provide steric stability, preventing them from aggregating into larger structures. Ortega et al. [107] found out that the addition of dodecyl-benzenesulfonic acid as a chemical surfactant was sufficient enough to significantly enhance the viscosity of the bitumen at 60°C (mild condition). Also, it was noted that there was a more significant reduction in the viscosity curves when the samples were thermally treated at temperatures around 170 °C. In another study, Kwon et al. [108] found that the use of surfactants with a short alkyl chain was the

best way to maximize the efficiency of asphaltene removal at atmospheric conditions. The viscosity of bitumen decreased by a factor of 6 times when it was compared with the cases in which surfactants were not used.

However, studies related to asphaltene cracking behavior in the presence of surfactants during high-temperature thermal upgrading ($>350^{\circ}\text{C}$) have not been documented in the literature. There is no clear correlation between the charge or concentration of the surfactant and its efficiency in asphaltene cracking and dispersion at high temperatures. This might be justified due to the fear of thermally decomposing the surfactants at elevated temperatures greater than 250°C . However, most surfactants, such as the ones chosen in this study, might be able to initiate some desirable free radical reactions at lower temperatures prior to their degradation [109], which means that even if the thermal upgrading was carried out at the elevated temperatures of $\sim 400^{\circ}\text{C}$, the effect of the surfactants in partial upgrading will remain a predominant factor. Any increase in temperature beyond 400°C would greatly reduce the influence of the surfactants, as most of them will be highly prone to decomposition. Therefore, the novel approach of studying the effect of the surfactant addition on the structure of asphaltene at the partial upgrading conditions between $360\text{-}400^{\circ}\text{C}$ is proposed. A series of anionic, cationic, and nonionic surfactants will be tested within bitumen and investigated through the thermal partial upgrading technique in a sealed autoclave reactor. In this study, surfactants will be preblended with bitumen at their optimum concentrations and tested at the elevated temperatures: 360°C , 380°C , 390°C , and 400°C to mimic the bitumen partial upgrading conditions and evaluate the effect of high thermal stress on the surfactant's ability to alter the asphaltene fraction and improve its rheological properties. It is important to note that temperatures greater than 400°C were ignored in this study because, in our preliminary experiments, it was noticed that upgrading bitumen at temperatures in the range of $400\text{-}500^{\circ}\text{C}$ tends to generate a noticeable amount of coke. Hence, temperatures above 400°C were greatly decreasing the liquid yield of the upgraded bitumen. $360\text{-}400^{\circ}\text{C}$ seems to be a more reasonable range that can significantly reduce the viscosity of bitumen while at the same time maximize the liquid yield of bitumen.

4.2 Experimental Methodology

4.2.1 Materials

a) Bitumen: Oil sand bitumen obtained from Alberta's Athabasca reservoirs was used as the main feedstock for the experimental analysis presented in this research work. Table 4.2 below represents the main physical properties of the bitumen used for this study. The viscosities of the samples were measured according to the ASTM D4402 standard using the ROTAVISC rotational viscometer (procured from IKA), a reproducibility of $\pm 1\%$, and a measuring range of 100 – 4,000,000 cP. The density measurements were obtained using a specific gravity hydrometer purchased from Fisher Scientific following the ASTM E100 standard. The SARA (Saturates, Aromatics, Resins, and Asphaltene) analysis was performed according to ASTM D2007-98 standard procedure and the average measurements of the original bitumen fractions are also reported in Table 4.2.

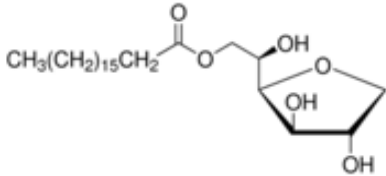
Table 4.2: Physical properties of the original bitumen of interest measured at room conditions.

	Properties	Measured values	Error Bar (+/-)
Physical properties	Viscosity (cP)	330,000	1%
	TAN (mgKOH/g)	4.32	0.1
	Density (kg/m ³)	1020	5
	API (°)	7.23	-
SARA Analysis	Saturates (wt%)	19	0.5
	Aromatics (wt%)	29	0.5
	Resins (wt%)	31	1
	Asphaltenes (wt%)	21	0.5

b) Surfactants:

All the surfactants (in solid form) that were tested were purchased from Fisher Scientific with purities > 97% and no further modifications were made to them. Their chemical structures are summarized in Table 4.3.

Table 4.3: List of surfactants of interest.

	Surfactant Name	Abbreviation	Type	Structure
1	Dodecyl trimethyl ammonium bromide	DTAB	Cationic	$\text{CH}_3(\text{CH}_2)_{10}\text{CH}_2-\overset{\text{CH}_3}{\underset{\text{CH}_3}{\text{N}^+}}-\text{CH}_3 \text{ Br}^-$
2	Span 60	Span 60	Non-ionic	
3	Sodium Dodecyl Sulfate	SDS	Anionic	$\text{CH}_3(\text{CH}_2)_{10}\text{CH}_2\text{O}-\overset{\text{O}}{\parallel}{\text{S}}-\text{ONa}$

1. Dodecyl trimethyl ammonium bromide:

DTAB is a cationic surfactant that has the molecular formula of $\text{CH}_3(\text{CH}_2)_{11}\text{N}(\text{CH}_3)_3\text{Br}$ [110]. This surfactant has been previously proven to promote oil recovery in petroleum reservoirs. The improvement in the oil recovery was due to the ability of the surfactants to (a) reduce the oil/water interfacial tension [111]; (b) generate foam in porous media [112] and (c) modify rock wettability so that it shifts toward water-wet conditions [113]. Furthermore, surfactants such as DTAB were proven by Kwon et al. [108] to greatly improve the bitumen properties through an effective deasphalting mechanism at low temperatures.

2. Span 60:

Span 60 is a nonionic surfactant which is also known as “sorbitan monostearate”, it has the molecular formula of $\text{C}_{24}\text{H}_{46}\text{O}_6$, and it has no net charge. Span 60 has proven its ability to induce the cracking reactions in favor of converting asphaltene and resins to smaller hydrocarbon molecules hence, improving the gas oil to resin ratios [114].

3. Sodium dodecyl sulfate:

Sodium dodecyl sulfate (SDS) belongs to a group of surfactants called alkyl sulfates, and it has the chemical formula of $\text{CH}_3(\text{CH}_2)_{11}\text{SO}_4\text{Na}$. SDS has a linear molecular structure that consists of twelve carbon atoms in the form of a hydrophobic chain attached to a negatively charged sulfate group [115]. Thus, SDS can significantly interact with asphaltene molecules at the interface between asphaltene molecules. Moreover, it can potentially reduce the π - π interactions between asphaltene molecules which are considered the main contributor to asphaltene stacking [116].

4.2.2 Sample Processing Method

The bitumen was preheated using hot water until it became flowable (oil temperature should be about 80 °C); then about 60 g of bitumen was added to the autoclave (Parr Bench Top Reactor of series 4590) that is shown in Appendix A-1. After that, the surfactant was added to bitumen and stirred at 300 rpm for 1 hour at 60°C to form a homogenous blend. The bitumen sample was then thermally treated at the preset temperatures (360-400°C) for 2 hours then was left to cool down to room temperature.

After each run, the upgraded bitumen was removed from the autoclave and its physical properties such as viscosity, density, and asphaltene content were measured. Later, the asphaltene fraction (insoluble in *n*-pentane) was extracted from the treated bitumen and subjected to detailed characterization tests.

4.2.3 Characterization Tests

1) Thermogravimetric analysis (TGA):

Thermogravimetric analysis was conducted on the liquid bitumen samples using the apparatus Pyris 1 TGA (Perkin-Elmer) under a nitrogen environment. Each run was conducted using ~10 mg of bitumen per run. During the TGA analysis, the samples were heated from 20°C to 600°C with a heating ramp of 30°C/min and N₂ flow rate of 30 ml/min.

2) X-ray diffraction (XRD):

The structural parameters of asphaltene particles were obtained by using the X-ray diffraction patterns within the range of 10–60° with a step size of 0.02°/step using the Rigaku DMax diffractometer. Before the analysis, a portion of the asphaltene sample was grounded for ~ 1 minute and then mounted with the help of ethanol as a solvent. The XRD results obtained were used to calculate La (diameter of the aromatic sheet), Lc (height of the stack of aromatic sheets), and d (layer distance between the aromatic sheets).

3) High-Resolution Transmission Electron Microscope (HRTEM):

The transmission electron microscope (Titan 80-300 LB) which is a high-resolution TEM that operates at 80 and 300 keV accelerating voltage with an ultimate lattice resolution of 0.24 nm was used to record the microstructural details of the upgraded asphaltene particles. After being ultrasonicated in ethanol for 10 minutes, the dried asphaltene samples were placed on a lacey carbon-coated, copper grid and the TEM images were obtained from different sites of the asphaltene samples.

4.3 Results and Discussion

4.3.1 Surfactant Effect on bitumen's Physical Properties

i) The effect of temperature on bitumen partial upgrading with no additives:

In the first step, bitumen was thermally upgraded at different temperatures within the range of 360–400°C with 10°C increment as described earlier in an autoclave reactor. This step will serve as a basis (control) to help compare the properties of the upgraded bitumen with and without the addition of surfactants. It was noticed that within the upgrading temperature range of interest, the liquid product yield of around 97~98% can be easily achieved without any significant coke formation. The SARA analysis was then performed on all the samples, and a summary of the obtained results is included in Table 4.4. The SARA analysis for the thermally upgraded bitumen samples suggests that, as the upgrading temperature increases from 360°C to 400°C, the fractions of asphaltenes and resins continuously decrease reaching their minimum at 400°C. At the same time, the fraction of aromatics readily increases with temperature, which suggests that the asphaltene and resins were primarily thermally cracked into aromatics. Rapid reduction of resin content to aromatics was also observed within the 380–390°C range, indicating that the resin

fraction was activated within this temperature range. Saturates were slightly decreasing with temperature, which might be due to some polymerization reactions that might convert them to aromatics. The rheology and physical properties of the original and thermally upgraded bitumen were also measured and compared in Table 4.5. The trends of those physical properties suggest that the thermal treatment is one of the effective means to reduce bitumen's viscosity. The viscosity of the original bitumen (measured at 25 °C) decreased from an initial value of 330,000 cP steadily with temperature, reaching a minimum value of 1,700 cP (for the upgraded bitumen at 400°C). Although similar trends were observed for the viscosity values measured at a lower temperature (7.5°C) that were mainly used to mimic the Canadian pipeline specification conditions, the lowest viscosity value observed at 400°C was 5,500 cP (measured at 7.5°C). This viscosity value that was achieved by thermally upgrading bitumen at 400°C on its own still stands way above the required criteria of 300 cP.

Table 4.4: SARA analysis for the upgraded bitumen at various temperatures.

Fractions	Original Bitumen	Bitumen	Bitumen	Bitumen	Bitumen	Error Bar (+/-)
		upgraded at 360°C	upgraded at 380°C	upgraded at 390°C	upgraded at 400°C	
Saturates (wt%)	18	20	20	20	19	0.5
Aromatics (wt%)	29	39	47	53	53	0.5
Resins (wt%)	30	23	19	14	10	1
Asphaltenes (wt%)	20	15	14	14	13	0.5

Table 4.5: Viscosity and density measurements for the upgraded bitumen at various temperatures.

Sample	Density (kg/m ³)	Viscosity (cP)		
		Measured @ 40°C	Measured @ 25°C	Measured @ 7.5°C
Original Bitumen	1020	200,000	330,000	N/A
Upgraded @ 360°C	1000	12,000	45,000	150,000
Upgraded @ 380°C	990	3,000	7,000	22,500
Upgraded @ 390°C	985	1,250	4,000	9,000
Upgraded @ 400°C	980	132	1,700	5,500

ii) The effect of surfactant addition to bitumen prior to thermal upgrading:

To determine the effect of surfactant on bitumen before conducting the thermal cracking reactions, various bitumen samples were premixed with an equal amount of the 3 different surfactants, in the form of solid powder, with different concentrations and charges. Physical properties such as viscosity, density, TAN, and SARA composition were measured for each sample accordingly. The results suggested that the viscosity and density measurements in addition to the SARA analysis were almost identical to the original bitumen samples. This means that the addition of small quantities of surfactants (up to 1wt%) on their own is not enough to alter any physical property within the original un-upgraded bitumen. Therefore, the properties of the original bitumen and the un-upgraded bitumen with surfactants are identical and the two terms hereafter are interchangeable. A better indication of the pre-upgrading results is shown in Table 4.6.

Table 4.6: The effect of surfactants on the physical properties of bitumen before thermal upgrading.

Properties	Bitumen + No surfactant (blank)	Bitumen + 0.25wt% surfactant	Bitumen + 0.5wt% surfactant	Bitumen + 1wt% surfactant
Saturates (wt%)	18	18	18	18
Aromatics (wt%)	29	29	29	29
Resins (wt%)	30	30	31	30
Asphaltenes (wt%)	20	20	20	21
Viscosity (cP)	330,000	330,000	330,000	330,000
Density (kg/m ³)	1,020	1,020	1,020	1,020

iii) The effect of surfactant charge on bitumen through thermal partial upgrading:

To study the effect of the surfactant charge on the thermal upgrading of bitumen, the samples were premixed with an equal amount (0.5wt%) of different surfactants with different charges. The samples were then thermally upgraded in the autoclave at 360°C (fixed temperature) for 2 hours. 360°C was chosen in this case as it was the minimum thermal upgrading temperature in this study. A low temperature will assist in identifying the magnitude of surfactants' effect on the bitumen's

viscosity for the best comparison. The viscosities of upgraded oil samples were measured, and the obtained results are shown in Table 4.7.

Table 4.7: Viscosity measurements of upgraded bitumen with differently charged surfactants.

Bitumen upgraded at 360°C	Viscosity (cP)		
	Measured @ 40°C	Measured @ 25°C	Measured @ 7.5°C
with No surfactant	12,000	45,000	150,000
with SDS (anionic)	8,000	30,000	85,000
with DTAB (cationic)	7,000	20,000	55,000
with Span 60 (nonionic)	10,000	38,000	105,000

As shown in Table 4.7, the bitumen sample that was premixed with the cationic surfactant (DTAB) and thermally upgraded at 360°C recorded the minimum viscosity of 7,000 cP (measured at 40°C). That is, the cationic surfactant was able to promote about a 42% reduction in viscosity as compared with the viscosity of the bitumen cracked at the same temperature with no additive (12,000 cP). The anionic surfactant was able to reduce the viscosity to about 8,000 cP (33% reduction) while the nonionic surfactant has the least influence on the viscosity of the bitumen, which was reduced only by about 16.7%. This concludes that the addition of surfactants to bitumen before upgrading indeed promotes viscosity reduction, but the cationic surfactant “DTAB” had the most significant effect when compared with the other surfactants used.

iv) The effect of surfactant concentration on bitumen’s properties via thermal partial upgrading:

Bitumen samples were premixed with different concentrations of DTAB (cationic surfactant) from (0–1.0 wt%) and thermally cracked at 360°C (fixed temperature). The viscosities of the cracked oil samples were then measured to determine the optimum surfactant concentration for viscosity reduction. The results of the thermally cracked bitumen viscosity versus surfactant concentration are shown in Figure 4.1.

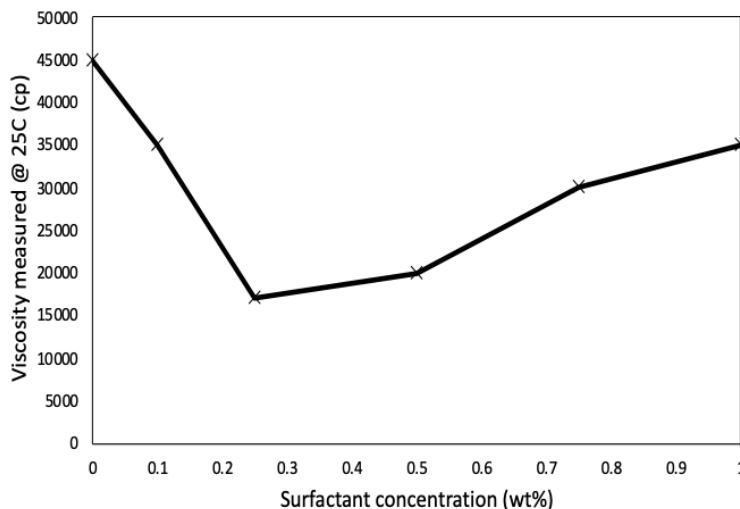


Figure 4.1: Viscosity measurements for bitumen upgraded at 360°C versus surfactant concentrations.

Figure 4.1 shows that the optimum surfactant concentration recorded was about 0.25wt%. At this concentration, the viscosity of the cracked oil was reduced to a minimum of 17,000 cP from initially 45,000 cP (measured at 25 °C). That is, the viscosity was reduced by about 62% as compared with the original sample at the same upgrading conditions. It is important to note that as the surfactant concentration increases beyond 0.25wt%, the viscosity of the thermally cracked oil tends to increase as well. This can be explained by the fact that higher surfactants concentrations can promote the development of large-sized aggregates or flocculates due to the increased surfactant-asphaltene interactions [107]. Consequently, greater shear forces will be required to overcome these interactions, and hence, larger viscosity values are recorded.

v)The effect of the temperature of partial upgrading on surfactant activity:

To study the effect of surfactants on bitumen under various thermal stresses and how the temperature affects the performance of the surfactants, a fixed concentration of 0.25wt% of DTAB (optimum concentration) was selected and premixed with bitumen samples and thermally upgraded under 360, 380, 390 and 400°C. The viscosities of the upgraded samples were then measured and tabulated in Table 4.8. Similarly, even with the addition of surfactant, as the upgrading temperature increases, the viscosity of the oil products also decreases proportionally. The addition of DTAB enhanced the viscosity reduction by 62.5% at 360 °C (from 12,000 to 4,500

cP); however, the effect of the surfactant reduced as the upgrading temperature increased to the 380-390°C range. At this range, the surfactant was still able to reduce the viscosity of bitumen by around 53%. As the temperature reached 400°C the thermal cracking dominated the reactions. The effect of the surfactant at this high temperature was further reduced and resulted in a viscosity reduction of only 22.7% from 132 cP to 102 cP (measured at 40°C) and 27% reduction from 5,500 to 4,000 cP (measured at 7.5°C).

Table 4.8: Viscosity measurements of bitumen upgraded at various temperatures with and without surfactants.

Bitumen partially upgraded at	Viscosity (cP)		
	Measured @ 40°C	Measured @ 25°C	Measured @ 7.5°C
360°C	12,000	45,000	150,000
360°C + DTAB	4,500	17,000	55,000
380°C	3,000	7,000	22,500
380°C + DTAB	1,400	3,200	10,500
390°C	1,250	4,000	9,000
390°C + DTAB	570	1,850	5,150
400°C	132	1,700	5,500
400°C + DTAB	102	1,300	4,000

The SARA analysis was performed on the upgraded oil samples with surfactants to study the effect of the surfactant (DTAB) on the compositional changes within the upgraded bitumen. The SARA results were summarized in Table 4.9 below. The results suggest that the addition of DTAB greatly affected the resins fraction which was mainly cracked into lighter fractions (aromatics and saturates). There is still a tiny fraction of aggregates formed due to the increased DTAB-asphaltene interactions which led to a slight increase in the asphaltene content as compared to the samples upgraded without surfactant. The sum of the heavy fractions of resins and asphaltenes decreased with elevated temperatures, from 33% at 360°C down to 22% at 400°C. Thus, it can be concluded that the overall contribution to the thermal cracking reactions induced by DTAB was more than the contribution of the polymerization reaction resulting in a net reduction in the shear forces within the hydrocarbon molecules and hence, reducing the viscosities. Compared to the summation of resins and asphaltenes shown in Table 4.4, the addition of the surfactant is deemed effective in

the reduction of resins and asphaltenes at relatively low temperatures. As the temperature increases, there is a slight reduction in the saturate fraction accompanied by a slight increase in the aromatics. Furthermore, the increased temperature resulted in further cracking reactions within the heavier fractions (resins and asphaltenes) which were readily decreasing with temperatures reaching their minimum values at 400°C.

Table 4.9: SARA analysis for the upgraded bitumen at various temperatures with surfactants.

Fractions	Original Bitumen	Upgraded at 360°C with DTAB	Upgraded at 380°C with DTAB	Upgraded at 390°C with DTAB	Upgraded at 400°C with DTAB	Error Bar (+/-)
Saturates (wt%)	18	25	24	22	21	0.5
Aromatics (wt%)	29	42	49	54	56	0.5
Resins (wt%)	30	14	10	7	6	1
Asphaltenes (wt%)	20	19	17	17	16	0.5

vi) The effect of surfactant addition on bitumen transportation properties:

As previously mentioned, to decrease the viscosity of bitumen to a value acceptable by the Canadian pipeline specification (i.e., 300 cP), about 33wt% of diluent must be premixed with bitumen before its transportation. Given this requirement and with the help of the diluent concentration correlation provided by Gray [13], the amount of diluent required by bitumen at various upgrading conditions was interpolated from the diluent concentration graph in [13] and tabulated in Table 4.10.

Table 4.10: Diluent concentrations required for bitumen to reach 300 cP.

Bitumen partially upgraded at	Viscosity (cP) Measured @ 25 °C	Diluent required (wt%)
Un-upgraded (original)	300,000+	33.0
360°C	45,000	26
360°C + DTAB	17,000	22
380°C	7,000	20
380°C + DTAB	3,200	16
390°C	4,000	17
390°C + DTAB	1,850	12
400°C	1,700	11
400°C + DTAB	1,300	10

According to the calculated diluent concentrations presented in Table 4.10, there is a continuous decrease in the diluent requirement with the increase in upgrading conditions. The addition of a small amount of DTAB has a noticeable effect in reducing the diluent requirement for the upgraded bitumen. At 390°C, for instance, with the addition of 0.25wt% DTAB, the upgraded bitumen sample had a viscosity of 1850 cP measured at 25°C. This viscosity now requires only 12wt% of diluent to reach the required pipeline specification of 300 cP instead of the earlier 33wt% that was needed. Thus, 21% of the diluent required for blending with original bitumen can be reduced, resulting in 21% of the pipeline capacity freed (originally occupied by the extra diluent) which can be used to transport more bitumen every time the partially upgraded bitumen is pumped. To confirm that the addition of 0.25wt% of the DTAB surfactant will not worsen the corrosivity of resulted bitumen, the total acid number (TAN) of the upgraded bitumen samples was measured and the results obtained are shown in Table 4.11.

Table 4.11: Measurements of the total acid number (TAN) of the upgraded bitumen products.

Bitumen upgraded at	Total acid number (mgKOH/g)	Error Bar (+/-)
Un-upgraded Bitumen	4.32	0.2
360 °C	3.46	0.2
360 °C + 0.25 wt% DTAB	3.41	0.2
360 °C + 0.25 wt% Span 60	3.98	0.2
360 °C + 0.25 wt% SDS	3.02	0.2

From the TAN measurements obtained in Table 4.11, it is observed that the acidity of the upgraded oil products did not increase with the addition of 0.25wt% of the tested surfactants. As a result, little to no extra corrosion is expected in this case.

4.3.2 Thermogravimetric analysis (TGA) of upgraded oil:

i) The effect of temperature on bitumen partial upgrading with no surfactant addition:

The oil vaporization tendency is a crucial parameter in identifying the changes within the oil fractions through determining the rate of weight loss as a function of temperature. Therefore, in order to identify those changes within the hydrocarbon fractions of both the original and upgraded bitumen samples, thermogravimetric analyses (TGA) were performed. The variations in oil weight loss versus temperature for the original and upgraded bitumen alongside their derivatives (DTG) were measured and plotted in Figure 4.2. It can be observed from the plots in Figure 4.2 that the original oil sand bitumen (represented by the black line) is quite heavy, the majority of which, 57.9wt%, is heavy gas oil while only containing about 1.7wt% of light naphtha. After the thermal treatment, the heavy gas oil is cracked into lighter products (mainly aromatics) which have drastically increased to 15.4wt% in the upgraded product treated at 400°C. Meanwhile, a slight fraction of heavy residue is also formed. The elevated thermal treatment resulted in a 2-3% increase in heavy residue because of polymerization. Therefore, this analysis indeed justifies the pattern represented earlier by the SARA analysis in which the thermal stress caused free radical reactions and initiated polymerization reactions to take place. At the same time, the thermal stress initiated some heavier fractions (resins and asphaltenes) to get cracked into lighter products. Looking at the DTG curves, it is observed that the maximum derivative (decomposition temperature) occurs at the temperature range between 480-490°C. At this temperature range, most of the heavy gas oil (HGO) fraction is decomposed into lighter fractions. Moreover, with the increase in upgrading temperature, the value of the maximum derivative peak tends to decrease, and the curve tends to flatten more over a wider temperature range. This phenomenon occurs since the cracking reactions were initiated at a lower temperature range than that of the original bitumen via thermal partial upgrading. The unique differences between the curves are mainly a result of the characteristics of the heavy hydrocarbon fractions (resins and asphaltenes). Asphaltene is the heaviest fraction in bitumen and doesn't contain any light compounds that can vaporize in the first phase of the TGA pyrolysis. Therefore, based on this TGA analysis, it can be suggested that the increase in the

thermal cracking temperatures led to a greater portion of the asphaltene fraction being cracked into smaller volatiles.

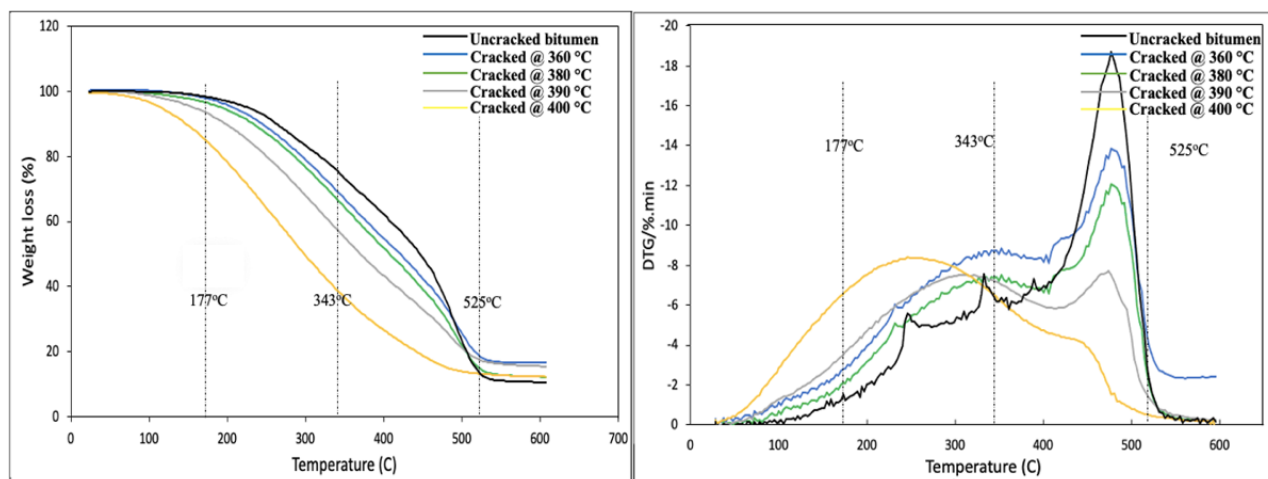


Figure 4.2: TGA and DTG curves for upgraded oil at various temperatures.

ii) *The effect of surfactant charge on bitumen's TGA:*

The variations in oil weight loss versus temperature for upgraded bitumen with the three differently charged surfactants at a fixed temperature of 360°C alongside their derivatives (DTG) were measured and plotted in Figure 4.3.

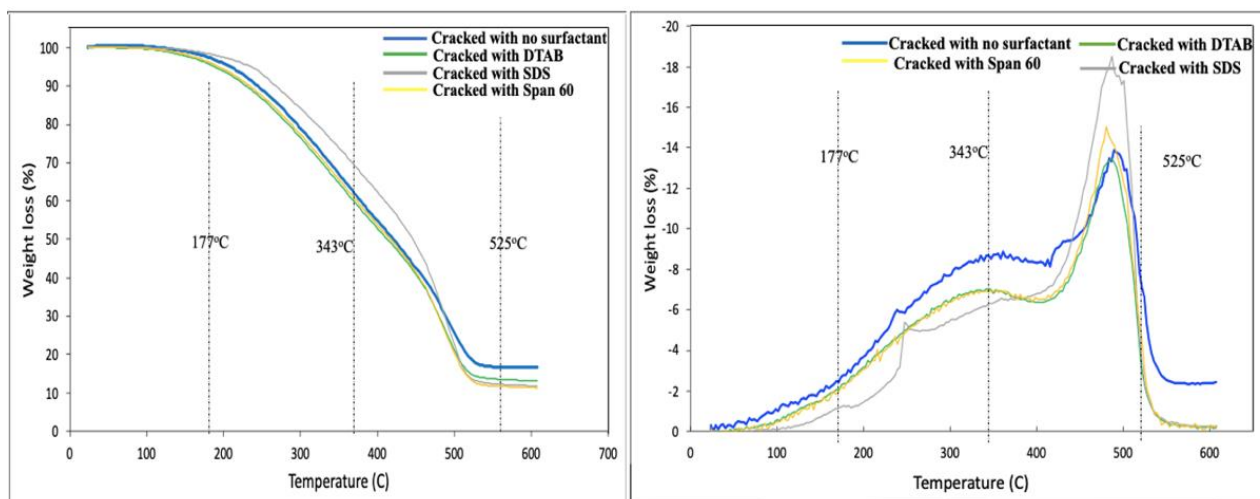


Figure 4.3: TGA and DTG curves for upgraded oil at 360°C with differently charged surfactants.

From the TGA graph, one can see that all the differently charged surfactants had almost the same effect on the thermal degradation of bitumen. The presence of surfactant (regardless of its charge) within the upgraded oil samples slightly lowered the maximum decomposition temperature from 500°C to about 480°C. This can further be witnessed by looking at the DTG peaks of the upgraded samples in which the derivative peaks are slightly shifted to a lowered temperature. Moreover, the surfactants caused a significant reduction in the (residue) coke fraction to about 10wt% as compared with the “no surfactant” sample which yielded about 18wt% at 600°C. These results further ascertain the hypothesis of the attachment of surfactant molecules to the asphaltenic fraction, which promoted the initiation of free radical reactions and ultimately resulted in the enhanced rheological properties of the upgraded bitumen.

iii) The effect of surfactant concentration on bitumen's TGA:

The variations in oil weight loss versus temperature for upgraded bitumen with different concentrations of the surfactant (DTAB) at 360°C alongside their derivatives (DTG) were also measured and plotted in Figure 4.4. From the thermograms, one can see that regardless of the surfactant concentration used, the temperature shift that occurred to all the upgraded bitumen samples with different surfactant concentrations was very similar to each other. The presence of the surfactant even in very low concentration (starting 0.25wt%) is still enough to result in a shift in the maximum decomposition temperature from 500 to about 480°C. This shift is more visible as the concentration of the surfactant increases. The induced shift can further be witnessed in the DTG peaks of the upgraded samples in which the derivative peaks are shifted to a lower temperature range (470-480°C). Moreover, the surfactants caused a significant reduction in the coke formation as they reduced the coke yield from 18wt% to 9wt%.

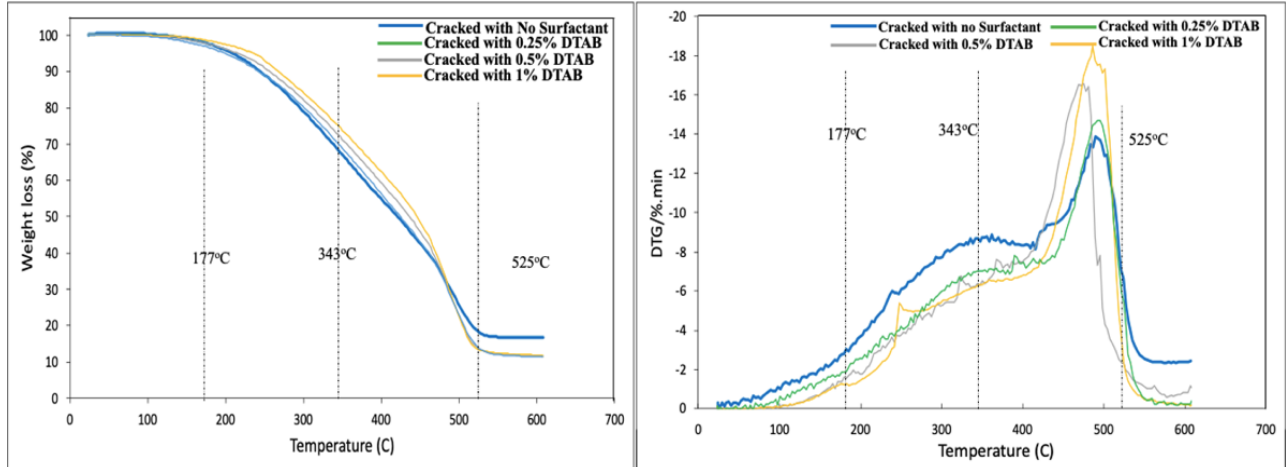


Figure 4.4: TGA and DTG curves for upgraded oil with different concentrations of DTAB.

iv) The effect of temperature and surfactant on bitumen's Activation Energy:

Further analysis of the thermal stability of the upgraded oil was performed by calculating the activation energy of oil cracking conversion using the kinetic model discussed in [117]. In this model, the oil fraction conversion (α) is defined as $\alpha = \frac{(M_0 - M_T)}{(M_0 - M_L)}$, with M_0 being the initial mass of the oil sample, M_T is the mass of partially converted oil at temperature T , and M_L is the leftover mass. The reaction model or conversion function is denoted by $g(\alpha)$ and it can be related to the oil fractional conversion (α) by the following equation:

$$\ln(g(\alpha)) = \ln\left(\frac{A}{B}\right) - \left(\frac{Ea}{RT}\right) \quad (\text{Eq. 4.1})$$

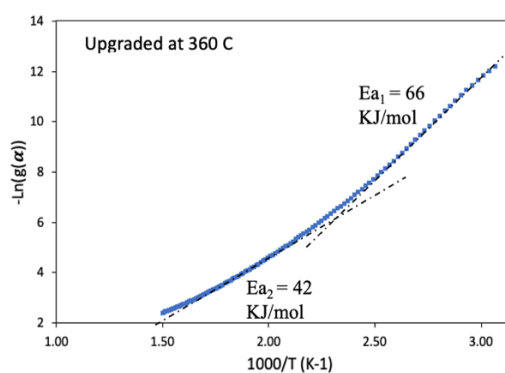
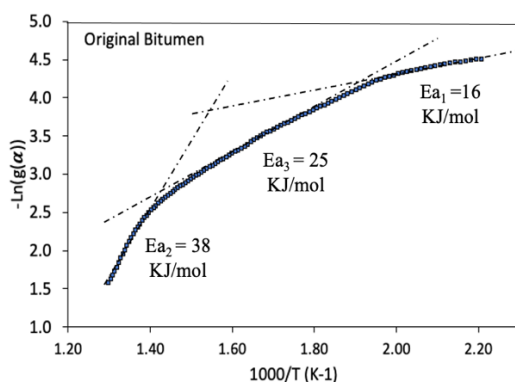
$$g(\alpha) = 1 - \frac{2\alpha}{3} - (1 - \alpha)^{2/3} \quad (\text{Eq. 4.2})$$

While obeying the Arrhenius equation, $k=Ae^{-(Ea/RT)}$, A is the pre-exponential factor, B is the constant heating rate dT/dt , Ea is the activation energy of oil conversion, and T is the temperature in ($^{\circ}\text{K}$) [118]. $-\ln(g(\alpha))$ is then plotted against $1000/T$ for all the oil samples (original, upgraded, and upgraded with surfactant) and the activation energies (Ea) were calculated from the slope of the best tangent lines to the curves. The plots of the conversion functions vs temperature are presented in Figure 4.5 and the calculated activation energies are shown in Table 4.12. The Ea plot for the original bitumen is different from those obtained for the thermally treated bitumen. Three sections of linearity appear to be for the original bitumen. While on the other hand, two linear

sections were observed for all the partially upgraded bitumen. This suggests that thermal cracking has modified the molecular structure of bitumen. The two sections in the upgraded bitumen samples represented the two activities (high temperature and low temperature) separated at a critical point, where a change in the slope occurs. This observation confirms that the thermal cracking process is preceded by a vaporization stage, but as the temperature increases more chemical cracking reactions are induced. The thermal reaction stages in the TGA results are represented by the activation energies E_{a1} and E_{a2} , corresponding to the vaporization and thermal cracking stages, and can be calculated from the slopes $-E_a/R$ of the straight lines [117]. The kinetic parameters of the vaporization and thermal cracking sections were obtained by linear regression. The activation energies, E_{a1} , and E_{a2} , that are calculated for all the upgraded bitumen samples at various conditions showed the coefficient of determination, R , greater than or equal to 0.98.

Table 4.12: Activation energies for upgraded oil samples.

Sample	Low Temp Activation Energy (E_{a1}) (KJ/mol)	High Temp Activation Energy (E_{a2}) (KJ/mol)	Critical Temperature ($^{\circ}$ C)
Original Bitumen	16	38	352
Upgraded @ 360 $^{\circ}$C	66	42	162
Upgraded @ 380 $^{\circ}$C	94	49	145
Upgraded @ 390 $^{\circ}$C	96	55	145
Upgraded @ 400 $^{\circ}$C	104	56	127
Upgraded @ 360 $^{\circ}$C with 0.25wt% DTAB	99	56	145



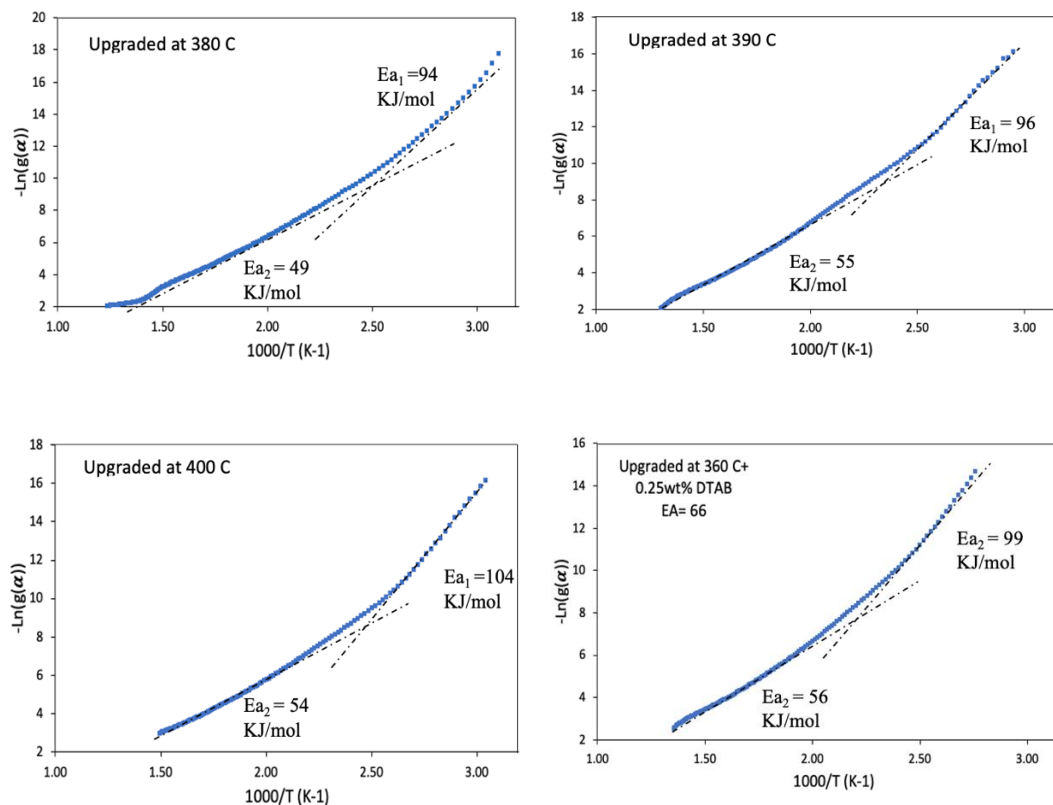


Figure 4.5: Activation energy lines from TGA plots of bitumen samples.

Significant differences in the activation energies of the bitumen samples were observed, starting with the lowest activation energy for the original bitumen which required 16 kJ/mol (E_{a1}) to initiate its vaporization phase and 38 kJ/mol (E_{a2}) to initiate the cracking phase beyond the critical temperature of 352°C. It is to be noted that there is an intermediate phase for the original bitumen (between the normally identified two phases) denoted with E_{a3} , the value of the activation energy of this intermediate phase was about 25 kJ/mol. However, after the partial upgrading of bitumen, this intermediate phase almost vanished. From the activation energy plots of the upgraded samples, one can see that there was a gradual increase in activation energies proportionally with the increase in upgrading temperatures reaching a maximum of 104 kJ/mol for E_{a1} and 56 kJ/mol for E_{a2} at 400°C. On the other hand, the bitumen sample upgraded at only 360°C with 0.25wt% DTAB had the activation energies of 99 kJ/mol and 56 kJ/mol for E_{a1} and E_{a2} respectively. That means that the addition of surfactant indeed promoted further cracking reactions and generated a more stable partially upgraded oil that almost has the same properties and activation energies as the oil samples processed at much higher upgrading temperatures such as 390 and 400°C.

4.3.3 XRD of Product's Asphaltene:

i) *The effect of temperature on Bitumen's asphaltene structure after partial upgrading:*

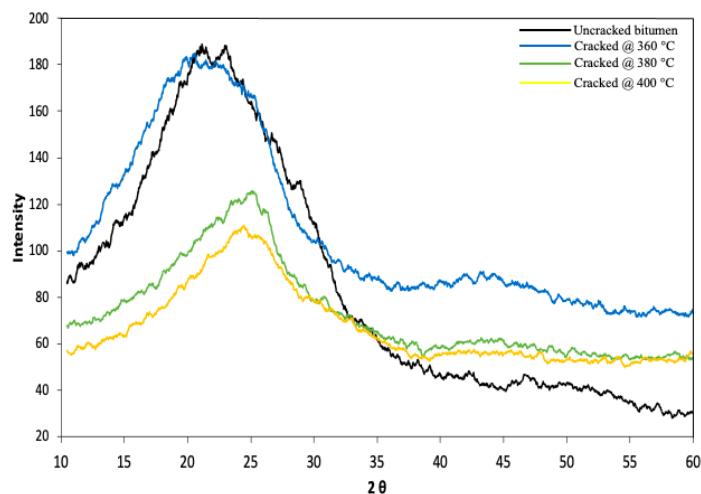


Figure 4.6: XRD pattern of asphaltene samples derived from upgraded bitumen.

To further understand the effect of temperature and surfactant addition on the heavier fractions of bitumen, the asphaltene fractions were extracted from the thermally upgraded bitumen and dried in the oven overnight until the asphaltene particles were solidified and became retrievable. The X-ray diffraction analysis was then performed on the asphaltene particles and the results are shown in Figure 4.6. The results of the analysis mainly showed two peaks at the 2θ scale at around 22° and 44° for the asphaltene treated at 360°C ; however, only one peak was observed at 44° for the un-upgraded sample. While the peaks for the 380°C and 400°C samples were located at around 25° and 45° , respectively. The peak in the range of $22\text{-}25^\circ$ is assigned to the (002) plane and it contains information about the interlayer spacing and the layer distance between the aromatic sheets [119]. The peak in the range of $44\text{-}45^\circ$ is assigned to the (100) plane and is an indicator of the average sizes of the aromatic sheets in the asphaltene sample. The quantitative analysis of these two peaks provides information about the nanostructure of the asphaltene fraction of bitumen under various thermal stresses. These parameters manifest in the d_{002} value as per Bragg's law (see Eq. 4.3), the nano-crystallite height (L_c) which indicates the height of the stack of aromatic sheets, using the Scherrer formula (see Eq. 4.4), and the nano-crystallite width (L_a) which provides the average diameter of the aromatic sheet using the Eq. 4.5. Moreover, the number of aromatic sheets per

stack or stacking number (M) and the number of aromatic rings per aromatic sheet (NO_{ar}) are also calculated using Eq. 4.6 and Eq. 4.7, respectively, as shown below:

$$d_{002} = \frac{\lambda}{2\sin\theta_{002}} \quad (\text{Eq. 4.3})$$

$$L_c = \frac{0.9\lambda}{B_{002}\cos\theta_{002}} \quad (\text{Eq. 4.4})$$

$$L_a = \frac{1.84\lambda}{B_{100}\cos\theta_{100}} \quad (\text{Eq. 4.5})$$

$$M = \frac{L_c}{d_{002}} + 1 \quad (\text{Eq. 4.6})$$

$$NO_{ar} = \frac{L_a}{2.667} \quad (\text{Eq. 4.7})$$

In these equations, λ = wavelength of X-rays (0.154 nm for Cu $K\alpha$), the Brags angles are θ_{002} and θ_{001} and the full width at half maximum (FWHM) values are B_{002} and B_{100} for the two peaks. The Brags angles and the FWHM were then obtained by the Gaussian fitting of the respective peaks using Matlab software as was done by Abdrabou et al. in [120]. The obtained values are listed in Table 4.13. To verify the repeatability of the results, each XRD result was repeated at least 3 times and then the arithmetic mean of the calculated values was reported in addition to their standard deviations. The SD (σ) was calculated by subtracting each result from the mean, then squaring the difference and adding the results. Then the sum of squares was divided by the number of trials minus one and taking the square root of the result.

Table 4.13: Asphaltene parameters calculated from XRD plots.

Properties	Definition	Bitumen	Upgraded at			σ
			360°C	380°C	400°C	
d_{002} (nm)	Layer distance between the aromatic sheets	4.16	3.82	3.62	3.60	± 0.01
L_a (nm)	Diameter of the aromatic sheet	7.50	12.00	32.0	35.0	± 0.5
L_c (nm)	Thickness of the stack of aromatic sheets	15.72	11.55	9.57	9.0	± 0.5
NO_{ar}	Number of aromatic rings in the aromatic sheet	2.81	4.50	12.00	13.12	-
M	Mean Stacking number	4.78	4.02	3.64	3.50	-

As evident from Table 4.13, the interlayer distance between the aromatic sheets is slightly decreasing with temperature due to the thermal stress exerted on the asphaltene particles, although the difference is still minor. Substantially, the reduced L_c values confirm that the nano-crystallites present in the thermally cracked asphaltene samples contains thinner and finer hydrocarbon stacks with a reduced number of graphene layers per stack compared to the original asphaltene sample. This decrease in aromatic sheet thickness was attributed to the loss of aliphatic carbon in the side chains and consequently, resulting in a decrease in the number of aromatic sheets per stack, aka stacking number (M). Similar results were also obtained in [121] by AlHumaidan et al.

On the other hand, the increasing values of L_a at elevated thermal stresses imply that the increase in thermal upgrading severity drives the asphaltene molecules towards the core nature structure. The asphaltene fraction is known to have an asphaltenic core which is sometimes referred to as the coke fraction in some studies [121],[122]. The asphaltenic core in extreme thermal upgrading conditions tends to undergo secondary reactions such as dealkylation of side aliphatic chains, cyclization of alkyl chains, and combination of aromatic rings radicals via polymerization [122]. These reactions are the possible reason for the noticeable increase in the diameter of the aromatic sheet (L_a) and hence the increase in the number of aromatic rings in a single aromatic sheet (NO_{ar}).

ii) The effect of surfactant on the upgraded asphaltene nanostructure:

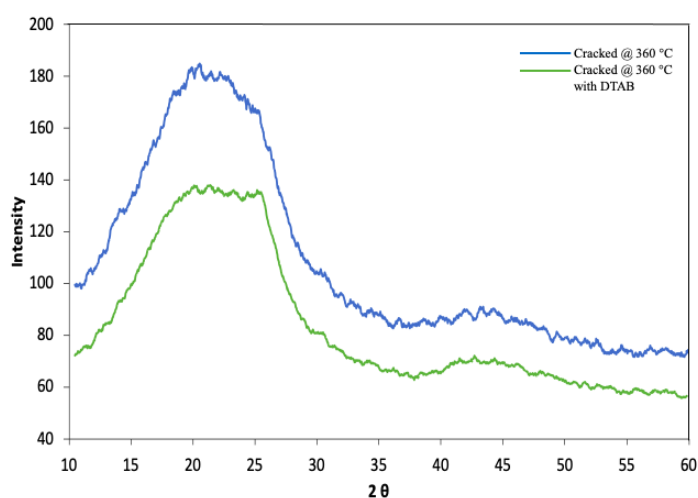


Figure 4.7: XRD pattern of asphaltene samples from cracked bitumen at 360°C with and without DTAB.

The X-ray diffraction analysis was performed on the asphaltene samples recovered from the thermally cracked bitumen at a fixed temperature (360°C) with and without the addition of DTAB surfactant, and the results are shown in Figure 4.7. The results showed some similarities to the previous analysis with two peaks at the 2θ scale at around 22° and 44°. However, it is noticed that there might be a third peak at 25° for the surfactant blended sample that didn't appear earlier. This additional peak is identified as the γ -band, and it is usually attributed to the loosely held long-chain aliphatic structure (i.e. highly amorphous carbon structure attached to the aromatic rings). Equations E3-E7 were again used in collaboration with the Matlab code to obtain the Bragg angles and the FWHM via Gaussian fitting of the XRD plots and the calculated parameters are shown in Table 4.14 below:

Table 4.14: Asphaltene parameters calculated from XRD plots.

Properties	Upgraded at 360 °C	Upgraded at 360 °C with 0.25wt% Surfactant (DTAB)	Standard deviation (σ)
D_m(nm)	3.82	4.15	± 0.01
L_a (nm)	12.00	22	± 0.5
L_c (nm)	11.55	5.7	± 0.5
NOar	4.50	8.25	-
M	4.02	2.37	-

The addition of 0.25wt% of DTAB to bitumen followed by thermal treatment resulted in an asphaltene that has a slightly greater layer distance between the aromatic sheets (D_m). The addition of the surfactant caused the L_c value to decrease to about 50% of its original value mimicking the effect of increasing the upgrading temperature which exerted additional stress on the asphaltene particles, the reduced L_c values confirm that the nano-crystallites present in the surfactant-containing asphaltene samples contains thinner and finer hydrocarbon stacks with a reduced number of graphene layers per stack as compared to the asphaltene sample with no surfactant. Similarly, the increase in the value of L_a to double the value with the addition of surfactant implies that the surfactant induced a similar effect on the asphaltene nanostructure as the increase in thermal upgrading severity due to temperature increase initially did. To verify the conclusions drawn from the XRD analysis, TEM images were obtained and carefully analyzed.

4.3.4 HRTEM of Product's Asphaltene:

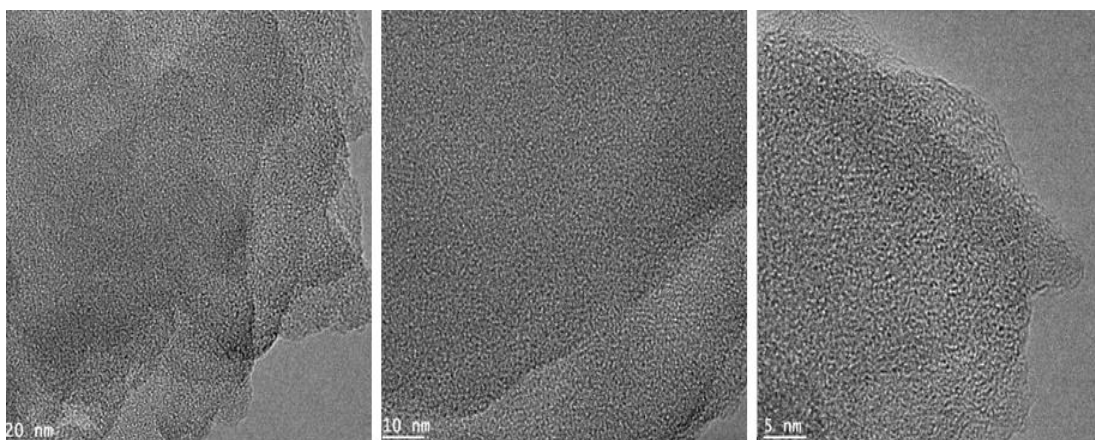


Figure 4.8: HRTEM images of the original bitumen asphaltene at different magnifications (20, 10, and 5 nm scale).

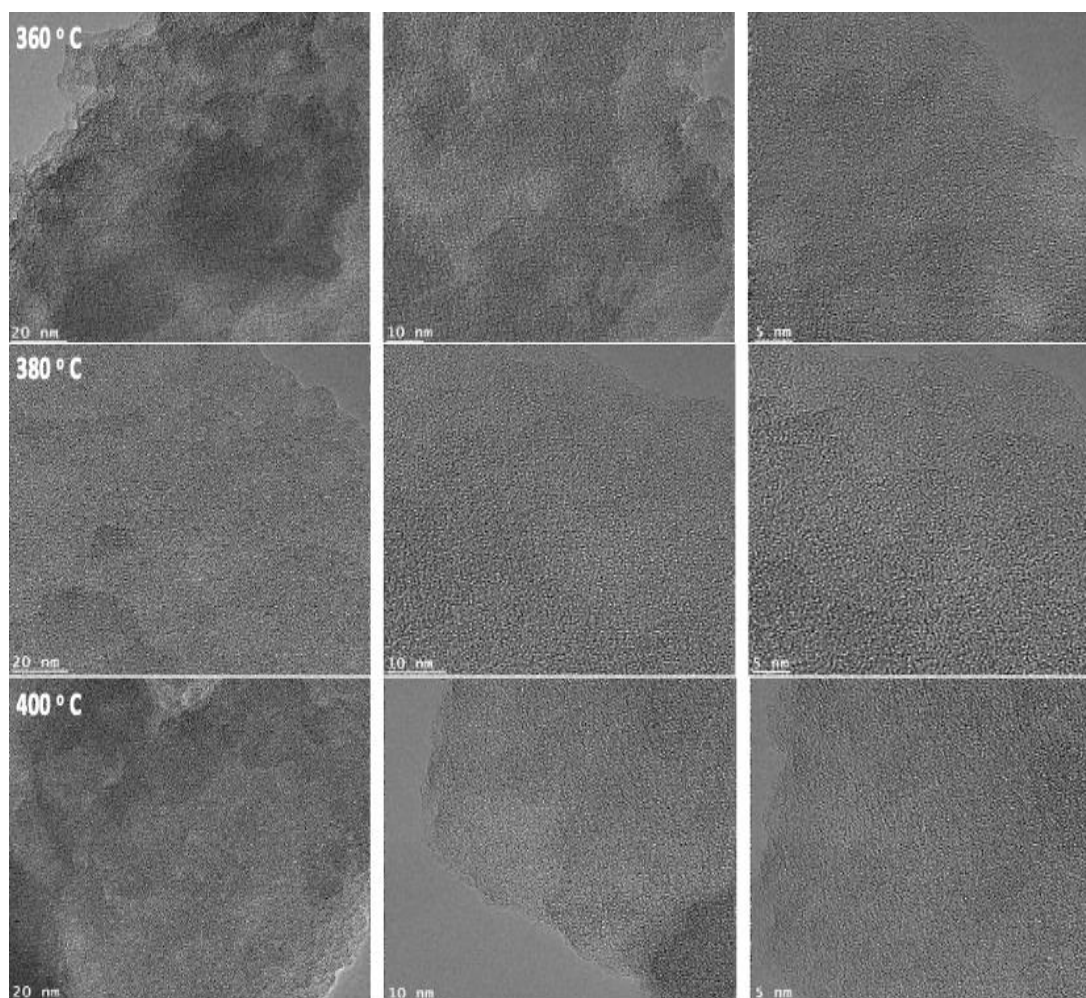


Figure 4.9: HRTEM images of the asphaltene of the partially upgraded bitumen at 360, 380, and 400°C at different magnifications (20, 10, and 5 nm scale) without surfactant.

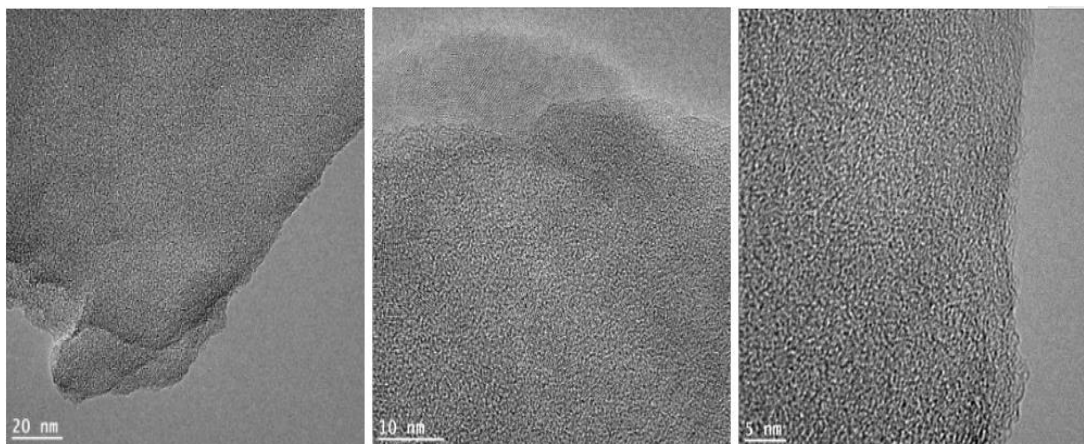


Figure 4.10: HRTEM images of the asphaltene of the partially upgraded bitumen with 0.25wt% DTAB at 360°C at different magnifications (20, 10, and 5 nm scale).

Figure 4.8 represents the HRTEM images of the original (un-upgraded) bitumen's asphaltene obtained at different magnifications (20, 10, and 5 nm scale). These images will be considered as the basis and will be used to draw comparisons with the thermally and chemically treated asphaltene particles under various conditions. Figure 4.9 represents HRTEM images of the asphaltene nanoparticles extracted of the partially upgraded bitumen at 360, 380, and 400°C at different magnifications (20, 10, and 5 nm scale) without the use of surfactant. It is clear from the micrographs that as the upgrading temperature increases, the severity of the cracking reactions within the asphaltene fragments also increases; hence, more tortuous and smaller fragments are observed. To further analyze the effect of the surfactant "DTAB" on the nanostructure of the asphaltene at low partial upgrading conditions, HRTEM images of the bitumen's asphaltene upgraded at 360°C with 0.25wt% DTAB were obtained and shown in Figure 4.10. The images in Figure 4.10 suggest that the addition of DTAB to the upgrading process of bitumen could indeed enhance the degree of cracking, leading to a reduction in the size of the asphaltene particles. Qualitatively from the images, it can be witnessed that the effect of DTAB at 360 °C in terms of asphaltene nano-structural disorder is very similar to that resulting from the upgraded bitumen at 400°C; however, this assumption must be proven further qualitatively. Therefore, this possibility of the nano-structural disorder within the asphaltene particles can be confirmed by analyzing the small stacking lines commonly referred to as the fused aromatic ring structures [123]. This process can be performed by estimating the graphene layers (fringes) length distribution and degree of tortuosity within the upgraded bitumen's asphaltene micrographs. A quantitative analysis of the

fringe length and tortuosity was performed using the Matlab code based on the algorithms reported by K. Yehliu et al. [124], where the HRTEM images were subjected to negative transformation and grayscale. The negative transformation is defined as $I_{\text{negative}} = L - 1 - I_{\text{original}}$, where I_{original} is the image pixel values before transformation and 'L' is the discrete intensity levels. On selected multiple regions of interest, operations like Gaussian filter, histogram equalization, and Tophat transformation were performed to eliminate errors due to non-homogeneous illumination across the image as well as to improve the fringe contrast. The branches from fringes were removed by a process called skeletonization using built-in functions in Matlab that uses a parallel thinning algorithm [125]. Relative to these branch points, fringe length was determined in all directions. The smallest branch was identified, and the branch connections were broken by setting the first pixel to this branch as zero. The detailed procedure, equations, and algorithms used are listed in detail in reference [124]. For each sample, an HRTEM image consisting of 50-100 particles is chosen for homogeneity of the primary particle structure, of which 5 high-resolution microstructural images of each primary particle are randomly chosen and subjected to Matlab image processing as discussed above. The mean values of the fringe length and fringe tortuosity are then calculated using the Matlab code. The analysis was repeated 5 times for each image and the arithmetic mean values were reported in addition to their error bars. Samples of the processed fringe images for the asphaltene particles are shown in Figure 4.11.

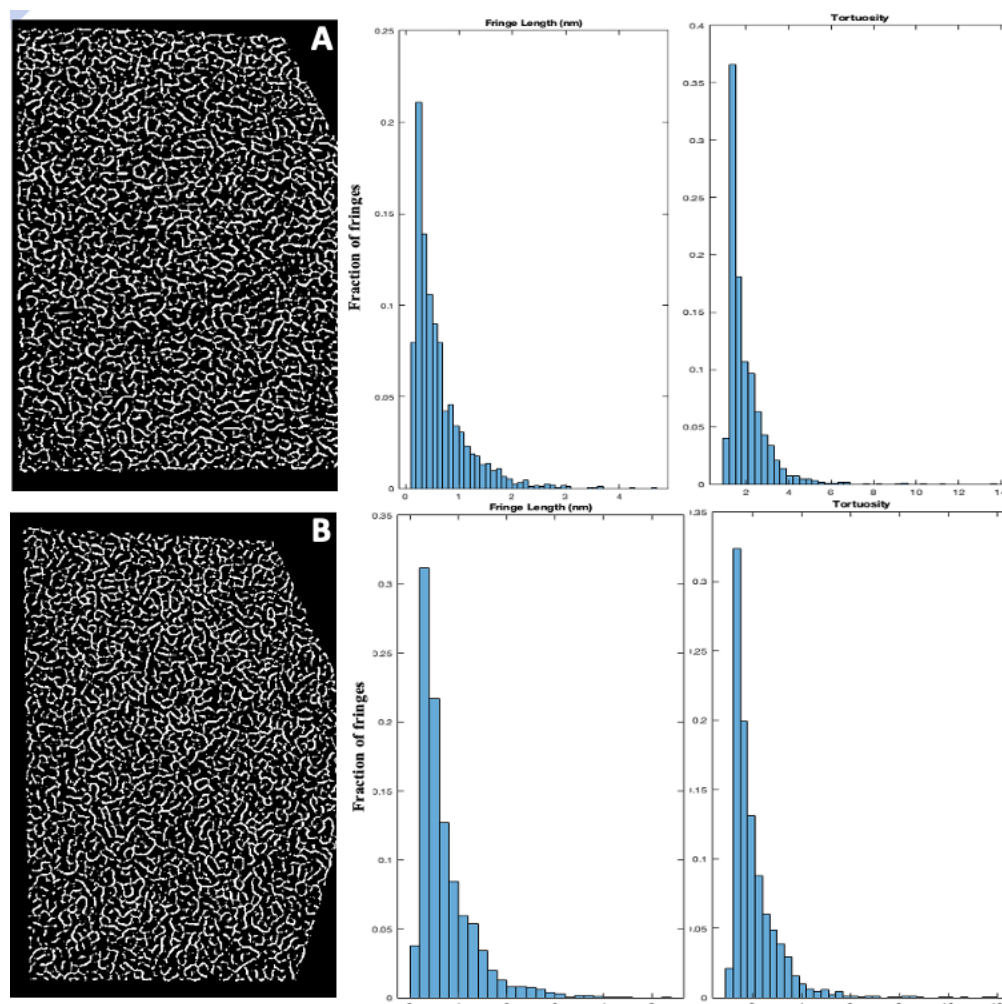


Figure 4.11: Matlab images, fringe length, and tortuosity index of asphaltene particles, for (A) bitumen upgraded with no surfactant and (B) bitumen upgraded with 0.25wt% DTAB.

Table 4.15: The calculated nanostructure parameters from HRTEM.

Asphaltene sample	Mean Fringe Length (nm)	Mean Fringe Tortuosity
Original (Un-upgraded) bitumen	0.81 ± 0.01	1.76
Upgraded at 360°C	0.78 ± 0.01	1.78
Upgraded at 380°C	0.78 ± 0.01	1.94
Upgraded at 400°C	0.78 ± 0.01	1.97
Upgraded at 360°C with 0.25wt% DTAB	0.72 ± 0.01	2.06

From Table 4.15, one can conclude that asphaltene particles obtained from the original bitumen had a mean fringe length of 0.81 nm which decreases to 0.72 nm in the case of upgraded bitumen using DTAB. Moreover, the analysis of the tortuosity index also suggests that the short fringes in the surfactant treated asphaltene had a higher curvature (2.06) as compared to original bitumen asphaltene (1.76). The tortuosity index measures the curvature of fringes within the planar aromatic framework of graphene layers. Such curvatures in aromatic layers prevent the development of long-range graphitic stacks, resulting in the reduction in the overall particle size of the asphaltene particle [126]. Therefore, it is more evident that the shorter fringe length and largely curved fringes make the asphaltene particles retrieved from the bitumen upgraded with DTAB surfactant highly disordered and amorphous. This suggests that the effect of increasing the upgrading temperatures on the asphaltene nanostructure can similarly be mimicked by adding a small quantity of DTAB to the bitumen and upgrading it at a much lower temperature.

It is important to note that it is difficult to come up with a new mechanism given the observations and results we currently have, and the complexity of the asphaltene fraction. Proposing a mechanism might be feasible when surfactants are studied on known model compounds. The purpose of this study was to determine whether the addition of surfactants to bitumen will improve its final rheological properties. And to understand what properties of the liquid and the asphaltene fraction changed with temperature and/or surfactant addition. Nevertheless, it is encouraging to adopt a combination of mechanisms proposed by some earlier studies. Kwon et al.[108], for instance, proposed that the cationic surfactants have an electric potential that is opposite that of the asphaltene–resin colloid, hence the electrostatic attraction plays an important role in the thermal cracking initiation reactions. Furthermore, considering the common adsorption behavior for both anionic and cationic surfactants, it can be confirmed that the dominant mechanism for the adsorption of surfactants is the hydrophobic interaction between the asphaltene–resin colloid and alkyl chain of the surfactant rather than the electrostatic forces.

Alternatively, in another study by Ortega et al. [107], it was shown that ionic surfactants such as dodecylbenzene sulfonic acid (DBSA) were able to affect the reaction mechanism of asphaltenes through the protonation of heteroatomic components in the asphaltenes, which are positively charged, whereas proton-donor DBSA molecules become negatively charged ions. Hence, this

process led to an ion pair with strong ionic bonding, and it can promote further electrostatic interactions with other ion pairs in neighboring molecules/aggregates.

4.4 Conclusion

A systematic investigation of the effect of adding ionic surfactants to bitumen before its thermal partial upgrading was performed. Bitumen was partially upgraded within the temperature range of 360-400°C with surfactants of different charges and concentrations. The physical properties such as viscosity, density, and SARA composition of the upgraded bitumen at all upgrading conditions were then measured. The results revealed that the addition of 0.25wt% of the cationic surfactant “DTAB” was the optimum condition for maximizing the reduction in bitumen’s viscosity. DTAB was able to reduce the viscosity of the upgraded bitumen by 62%, 53%, and 27% at the upgrading conditions of 360, 380, and 400°C, respectively, as compared with the bitumen upgraded without any additives. To further understand the hydrocarbon fractions compositional changes within the bitumen samples, thermogravimetric analysis was performed on the partially upgraded bitumen samples both with and without surfactant. The results revealed that the addition of surfactants led to a significant reduction in the Heavy Gas Oil (R3) fraction and induced an earlier mass reduction plateau as compared with the original samples. This indicates that the surfactants were able to promote more cracking reactions at high temperatures and cause the heavier hydrocarbon fractions (R3 and R4) to break down into smaller and lighter fractions within the upgraded bitumen. Furthermore, the upgraded bitumen with surfactants showed significantly higher initial activation energies as compared to samples with no surfactant. This E_a calculation acts as an indicator for the enhanced stability that the surfactants induced within the upgraded bitumen samples. Solid asphaltene samples were then recovered from the upgraded bitumen and subjected to XRD and HRTEM analysis to understand the effect of surfactants on bitumen’s heaviest fractions. The detailed morphological characterization of the asphaltene samples using HRTEM and XRD techniques revealed an increase in the hydrocarbon structural disorder (greater fringe tortuosity and shorter fringe length), within the asphaltene nanostructure with the addition of DTAB. This change in the asphaltene nanostructure may be an indication of the additional cracking reactions that the surfactants induced during the thermal upgrading process.

Chapter 5 - Optimization of Iron-Based Catalyst for Partial Upgrading of Athabasca Bitumen: The Role of Fe Oxidation State, Particle Size, and Concentration

5 Abstract

The present investigation examines the prospective application of Fe-based catalysts for catalyzing the partial upgrading of Athabasca oil sand bitumen, aiming for developing an economically viable and environmentally sustainable process. The primary focus is to analyze the impact of the oxidation state of iron, catalyst particle size, and catalyst concentration on partial upgrading efficiency to optimize bitumen resource utilization without the need of an external source/supply of hydrogen gas using an autoclave reactor. The experimental results demonstrate that Fe-based catalysts, particularly those with lower oxidation states such as FeS, FeO, and Fe₃O₄, significantly improve the oil quality and reduce bitumen's viscosity through increasing saturates and substantially reducing the asphaltene fractions. Furthermore, it is also identified that those catalysts can promote hydrogenation and cracking reactions that transform heavier fractions into lighter ones while achieving up to 59% vacuum residue conversion. A comprehensive screening process using Minitab statistical software was made to identify the best catalyst based on the catalyst's oxidation state, concentration, and particle size range. As a result, Fe₃O₄ nanoparticles at a 0.5wt% loading have been identified as the optimal catalyst combination for achieving the maximum liquid yield, while simultaneously producing the minimum asphaltene content, and maximum viscosity reduction. An assessment of the fresh and spent Fe₃O₄ catalyst yielded valuable insights concerning the catalytic partial upgrading of bitumen, unveiling a reaction mechanism involving iron catalyst sulfidation, desulfurization reactions, C-H scission, and hydrocarbon cracking, in addition to the formation of coke. The potential role of various alloy materials employed in the fabrication of reactors for bitumen partial upgrading has also been studied and compared, discussing their unique advantages and limitations in terms of product quality and liquid yield. The findings presented in this study contribute significantly to the development of more efficient and sustainable upgrading processes, paving the way for optimizing catalyst properties for bitumen upgrading applications and providing a valuable perspective on the role of catalysts in the upgrading of heavy oils.

5.1 Introduction

Canadian pipeline specifications demand strict adherence to the requirement that any transported oil must have a viscosity of 350 cSt or less and a density of less than 940 kg/m³ at reference temperatures of 7.5°C for winter and 15°C for summer [12]. Unfortunately, bitumen, a commonly transported oil in Canada, is highly viscous and cannot meet these standards without undergoing processing. Upgrading refers to the process of converting bitumen into lighter oil or synthetic crude oil (SCO) that can be easily treated at refineries while adhering to Canadian pipeline standards. The SCO product is then sent to downstream refineries for conversion into more useful products. While full upgrading techniques are expensive and highly energy-consuming, partial upgrading, on the other hand, offers a more economical and practical alternative. Partial upgrading is a newly proposed upgrading technique that can upgrade bitumen to a heavy crude that meets pipeline transportation specifications at a low cost and lower GHG emissions [22].

To further reduce the preparation and implementation costs associated with on-site partial upgrading processes, catalytic partial upgrading is proposed. The catalytic partial upgrading differs from conventional upgrading technologies, such as thermal cracking and hydrocracking, which mainly rely on extremely high temperature cracking to reduce the molecular weight of heavy crude oils [127]. Visbreaking, for instance, is a mild thermal cracking process that involves heating the crude oil to temperatures typically below 450°C, aiming to break down heavy hydrocarbons into lighter fractions. Unlike the more intense thermal cracking processes, visbreaking is designed to avoid coke formation by carefully selecting the temperature and residence time. It should be noted that the thermal cracking processes with coke formation are commonly referred to as coking, where significant carbon residues are produced [128]. Hydrocracking, on the other hand, is a more severe form of hydroprocessing that uses both a source of hydrogen gas and a catalyst to upgrade heavy crude oils at high temperatures and pressures (typically exceeding 400°C and 10 MPa) [46]. While thermal cracking and hydrocracking are effective in reducing the viscosity and sulfur contents of crude oils, they have major drawbacks. Hydrocracking, for instance, is limited by its high cost, high energy consumption, its dependence on a continuous external source of H₂ and finally its production of significant amounts of CO₂ emissions [129]. In contrast, catalytic partial upgrading utilizes inexpensive catalysts to selectively crack heavy hydrocarbons under milder operating conditions (below 400°C and at atmospheric pressures) without the direct use of hydrogen gas

[130]. As a result, an intermediate oil that satisfies the pipeline transportation criteria is achieved with lower energy consumption, lower CO₂ emissions, and higher yields of lighter hydrocarbon products [131]. Therefore, catalytic partial upgrading is considered a more sustainable and efficient approach for processing heavy crude oils when compared to visbreaking and hydrocracking.

Choosing an appropriate catalyst is a crucial aspect of achieving the objectives of catalytic partial upgrading. To achieve cost-effectiveness, a low-cost easily recoverable catalyst that doesn't require the use of hydrogen gas is highly desirable [22]. Metal-based heterogeneous catalysts, particularly the magnetic ones, offer the added advantage of recyclability via magnetic collection [132]. Extensive research has shown that metal-based catalysts can substantially decrease the activation energy required for cracking reactions during oil upgrading [58], [133]. This development has enabled the mitigation of coking issues during extraction and upgrading processes, making the process more efficient and sustainable. The catalytic activity leads to the fragmentation of complex hydrocarbon molecules into smaller hydrocarbon molecules, thus reducing the viscosity of heavy oil [51].

With the increasing demand for cost-effective and environmentally sustainable partial upgrading catalysts for heavy crude oils and bitumen, the utilization of iron-based catalysts is emerging as a promising option [134]. These catalysts possess several advantages, including high thermal stability, low cost, and strong paramagnetic properties, making them a sustainable and scalable alternative to traditional catalysts [51]. In addition, dispersed nano-catalyst technology will allow the iron particles to remain suspended in the oil layer, ensuring they don't sink to the bottom of the reactor [55]. Iron-based catalysts have been shown to have comparable or superior performance in terms of activity and selectivity towards the production of light hydrocarbons [135]. Various studies have demonstrated the efficiency of iron-based catalysts in viscosity reduction, particularly nano-sized Fe, Fe₂O₃, and Fe₃O₄ catalysts [136]. Recent research has highlighted the importance of factors such as oxidation state, particle size, and concentration of iron species in determining the performance of iron-based catalysts [137]. To achieve optimal results, it's crucial to choose the right temperature range, reaction time, and metal iron dosage. AlMarshed et al. [138] have demonstrated that catalytic upgrading experiments conducted under specific conditions can optimize the light and intermediate components of crude oil while minimizing coke yield.

However, the viscosity of the oil may increase if metal particles are not used appropriately [139]. Therefore, the concentration, particle size, and type of catalyst particles should be selected carefully to ensure all the particles are consumed during high-temperature hydrogenation and desulfurization reactions. As a catalyst, Fe attacks the C-S bonds within the hydrocarbon chain, leading to the formation of FeS, which is fortunately an effective catalyst in hydrocarbon cracking and C-S bond scission, moreover, part of the sulfur interacts with hydrogen to form H₂S [140]. Despite the notable advances made in developing iron-based catalysts for various fuel upgrading processes, several research gaps remain in the literature. There are very few reports on using iron catalysts to partially upgrade bitumen. One of the main challenges is related to the lack of understanding of the relationship between the catalyst properties and the catalytic performance in bitumen partial upgrading, which limits their practical applications [135]. This study proposes a novel and comprehensive investigation of the effects of various catalyst parameters, such as Fe oxidation state, particle size, and concentration, on the catalytic performance of iron-based catalysts in bitumen partial upgrading. Additionally, the study will describe the reaction mechanisms and kinetics involved in the catalytic process, further contributing to the development of efficient and selective catalysts.

In this study, the proposed methodology involves testing and characterization of iron-based catalysts with varying Fe oxidation states, particle sizes, and concentrations. The best catalysts will be characterized using various techniques, such as X-ray diffraction (XRD), scanning electron microscopy (SEM), and X-ray photoelectron spectrometry (XPS). The catalytic performance of the catalysts will be evaluated for the partial upgrading of Athabasca bitumen under various reaction conditions using an autoclave reactor system. The products will be analyzed using gas chromatography (GC) for the gas and thermogravimetric analysis (TGA) and SARA analysis for the liquid to determine the product distribution and composition.

5.2 Experimental Methodology

5.2.1 Materials

The properties and characteristics of bitumen derived from the Athabasca oil sands in Alberta were investigated, serving as the primary feedstock for experimental evaluation. Table 5.1 presents a summary of the key physical attributes of the bitumen investigated. Viscosity measurements were determined in accordance with ASTM D4402 standard using an IKA ROTAVISC rotational viscometer, which has a measurement range of 100-4,000,000 cP and a reproducibility of $\pm 1\%$. Density measurements were acquired using a DensitoPro Handheld Density Meter purchased from Mettler Toledo, following the ASTM D7777 standard. To gain a comprehensive understanding of the bitumen's composition, a SARA (Saturates, Aromatics, Resins, and Asphaltenes) analysis was conducted using the ASTM D2007-98 standard procedure. Additionally, the sulfur content was determined via X-ray fluorescence (XRF) analysis and the distillation cuts were estimated from thermogravimetric analysis (TGA) of the oil samples.

Table 5.1: Measured properties of the original bitumen of interest.

Property	Athabasca Bitumen	Reproducibility (+/-)
Density (kg/m ³)	1020	5
Viscosity (mPa.s or Cp) at 20°C	300,000	1%
TAN (mg KOH/g)	4.32	0.1
Sulfur Content (wt%)	4.67	0.05
SARA fractions (wt%)		
Saturates	19.1	0.2
Aromatics	28.9	0.3
Resins	30.8	0.3
Asphaltenes	21.2	0.2
Distillation Fractions via TGA (wt%)		
(<175°C) Naphtha	1.7	0.1
(175 -343°C) Light Gas oil	11.3	0.1
(343-525°C) Heavy Gas oil	37.9	0.1
(525°C+) Vacuum residue	49.1	0.1

Iron-based nanoparticles, including Fe, Fe₂O₃, FeO, Fe₃O₄, and FeS powders, with particle sizes of <50 nm, <100 nm, and < 1 μm , were purchased from Sigma-Aldrich and employed as received. A detailed description of these materials is presented in Table 5.2. To ensure consistency and

reliability in the analysis, the liquid products were characterized using SARA analysis, viscosity, density, and thermogravimetric analysis (TGA) following the methodologies outlined in previous work conducted by our research team [73].

Table 5.2: Specifications of the iron particles used as catalysts.

Catalyst Used	Particle Diameter	Form	Multi-point BET-specific surface area (m ² /g)
Iron (Fe)	<100 nm	Nano powder	36.3
	< 1 μ m	Powder	5.8
Iron (II) Oxide (FeO)	<100 nm	Nano powder	12.5
Iron (III) Oxide (Fe ₂ O ₃)	<50 nm	Nano powder	46.4
	< 1 μ m	Powder	11.1
Iron (II, III) Oxide (Fe ₃ O ₄)	<50 nm	Nano powder	42.6
	< 1 μ m	Powder	10.7
Iron Sulfide (FeS)	<100 nm	Nano powder	9.2

To achieve a flowable fuel, a hot water bath was utilized to preheat the bitumen. Subsequently, approximately 80 grams of bitumen were introduced into a Parr Bench Top Reactor (Series 4590 autoclave). A predetermined amount of iron powder catalyst was added to the reactor, and the resulting mixture of bitumen and catalysts was agitated at 600 rpm for one hour at 60°C to ensure uniform dispersion of catalyst powders. Subsequently, the bitumen sample was subjected to thermal treatment at 400°C for two hours. After completion of the reaction, the mixture was allowed to cool to room temperature, and the resulting oil was extracted from the autoclave. Physical properties such as viscosity, density, and SARA composition of the upgraded bitumen were assessed after each trial.

5.2.2 Product analysis and Characterization

The main products of the upgrading reactions were a) upgraded liquid oil, b) non-condensable gas, and c) coke. Equation 1 was used to compute the yields of each product as a proportion of the mass of feeding oil.

$$\text{Yield (wt\%)} = \frac{M_i}{M_{\text{feed}}} \times 100\% \quad (\text{Eq. 5.1})$$

where M_i represents the mass of component i . The liquid yield was calculated based on the weight of the direct filtrate. After the reaction, the samples were centrifuged and filtered to separate the liquid phase from the solid catalyst particles. The weight of the collected liquid phase, which represents the converted product, was used to calculate the liquid yield. The mass of produced gas was calculated based on the final pressure and average molecular weight determined by gas chromatography (GC) analysis. The gas weight was calculated using the formula: Gas weight = Average gas molecular weight * number of moles. The number of moles was determined using the ideal gas law equation: $PV = nRT$, where P is the gas pressure in atm, V is the gas volume in liters (0.3427 L in this case), R is the ideal gas constant (0.08205 L.atm/mol.K), and T is the temperature in Kelvin (298 K in this case). Finally, the coke yield was based on the carbon residue in the sample. After the reaction, the spent catalyst was collected and analyzed to determine the carbon residue content.

Asphaltene content was evaluated using the ASTM D2007-98 standard with *n*-pentane as a solvent. Upgraded oil samples were further analyzed for API gravity, viscosity, and liquid fraction distribution via SARA and thermogravimetric analysis (TGA). GC was employed to determine the composition and concentration of gaseous products. Spent catalysts were characterized using X-ray photoelectron spectroscopy (XPS), X-ray diffraction (XRD), scanning electron microscopy (SEM), and vibrating sample magnetometry (VSM).

The surface area and porosity of the catalysts were determined using the Brunauer-Emmett-Teller (BET) analysis using a QuantaChrome Nova 1200E analyzer. Liquid bitumen samples were subjected to thermogravimetric analysis (TGA) analysis using a Perkin-Elmer Pyris 1 TGA instrument under a nitrogen environment with a heating ramp of 30°C/min and an N_2 flow rate of 30 ml/min. Sulfur content in bitumen samples was measured through X-ray fluorescence (XRF), following the ASTM D4294 standard. X-ray photoelectron spectrometry (XPS) was utilized to track the oxidation state changes in iron, the concentrations of oxygen species, and potential carbon deposition on iron catalysts, using a Kratos AXIS Supra instrument with a monochromatic Al K(α) source. Magnetic properties of catalyst samples were measured using Vibrating sample magnetometry (VSM) on a Quantum Design PPMS® DynaCool™ instrument, performing a

magnetic field sweep from -30000 Oe (-3T) to 30000 Oe (3T) at room temperature. Structural parameters of Fe catalyst particles were provided via X-ray diffraction (XRD) analysis, which was conducted using a Rigaku DMax diffractometer. Finally, detailed sample imaging was achieved through scanning electron microscopy (SEM) using a Hitachi SU8230 Regulus Ultra High-Resolution Field Emission SEM.

5.2.3 Uncertainties in analysis

The reliability of the experimental results is crucial for the validity of this research. To ensure that the results reported are reproducible and robust, the following uncertainties were identified and meticulously addressed in a similar manner to [141], [142]:

- 1) **Errors from Sample Preparation and Size Differences:** Uniformity in sample preparation was maintained by employing consistent procedures across all experiments. Variations in sample size were minimized by using standard protocols, ensuring that all samples were prepared to the same specifications.
- 2) **Accuracy Errors from Product Yield Measurements:** The measurements of product yields were performed multiple times (at least 3 times at each condition), and only the arithmetic average values were reported. The deviations were confirmed to be within an acceptable range of less than 5%, enhancing the accuracy of these results.
- 3) **Uncertainties in Oil Physical Properties Measurements (Density, Viscosity, Sulfur Content):** Rigorous calibration and validation of the analytical tools used for measuring these properties were carried out. Each measurement was repeated at least three times, and the average values were reported, with the observed deviations well within acceptable limits.
- 4) **Errors in SARA Fractions Measurements:** The analysis of Saturates, Aromatics, Resins, and Asphaltenes (SARA) fractions was conducted with precision, and any potential error was eliminated by adhering to standardized procedures and repeating the analysis to confirm consistency. The total mass of all the recovered fractions were > 97% (which satisfies the ASTM-2007 requirements).

- 5) **Process Condition Error in TGA Analysis:** Special attention was given to potential errors that might occur during Thermogravimetric Analysis (TGA). The TGA analyzer was purged with an inert gas (such as N_2) to minimize the effects of residual air on the thermogram analysis, in alignment with best practices.
- 6) **Statistical Analysis of Uncertainties:** Comprehensive statistical analyses were conducted to quantify the uncertainties and ensure that the reported results are grounded in robust experimental evidence. This includes the use of confidence intervals and other statistical tools to gauge the reliability of the findings.

5.3 Results and Discussion

5.3.1 Catalyst Morphology

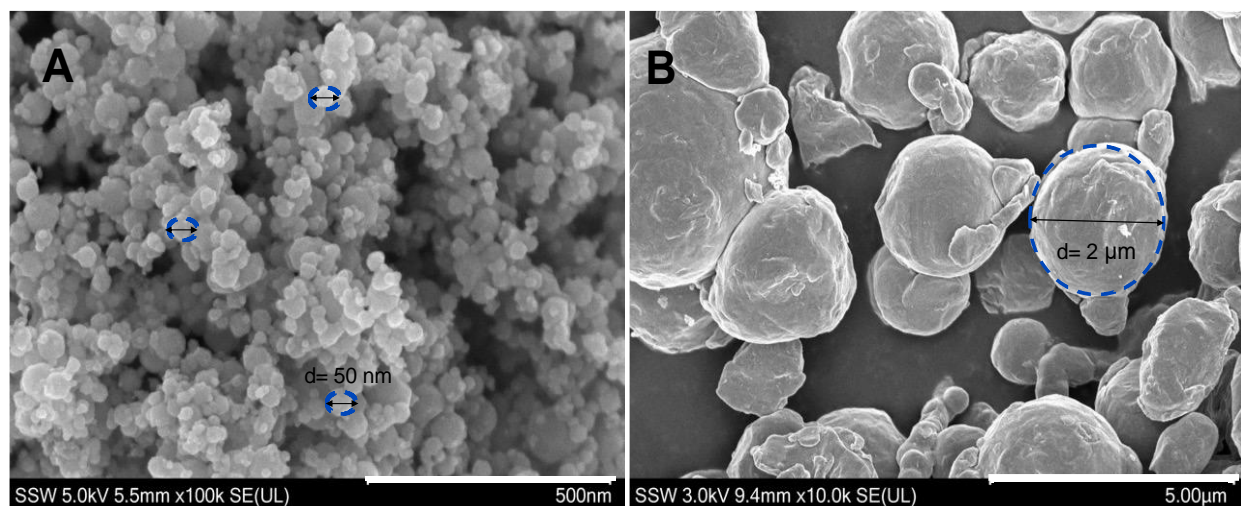


Figure 5.1: SEM images of Fe_3O_4 A) Nano-particles and B) Micro-particles used as catalysts.

The initial SEM images revealed that the catalysts of interest for this investigation were predominantly non-porous in nature. The nano-sized Fe_3O_4 particles had an average diameter of approximately 50 nm, while the micro-sized particles had an average diameter that primarily fall in the range of 1-2 μm . The particles had smooth surfaces and dense morphologies, indicating a high level of homogeneity. More SEM images can be found in Appendix B. Energy dispersive X-ray analysis (EDX) confirmed the presence of iron, oxygen, and carbon, which was consistent with the expected composition of iron oxide catalysts, in addition to sulfur in the FeS catalyst, as

expected. The absence of other elements or impurities suggested a high degree of purity in the particles. These observations suggest that the non-porous particles possess favorable properties for application as a catalyst in bitumen upgrading processes.

5.3.2 Catalytic Effect of Fe-based Nano-Catalysts

The effect of iron oxidation state

Table 5.3: Property measurements for the upgraded oil with and without 0.5wt% of Fe-based nanocatalysts upgraded at 400°C for 120 minutes.

Property	Upgraded with no catalyst	Upgraded with Fe Nanoparticles	Upgraded with FeO Nanoparticles	Upgraded with Fe ₂ O ₃ Nanoparticles	Upgraded with Fe ₃ O ₄ Nanoparticles	Upgraded with FeS Nanoparticles
Yield (wt%)						
Gas	5.2	6.0	7.7	7.4	7.6	7.9
Liquid	93.8	87.0	84.6	86.5	86.0	86.6
Coke	0.0	4.9	5.4	4.9	5.1	5.5
Physical Properties						
Density (kg/m ³)	990	980	970	980	975	970
Viscosity (mPa.s or Cp) at 20°C	1700	500	270	560	320	230
Sulfur Content (wt%)	3.54	3.30	3.19	3.22	3.21	3.25
Desulfurization (%)	24.2	29.4	31.7	31.1	31.3	30.4
SARA fractions (wt%)						
Saturates	19.0	23.1	23.5	23.1	23.4	24.1
Aromatics	53.1	40.2	37.9	41.0	40.9	40.4
Resins	10.8	26.3	29.8	23.7	26.0	27.3
Asphaltenes	13.2	7.4	6.7	9.2	6.8	6.2
R/A ratio	0.82	3.55	4.45	2.58	3.82	4.40
Distillation Fractions via TGA (wt%)						
(<175°C) Naphtha	8.3	5.6	5.6	6.8	6.2	6.1
(175-343°C) Light Gas oil	30.9	36.4	33.1	31.7	30.6	34.2
(343-525°C) Heavy Gas oil	25.6	37.7	41.0	39.2	43.0	38.1
(525°C+) Vacuum residue,	35.2	20.2	20.3	22.3	20.2	21.6
Res. Conversion (%)	(28.3)	(58.8)	(58.7)	(54.6)	(58.8)	(56.0)

Viscosity and Density:

Table 5.3 demonstrates the significant impact of various iron-based catalysts on the physical properties of upgraded bitumen. The uncatalyzed sample resulted in a density of 990 kg/m³ and a viscosity of 1700 cP, whereas samples upgraded with Fe, FeO, Fe₂O₃, Fe₃O₄, and FeS catalysts displayed substantially lower viscosity values while minorly reducing the density values, indicating successful partial upgrading. FeS, FeO, and Fe₃O₄ nanoparticles were particularly effective in reducing the viscosity to the final values of 230, 270, and 320 cP, respectively. These results primarily indicate that the Fe valence state plays a crucial role in bitumen's partial upgrading. Catalysts like FeS, FeO, and, to a lesser extent, Fe₃O₄ nanoparticles (which can be regarded as an equimolar mixture of FeO and Fe₂O₃), contain Fe in its lower valence state (Fe²⁺), demonstrated the most effective viscosity reduction. This finding suggests that a lower Fe valence state promotes hydrocarbon cracking. Conversely, the Fe₂O₃ nanoparticles catalyst, containing Fe in its highest valence state (Fe³⁺), proved least effective as the obtained bitumen exhibits relatively higher density and viscosity. This outcome could be attributed to the fact that Fe³⁺, which has higher electronegativity, is less active at activating the C-H bond than Fe²⁺ [143]. These findings indicate that the catalytic activity of iron-base catalysts for bitumen partial upgrading is strongly influenced by the Fe valence state, with lower valence states of Fe demonstrating greater efficiency in activating the C-H bond so that the viscosity of upgraded bitumen is significantly reduced. To gain a deeper insight into the underlying mechanisms governing these observations and optimize catalyst properties for bitumen upgrading applications, further investigations are needed, which will be explored in the following sections.

SARA Analysis:

The introduction of iron-based catalysts had a significant impact on the SARA fractions of the upgraded bitumen, leading to significant improvement in the oil stability and quality compared to the bitumen upgraded without using a catalyst, as evidenced by the data shown in Table 5.3. In the presence of catalysts, the saturates and resins fractions in the upgraded bitumen were higher compared to those without catalysts, while the aromatics and asphaltenes fractions were lower. Among the catalysts, FeS, FeO, and Fe₃O₄ nanoparticles exhibited the highest increase in saturates, highlighting their effectiveness in breaking down larger molecules into smaller, saturated

hydrocarbons. A reduction in the aromatics fraction was observed for all iron-based catalysts, with FeO showing the most significant decrease. The reduction indicates that the catalysts encourage direct scission of the C-H bond, converting resins and asphaltene into saturates and lighter products. The higher resins content in upgraded bitumen (with the presence of catalysts) helps maintain the stability of the upgraded bitumen, as resins act as natural surfactants stabilizing asphaltenes. The stability of asphaltenes in the upgraded oil was evaluated by assessing the resin-to-asphaltene (R/A) ratio, a commonly used qualitative indicator of asphaltene aggregation and precipitation in the literature [144]. The R/A ratio provides insights into the stability of the upgraded oil and the effects of the Fe catalysts on asphaltene behavior. In this study, the addition of Fe catalysts led to a significant increase in the R/A ratio compared to the non-catalyzed sample. Specifically, the R/A ratio of the upgraded oil increased from 0.82 to values ranging between 3-4, depending on the specific catalyst used. This elevated R/A ratio suggests an enhancement in asphaltene stability within the upgraded oil. The catalysts also effectively reduced the asphaltene fraction within the upgraded oil, with the most significant reduction observed for FeO nanoparticles, followed closely by FeS and Fe₃O₄. The decrease in asphaltene results from the promotion of reactions like hydrogenation, cracking, or dealkylation, transforming these heavy compounds into lighter and more stable components [15]. As a result, the use of iron-based catalysts, particularly those with lower Fe valence states, positively affected the SARA fractions, leading to enhanced stability and quality of the upgraded bitumen.

Liquid product distribution via TGA:

Thermogravimetric Analysis (TGA) involves measuring the sample's weight loss as it is heated at a constant rate, and this loss of weight can be used to determine the amount and timing of the different fractions that are released during thermal decomposition. The liquid fraction distribution can be inferred from the TGA curves by analyzing the rate of weight loss at different temperature ranges and correlating these with the boiling points of the different fractions in the bitumen. Several studies have successfully used TGA to analyze the liquid fraction distribution in bitumen and its products of upgrading, including the work by Kök et al. [145] and Wang et al. [146].

The results presented in Figure 5.2A and Table 5.3 illustrated the mass fractions of different fractions in the upgraded bitumen samples that were treated using different Fe-based catalysts. The

mass fractions were determined for four fractions: light naphtha (R1), light gas oil (R2), heavy gas oil (R3), and vacuum residue (R4). The results indicated that the use of Fe-based catalysts had a significant impact on the mass fraction distribution of the different fractions. For instance, the light naphtha fraction was found to be the highest for the sample that was upgraded without catalyst (8.3 wt%), followed by that upgraded with Fe_2O_3 (6.8 wt%) and Fe_3O_4 (6.2 wt%). These results suggest that the Fe_2O_3 catalyst is particularly effective in promoting the formation of lighter products. On the other hand, the vacuum residue fraction is lowest for the samples upgraded with Fe, FeO, and Fe_3O_4 accounting for more than 58% residue conversion, indicating that these catalysts are more effective in reducing the vacuum residue content compared to the other catalysts. The highest vacuum residue fraction is found in the sample upgraded with no catalyst which resulted in only 28% residue conversion from the original bitumen, suggesting that the presence of Fe-based catalysts generally results in a lower vacuum residue content. As a result, it can be concluded that all the Fe-based catalysts had a great impact on the degree of residue conversion; however, different valency states of Fe-based catalysts influenced the product distribution of the upgraded bitumen differently.

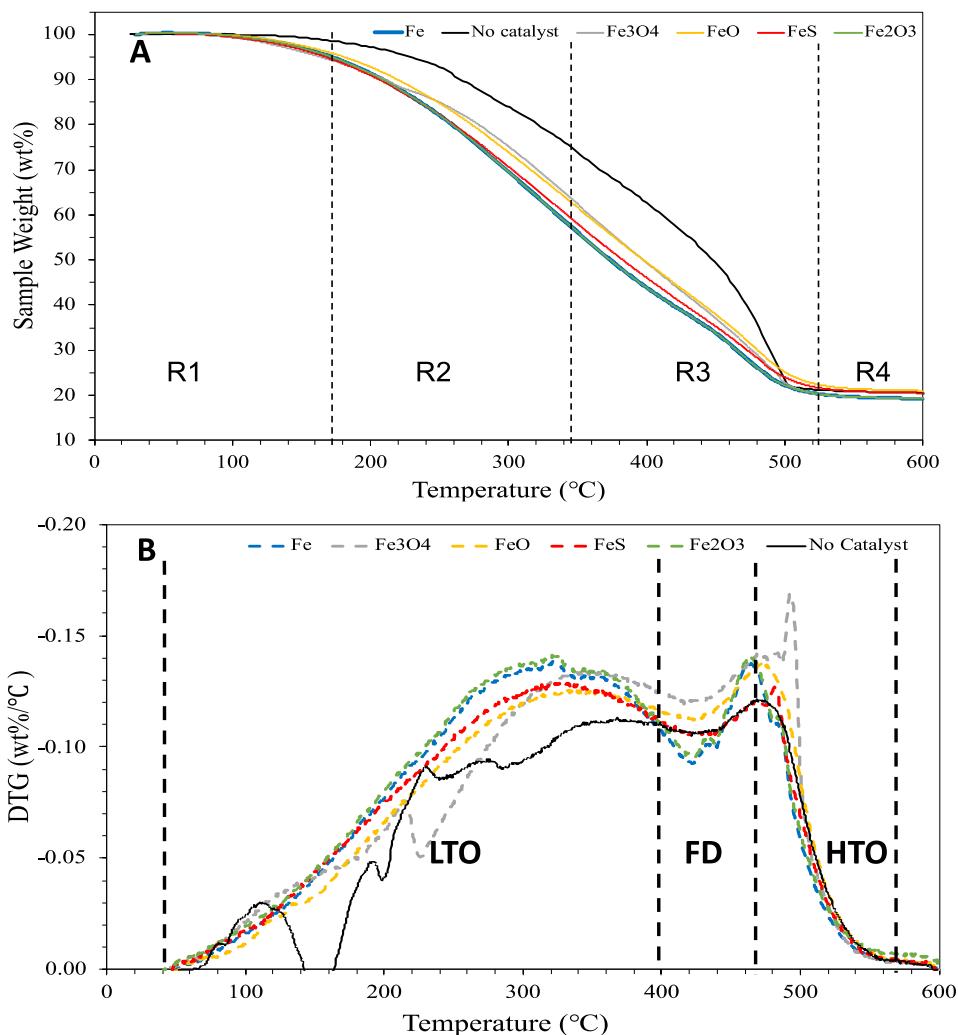


Figure 5.2: A) TGA and B) DTG plots for liquid oil samples upgraded with 0.5wt% Fe-based catalysts.

Figure 5.2B showed the DTG curves for upgraded bitumen samples obtained using different Fe-based catalysts. Despite being heated in an inert (N_2) environment, the DTG results exhibit an excellent fit with the combustion kinetics of heavy oil. The curves were segmented into three distinct reaction zones, namely low-temperature oxidation (LTO), fuel deposition (FD), and high-temperature oxidation (HTO) that were identified and extensively investigated for in situ combustion of heavy oil [147]. The temperature intervals for each of the three reaction zones (LTO, FD, HTO) were identified using the endpoints of the DTG curves. These endpoints were determined by locating the inflection points on the DTG curves, which is used to establish the starting and ending temperatures of each zone, referred to as T_{min} and T_{max} , respectively. A

summary of the reaction intervals and total mass loss at different heating rates is provided in Table 5.4.

Table 5.4: Reaction interval and mass loss for each reaction zone for the upgraded oil with Fe-based catalyst.

Sample	LTO			FD			HTO		
	T _{min}	T _{max}	Mass loss (%)	T _{min}	T _{max}	Mass loss (%)	T _{min}	T _{max}	Mass loss (%)
No Catalyst	60	380	78.2	380	490	9.4	490	600	12.4
Fe	60	420	60.2	420	490	15.9	490	600	23.9
Fe ₃ O ₄	60	420	55.6	420	500	21.6	500	600	22.8
FeO	60	430	57.4	430	480	12.5	480	600	30.1
FeS	60	440	62.6	440	480	9.2	480	600	28.2
Fe ₂ O ₃	60	420	60.2	420	490	15.9	490	600	23.9

The data presented in Table 5.4 revealed a significant mass loss in the LTO zone, attributed to the evaporation of lighter components. The addition of 0.5 wt% of Fe-based nanocatalysts resulted in a decrease in the mass loss within the LTO zone, indicating the occurrence of catalyzed LTO reactions. In the FD zone, cracking reactions took place, causing heavier components and LTO products to produce lighter components with higher H/C ratios and coke residue. To develop a kinetic model from the TGA results, the methodology reported by Esmailnezhad et. al. [148] was employed in this work. First, the extent of conversion (α) vs. temperature (T) data for the three reaction zones were analyzed (Figure 5.3). TG data was converted to the oil fraction conversion (α) for the three reaction zones of all experiments, in which α is defined as

$$\alpha = \frac{(M_0 - M_T)}{(M_0 - M_L)} \quad (\text{Eq. 5.2})$$

With M_0 being the initial mass of the oil sample at T_{\min} of each reaction zone, M_T being the mass left at the particular temperature in which the conversion is being determined and M_L being the mass of the sample left at the end point temperature (T_{\max}) of each reaction zone as determined in Table 5.4. For each of the zones (LTO, FD and HTO), Equation 2 was applied separately to

calculate the conversion (α) within that specific zone. This was used to normalize the conversion for each individual zone to a range of 0-1.0. This normalization enables a detailed analysis of each reaction zone independently. As a result of the above approach, each zone has its own conversion profile ranging from 0 to 1.0 as shown in Figure 5.3. The α -T curves in the LTO zone follow a power-law trend, indicating acceleratory rate reactions. The α -T curves in the FD zone follow a linear trend, while those in the HTO zone follow a sigmoid trend, suggesting controlling mechanisms in the reaction pathway.

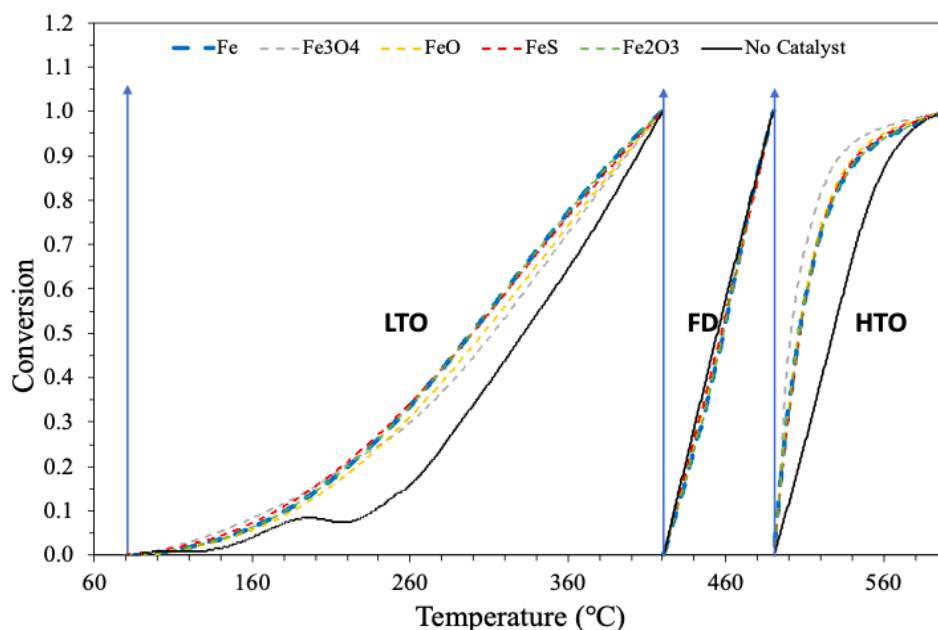


Figure 5.3: Conversion (α) vs Temp curves of different oxidation zones of upgraded oil + 0.5 wt% Fe-based nanocatalysts.

Next, the modified distributed activation energy model (DAEM) was used to determine the apparent activation energy and pre-exponential factor for each reaction zone (Figure 5.4). The variation of activation energy is evaluated and compared for the 3 different reaction regions of all samples. Miura and Maki [149] simplified the DAEM to directly evaluate both $E\alpha$ and $A\alpha$ in different conversions. The simplified DAEM may be written as Eq. (3).

$$\ln\left(\frac{\alpha}{T^2}\right) = \ln\left(\frac{A^*R}{E\alpha}\right) + 0.6075 - \frac{E\alpha}{RT} \quad (\text{Eq. 5.3})$$

By plotting $\ln(\alpha/T^2)$ versus $1/T$ at each conversion degree, the slope will yield the activation energy and the y-intercept will yield $\ln(AR/E_a)$ at that conversion. The results suggested that the complex components of the oil samples underwent diverse reactions at different temperatures. To capture these multiple reactions, a kinetic model can be utilized by varying the apparent activation energy with conversion.

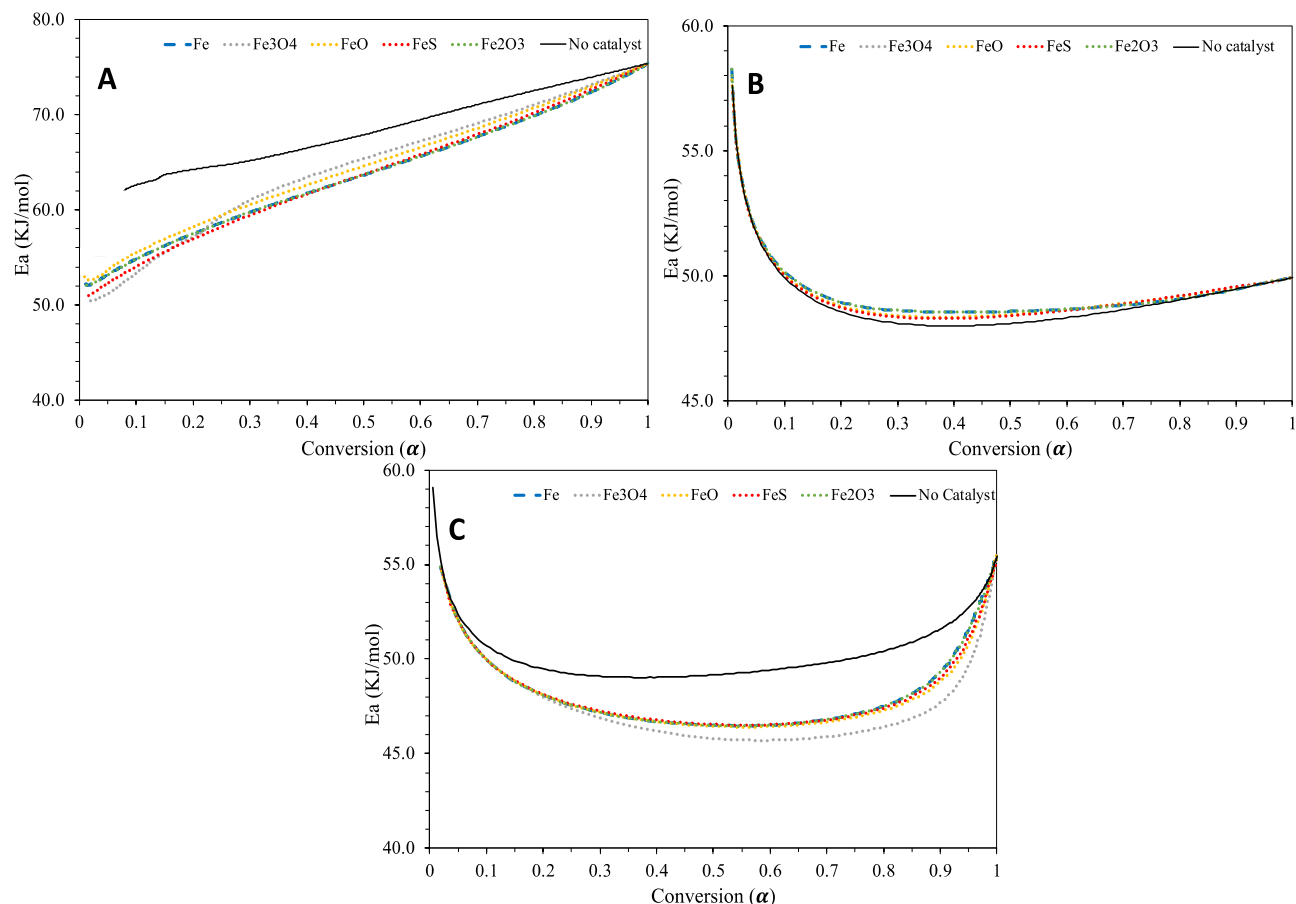


Figure 5.4: Variation of activation energy with conversion during (a) LTO, (b) FD, and (c) HTO reaction zones of upgraded bitumen with 0.5 wt% of Fe-based nanocatalysts.

The investigation of the upgraded oil with different Fe-based nano-catalysts revealed the presence of three distinct reaction zones (LTO, FD, and HTO). These zones exhibited unique trends in apparent activation energy distribution with conversion, suggesting the need for different model representations for each zone. The analysis of conversion-temperature curves and determination of the activation energies and pre-exponential factors for each reaction zone indicated that Fe-based catalysts effectively catalyze LTO reactions, leading to a reduction in endpoint temperature,

peak temperature, and mass loss in this zone. Furthermore, the adapted kinetic model highlights the influence of Fe-based catalysts on the reaction mechanisms, as evidenced by distinct trends in α -T curves for each zone. The variation of apparent activation energy with conversion highlights the involvement of multiple components in various reactions at different temperatures. It is important to note that in the present study, the kinetic analysis was conducted using a single heating rate, focusing on the qualitative observation of the effect of the Fe-based catalyst on the apparent activation energy (E_a) of the upgraded oil. While this approach provided valuable insights, it must be noted that a more rigorous and accurate determination of E_a values would necessitate conducting thermal gravimetric analysis (TGA) at a minimum of four different heating rates, in line with the recommendations set forth by the ICTAC Kinetics Committee [150]. However, this study sets the stage for future work that can build upon our findings, employing more detailed kinetic modeling with varied heating rates to refine the understanding of the catalytic effects on bitumen upgrading.

Desulfurization

The XRF results presented in Table 5.3 demonstrated the positive impact of all catalysts used in the study on reducing the sulfur content of the upgraded bitumen samples in comparison to the original bitumen sample. This finding indicated that the catalysts were effective in promoting the desulfurization reactions during the upgrading process. The FeO catalyst was observed to produce the greatest reduction in sulfur content, where the original bitumen sample with a sulfur content of 4.67 wt% was reduced to 3.19 wt%. This suggested the superior efficiency of the FeO catalyst in promoting desulfurization reactions without the use of an external supply/source of hydrogen gas. The upgraded bitumen samples using Fe₂O₃, and Fe₃O₄ catalysts also showed a great reduction in sulfur content compared to the original bitumen sample, with a comparable effect to the FeO catalyst. Interestingly, the upgraded bitumen sample using the FeS catalyst exhibited a slightly higher sulfur content compared to the other upgraded samples, possibly indicating its inferior effectiveness in promoting desulfurization reactions relative to the other catalysts used in the study.

Gas product analysis

The data in Table 5.5 shows the concentrations of gas products and the average molecular mass obtained from the upgrading of bitumen using different Fe catalysts. It can be observed that the

use of Fe-based catalysts leads to an increase in the concentrations of the lighter hydrocarbons especially CH₄, while the concentrations of heavier hydrocarbons such as C₃H₈, C₄H₁₀, and n-C₅H₁₂ decrease compared to the upgrading without a catalyst. This indicates that the Fe catalysts promote cracking and fragmentation of heavy hydrocarbons into lighter ones. The average molecular mass of the gas products is also significantly reduced when using the Fe catalysts, with the lowest average molecular mass observed for the upgrading with Fe₃O₄. This again suggests that the Fe-based catalysts promote cracking and fragmentation of the heavy hydrocarbons, leading to the production of lighter hydrocarbons. Furthermore, the data analysis reveals a significant reduction in H₂S content in the gas products when bitumen is upgraded with Fe-based catalysts, particularly Fe₃O₄. This observation indicates that Fe-based catalysts effectively react with the H₂S produced during the reaction, resulting in a decrease in its content. The interaction between Fe-based catalysts and H₂S most probably facilitates the formation of metal sulfides during the bitumen upgrading process. It is worth noting that this phenomenon was not observed in the sample treated with FeS nanoparticles. In this case, the presence of FeS nanoparticles led to an increase in the overall sulfur (S) content in the system, resulting in a slight increase in H₂S emission levels.

Table 5.5: Concentrations and average molecular mass of gas products using different Fe catalyst– Ave. values (values are recorded as mass fractions per gram of gas released per gram of bitumen reacted).

Composition (ppm)	Upgraded with No catalyst	Upgraded with Fe	Upgraded with FeO	Upgraded with Fe ₂ O ₃	Upgraded with Fe ₃ O ₄	Upgraded with FeS
CH ₄	27499	33748	32518	32433	37089	35634
C ₂ H ₄	206	52	676	112	546	148
C ₂ H ₆	6879	5204	4598	5884	6056	5777
C ₃ H ₈	4558	1256	127	3209	857	675
C ₄ H ₁₀	295	26	371	112	24	66
C ₅ H ₁₂	723	240	153	326	263	245
n-C ₅ H ₁₂	976	209	79	370	215	169
CO	2632	1060	1658	2140	972	1253
CO ₂	1372	733	689	1118	713	772
H ₂ S	4985	1147	2748	2869	1135	6340
Ave. molecular mass (g/mol)	24.56	20.35	20.43	22.68	20.08	21.43

The Effect of Catalyst Particle Size

Table 5.6 presents the results of an investigation into the effect of particle size on the catalytic activity of iron-based catalysts, demonstrating the variation in activity with different particle sizes. The results presented in Table 5.6 indicated that particle size had an impact on the catalytic activity of iron-based catalysts in the partial upgrading of bitumen. The comparison of the density and viscosity of upgraded bitumen samples treated with nano-sized and micro-sized iron-based catalysts revealed that nanoparticles exhibited superior viscosity reduction. For instance, employing Fe nanoparticles yielded a viscosity of 500 cP, while Fe microparticles yielded a higher viscosity of 790 cP. Similarly, Fe₂O₃ and Fe₃O₄ nanoparticles demonstrated slightly lower viscosities (560 cP and 320 cP, respectively) compared to their microparticle counterparts (620 cP and 370 cP, respectively). These findings suggested that smaller particle size and high specific surface of iron-based nanoparticles enhances the catalytic activity. The difference in viscosity reduction is especially evident when comparing the performance of Fe nanoparticles with microparticles, which could be attributed to the unique properties of Fe catalysts or differences in their interaction with bitumen components [139]. The underlying mechanisms responsible for this enhanced performance of nanoparticles required further investigation.

However, when evaluating other parameters such as coke suppression, SARA fractions, and the degree of desulfurization, no substantial improvement was observed for nanoparticles compared to microparticles. This observation aligns with a study conducted by AlMarshed et al. [151], which demonstrated that unsupported Fe₂O₃ catalysts of different particle sizes exhibited similar activity in terms of product distribution, physical properties, and product quality of the produced oil under high reaction conditions. Despite the higher surface area-to-volume ratio of the 50 nm particles compared to the 5 μm particles investigated, their size did not significantly impact the upgrading or coke deposit.

Table 5.6: Measurements for the upgraded oil using 0.5wt% of Fe-based nano and micro-catalysts at 400°C.

Property	No catalyst	Fe Nano (<100nm)	Fe Micro (<1µm)	Fe ₂ O ₃ Nano (<50nm)	Fe ₂ O ₃ Micro (<1µm)	Fe ₃ O ₄ Nano (<50nm)	Fe ₃ O ₄ Micro (<1µm)
Yield (wt%)							
Gas	5.2	6.0	5.6	7.4	5.9	7.6	7.2
Liquid	93.8	87.0	87.6	86.5	87.8	86.0	86.3
Coke	0.0	4.9	4.7	4.9	4.5	5.1	5.0
Physical Properties							
Density (kg/m ³)	990	980	980	980	980	975	975
Viscosity (Cp)	1700	500	790	560	620	320	370
Sulfur Content (wt%)	3.54	3.30	3.45	3.22	3.39	3.21	3.21
HDS (%)	24.2	29.4	26.1	31.1	27.4	31.3	31.2
SARA fractions (wt%)							
Saturates	19.0	23.1	22.4	23.1	22.3	23.4	23.2
Aromatics	53.1	40.2	40.6	41.0	43.0	40.9	39.0
Resins	10.8	26.3	22.8	23.7	20.9	26.0	26.1
Asphaltenes	13.2	7.4	11.2	9.2	10.8	6.7	6.9

The Effect of Catalyst Concentration

To determine the optimal catalyst concentration for achieving the highest degree of bitumen upgrading, various catalyst concentrations ranging from 0 to 1.0 wt% were examined to understand the variation of bitumen conversion with catalyst concentration and the results are shown in Figure 5.5. It is important to note that the data in Figure 5.5 was presented using a continuous line to show the trend of viscosity reduction as the concentration of Fe-based catalysts increased. The purpose of the “dashed interpreted lines” was to illustrate the general trend of viscosity reduction based on the measured data points, which were represented by dots.

The results as shown in Figure 5.5 indicated that the optimal catalyst concentration for all iron-based catalysts is 0.5 wt%, resulting in the lowest viscosity values, indicating a higher degree of bitumen upgrading. Increasing the concentration beyond 0.5 wt% led to a rise in viscosity. Among the tested catalysts, FeS exhibits the most effectiveness in reducing bitumen viscosity at the optimal concentration of 0.5 wt%, followed by FeO and then Fe₃O₄. These results enhance our

understanding of the role of iron-based catalysts in bitumen upgrading and provide valuable insights for optimizing catalyst concentrations to achieve improved upgrading performance.

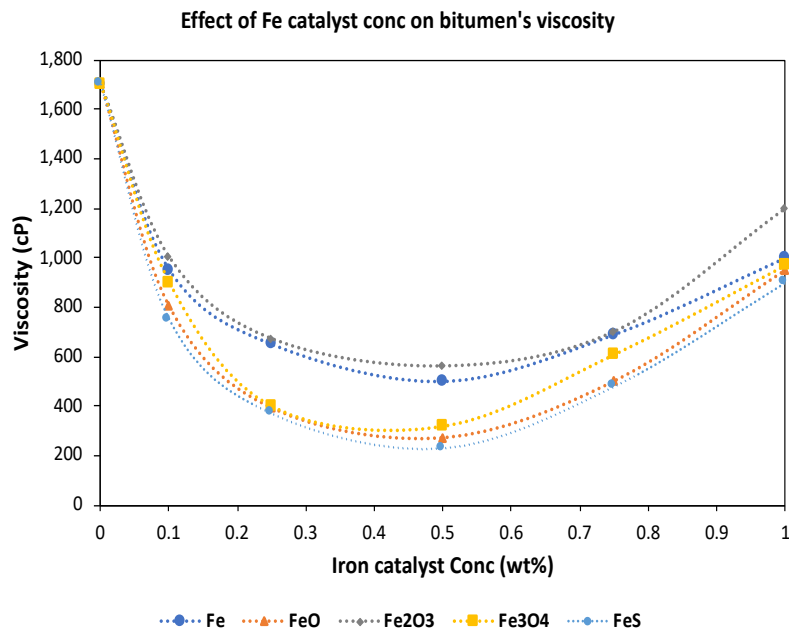


Figure 5.5: Viscosity of the upgraded bitumen at various catalyst concentrations.

The increase in viscosity observed at higher catalyst concentrations beyond 0.5 wt% in the bitumen upgrading process can be attributed to several factors. One explanation is the occurrence of undesired side reactions, such as polymerization or condensation, which can lead to an increase in molecular weight and, subsequently, viscosity. Another possibility is the formation of solid or semi-solid compounds by the catalyst, which may contribute to the viscosity increase [51]. The coordination of metal species with asphaltene structures is considered a detrimental process that can increase the viscosity beyond the optimal concentration. This reaction is metal concentration-dependent, with higher concentrations promoting increased complexity in asphaltenic structures through coordination reactions, thereby elevating oil viscosity [152]. Additionally, the attachment of asphaltene molecules to metal particles, primarily due to the Ostwald ripening process, could serve as a non-chemical mechanism for viscosity reduction [139]. Therefore, several factors must be considered when optimizing catalyst concentrations for the bitumen upgrading process to avoid unintended consequences on the viscosity of the upgraded product.

5.3.3 Screening for the Best Catalyst

To systematically identify the optimal catalyst for the partial upgrading of bitumen, a comprehensive screening process using Minitab statistical software was used to analyze and compare the performance of the five investigated catalysts. This analysis aimed to determine the best combination of factors that maximize liquid oil yield, minimize asphaltene content, and enhance viscosity reduction in the upgraded bitumen. A Pareto chart was generated to visualize the relative impact of each factor on the upgrading process, enabling us to prioritize the most influential parameters.

Employing a multi-objective optimization approach, the ideal combination of catalyst type, concentration, and particle size to achieve the desired performance metrics was examined. Utilizing Minitab's advanced statistical tools, a Design of Experiments (DOE) analysis was conducted to systematically study the relationships between these factors and their influence on the upgrading process. To provide a better understanding of the input parameters used for the DoE and validation process, the following examples are provided: a) Catalyst concentration: The levels were defined as low (e.g., 0.1 wt%), medium (e.g., 0.5 wt%), and high (e.g., 1.0 wt%). b) Catalyst particle size: The levels were defined as small (e.g., 10 nm), medium (e.g., 50 nm), and large (e.g., 100 nm). c) Oxidation state of iron: The levels were defined as high (e.g., Fe_2O_3), medium (e.g., Fe_3O_4), and low (e.g., FeO).

The analysis of the resulting data was used to establish a model that accounts for the interactions and main effects of these factors on the bitumen upgrading process. As illustrated in Figure 5.6A, the catalyst type emerged as the primary contributor to the overall upgrading process, followed by catalyst concentration and then the particle size. Using Minitab's optimization algorithms, the optimal combination of catalyst type, concentration, and particle size that simultaneously maximizes liquid yield, minimizes asphaltene content and maximizes viscosity reduction for the best partial upgrading results were identified. Figure 5.6B demonstrates that the optimum condition achieves a viscosity of 370 cp, with a maximum 86% liquid yield, and an asphaltene content of 7wt%. This optimal performance can be attained by employing Fe_3O_4 nanoparticles at a 0.5wt% loading. Consequently, this combination was selected for further study, and additional characterization tests for both the fresh and spent Fe_3O_4 catalyst will be conducted to better understand the bitumen partial upgrading mechanism in the following sections.

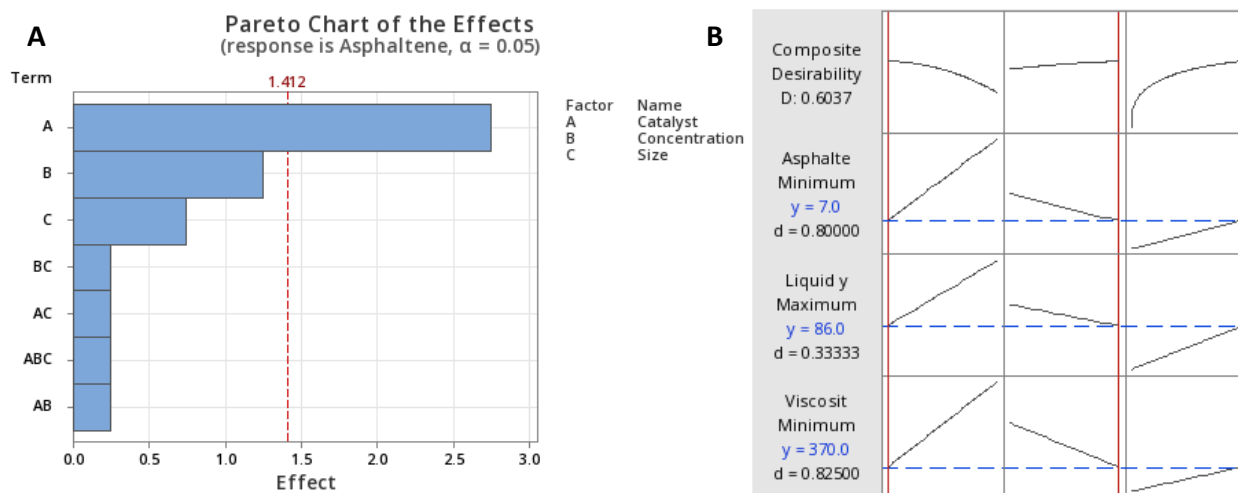


Figure 5.6: A) Pareto chart for the effects of various catalyst parameters B) Minitab optimized results for max liquid yield, viscosity reduction, and minimum asphaltene content.

5.3.4 Catalyst Characterization

Magnetic properties Via VSM

Figure 5.7 displays the Vibrating Sample Magnetometer (VSM) results for the Fe_3O_4 catalyst both before and after the catalytic upgrading process. The VSM results reveal that the Fe_3O_4 nanocatalysts exhibit significant magnetic properties prior to and following the upgrading reaction, indicating their potential for easy magnetic adsorption in order to facilitate recycling or reuse in partial upgrading facilities. Fe_3O_4 is a ferrimagnetic material, meaning that it exhibits spontaneous magnetization even in the absence of an external magnetic field. This property also makes Fe_3O_4 a superior catalyst when compared to other previously discussed catalysts such as FeS or FeO . However, a noticeable decrease in the magnetic saturation point, from approximately 80 emu/g to 15.5 emu/g after the upgrading process, can be attributed to the effects of elevated temperature on the magnetic nanoparticles as well as potential coke deposition on the catalyst's surface.

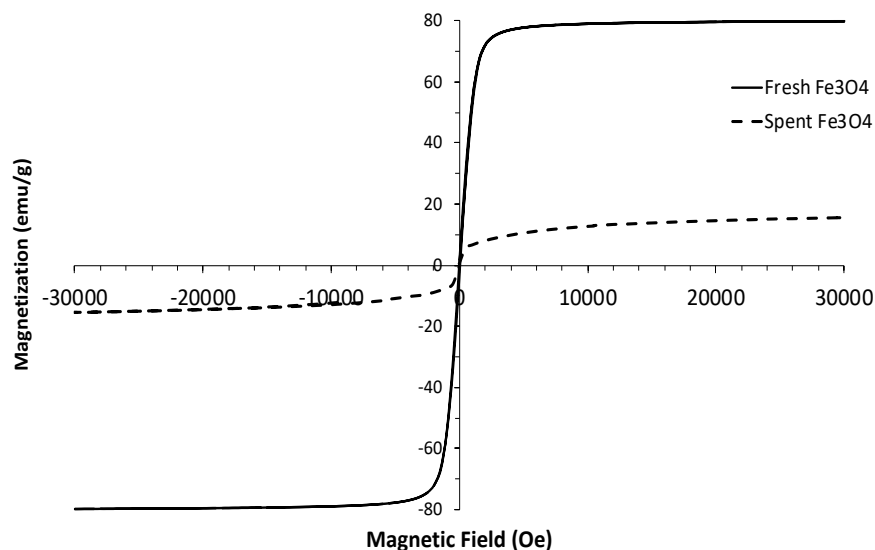


Figure 5.7: Magnetization saturation measurements for fresh and spent Fe_3O_4 nanocatalyst.

Catalyst characterization Via SEM

The Scanning electron microscopy (SEM) images presented in Figure 5.8 revealed that there were no significant visible alterations in the morphology of the catalysts before and after the upgrading reactions, nor evidence of bulk aggregation or fragmentation during the upgrading process. A comparison of particle diameters before and after upgrading showed minor to no changes. While new phase formation and alterations in the crystalline structure are still possible, such conclusions can be only confirmed by XRD and XPS analysis which will be discussed in the subsequent sections.

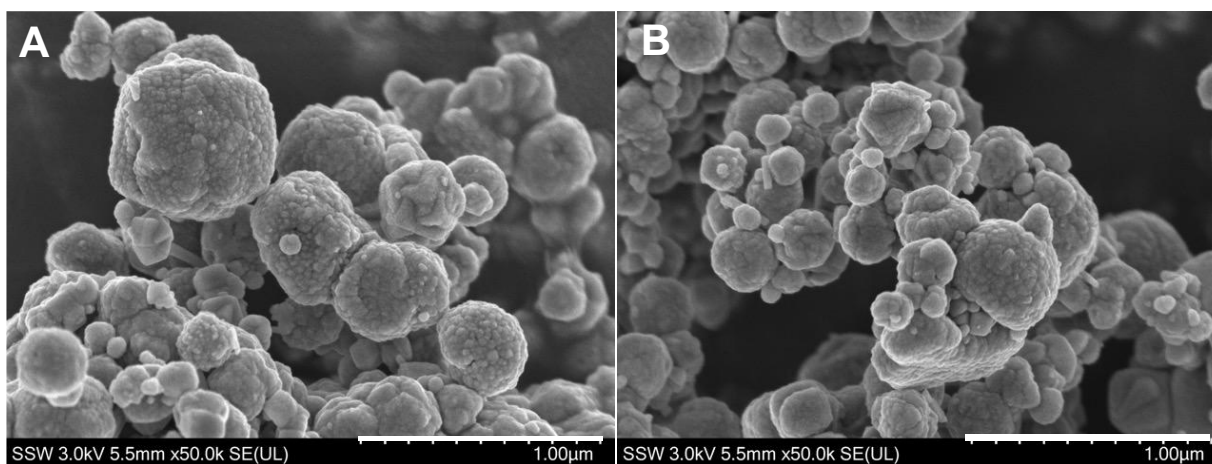


Figure 5.8: SEM images of A) fresh Fe_3O_4 nanocatalyst and B) spent Fe_3O_4 nanocatalyst.

Catalyst characterization Via XRD

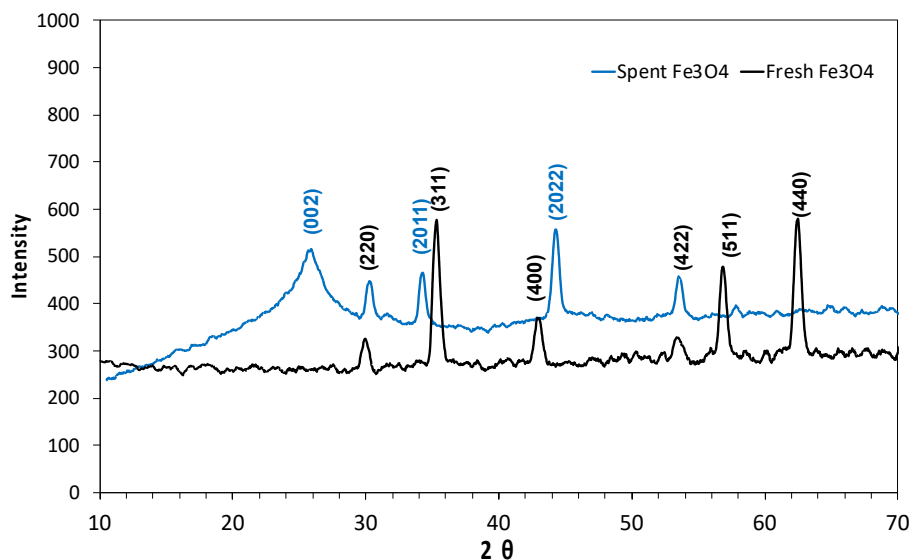


Figure 5.9: XRD for the fresh and spent Fe₃O₄ nanocatalyst.

The X-ray diffraction patterns for both fresh and spent Fe₃O₄ catalysts are shown in Figure 5.9, revealing several crystalline phases. The fresh catalyst displayed reflections at $2\theta = 30.1^\circ$, 35.4° , 43.1° , 53.1° , 56.9° , and 62.5° , corresponding to the planes (220), (311), (400), (422), (511), and (440) respectively, indicating the presence of the magnetite phase (Fe₃O₄) as reported in [153]. On the other hand, the spent catalyst exhibited additional reflections at $2\theta = 33.8^\circ$, 43.7° , and 53.1° , corresponding to the planes (2011), (2022), and (422) respectively, representing the pyrrhotite phase (Fe_{1-x}S). These results demonstrated that dispersed catalysts are activated during the heating and reaction stages, consistent with previous studies on transition metal catalysts [151]. This observation suggests that the first step of the reaction mechanism is the sulfidation of iron nanoparticles, where the iron or iron oxide particles react with S to generate an active iron sulfide species (Fe_{1-x}S) during the heating stage. Another notable difference is the presence of the (002) peak at 26° , which indicates coke deposition on the Fe₃O₄ catalyst's surface. This observation suggests that the final step of the reaction mechanism contains some side reactions such as polymerization or condensation of aromatic compounds which in turn lead to coke formation on the catalyst surface. Using Scherrer's formula and the (311) diffraction peak, the crystallite size of the Fe₃O₄ nanoparticles was calculated. The fresh catalyst's crystalline size was determined to be 33.6 nm, while the spent catalyst's size was 35.2 nm. The similar crystalline structures in both fresh and spent Fe₃O₄ nanoparticles suggest their structural consistency [148].

Catalyst characterization Via XPS

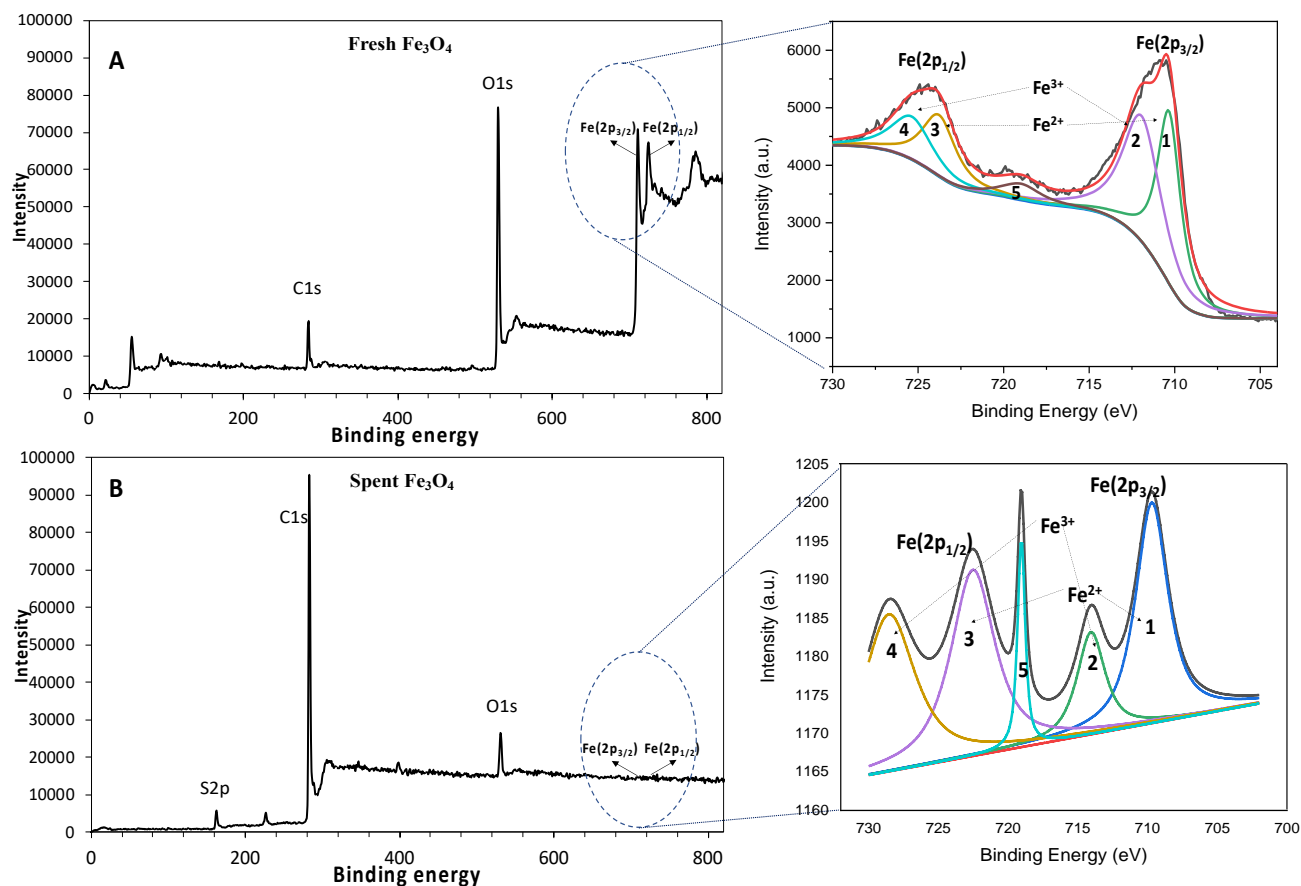


Figure 5.10: XPS plot for the Fe 2p peak for the A) fresh Fe_3O_4 nanocatalyst and B) spent Fe_3O_4 nanocatalyst.

Figure 5.10 presents the X-ray Photoelectron Spectroscopy (XPS) spectra for both the fresh and spent Fe_3O_4 nanocatalysts, providing insights into their chemical composition and the oxidation state of Fe within the catalyst before and following the upgrading reaction. In the binding energy range of 705 to 730 eV, five peaks were fitted, corresponding to the binding energies of 710, 712, 723, 725, and 717 eV, signifying the presence of both Fe^{2+} and Fe^{3+} species. Peaks 1 and 3 were associated with Fe^{2+} species, while peaks 2 and 4 were associated with Fe^{3+} species. By analyzing the area of these peaks, a $\text{Fe}^{2+}/\text{Fe}^{3+}$ ratio of approximately 52:48 was determined.

In the case of the spent catalyst, the signal corresponding to O1s showed a considerable decrease, while the signal associated with C1s exhibited a significant increase. Additionally, a small peak corresponding to the S2p signal emerged at a binding energy of 162 eV, further confirming the

formation of a Fe-S bond and hence the conversion of some of the Fe_3O_4 to FeS as a result of the upgrading reaction. As a result, the signals for the Fe2p peak diminished considerably for the spent catalyst; however, small peaks were still detected, and the area of these peaks indicated a similar $\text{Fe}^{2+}/\text{Fe}^{3+}$ ratio as observed in the fresh catalyst signal.

5.3.5 Proposed Mechanism for Bitumen Partial Upgrading Using Fe-based catalyst

Drawing based on the experimental data collected and discussed earlier, it is possible to propose a detailed discussion of the reaction mechanism to explain the effect of Fe-based catalysts on bitumen partial upgrading. This proposed mechanism is based on our understanding of the witnessed changes and the general principles of catalytic upgrading which in turn will serve as a conceptual framework to explain the observed changes in the upgraded bitumen samples and to provide a basis for further investigations. The mechanism is composed of five main steps, as follows:

Sulfidation of iron nanoparticles (Step 1): in this initiation step the catalyst is activated in situ through a sulfidation reaction between iron nanoparticles and sulfur in heavy oil. At elevated temperatures, the iron catalysts react with the C-S bonds in heavy oil to generate active iron sulfide species (Fe_{1-x}S). The presence of the pyrrhotite phase in the spent catalyst, as confirmed by the XRD analysis (Figure 5.9), supports this step of the proposed mechanism. Sulfidation is crucial for activating the Fe-base catalyst and initiating the subsequent upgrading reactions.

Scission of C-H bond (Step 2): The activated iron sulfide catalyst promotes the scission of the C-H bond, breaking down large asphaltene clusters and resin molecules within the large complex hydrocarbon structure. This leads to increased paraffin structures, improved heavy fraction conversion, and reduced bitumen viscosity. The catalyst's impact on SARA fractions is evident in the increased saturates and reduced asphaltenes, resulting in a decrease in aromatic and naphthenic ring numbers. This step plays a crucial role in upgrading the heavy oil by altering its composition and improving its properties [154].

Cracking reactions (Step 3): In addition to the C-H scission, the Fe-based catalyst also promotes cracking reactions, leading to a higher yield of gas products and a reduction in vacuum residue

content. The concentrations of various gas products, such as CH₄, C₂H₆, and H₂S, are influenced by the specific catalyst used. Different Fe-based catalysts show variations in their gas product profiles. Cracking reactions contribute to the upgrading process by breaking down larger molecules into smaller, less condensed structures [155].

Desulfurization reactions (Step 4): The in-situ generated and then activated FeS species also promotes desulfurization reactions, further removing sulfur from the heavy oil and converting it into hydrogen sulfide (H₂S). This process leads to a general reduction in sulfur content within the upgraded oil, as evidenced by the significant decrease in sulfur content in all the upgraded samples.

Side reactions (Step 5): During the upgrading process, side reactions, such as polymerization or condensation of aromatic compounds, might occur, leading to coke formation, which is mainly influenced by the catalyst type and particle size. Generally, the presence of a catalyst increases coke formation compared to the no catalyst case, but there is variation in coke yield among different types of catalysts and catalyst particle sizes. This suggests that catalysts participate in the side reactions leading to coke formation. It seems that the more active the catalyst is in the cracking reactions, the more coke will be expected to form, as observed by the large carbon peaks detected both by the XRD and XPS spectra.

5.3.6 Comparison of Fe₃O₄ nanoparticles with metallic alloys

A subsequent investigation was carried out to assess and compare the effectiveness of the previously explored iron-based catalysts to the metallic alloys that are frequently used to construct bitumen upgrading reactors. The selected metal alloys, if proven efficient in catalyzing bitumen upgrading, could offer considerable advantages due to their abundance, versatility, and low costs. Furthermore, the process of separation of the catalyst from bitumen oil can be eliminated. However, the use of metallic alloys to construct a bitumen upgrading reactor may raise concerns regarding the dependability and durability of the reactor given that these alloys are involved in catalyzing the bitumen upgrading process.

A thorough elemental analysis was conducted on the three catalyst alloys of interest, as detailed in Table 5.7, to understand how the addition of some extra elements can influence the performance of iron.

Table 5.7: Chemical composition of the Catalyst alloys in (wt%).

Materials	Fe	C	Mn	Cr	Mo	Ni	Si	Cu	P	Co	N	V	Al
Alloy 1	98.23	0.17	1.15	0.04	0.01	0.03	0.34	0.03	0.01	0.00	0.00	0.00	0.00
Alloy 2	89.44	0.11	0.47	8.36	0.90	0.07	0.33	0.00	0.02	0.00	0.04	0.23	0.03
Alloy 3	69.05	0.02	1.19	16.58	2.00	10.01	0.33	0.42	0.03	0.30	0.07	0.00	0.00

Alloy 1 is primarily comprised of 98% Fe, 1.2% Mn, and trace amounts of other metals. Alloy 2, representing an example of ferritic stainless steel, mostly comprising Fe (89%) and Cr (8.4%), with the remainder being minor trace elements. Lastly, Alloy 3, which corresponds to a typical composition of austenitic stainless steel, contains 69% Fe, 16.6% Cr, 10% Ni, 2% Mo, and then some trace elements. The unique compositions of three alloys, which are often employed as building materials for reactors, serve as a foundation for a comprehensive comparison, allowing the identification of alloy elements that play a significant role in upgrading reactions.

Based on the experimental results presented in Table 5.8, the alloys (1, 2, and 3) examined in this study showed a significant catalyzing role in upgrading bitumen at 400°C, compared to the Fe₃O₄ catalyst and the reaction without catalyst. Alloy 1, mainly composed of Fe, exhibited effects similar to those of the Fe₃O₄ catalyst, with comparable impacts on viscosity and SARA fractions and similar mass distributions of gas, liquid, and coke fractions. Alloy 2, a ferritic stainless steel, promoted cracking reactions, resulting in the highest gas yield and lowest liquid yield, but also led to the highest coke formation, indicating a potential for catalyst deactivation and reactor fouling. Lastly, Alloy 3, austenitic stainless steel, displayed similar performance to alloy 2 in terms of viscosity reduction and SARA content, but with reduced coke formation due to the presence of nickel, indicating increased resistance to deactivation. Each alloy possesses unique advantages and limitations in terms of product quality and liquid yield; therefore, a techno-economic analysis is recommended in order to evaluate their feasibility for industrial-scale upgrading processes.

Table 5.8: Property measurements for the upgraded oil using synthesized catalyst alloys at 400°C.

Property	No catalyst	Fe ₃ O ₄ nanocatalyst	Alloy 1	Alloy 2	Alloy 3
Yield (wt%)					
Gas	5.2	7.6	8.4	19.2	10.1
Liquid	93.8	86.0	87.2	58.5	73.5
Coke	0.0	5.1	3.8	22.1	16.3
Physical Properties					
Density (kg/m ³)	990	975	975	970	970
Viscosity (mPa.s or Cp) at 20°C	1700	320	340	90	90
SARA fractions (wt%)					
Saturates	19.0	23.4	22.4	25.2	25.1
Aromatics	53.1	40.9	43.5	48.1	47.5
Resins	10.8	26.0	23.7	17.2	19.2
Asphaltenes	13.2	6.7	9.2	8.4	8.1

5.4 Conclusion

This study investigated the impact of Fe-based catalysts on the partial upgrading of bitumen, demonstrating their effectiveness in promoting upgrading and enhancing the quality of the upgraded oil. The type of catalyst was found to be the most significant factor affecting the upgrading process, with lower valency states of Fe being particularly effective in transforming heavier fractions into lighter ones. FeS, FeO, and Fe₃O₄ catalysts were the most effective in reducing viscosity and increasing the saturate fractions while decreasing the content of aromatics and asphaltenes fractions. Catalyst concentration was also found to be an important factor, with the optimal concentration for all iron-based catalysts being around 0.5 wt%. The use of Fe-based nano-catalysts was shown to have an impact on the physical and chemical properties of upgraded bitumen, leading to a reduction in the endpoint temperature and peak temperature of the LTO zone, as well as promoting cracking and fragmentation of heavy hydrocarbons into lighter ones. Through the use of Minitab statistical software, Fe₃O₄ nanoparticles at a 0.5wt% loading were identified as the optimal concentration for achieving maximum liquid yield, minimum asphaltene content, and maximum viscosity reduction. The VSM results indicated the suitability of Fe₃O₄ nanocatalysts for easy magnetic adsorption, facilitating recycling or reuse in partial upgrading facilities. The XPS spectra revealed the chemical composition and oxidation state of Fe within the catalyst before

and after the upgrading reaction. The XRD patterns revealed the presence of Fe_3O_4 and Fe_{1-x}S phases in fresh and spent catalysts, respectively. Based on the experimental data, a proposed reaction mechanism was established, providing insights into the sulfidation of iron nanoparticles, scission of C-H bond and hydrocarbon cracking, desulfurization reactions, and the formation of undesirable compounds such as coke. These findings provide valuable insights into the catalytic upgrading of bitumen, paving the way for optimizing catalyst properties for bitumen upgrading applications, contributing to the optimization of bitumen resource utilization, and the reduction of environmental impacts associated with the bitumen industry.

Chapter 6 - Enhancing Bitumen Processing with Fe₃O₄ Coated Cenospheres and ANN-Driven Process Optimization: A Novel Approach to Sustainable Partial Upgrading

6 Abstract

This chapter introduces an innovative and greener approach to partially upgrade oil sand bitumen with the aid of a novel catalyst composed of iron-coated cenospheres (Fe-Ceno). Through the use of a combination of Fe²⁺ and Fe³⁺ precursors, the cenospheres were coated with a layer of Fe₃O₄, and the formed catalyst was then characterized in details using Scanning Electron Microscopy (SEM), Energy-Dispersive X-ray Spectroscopy (EDX), X-ray Diffraction (XRD), and X-ray Photoelectron Spectroscopy (XPS) techniques. The characterization tests investigated the new catalyst's morphology, microstructure, crystalline structure, and surface chemistry and confirmed that the coating layer of Fe₃O₄ was uniform and successfully applied. During the catalytic upgrading process, the Fe-Ceno catalyst was dispersed in a liquid hydrogen donor solution to facilitate the transformation of oil sand bitumen into a partially upgraded liquid oil product. The produced (upgraded) oils were subsequently subjected to rigorous Saturates, Aromatics, Resins, and Asphaltenes (SARA) analysis, as well as viscosity, density, Total Acid Number (TAN), oil-asphaltene stability, and olefin content measurements. The findings demonstrated that the introduction of only 1wt% of the Fe-Ceno led to a significant enhancement within the quality of the upgraded oil, noted by the reduced olefin content to below 1 wt%, improved phase stability, and a great reduction in the oils' viscosity and density to values below 300 cP and 940 kg/m³ respectively to meet the pipeline specifications. Additionally, this study builds beyond the experimental approach and develops a customized Artificial Neural Network (ANN) model that can accurately predict the rheological properties of the upgraded bitumen (experimental output) without the need to perform extra time-consuming experiments. The developed AI model can successfully predict values such as viscosity and density for the upgraded oil samples under different catalysts and operating conditions with an R² of more than 0.99, an Average Absolute Deviation (AAD) of < 0.1%, and a Root Mean Square Error (RMSE) of less than 0.2. With the further leveraging of more extensive datasets and improving generalization, this methodology shall exhibit the promising potential of ANN models to accelerate advancements in catalyst discovery and optimization to enhance upgrading process efficiency.

6.1 Introduction

Despite the global trend towards renewable energy sources, the demand for hydrocarbons as a primary energy resource continues to rise. This increase in energy demand is fueled by the ongoing population growth and the pursuit of better living conditions [1]. Even though the reserves of conventional light and middle crude oils are declining worldwide, there's still a growing market for unconventional hydrocarbon resources such as heavy crude oils and bitumen. Bitumen which is a highly dense and viscous petroleum oil found in the oil sand formations in countries like Canada and Venezuela faces significant production and transportation challenges due to its extreme viscosity and density values. For instance, in order to meet the North American pipeline standards, which require an API gravity $\geq 19^\circ$ (density $\leq 940 \text{ kg/m}^3$), a kinematic viscosity $\leq 350 \text{ cSt}$ at 15.6°C , and an olefin content of less than 1 wt% by H NMR [2, 3], bitumen is often diluted with up to 30 vol% of light hydrocarbons or diluents. As a result, this practice causes a 30% volume loss in pipeline capacity, and it also significantly increases the cost of bitumen, raising the total cost of a barrel of bitumen by almost 20% [34]. Alternatively, raw bitumen can be sent to a full upgrading unit to be converted into synthetic crude oil (SCO); however, this is also costly and comes with its own environmental restrictions [6]. The capital and operating costs of the current upgraders located in Canada are massive and the Canadian government has no intentions of investing in any additional full upgraders as they are cost-ineffective [7]. Another drawback of the full upgraders is that they produce significant greenhouse gas (GHG) emissions during the refining process. The oil sands operations currently emit 70 to 80 million tons of CO_2 equivalent (CO_2e) per year, accounting for about 10-12% of Canada's total GHG emissions [8].

Therefore, using onsite upgrading units which can partially reduce the viscosity and density of bitumen instead of fully upgrading it, might offer a viable option to optimize the cost, operational efficiency, and product quality. As a result, partial upgrading techniques have been viewed as a more promising approach to lower the viscosity, density, and sulfur content of the oil while avoiding the costs and environmental issues tied to fully upgrading to synthetic crude oil [9]. This technology includes different pathways ranging from thermal cracking to hydrotreating under mild conditions [10]. However, thermal or catalytic cracking alone produces a significant amount of olefins, consequently leading to much lower P-Values or higher product instability. Moreover, these olefins tend to react with persistent free radicals in heavy oils, creating even heavier end products [11]. Table 1 compares the properties of various forms of existing bitumen

against pipeline specifications and shows that while partial upgrading via thermal cracking improves some properties, unlike dilution or full upgrading techniques, it still falls short of satisfying all the transportation standards.

Table 6.1: Comparison between the physical properties of bitumen under various treatment conditions with the Canadian pipeline specifications adapted from Gray [4].

Property	Pipeline specs	Athabasca bitumen	Diluted bitumen	Fully upgraded synthetic crude oil	Partially upgraded by thermal cracking
VISCOSITY (cSt)	< 350	1x10 ⁶ (Average)	200-300	10	1500- 1700
DENSITY (kg/m ³)	< 940	>1000	920	850	980
API	> 19°	> 8°	> 20°	> 30°	12 -13°
OLEFIN CONTENT (wt%)	< 1	~0	~0	~0	> 1
T.A.N (mgKOH/g)	< 1	4.32	4.32	0.3	2-3
P-VALUE	> 1.1	3.4	3.4	> 1.1	< 1

To address some shortcomings of partially upgrading bitumen using only thermal cracking, a hydrogen source is usually introduced to the system to promote hydrogenation reactions during the hydrocarbon cracking which can greatly stabilize the produced olefins. Unfortunately, the cost and safety of using high pressure hydrogen are not justified, and producing hydrogen in large quantities for this process is also not currently feasible [10]. The emerging field of olefin treatment is thus focusing on reducing bitumen's viscosity and density while enhancing the product's stability by using cost-effective liquid organic hydrogen donors and metal-based nanocatalysts instead of the direct use of hydrogen gas [12–14]. The choice of hydrogen donor can influence the distribution of the products by promoting hydroconversion reactions over simple cracking [15]. Cycloalkyl aromatic hydrocarbons, such as tetralin, decalin, cyclohexane, and indane, can release hydrogen atoms under heat with or without a catalyst. These atoms transfer to and stabilize reaction intermediates, preventing condensed coke layers from forming [12]. In a recent study, Hart et al. [16] compared the use of cyclohexane to hydrogen gas, finding that a hydrogen atmosphere significantly reduced coke yield by 41.3% compared to a nitrogen atmosphere. Introducing cyclohexane under a nitrogen environment reduced the coke yield by 6.2–45.4% as the cyclohexane: oil ratio increased from 0.01 to 0.08 (g/g). In another study, Peparah [17] explored hydrogen donors beyond tetralin, including compounds like tetrahydroquinoline, 2-propanol, and

indoline, to examine whether their strong adsorption could speed up dehydrogenation and hydrogen transfer. The results concluded that strongly basic hydrogen donors, especially indoline, proved the most effective (up to 99% hydrogenation/conversion). However, these H donors have to be coupled with an appropriate catalyst to aid in effectively inducing the hydrogenation process.

Cenospheres, also known as fly ash cenospheres (FACs), are a by-product of coal combustion in power plants and consist mainly of silica and alumina with traces of metal oxides [18]. Cenospheres are one of the most value-added fractions of coal fly ash. They have a hollow spherical structure and can be applied in various industries due to their superior properties, such as low bulk density, high thermal resistance, high workability, and high strength [18]. Their high silica content and surface acidity make them not only easily recovered from power plants as a cost-effective waste material but also suitable for catalysts or catalyst support. This material has been effectively used in different chemical reactions, including esterification of n-octanol with acetic acid, deNO_x processes, pollutant degradation, and water cleanup [13–15]. Furthermore, the cenosphere-supported catalysts showed relatively high activity and good stability in the applications of dry reforming of methane (DRM) [22]. These factors enable it as a strong supporter candidate for bitumen partial upgrading. In addition, our recent study indicated that Fe nanoparticles, specifically Fe₃O₄, can significantly enhance vacuum residue conversion, effectively reducing the viscosity and density of upgraded oil [23].

Therefore, this study intends to introduce Fe₃O₄ coated cenospheres as a novel catalyst for bitumen partial upgrading which has not been studied before. The catalyst, developed through a cost-efficient method using economical precursors, will be integrated into the bitumen upgrading process. Furthermore, the catalyst will be tested in the presence of several hydrogen donor solvents including tetralin, decalin, indoline, cyclohexane, and n-heptane, aiming to replicate aspects of Husky's Diluent Reduction technology with a process that employs mild thermal cracking facilitated by organic hydrogen donors in volumes of less than 15% [24]. This partial upgrading approach seeks to transform the molecular structure of bitumen on-site, thereby decreasing both the type and amount of diluent necessary for transportation.

In addition to the experimental component of this study, an Artificial Neural Network (ANN) will be developed to model the effects of various partial upgrading parameters, including temperature,

reaction time, catalyst type, and hydrogen donor type, on the physical parameters of the upgraded oil. This computational approach is crucial for several reasons. Firstly, ANNs are capable of handling complex, nonlinear relationships between input variables and outcomes, making them particularly suitable for modeling the intricate processes involved in bitumen upgrading processes [165]. By accurately predicting how changes in upgrading conditions affect the properties of the oil, the ANN model will enable the optimization of these processes in a way that is both efficient and cost-effective. The decision to employ an ANN was driven by its flexibility and power in modeling complex systems, its ability to learn from data, and its utility in predicting outcomes based on a set of inputs without the need for explicit programming of the relationships between those inputs. Ultimately, this computational modeling aspect of the study is expected to be a transitional part in the future of bitumen upgrading research. It opens up new possibilities for the precise control and optimization of upgrading processes, contributing to the development of more efficient, environmentally friendly, and economically viable methods for transforming heavy oil into valuable resources. Through the integration of experimental and computational methods, this study aims to advance the field of bitumen partial upgrading and pave the way for innovative solutions to the challenges faced by the current oil and gas industry.

6.2 Experimental Methodology

6.2.1 Synthesis of Fe₃O₄ Coated Cenospheres

Gray cenospheres with a particle diameter range of 50 to 150 μm (average $\sim 100 \mu\text{m}$), a melting point of approximately 1500°C , and a true particle density between 0.32 and 0.45 g/cm^3 were sourced from Cenostar Corporation. The cenospheres' chemical composition, determined by X-ray fluorescence (XRF) analysis was provided by the manufacturer and is outlined in Table 6.2. Furthermore, analytical grade reagents, including ferric trichloride hexahydrate ($\text{FeCl}_3 \cdot 6\text{H}_2\text{O}$), iron sulfate heptahydrate ($\text{FeSO}_4 \cdot 7\text{H}_2\text{O}$), aqueous ammonia ($\text{NH}_3 \cdot \text{H}_2\text{O}$), and hydrofluoric acid (HF), were all purchased from Fisher Scientific without any further purification. Deionized water was used for all experimental procedures as a solvent and for washing.

Table 6.2: Chemical composition of cenospheres (wt%) as determined by XRF.

COMPOUND	Percentage Range (wt%)
SiO ₂	50 - 60
Al ₂ O ₃	30 - 38
Fe ₂ O ₃	1.4 – 2.0
K ₂ O	0.4- 0.8
CaO	1.4 – 2.5
MgO	0.3 – 0.8
Na ₂ O	0.4 – 1.3

The synthesis of the Fe₃O₄ coated cenospheres was carried out through a multi-step procedure using the precipitation method to ensure uniform coating and adherence of Fe₃O₄ nanoparticles to the cenosphere surfaces in a procedure similar to that performed by J. Zhan et al. [166]. Initially, a stoichiometric solution was prepared by dissolving 5.4 g of ferric chloride hexahydrate (FeCl₃·6H₂O) and 5.56 g of iron sulfate heptahydrate (FeSO₄·7H₂O) in 200 ml of deionized water. This solution, aimed at achieving a 0.1 M concentration for each iron ion, was vigorously stirred at 30°C to promote the complete dissolution of the precursors while maintaining an equimolar ratio of Fe²⁺ to Fe³⁺. Then the cenospheres were etched in a 1% HF solution at 40°C for 10 minutes to enhance their surface roughness to facilitate better nanoparticle adherence. After that, the cenospheres were rinsed with anhydrous ethanol and thoroughly washed with deionized water before being dried at 110°C for 12 hours. The prepared cenospheres were then introduced to the iron solution, with continuous stirring to promote uniform coating. The precipitation of Fe₃O₄ nanoparticles was initiated by adding aqueous ammonia (28 wt%) dropwise to the reaction mixture while continuously stirring at 500 rpm. The pH was carefully adjusted to 9, and the transition of the solution's color from pink to brown and then to black indicated the successful formation of the Fe₃O₄ particles. To ensure the completion of the reaction, the mixture was stirred for an additional 2 hours. Finally, the Fe₃O₄ coated cenospheres were then thoroughly washed using acetone, ethanol, and deionized water, each for 15 minutes, to remove any residual impurities and by-products. The washed cenospheres were filtered and subsequently dried in a vacuum oven at 60°C for 12 hours to eliminate all moisture, yielding the desired Fe₃O₄ coated cenospheres ready for further characterization and application in the partial upgrading of bitumen.

6.2.2 Characterization of the Catalyst:

Characterization of the Fe_3O_4 coated cenospheres utilized an integrated approach employing several advanced analytical techniques to provide a comprehensive understanding of their morphological, magnetic, structural, and chemical properties. Firstly, Field Emission Scanning Electron Microscopy (FESEM) was performed with a Hitachi SU8230 Regulus Ultra High-Resolution instrument to facilitate detailed images of the cenospheres before and after coating. At the same time, Energy-Dispersive X-ray Spectroscopy (EDX) analysis was conducted for precise determination of the chemical composition at various surface locations of the cenospheres. To assess the magnetic properties of the coatings, Vibrating Sample Magnetometry (VSM) was conducted using a Quantum Design PPMS® DynaCool™ system, measuring the magnetic response across a wide field range from -30,000 Oe to +30,000 Oe at ambient temperature.

Further structural analysis was performed through X-ray Diffraction (XRD) using a Rigaku DMax diffractometer, which provided detailed insights into the phase composition and crystallinity of the Fe_3O_4 coated cenospheres before and after treatments. The diffractometer, set with $\text{CuK}\alpha_1$ radiation at a wavelength of 0.154056 nm, operated at 40kV and 40mA, scanning over a 2θ angle range from 10 to 70 degrees at a rate of 2° per minute. X-ray Photoelectron Spectroscopy (XPS), performed on a Kratos AXIS Supra instrument equipped with a monochromatic Al $\text{K}\alpha$ source, played a crucial role in determining the oxidation states of iron, the presence of various oxygen species, and the detection of carbon deposition on the catalyst surfaces.

6.2.3 Upgrading of Oil Sand Bitumen:

For the thermal upgrading setup, approximately 80 grams of the Athabasca bitumen were preheated using a hot water bath to achieve a flowable state before being introduced into a Parr Bench Top Reactor (Series 4590 autoclave). The upgrading process utilized a blend of organic H-donor liquids and the iron-coated cenospheres catalyst to facilitate the bitumen's thermal cracking and hydrogenation. The H-donor solution, comprising of either tetralin, decalin, indoline, cyclohexane, and N-heptane, was prepared with each H-donor liquid accounting for 15wt% of the solution. These H-donors were all procured from Fisher Scientific with purities >98% and no further modifications were made to them. Additionally, 1wt% of the cenosphere catalyst was dispersed within the H-donor liquid, ensuring a homogeneous mixture. This catalyst-H-donor

mixture was then added to the reactor containing the bitumen, and the assembly was subjected to agitation at 600 rpm for one hour at 60°C to ensure even distribution of the catalyst throughout the bitumen. The thermal upgrading process was then conducted at 400°C under a nitrogen environment at the atmospheric pressure (1 bar) for two hours. Following the thermal treatment, the reactor was allowed to cool to room temperature, after which the upgraded bitumen was extracted for analysis. The effectiveness of the upgrading process was assessed by examining changes in the physical properties of the bitumen, including viscosity, density, and the composition of saturates, aromatics, resins, and asphaltenes (SARA).

6.2.4 Analysis of the Upgraded Bitumen

Viscosity measurements were determined in accordance with ASTM D4402 standard [21] using an IKA ROTAVISC rotational viscometer, which has a measurement range of 100-4,000,000 cP and a reproducibility of $\pm 1\%$. Density measurements were acquired using a DensitoPro Handheld Density Meter purchased from Mettler Toledo. To analyze the bitumen's complex composition, a SARA (Saturates, Aromatics, Resins, and Asphaltenes) analysis was carried out following the ASTM D2007 procedure [168], further supplemented by H NMR spectroscopy to quantify the olefin content within the upgraded oil. This involved mixing the bitumen sample in a known amount of dichloromethane (DCM) and then dissolving it in chloroform, which is used as the main solvent, the final mixture is analyzed using a Bruker 600 NMR spectrometer for detailed molecular insight.

To assess the stability of the upgraded bitumen oil, the P-value measurement method was used as per the ASTM D8253-21 [169] standard. Initially, the density of the bitumen sample was accurately recorded then a precise 1 g of bitumen was introduced into the vial, to which a 10 ml mixture of heptane and toluene in a 9:1 ratio was added under continuous stirring. This volume was adjusted based on the anticipated stability of the sample. Subsequently, the mixture was stirred for 5 minutes. Post-stirring, drops from the mixture were placed on a microscope slide and examined at a magnification range of 80 \times to 200 \times , with the images and observations of the asphaltenes being systematically recorded. The procedure was further extended by the incremental addition of toluene, starting with 1 mL, after which the mixture was stirred for another 5 minutes. This step was repeated, each time reducing the toluene volume, and the mixture drops were again observed microscopically after every toluene addition. The iterative addition of toluene continued

until the asphaltenes dispersed completely and were no longer detectable under the microscope as shown in Figure 6.9. The total volume of toluene required to achieve this endpoint was recorded. To ensure reproducibility and accuracy, the entire process was replicated with increased bitumen quantities of 2 g and 3 g. The endpoint data obtained from these tests were plotted to derive the solubility parameters, which were indicative of the bitumen's stability. Details of the calculations performed are shown in Appendix C.

6.3 Results and discussion

6.3.1 FESEM

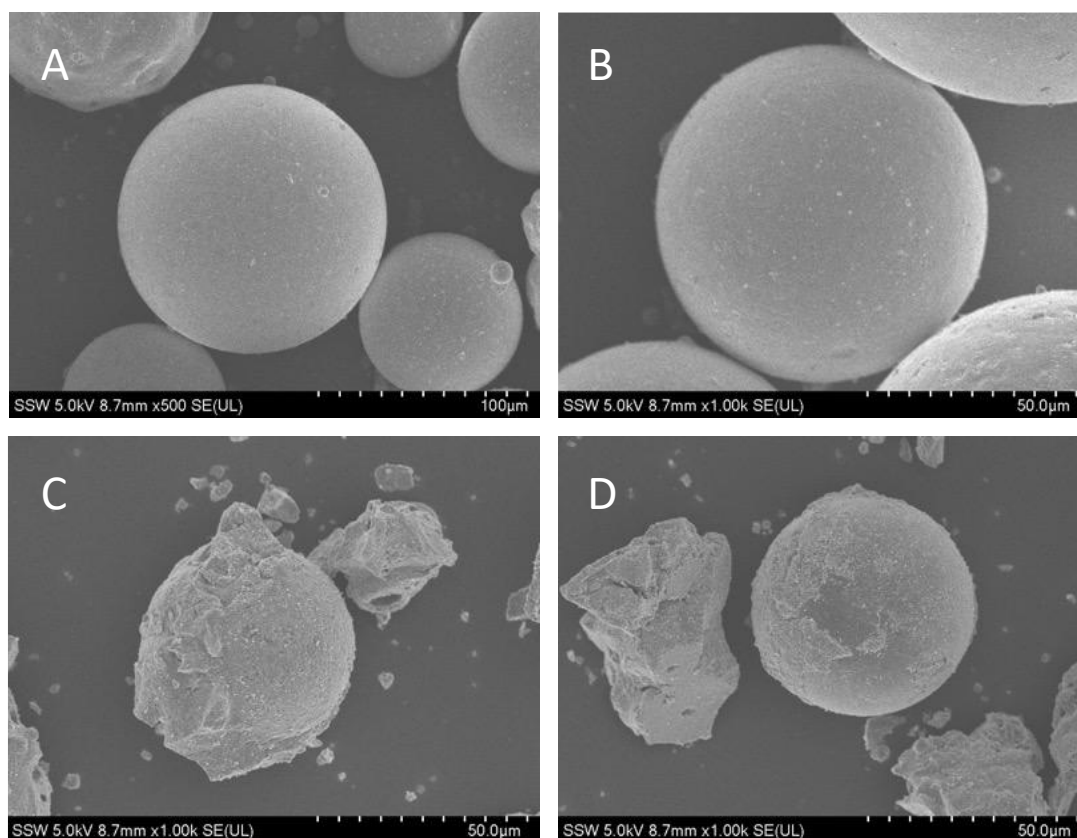


Figure 6.1: SEM images of cenospheres A&B) Before and C&D) After coating with Fe₃O₄.

Initially, the cenospheres were subjected to FESEM analysis, and the observed changes in the morphology of the cenospheres before and after the application of the Fe₃O₄ coating are shown in Figure 6.1. Images A and B reveal that the surface of the untreated cenospheres is relatively smooth and free of impurities. This initial condition provides a clear baseline for comparing post-treatment modifications.

The subsequent application of an HF solution initiates a transformation, as evidenced by the emergence of small, uniformly distributed pits across the surface of the cenospheres. This etching process is designed to increase the surface area and enhance coating adhesion which prepares the cenospheres for the next treatment phase. The introduction of $\text{FeSO}_4 \cdot 7\text{H}_2\text{O}$ and $\text{FeCl}_3 \cdot 6\text{H}_2\text{O}$ resulted in a noticeable change in the cenosphere surface. Images C and D from Figure 6.1 illustrate that the previously smooth cenosphere is now enveloped in a compact layer of Fe_3O_4 , signifying a successful coating procedure. Notably, despite this substantial surface modification, there are no significant morphological changes to the overall structure of the cenospheres, indicating that the integrity of the cenospheres is preserved even after the application of the Fe_3O_4 coating.

6.3.2 EDX analysis:

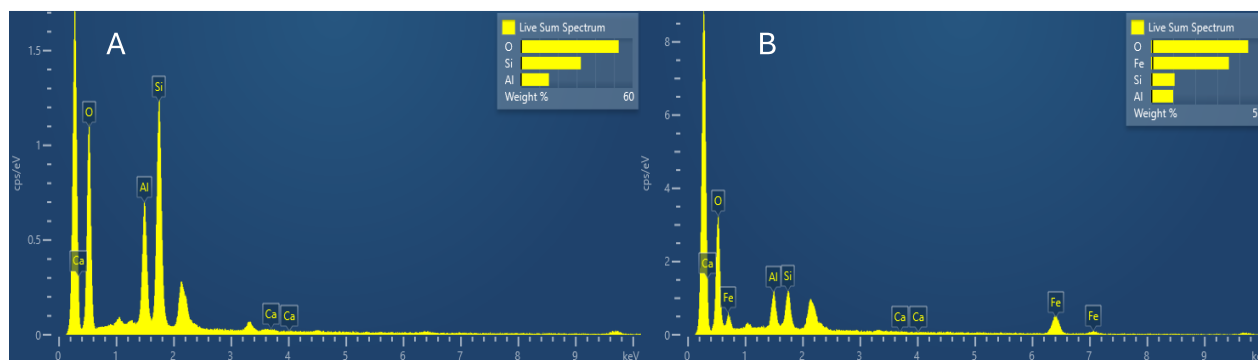


Figure 6.2: EDX survey spectra of cenospheres A) before and B) after coating with Fe_3O_4 .

The chemical compositions of the cenospheres before and after treatments are characterized by EDX survey spectra, as depicted in Figure 6.2, with the corresponding quantitative results summarized in Table 6.3. Prior to coating, the analysis (Figure 6.2A) reveals that the cenospheres' composition predominantly consists of oxygen (O) at 52.7%, silicon (Si) at 32.3%, and aluminum (Al) at 15.0% by mass percent, underscoring the expected presence of silica (SiO_2) and alumina (Al_2O_3). Notably, this initial composition lacks significant traces of other elements, highlighting the purity of the cenospheres.

Upon the coating of Fe_3O_4 nanoparticles, as shown in (Figure 6.2B), a distinct shift in the chemical makeup is observed. The oxygen content decreased to 44.1%, while silicon and aluminum were significantly reduced to 10.8% and 10.1% respectively. Most notably, iron (Fe) emerges as a major constituent, comprising 35.0% of the mass, directly attributed to the Fe_3O_4 nanoparticle deposition.

This substantial increase in iron content, alongside the modifications in silicon and oxygen percentages, validates the successful coating of the cenospheres with Fe_3O_4 .

Table 6.3: The chemical compositions of cenospheres before and after coating with Fe_3O_4 (EDX Analysis).

Elements	Untreated Cenospheres (wt%)	σ	Fe_3O_4 Coated Cenospheres (wt%)	σ
O	52.7	0.4	44.1	0.6
Si	32.3	0.3	10.8	0.3
Al	15.0	0.3	10.1	0.3
Fe	-	-	35.0	0.7

In order to verify the uniformity of the Fe_3O_4 nanoparticle coating on the cenospheres, EDX analyses were conducted at four distinct sites on each cenosphere sample after coating. The sites were carefully chosen to represent distinct areas, including the top, side, bottom, and an intermediate position between these points, to ensure a comprehensive assessment of the coating distribution. The EDX data collected from these four sites are presented in Table 6.4, which compares the elemental compositions across the selected sites, highlighting the consistency in the percentages of oxygen (O), silicon (Si), aluminum (Al), and iron (Fe) across all measured points. The uniformity in iron content across different sites particularly underscores the even distribution of the Fe_3O_4 coating. The consistency in composition across different sites indicates a homogeneous coating of Fe_3O_4 nanoparticles on the cenospheres. Notably, the minor variations observed are within the standard deviation range, affirming the reproducibility of the coating process. This even distribution is crucial for the enhanced performance of the coated cenospheres in their application, ensuring uniform catalytic activity and magnetic properties across the entire surface area.

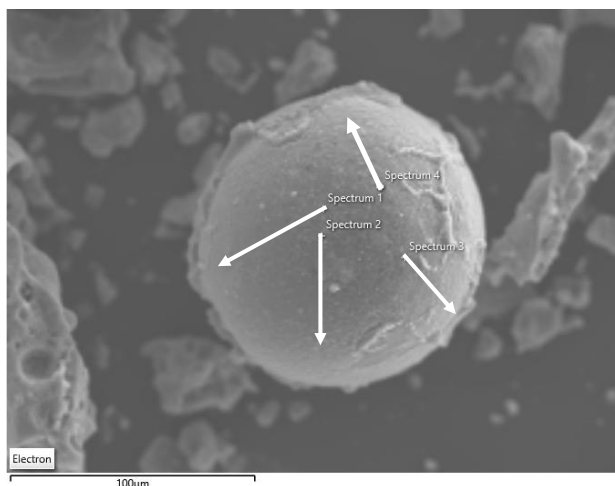


Figure 6.3: Locations of the 4 selected sites for EDX comparison.

Table 6.4: Elemental Composition of Fe₃O₄ Coated Cenospheres at Selected Sites (EDX Analysis).

Site	O (wt%)	Si (wt%)	Al (wt%)	Fe (wt%)
1	44.2	10.7	10.0	35.1
2	44.3	10.9	10.2	34.6
3	44.0	11.0	10.3	34.7
4	44.1	10.8	10.1	35.0

6.3.3 VSM analysis

Vibrating Sample Magnetometry (VSM) was used to investigate the magnetic characteristics of the cenospheres coated with Fe₃O₄ nanoparticles denoted as (Fe-Ceno). The magnetic hysteresis loops obtained at room temperature are depicted in Figure 6.4. The VSM results demonstrate that the magnetization of the prepared Fe-Ceno enhances progressively with the increasing magnetic field and exhibits a saturation magnetization (M_s) value of approximately 40 emu/g. This magnetization behavior suggests that the Fe₃O₄ nanoparticles have provided the cenospheres substantial magnetic properties after coating. In comparison with the original saturation magnetization value of pure Fe₃O₄ nanoparticles, which is around 80 emu/g, the Fe₃O₄ coated cenospheres (Fe-Ceno) exhibit a relatively lower M_s value. The observed M_s of 40 emu/g for the Fe-Ceno samples, although lower than that of pure Fe₃O₄, is significant and indicative of the enhanced magnetic properties gained by the cenospheres post-coating. These findings suggest that

the Fe_3O_4 coating process effectively induces strong magnetic properties in the cenospheres, potentially enhancing the ease of their separation from the upgraded bitumen for regeneration and reuse.

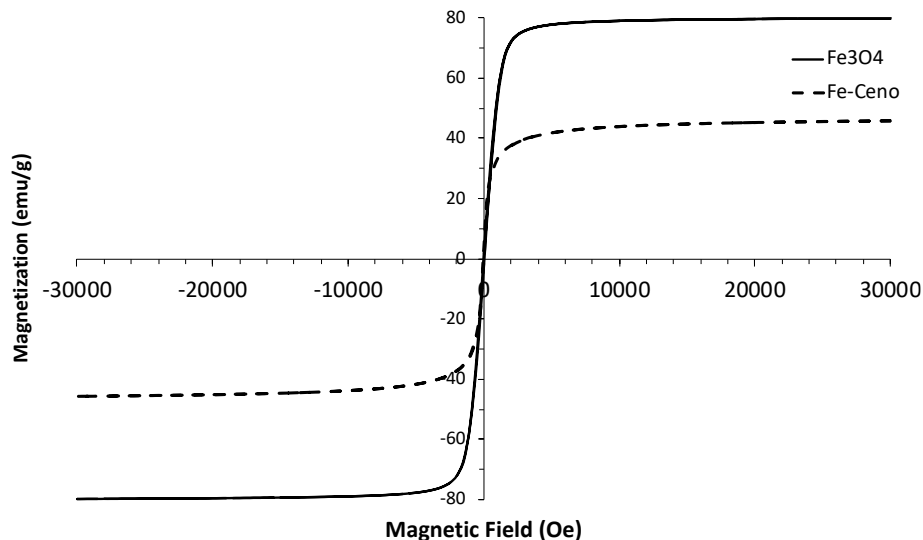


Figure 6.4: Magnetization saturation measurements of Fe-Ceno as compared with pure Fe_3O_4 nanoparticles.

6.3.4 XRD analysis

The XRD analysis provided a clear distinction between the crystalline structure of cenospheres before and after Fe_3O_4 coating. Figure 6.5 illustrates the distinct diffraction peaks corresponding to the crystalline phases present. For the untreated cenospheres, prominent peaks were observed for silica (SiO_2) at 26° [24, 25] and for aluminum oxide (Al_2O_3) at several angles including 25.4° , 35.0° , 37.7° , 43.8° , 52.5° , 57.4° , and 66.5° . These peak positions correspond to the known crystalline phases of $\alpha\text{-Al}_2\text{O}_3$, as confirmed by ICDD card number 00-010-0173 [172], denoting a polycrystalline and rhombohedral structure.

Upon application of the Fe_3O_4 coating, the XRD pattern reveals additional peaks at 2θ values of approximately 30° , 36° , 43° , 54° , 57° , 63° , and 75° . These peaks match those listed on JCPDS card no.19-0629 [166], signifying the successful deposition of Fe_3O_4 nanoparticles onto the cenosphere surface. Specifically, the diffraction peaks at 2θ of 30° , 36° , 43° , 54° , 57° , and 63° correlate to the $\{220\}$, $\{311\}$, $\{400\}$, $\{422\}$, $\{511\}$, and $\{440\}$ planes of the magnetite Fe_3O_4 phase,

indicative of a cubic inverse spinel structure [173]. The comparative reduction in the intensity of SiO_2 peaks in the Fe-coated samples suggests that the Fe_3O_4 particles contribute significantly to the surface composition, displaying an overlay of iron oxide peaks and demonstrating the presence of a coherent crystalline structure characteristic of Fe_3O_4 . The uniformity of the Fe_3O_4 peaks in the XRD diffractogram across the surface of the cenospheres suggests that the coating has been evenly distributed. The XRD pattern did not reveal any anomalous peaks, confirming the purity of the Fe_3O_4 coating and indicating no major contamination or unwanted by-product phases. Thus, the XRD analysis validates the integrity and homogeneity of the Fe_3O_4 coating process, supporting the cenospheres' potential for application in bitumen upgrading.

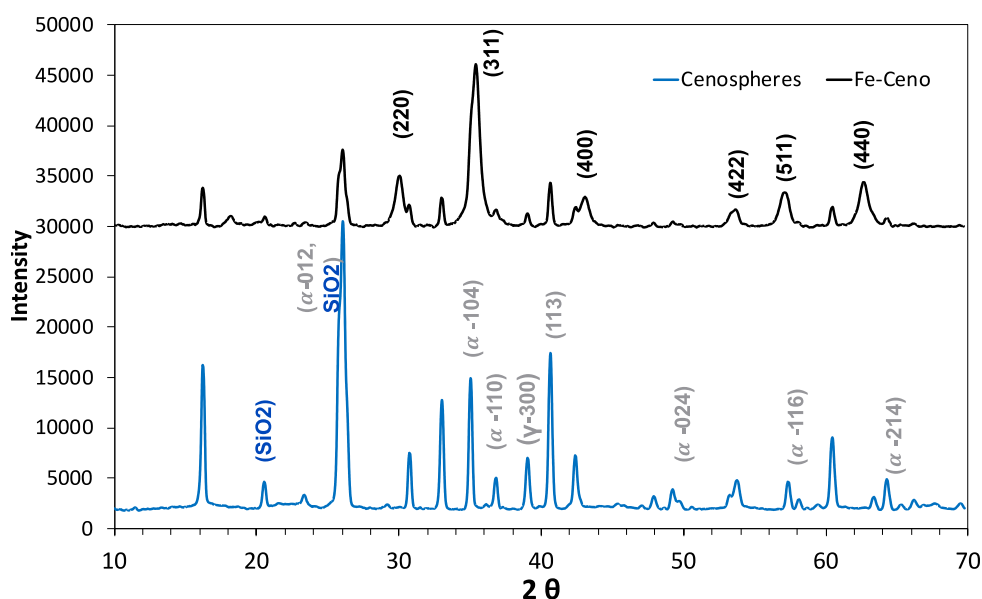


Figure 6.5: XRD patterns for coated and uncoated cenospheres.

6.3.5 XPS analysis

Analyzing the X-ray Photoelectron Spectroscopy (XPS) spectra of the Fe_3O_4 coated cenospheres, which is represented in Figure 6.6, provides a thorough understanding of the chemical states present within the catalyst prior to the upgrading reaction. The XPS spectra reveal multiple peaks within the binding energy range of 705 to 730 eV. These peaks were fitted and identified at binding energies of 710, 712, 723, 725, and 717 eV, which are indicative of the existence of iron in both Fe^{2+} and Fe^{3+} oxidation states. The first and third peaks were attributed to the Fe^{2+} species, while the second and fourth peaks are indicative of the Fe^{3+} species. The fifth peak at 717 eV represents the satellite peak commonly associated with Fe^{3+} . The integral area under these peaks, after

deconvolution, has allowed for the calculation of the $\text{Fe}^{2+}/\text{Fe}^{3+}$ ratio. The derived ratio of approximately 52:48 closely mirrors the stoichiometry of pure magnetite (Fe_3O_4), which ideally possesses an equimolar ratio of iron ions in the +2 and +3 oxidation states. This close resemblance in the $\text{Fe}^{2+}/\text{Fe}^{3+}$ ratio between the coated cenospheres and pure Fe_3O_4 indicates that the coating process has successfully replicated the natural stoichiometry of magnetite on the surface of the cenospheres. The presence of both oxidation states is essential for the catalytic activity that is exploited during the bitumen upgrading process, offering potential redox sites for chemical reactions. The XPS analysis not only confirms the composition and oxidation states of the iron but also underscores the efficiency of the coating procedure in creating a catalytically active surface on the cenospheres.

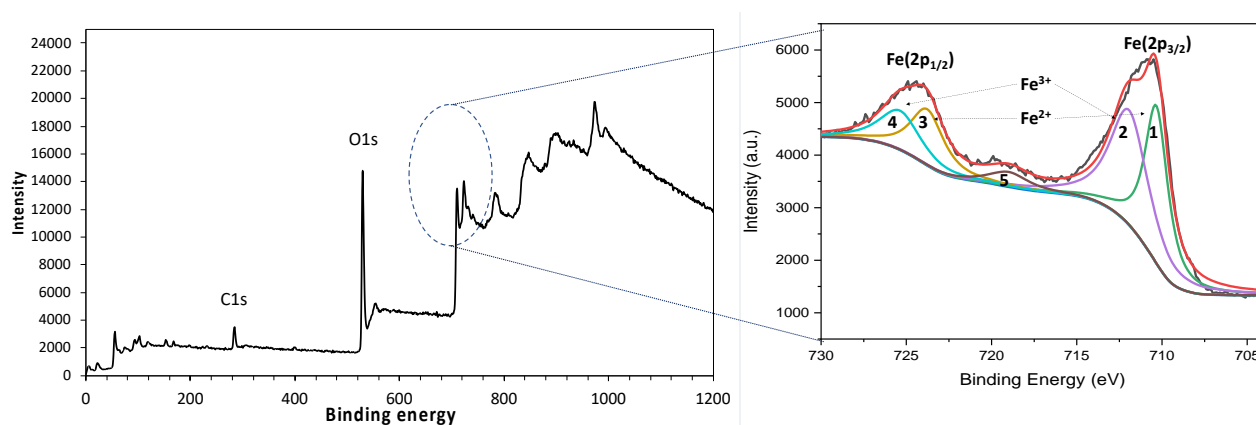


Figure 6.6: XPS plot for the Fe 2p peak coated cenosphere catalyst (Fe-Ceno).

6.3.6 Catalytic effect of Fe-coated cenospheres in bitumen upgrading

The catalytic effect of iron-coated cenospheres (Fe-Ceno) on the thermal upgrading of bitumen was studied under conditions that mimic the industrial partial upgrading conditions, with a focus on improving the liquid yield and the overall oil quality to meet the Canadian pipeline specifications. The upgrading process, conducted at 400°C for two hours using Fe-coated cenospheres dispersed in various hydrogen donor solutions, achieved product liquid yields between 84-86% for all the runs. While the coke production was limited to 4-5 wt%, with the remainder of the yield constituting gaseous products. Figure 6.7 illustrates the viscosity and density outcomes for the oil products post-upgrading. Notably, the viscosity of all upgraded oil was

recorded to be below 350 cP, aligning with pipeline standards, and marking a significant reduction from the original bitumen viscosity of 300,000 cP measured at 20°C. On the other hand, the density measurements were H donor dependent, with most oil products showing a decrease from the initial 1020 kg/m³ to approximately 970 kg/m³ and stopping there. However, the use of cyclohexane and N-heptane as H donors yielded much lower densities of 955 kg/m³ and 937 kg/m³, respectively, making N-heptane the only H donor able to fulfill the pipeline specification of 940 kg/m³.

The variation in performance between the H donors can be attributed to the molecular structure and bond dissociation energies of each H-donor. For instance, cyclohexane and N-heptane, with their aliphatic structures, facilitate a more substantial reduction in viscosity due to their saturated hydrocarbon configurations that may offer a more straightforward pathway for hydrogenation reactions under the catalytic influence of Fe-Ceno. In contrast, aromatic H-donors like tetralin, decalin, and indoline, despite their potential for easier hydrogen release due to lower bond dissociation energies adjacent to aromatic rings [64], show a varied impact on the bitumen's physical properties, possibly due to the complexities of their interactions with the asphaltenic components of the bitumen. The data interestingly indicate that the choice of H-donor significantly impacts the efficiency of the upgrading process, with N-heptane emerging as the most effective donor under the experimental conditions. This efficiency is closely linked to the chemical properties of the H-donors, including their molecular structures and the energies required to break the C-H bonds, which in turn influence their ability to donate hydrogen for the hydrocracking of heavy hydrocarbons.

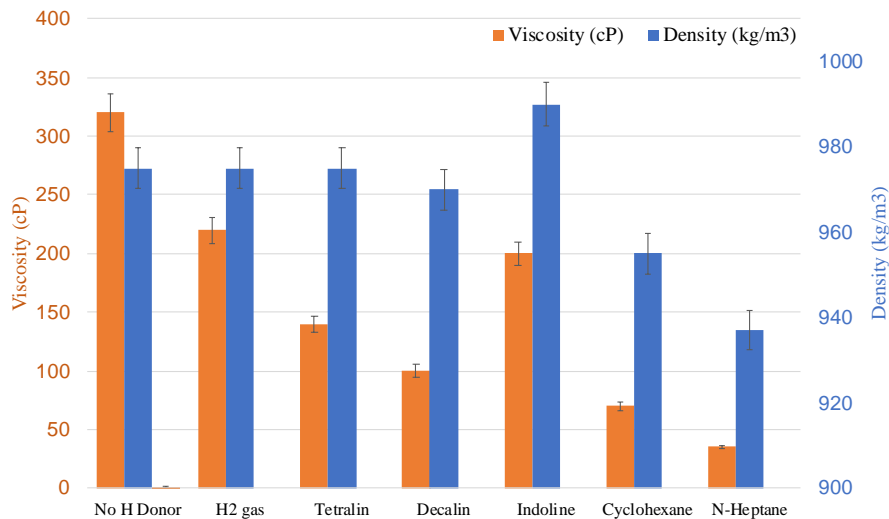


Figure 6.7: Oil product viscosity and density after upgrading at 400°C in the presence of Fe-Ceno using various H donors.

These preliminary results prompted further analyses, focusing on oil products derived from N-heptane and cyclohexane due to their superior density and viscosity parameters. Table 6.5 summarizes the comprehensive properties of the upgraded bitumen. The use of iron-coated cenospheres in synergy with hydrogen donors, particularly N-heptane and cyclohexane, resulted in enhanced oil properties, including increased saturates, decreased asphaltenes, and significantly reduced viscosity and density. This suggests a more efficient molecular breakdown during the upgrading process. Interestingly, while there was a rise in olefin content in samples thermally cracked without H donors, the incorporation of a suitable H donor into the system, coupled with the Fe-Ceno catalyst, greatly reduced olefin content through hydrogenation. Additionally, observed decreases in Total Acid Number (TAN) by more than 50% indicate the production of less corrosive and more environmentally friendly oil. The crucial role of the Fe-ceno catalyst in the observed improvements points to its effectiveness in facilitating the breakdown and removal of heavier oil fractions. These findings carry significant industrial relevance, marking a stride towards cost-effective and sustainable bitumen upgrading processes. The outlined advancements also offer valuable insights into the mechanics of heavy oil processing, highlighting the potential of tailored catalytic solutions in enhancing oil quality.

Table 6.5: Measured properties of the upgraded oil at various conditions.

	Raw Bitumen	Thermally Upgraded	Upgraded with Fe-Ceno	Upgraded with Fe-Ceno in N-Heptane	Upgraded with Fe-Ceno in Cyclohexane
Saturates (wt%)	19.1	19.7	23.4	23.6	12.6
Aromatics (wt%)	28.9	53.4	50.9	53.7	61.8
Resins (wt%)	30.8	10.5	16.0	15.0	16.8
Asphaltenes (wt%)	21.2	13.4	6.7	5.7	5.8
R/A	1.45	0.78	2.39	2.63	2.9
Viscosity (cP)	300,000	1700	340	35	70
Density (kg/m³)	1020	1000	975	937	955
TAN (mgKOH/g)	4.32	2.58	2.44	2.06	2.34
Olefin content (wt%)	0.5	1.65	0.78	0.54	0.54
P- value	3.4	0.95	1.62	1.76	1.76

A crucial aspect of evaluating the quality of the thermally upgraded oil samples, particularly in the context of pipeline specifications, is the olefin content, which was carefully analyzed using H-NMR spectroscopy. Figure 6.8 presents the H-NMR spectra for the various samples: thermally

upgraded, upgraded with the Fe-Ceno catalyst, and upgraded with both the Fe-Ceno catalyst and an H donor. The spectra indicate subtle variations in the molecular structure, especially in the aliphatic (0.5–4.5 ppm) and aromatic (6.5–9 ppm) regions [174]. It is noteworthy to mention that there is a significant peak at 5.3 ppm which corresponds to dichloromethane (DCM) which was used as a solvent in the NMR analysis and served as a reference for quantifying the olefinic content. In the olefinic range (4.5–6.5 ppm), two major peaks are observed at 5.2 and 5.5 ppm. Interestingly, the sample upgraded with an H donor shows these olefinic peaks, but the overall intensity within this region is markedly reduced compared to the sample upgraded thermally without an H donor. Quantitative assessment of the olefin content revealed a decrease from 1.65 wt% in the thermally upgraded sample to 0.78 wt% upon the introduction of the Fe-Ceno catalyst. A further reduction to 0.54 wt% was achieved with the addition of any H donors, bringing the olefin content below the threshold of <1 wt%, thereby meeting pipeline specifications. This trend is consistent with existing literature on hydrotreating, hydrogenation with hydrogen donor solvents, and the thermal cracking of vacuum residues [29, 30], underscoring the efficiency of Fe-Ceno catalysts and H donors in reducing the olefin content. The reduction in olefins highlights the dual role of the catalyst in facilitating hydrogenation reactions and the H donors in providing the necessary hydrogen atoms for saturating olefinic bonds. These findings are significant as they indicate that the integration of Fe-Ceno catalysts with H donors can enhance the quality of bitumen beyond the limitations of thermal upgrading alone, ensuring compliance with strict pipeline specifications for the olefin content.

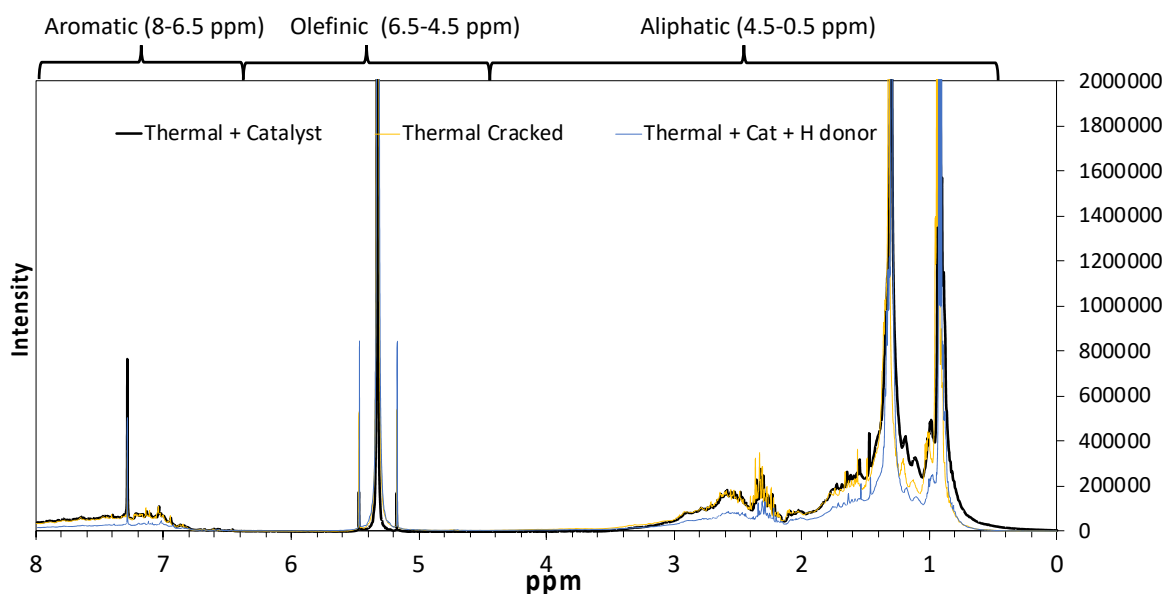


Figure 6.8: ¹H NMR spectra of the upgraded bitumen with and without the use of H donors.

A critical measure of asphaltene's stability in oil is the P-value, which is defined as the propensity of asphaltenes to remain solubilized within the crude oil. The P-values for various samples—thermally upgraded, upgraded with the Fe-Ceno catalyst, and upgraded with both the Fe-Ceno catalyst and a hydrogen donor—were all measured. The measurements are summarized in Table 6.5, with raw bitumen typically exhibiting a P-value of 3.4. This value stands well above the stability threshold of 1.15 [177], reflecting the natural stability of the unprocessed material. Figure 6.9 captures the microscopic photographs utilized in assessing the P-value of the bitumen samples, showcasing the point at which asphaltenes become undetectable under a microscope after the incremental addition of toluene.

Asphaltenes, known to be the heaviest fraction of crude oil, maintain stability in the presence of heavier fractions such as resins due to closely matched solubility parameters [178]. The process of thermal cracking on its own reduces the molecular weight of various oil fractions, which consequently affects the stability of asphaltenes, evident in the decreased P-value from 3.4 to 0.95. This reduction is also attributed to structural changes in the asphaltenes, particularly hydrogen deficiency, which is more pronounced in the context of lighter oil products [179]. However, on the other hand, the introduction of the Fe-Ceno catalyst to the upgrading process led to an increased P-value of 1.62, signaling an improvement in asphaltene stability. The addition of an H donor to the system further enhanced this stability, raising the P-value to 1.76. This increase suggests that both the Fe-Ceno catalyst and H donors play a significant role in stabilizing asphaltenes. This improved stability is indicative of a successful alteration in the bitumen's composition, aligning with the objectives of creating a more stable, pipeline-ready oil product.

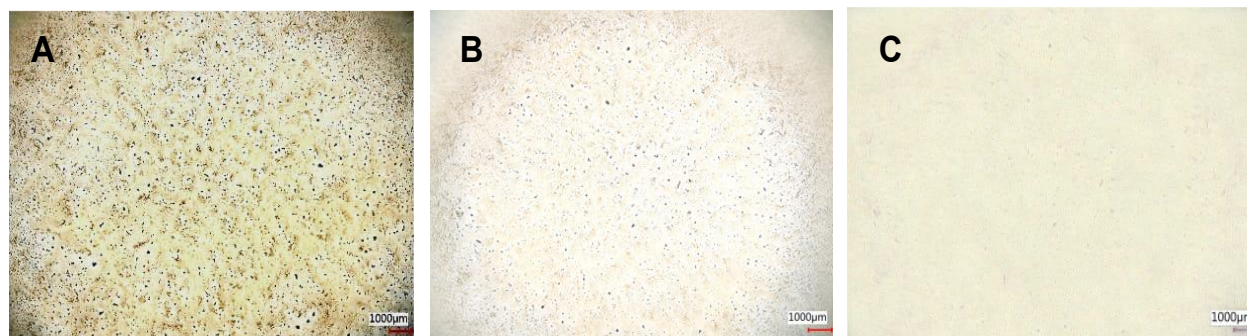


Figure 6.9: Microscopic images of upgraded oil diluted with toluene at A) 5 ml B) 10 ml C) at complete dilution.

As shown above, the Fe₃O₄-coated cenospheres (Fe-Ceno) shall offer several advantages as a catalyst for bitumen partial upgrading. Firstly, the cost of preparing Fe-Ceno is significantly lower than conventional upgrading catalysts such as nickel-molybdenum (Ni-Mo) and cobalt-molybdenum (Co-Mo), which can cost thousands of dollars per ton compared to a few hundred dollars per ton for Fe-Ceno. Secondly, Fe-Ceno can be reused after separation from the upgraded oil with the aid of a magnet, as demonstrated by the VSM results which show a saturation magnetization value of approximately 40 emu/g. Furthermore, our preliminary studies suggest that the catalyst retains its activity over multiple cycles, although further research is required to fully determine its lifespan and regeneration methods but given the cost and the availability of the cenospheres, the catalyst shows the potential for multiple cycle application. Finally, the use of Fe-Ceno contributes to environmental benefits as it utilize fly ash cenospheres, a by-product of coal-fired power plants. The enhanced efficiency of the bitumen upgrading process can lower energy consumption and reduce associated greenhouse gas emissions. While a detailed life cycle assessment (LCA) study is needed to accurately assess the greenhouse gas emissions of this process compared to traditional methods, the utilization of waste materials as catalysts underscores the green economic and environmentally friendly potential of this approach.

6.3.7 Artificial Neural Network (ANN) Model:

Description of the ANN Model

A crucial part of this chapter was the construction of a feedforward neural network model utilizing backpropagation algorithms to predict the viscosity and density of the partially upgraded bitumen. The model's input parameters included temperature, reaction time, catalyst type, and hydrogen donor type. This model was implemented in Python using TensorFlow's Keras API, which was chosen for its ease of use and flexibility in defining and training neural networks. The dataset for the model was imported and processed using the Pandas library, a library that can efficiently manage the data and prepare it for modeling [180]. The ANN model structure consisted of an input layer, multiple hidden layers (ranging from 1 to 3 layers) with varying numbers of neurons (ranging from 8 to 128), and an output layer with a linear activation function to predict the continuous target variables of viscosity and density. The ReLU activation function was applied within the hidden layers to introduce non-linearity into the model. The Adam optimizer was chosen for its adaptive

learning rate capabilities, as was done by Ssebadduka et al. [181], and to improve efficiency in the model's convergence.

The model employed the “train_test_split” method from the scikit-learn library to divide the dataset into training and testing subsets, with approximately 60% of the data used for training and 40% reserved for testing. This split was chosen to ensure sufficient data was available for learning while still providing a robust test set for evaluation. Feature scaling was a crucial step in the preprocessing pipeline, achieved through scikit-learn's StandardScaler, to normalize the input features and target variables, enhancing the model's convergence during training. To mitigate the risk of overfitting, the model incorporated an early stopping mechanism. This callback monitored the validation loss, pausing the training process if no improvement was observed for 10 consecutive epochs (patience parameter), thereby ensuring the model generalized well to any unseen data. Finally, post-training evaluation metrics such as the Average Absolute Deviation (%AAD), Root Mean Square Error (RMSE), and Coefficient of Determination (R^2) were calculated using scikit-learn's capabilities to provide a comprehensive assessment of the model's predictive accuracy. The model's initial structure is visually represented in Figure 6.10, depicting the sequence and connection of the layers and the possible number of neurons to be tested in each hidden layer. The trained model, alongside the feature and target scalers, was saved, facilitating future predictions and the assessment of bitumen properties under variable conditions.

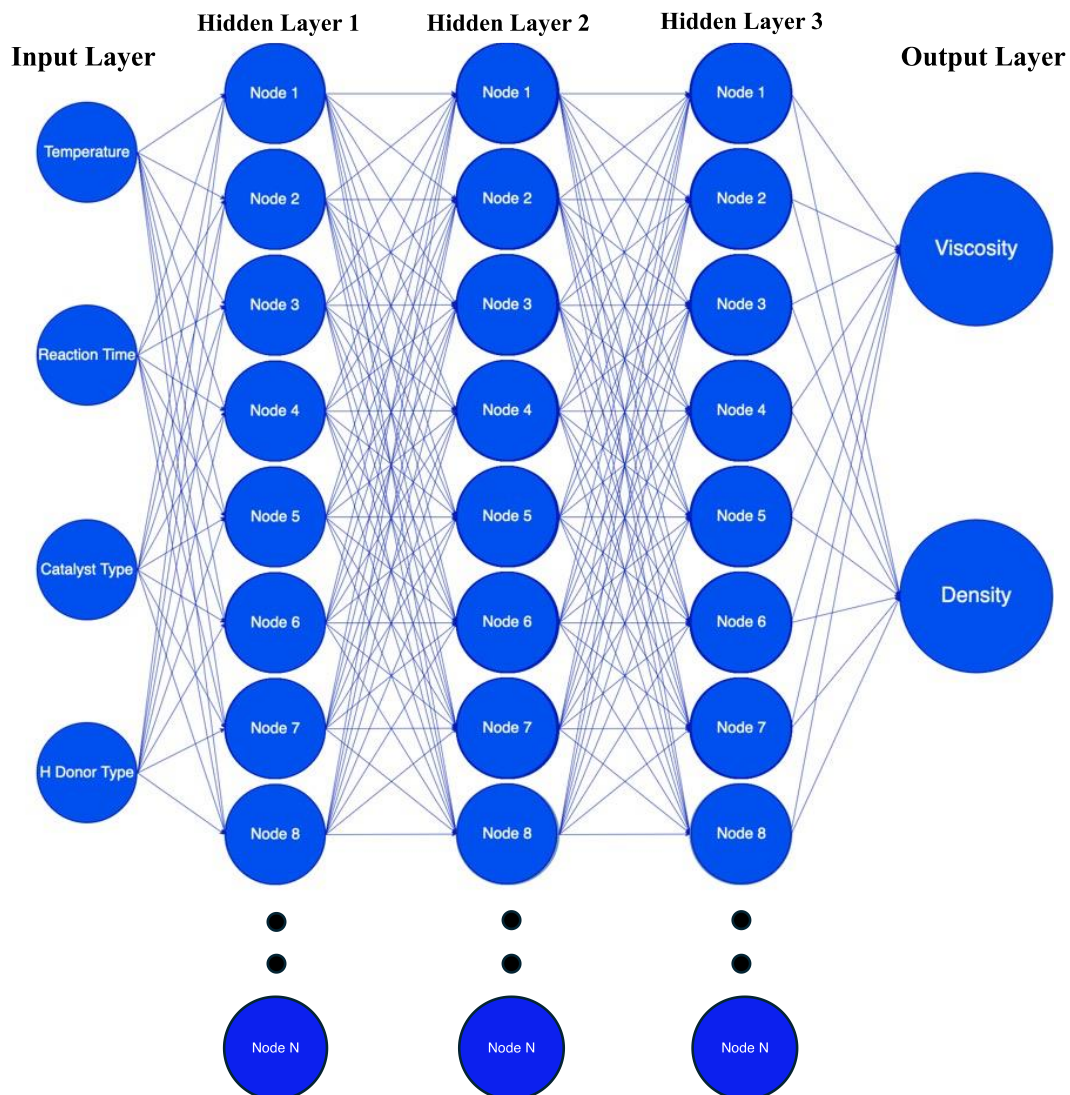


Figure 6.10: Schematic of the architecture of the ANN model proposed.

Fine-Tuning of the ANN Model

In practical applications, especially within specialized fields such as materials science, large datasets may not always be readily available. The cost and effort to acquire extensive experimental data can be a limiting factor. Recognizing this challenge, we utilized a relatively small dataset, comprised of experimentally obtained data points from this study alongside two of our previous studies [17, 36], to train the ANN model. The fine-tuning process was crucial to adapt the model to work effectively with the limited data at our disposal.

The model's architecture and hyperparameters underwent careful adjustments to optimize its performance. One key area of focus was the model's depth and width, specifically the number and size of hidden layers. Our exploratory tests encompassed models with one to three hidden dense layers. While adding more layers can theoretically increase the model's capacity to learn complex relationships, it was observed that beyond two hidden layers, the model began to overfit, which was evidenced by deteriorating performance on the test data. This was an important finding, as it underscored the delicate balance between model complexity and the generalization capability. Moreover, we experimented with varying the number of neurons in each hidden layer, starting from 8 and extending up to 128 neurons. This adjustment aimed to find an optimal level of model complexity that could capture the underlying patterns in the data without overfitting. The evaluation of the accuracy of the ANN models with various architectures was based on the three parameters previously mentioned: R^2 , %AAD, and RMSE which were calculated as shown in Equations 6.1-3.

$$R^2 = 1 - \frac{\sum_{i=0}^n (y_{exp} - y_p)^2}{\sum_{i=0}^n (y_{exp} - y_{ave})^2} \quad \text{Eq (6.1)}$$

$$\%AAD = \frac{100}{n} \sum_{i=0}^n \left| \frac{y_{exp} - y_p}{y_{exp}} \right| \quad \text{Eq (6.2)}$$

$$RMSE = \sqrt{\frac{1}{n} \sum_{i=0}^n (y_{exp} - y_p)^2} \quad \text{Eq (6.3)}$$

where n is the number of observations, y_{exp} is the actual experimental value, y_p is the predicted value from the model and y_{ave} is the mean of the predicted values y_p across all the n observations.

A summary of the testing results of the best selected models within the various structures is shown in Table 6.6. The findings suggested that increasing the number of neurons in the first two hidden layers to at least 32 neurons significantly enhanced the model's predictive accuracy, with the coefficient of determination (R^2) reaching as high as 0.9966 during testing as represented by Model-9. When comparing the performance of all the models tested based on the R^2 , %AAD, and RMSE values, it appears that Models 7, 9, and 15 outperformed all the others with each reaching an R^2 of more than 99%, an Average Absolute Deviation of $< 0.1\%$ and a Root Mean Square Error of less than 0.2.

Table 6.6: Comparing the accuracy of different multilayered ANN models.

Model #	# of Hidden Layers	Neurons in layer 1	Neurons in layer 2	Neurons in layer 3	R ²	% AAD	RMSE
1	1	32	0	0	0.78	0.2042	0.3428
2	1	64	0	0	0.8097	0.1697	0.3102
3	1	128	0	0	0.8715	0.1777	0.3065
4	2	32	16	0	0.8921	0.1234	0.2865
5	2	64	16	0	0.931	0.1395	0.2265
6	2	128	16	0	0.9025	0.1686	0.2908
7	2	32	32	0	0.9902	0.0997	0.1627
8	2	64	32	0	0.9885	0.1567	0.1735
9	2	128	32	0	0.9966	0.0964	0.1568
10	3	32	16	8	0.9232	0.1504	0.2745
11	3	64	16	8	0.9426	0.156	0.2325
12	3	128	16	8	0.9557	0.1014	0.2027
13	3	32	32	8	0.9444	0.1408	0.2359
14	3	64	32	8	0.9752	0.1356	0.1901
15	3	128	32	8	0.9917	0.0924	0.1964

Validation of the ANN Model with experimental data

Among the developed models, Models 7, 9, and 15 emerged as the top performers based on their preliminary evaluations as highlighted in Table 6.6. These models were advanced to the testing phase, where their predictions were directly compared with the actual experimental measurements. The primary objective was to assess the models' efficiency in predicting the viscosity and density of bitumen upgraded with the Fe-Ceno catalyst in conjunction with various hydrogen donors at 400°C for two hours. Model-9, in particular, demonstrated remarkable predictive accuracy during this phase. Figure 6.11 represents a visual comparison between the predicted and experimentally measured values for both the viscosity and density of the upgraded oil samples. Notably, the density predictions from Model-9 exhibited an almost perfect alignment with the measured data, underscoring the model's robustness in capturing the underlying physical transformations resulting from the upgrading process. On the other hand, although the viscosity predictions were slightly deviating from the experimental measurements they still remained within a very narrow margin of

error. This slight deviation was quantified by an RMSE of 0.1568 and an AAD of 0.0964, indicative of the model's high precision. Such minor variances are acceptable within the context of complex chemical processes and highlight the potential of the ANN model as a reliable tool for predicting bitumen's physical properties post-upgrading.

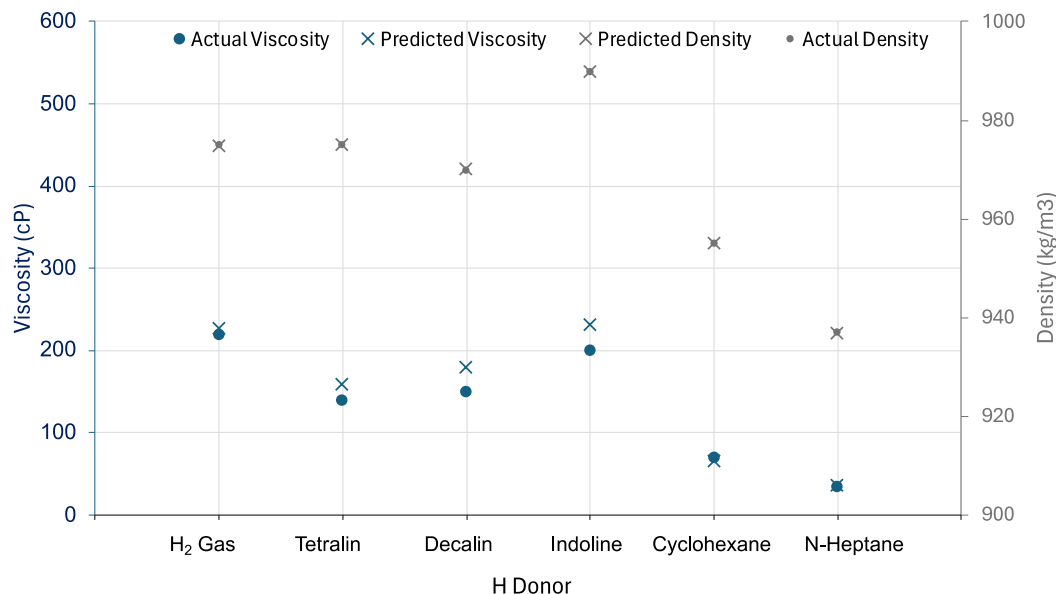


Figure 6.11: Comparison of the ANN predicted viscosity and density values for the upgraded oil with Fe-Ceno catalyst with different H donors to the experimental values.

In addition to the visual comparisons illustrated in Figure 6.11, a detailed quantitative analysis further emphasizes the predictive power of the ANN models, particularly Model-9. Table 6.7 presents a comparative view of the experimental viscosity values (measured in cP) for upgraded oil using different hydrogen donors against the predictions made by Models 7, 9, and 15.

Table 6.7: Predicted vs. Experimental Viscosity Values for Upgraded Oil Using Various H Donors.

H Donor	Experimental Value (cP)	Model-7 (cP)	Model-9 (cP)	Model-15 (cP)
H ₂ gas	220	154.63	226.89	197.37
Tetralin	140	120.68	159.06	67.47
Decalin	150	127.67	199.69	38.7
Indoline	200	326.81	231.65	322.39
Cyclohexane	70	60.36	65.82	50.51
N-heptane	35	12.1	36.45	48.86

Table 6.7 not only showcases the varying degrees of success each model had in approximating the viscosity values for different hydrogen donors but also highlights the exceptional accuracy of Model-9 across multiple scenarios. Notably, for donors like H₂ gas and N-heptane, Model-9's predictions closely align with the experimental values, demonstrating its capability to accurately model the outcomes of the upgrading process under these specific conditions. By closely mirroring the actual experimental results, the model demonstrates its potential to serve as an invaluable asset in refining and optimizing the parameters for bitumen partial upgrading, potentially reducing the need for extensive physical experimentation.

Limitations of the ANN Model

It is important to note that the AI model described in the above section was trained on a limited dataset that was acquired through experimentation and the authors of this paper recognize the need for a larger dataset to improve the generalizability and accuracy of this model for large-scale and industrial implementations. Cross-validation, early stopping, and careful hyperparameter tuning were employed to mitigate overfitting, which led to the current specialized model achieving high predictive accuracy, with R² values exceeding 99% and low %AAD and RMSE values. However, there is still a need to expand the dataset through additional experiments and explore advanced techniques such as transfer learning to enhance the model's robustness for final industrial application.

Introducing this neural network model in the context of a complicated bitumen upgrading process is unique and novel and still in its early stages, with no known implementation in existing literature. Initially, the model is specific and limited to the training data range, but it serves as a specialized model with significant growth potential. The results were experimentally validated, demonstrating its current and future utility. The model is strictly accurate only within the specific operational conditions it was trained on which were: reaction temperatures of 360-400°C, reaction times of 1-2 hours, Fe-based catalysts (Fe-Ceno, iron oxides, and iron sulfides), and selected H donors (tetralin, decalin, indoline, cyclohexane, heptane, and H₂ gas).

Many successful AI models, started with limited data and capabilities, gradually improving as more data and computational resources became available. This incremental approach allows for the further refinement of models over time, ensuring that they become more accurate and

generalizable. Similarly, the ANN model developed in this study is a starting point that highlights the feasibility and potential benefits of integrating AI in bitumen upgrading processes. With the accumulation and incorporation of more data into this model, significant improvements in the model's performance and applicability will be anticipated. Furthermore, the ongoing development of this model can help pave the way for more comprehensive and data-driven approaches in similar fields, encouraging further research and collaboration. Sharing the findings and methodologies of this study might be a step towards contributing to the broader scientific community's efforts to leverage AI for optimizing industrial processes, ultimately leading to more efficient and sustainable practices.

6.4 Conclusion

This chapter explores a novel approach for the partial upgrading of bitumen using Fe_3O_4 -coated cenospheres as catalysts combined with various hydrogen donors. The synthesis of the Fe_3O_4 -coated cenospheres was achieved through a multi-step precipitation process, ensuring uniform coating and significant magnetic properties, as confirmed by FESEM, EDX, VSM, XRD, and XPS analyses. These characterizations demonstrated the successful deposition of Fe_3O_4 on the cenospheres, enhancing their suitability as catalysts for bitumen upgrading. The experimental results showed that the Fe_3O_4 -coated cenospheres, when used with hydrogen donors such as n-heptane and cyclohexane, significantly improved the viscosity and density of the upgraded bitumen, meeting pipeline specifications. Notably, the introduction of n-heptane as a hydrogen donor resulted in the best performance, reducing the bitumen's viscosity to 35 cP and density to 937 kg/m^3 . The reduction in olefin content and improvement in P-value further underscored the efficiency of this catalytic system in stabilizing the upgraded oil. Complementing the experimental work, a robust Artificial Neural Network (ANN) model was developed to predict the outcomes of the upgrading process based on key parameters. Among the various ANN models tested, Model-9 exhibited the highest predictive accuracy, with an R^2 of 0.9966, an AAD of 0.0964, and an RMSE of 0.1568. This model's ability to closely mirror experimental results underscores its potential as a valuable tool for optimizing upgrading parameters and reducing the need for extensive physical experimentation. In conclusion, the integration of Fe_3O_4 -coated cenospheres with hydrogen donors presents a promising, cost-effective solution for bitumen upgrading, improving both the economic viability and environmental impact of the process.

Chapter 7 - Harnessing the Power of Microwave Irradiation: A Novel Approach to Bitumen Partial Upgrading

7 Abstract

The partial upgrading of the “tar-like” Canadian bitumen is one essential process to reduce its viscosity to an acceptable range that meets the required pipeline specifications. An innovative and potentially greener solution has emerged in the form of microwave irradiation. This work proposes and demonstrates the use of electrically powered commercial microwave along with carbon-based microwave susceptors (activated carbon, biochar, coke, and graphite) to promote localized thermal cracking within bitumen at a temperature as low as 150°C, compared to the conventional method of 400°C. Remarkable results have shown that just 0.1wt% of carbon additives can reduce the viscosity of bitumen by 96% with just 10 minutes of microwaving at 200°C. The Saturates, Aromatics, Resins, Asphaltenes (SARA) analysis revealed that the mass fractions of light components (saturates) were almost doubled and that almost one-third of heavy polar hydrocarbon constituents were cracked and decomposed into much lighter molecules, resulting in higher-quality, less viscous bitumen. Furthermore, the study highlights the key role of the surface area and porosity of the carbon microwave susceptor in absorbing microwave radiation, offering exciting new avenues for optimization. Microwave-assisted partial upgrading of bitumen is a cost-effective and eco-friendly alternative to conventional upgrading, producing upgraded bitumen that requires significantly less diluent at a lower cost prior to pipeline transportation.

7.1 Introduction

Bitumen, a highly viscous oil that represents over 50% of the current global oil reserves [5], presents a significant challenge for pipeline transportation due to its extremely high viscosity, density, and asphaltene content, which accounts for over 15% of its total weight [10]. Consequently, bitumen modification processes are needed to meet the pipeline specifications, which mandate a maximum viscosity of 350 cSt and a density of less than 940 kg/m³ at the reference temperatures [12]. Currently, the sole dilution of bitumen with expensive diluents such as condensate or light naphtha increases its production costs by approximately \$14 per barrel of bitumen and occupies about 30-33% of the pipeline capacity [15]. Alternatively constructing new upgrading plants is no longer economically viable [16]. In addition to that, the current operating

upgraders are contributing significantly to the greenhouse gas (GHG) emissions, with oil sand operations currently accounting for around 8% of Canada's total GHG emissions [19]. As a result, some partial upgrading techniques that involve a combination of heating, diluent mixing, and upgrading to reduce viscosity by cracking macromolecules are alternatively being used [182]. Nonetheless, substantial viscosity reduction is typically achieved at relatively high temperatures of 400°C+ in processes such as visbreaking and/or coking [42], making traditional thermal upgrading techniques both energy-intensive and time-consuming [73], and ultimately leading to substantial GHG emissions. As such, the exploration of new innovative, green, and sustainable partial upgrading techniques is required.

This chapter introduces the concept of microwave irradiation as a promising alternative to conventional bitumen partial upgrading techniques. Unlike traditional heating methods, which heavily rely on natural gas combustion and have a high carbon footprint, microwave technology can be integrated with renewable energy sources, potentially reducing CO₂ emissions to nearly zero. Despite higher operating costs currently preventing its adoption in refineries, microwave irradiation offers promising benefits including selective and volumetric heating and a more convenient plug-on-and-plug-off mode for remote operation [74]. Figure 7.1 illustrates a proposed schematic for the upgrading process of bitumen via microwave irradiation.

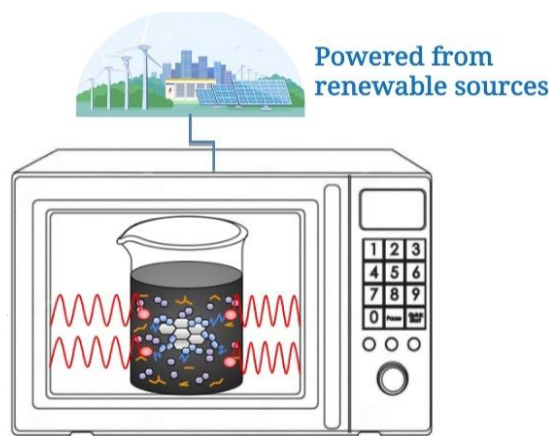


Figure 7.1: Schematic for the microwave heating of bitumen.

Studies show that microwave heating can selectively target and crack highly polar hydrocarbon fractions within bitumen [183], greatly enhancing the quality of the upgraded oil. Evidence suggests that heavy oils rich in heteroatoms, like bitumen, can absorb more microwave energy,

resulting in a significant reduction in viscosity under relatively mild conditions [183]. The ability of the oil to absorb and utilize the energy induced by microwave radiation greatly depends on two crucial parameters: the dielectric constant and the dielectric loss factor. The former parameter quantifies a material's aptitude to store electromagnetic energy and undergo polarization, while the latter measures the conversion of this energy into heat [184]. Studies report that the dielectric constant for crude oil typically lies between 1.72 and 2.34 [10-12]. However, when examined in isolation, oil's hydrocarbon fractions show distinct dielectric properties. Asphaltenes exhibit the highest dielectric constant values, ranging from 3.30 to 5.00 [10-12]. In contrast, the resin and aromatic fractions display lower dielectric constants, within the range of 1.80–2.61 and 2.0-2.7, respectively [10-13], while the dielectric constant of the saturate fraction ranges from 1.58 to 1.91 [11,14,15]. Despite its varying dielectric properties, heavy oil demonstrates some microwave absorption capabilities. To enhance this, some propose introducing a superior microwave-absorbing material that is cheap and compatible with oil such as carbon [188]. Given its dielectric constant of roughly 8.0 [189], carbon's absorption capacity is nearly quadruple that of crude oil. This addition could potentially facilitate thermal cracking at temperatures as low as 150°C [184].

Microwave-induced selective heating leads to uneven temperature distribution or formation of "hot-spots" [190]. These hot-spots, characterized by temperature gradients within the material, expedite the breakdown of complex hydrocarbons into smaller molecules, thereby reducing viscosity. Localized areas within heavy oil can exhibit temperatures 100–200°C higher than the bulk fluid under microwave radiation, causing localized overheating [75]. The formation of these hot-spots could potentially accelerate cracking reactions compared to traditional heating methods.

This chapter aims to bridge the gap in the existing literature by exploring the effects of different carbon susceptors on microwave utilization in bitumen upgrading. The study investigates the influence of various parameters like microwaving time, operating temperature, carbon additive concentration, and agitation rate on the extent of reaction and viscosity reduction. The effect of different carbon susceptors such as activated carbon, graphite, biochar, and coke on the viscosity of Canadian bitumen oil under microwave irradiation will be also assessed. The goal is to optimize physical operating conditions to better understand their impact on bitumen's physical and chemical properties and hydrocarbon fractions composition.

7.2 Experimental Methodology

7.2.1 Materials

The main feedstock for this study was oil sand bitumen sourced from the Athabasca reservoirs in Alberta. The key physical properties of this bitumen were provided earlier in Table 4.2. Viscosities were measured using the ROTAVISC rotational viscometer from IKA, with a measurement range of 100–4,000,000 cP and a repeatability of 1%, following the ASTM D4402 standards [191]. Density measurements were conducted using a specific gravity hydrometer from Fisher Scientific, adhering to the ASTM E100 standard. The Saturate, Aromatic, Resin, and Asphaltene (SARA) analysis was performed to classify the crude oil constituents based on their polarizability and polarity, following the ASTM D2007-98 standard process.

All carbon-based susceptors used in the study except biochar were procured from Fisher Scientific, each with a purity > 99%, and negligible ash and trace metal content. This study employed four distinct carbon-based materials. Firstly, the commercially available DARCO G-60 activated carbon, a highly porous powder with a mesh size between 100–325 (149-45 μ m), was used. Secondly, synthetic graphite powder was utilized, having a composition of 99% carbon and 0.2% ash and a mesh size ranging from 100-200 (149-74 μ m). The third material was calcined petroleum coke powder, a crystalline structured substance with a mesh size of approximately 325 (~45 μ m). Lastly, the study incorporated synthesized biochar, a product of pyrolyzing pinewood sawdust, a waste biomass that is readily available, at 300°C for 30 minutes with K₂CO₃ as a catalyst. The resulting biochar exhibited a mesh size between 100–325 (149-45 μ m).

7.2.2 Experimental Design

The microwave irradiation experiments were conducted using a standard commercial microwave oven, specifically the Danby 0.7 cu. ft. Countertop Microwave. This microwave oven operates at a power of 700 watts. The choice of a commercially available microwave oven was driven by the aim of the study to explore the feasibility of microwave-assisted bitumen upgrading using readily accessible and cost-effective equipment. This choice presents a realistic scenario for potential applications in smaller-scale or preliminary industrial trials.

Moreover, it is important to note that in microwave-assisted processes, the reactor's fabrication material plays a critical role due to its interaction with microwaves. Therefore, Polytetrafluoroethylene (PTFE), a microwave-transparent plastic, was chosen for this study over other potential materials such as glass or ceramic. PTFE offers superior chemical resistance, physical durability, and ease of cleaning, in addition to its resilience to sudden thermal shocks. While PTFE starts to degrade at temperatures higher than 260°C, this isn't a concern for this study, as we made sure that the oil temperature does not exceed 200°C providing a safety margin of 60°C. Temperature measurements during the microwave irradiation process were conducted using a carefully shielded fiber optic temperature sensor (FOTS). The sensor was precisely positioned within the PTFE reactor to ensure contact with the bitumen mixture, without touching the reactor's sides. Before each experiment, the sensor was calibrated, with the temperature readings displayed in real-time during the irradiation process. This ensured that the microwaves interacted exclusively with the bitumen mixture, not the sensor. The agitation method involved a metallic stirrer, typically not recommended due to the potential for metal-microwave interactions. However, some measures were taken to mitigate such interactions. The stirrer was aligned parallel to the electromagnetic field, minimizing potential interference. In addition, the stirrer was designed with a smaller diameter and smoother surface to decrease the risk of arcing and heating by reducing the exposed surface area to the microwave field. Pictures of the experimental setup used in the microwave partial upgrading series of tests is shown in Figure 7.2.

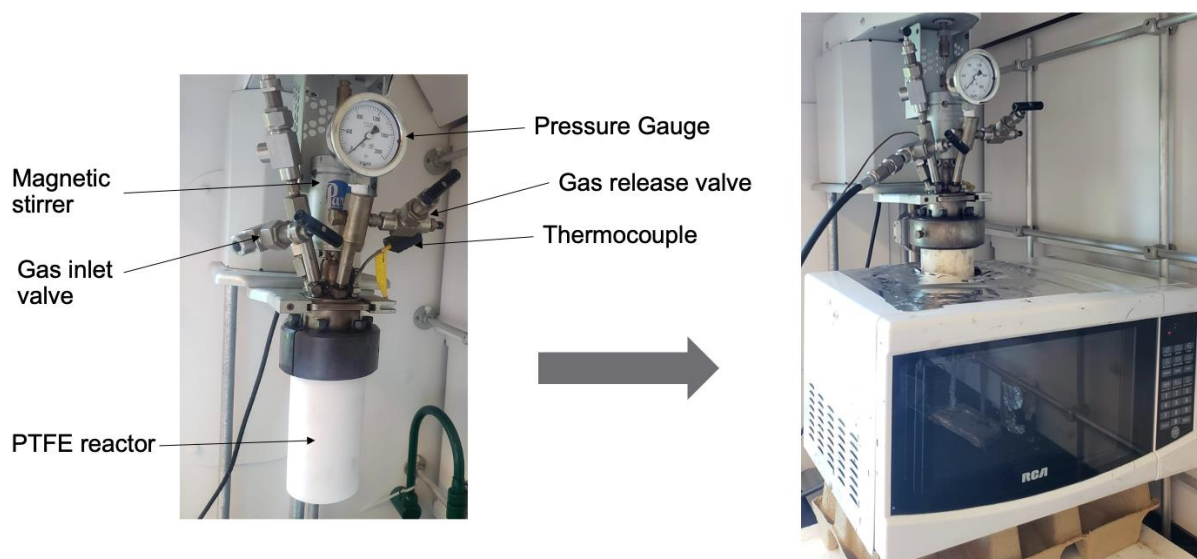


Figure 7.2: Pictures of the experimental setup used for microwave upgrading.

7.2.3 Sample Processing Method

Approximately 50 g of bitumen was initially heated in a hot water bath until flowable (approximately 80°C), then introduced into the PTFE reactor. This was combined with carbon additives and agitated at 300 rpm for 10 minutes to ensure a homogeneous mixture. The bitumen sample was subsequently heated using the commercial microwave, operating at 2.5 GHz and 700W. To maintain a non-reactive environment, the reactor assembly was filled with nitrogen gas. Post-heating, the upgraded bitumen was extracted from the PTFE reactor, and its physical properties - viscosity, density, and SARA hydrocarbon composition - were measured. All microwave upgrading reactions yielded approximately 97-98% liquid, with no observed coke formation.

The initial biochar utilized in this study was derived from the pyrolysis of pinewood biomass. However, the inherent surface area and porosity resulting from the pyrolysis process were relatively low; therefore, an activation process was used to elevate these parameters. This was crucial to equate the characteristics of the biochar to the commercially available activated carbon, thereby enabling a comparative study on the influence of the surface area and porosity on the heating efficiency of microwave irradiation. The activation procedure is comprised of several steps. Initially, 6 g of biochar was amalgamated with 6 g of KOH and 20 mL of pure water within a centrifuge tube. This mixture was then agitated for approximately 2 hours. Following this, the solution underwent filtration, with the biochar residue subjected to washing using a diluted acid solution until neutrality was attained. After neutralization, the residue was dehydrated at 80°C for 48 hours. To complete the activation, the dried biochar was placed within a ceramic crucible and exposed to a heating rate of 10°C/min until a temperature of 800°C was reached. This temperature was maintained for 2 hours under an inert atmosphere within an activation unit.

7.2.4 Characterization Methods

The Nova 1200E BET analyzer from QuantaChrome was used for surface area analysis of the four carbon-based susceptors. Before measurements, samples were degassed at 150°C for over 3 hours in a vacuum. The BET Nitrogen adsorption and desorption method was used at 77°K to determine the specific surface area and pore size distribution, following the BET and BJH equations respectively.

The sulfur percentage in hydrocarbons was determined following the ASTM D4294 standard [192]. The sample was injected into a measurement cell and exposed to an X-ray tube beam. The emitted characteristic X radiation was measured, and the collected count was compared with those from calibration standards to determine the sulfur concentration in mass percent. Three concentration ranges were covered by calibration samples: 0.0 to 0.1 mass%, 0.1 to 1.0 mass%, and 1.0 to 5.0 mass% sulfur.

7.3 Results and Discussion

7.3.1 Effects of Carbon Susceptors on Bitumen Upgrading

The Role of Carbon Susceptors in Microwave Absorption and Heating Rates

The impact of carbon susceptors on the microwave heating rate and the time taken to reach a target temperature of 200°C in oil samples is illustrated in Figures 7.3a and b. The heating rate under microwave irradiation depends on the oil sample's ability to absorb and convert microwave energy into heat. Four types of carbon susceptors - activated carbon, coke, graphite, and biochar - at concentrations ranging from 0 to 1.0 wt%, were tested in bitumen samples to evaluate their effect on heating rates. The results, demonstrating different absorption capabilities among the susceptors, can be attributed to factors such as the dipole moment of a molecule, the contact surface area, and the elemental composition [188].

In the absence of a carbon susceptor, bitumen reached a peak temperature of 125°C after 15 minutes of microwave heating (heating rate of 6°C/min). Conversely, the addition of a small quantity of 0.1wt% of activated carbon (AC) allowed the bitumen sample to hit the 200°C mark within 9 minutes, enhancing the heating rate to 20.8°C/min. With increasing the AC concentration, the time to reach 200°C was significantly reduced, taking only 5 minutes at 0.5 wt% and 4 minutes at 1.0 wt% AC.

Biochar and coke exhibited similar trends, needing a minimum of 4 minutes to reach 200°C at 1 wt%. At a lower concentration of 0.1 wt%, however, it took about 25 minutes to reach the desired temperature. At 0.5 wt%, both biochar and coke reached 200°C in around 7-8 minutes, corresponding to a heating rate of 25°C/min, comparable to 0.1wt% AC. Graphite, in comparison, showed the least absorption capabilities. Its most efficient heating rate of 21°C/min was achieved

at 1wt%, taking approximately 8.8 minutes to reach 200°C. This rate was comparable to 0.1wt% AC or 0.5wt% of either biochar or coke. At 0.5wt% and 0.1wt%, graphite needed roughly 16 and 25 minutes of microwave heating, respectively.

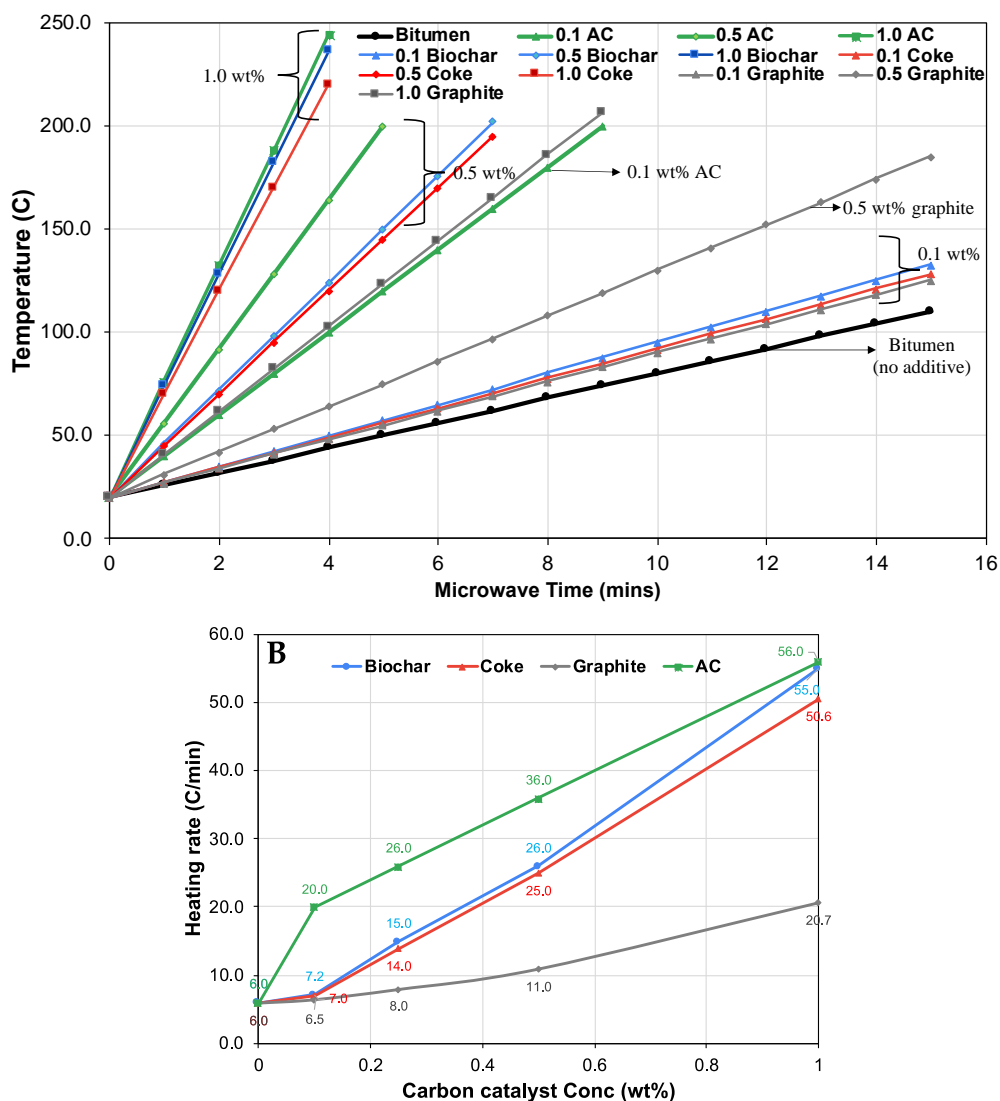


Figure 7.3: A) Recorded temperatures with carbon susceptors at different concentrations.

B) The effect of different carbon susceptor concentrations on the heating rates.

The Effect of Carbon Susceptors on Bitumen's Viscosity

Figure 7.4 outlines the viscosity changes for the upgraded oil samples at different carbon susceptor concentrations under microwave irradiation. After reaching 150°C, or the maximum feasible temperature for samples with lower carbon susceptor concentrations, the samples were maintained

at that temperature for 10 minutes. Viscosity measurements were taken 3 times for each condition at room temperature (20°C), and the average value is presented in Figure 7.4. Remarkably, with the assistance of a carbon susceptor under microwave irradiation for merely 10 minutes, bitumen viscosity dropped from its initial value of 100,000 cP to 18,000 cP. However, this significant reduction was achieved at varying carbon susceptor concentrations. Only 0.1wt% of activated carbon (AC) was needed for the maximum viscosity reduction, with any further AC concentration increase failing to significantly alter the final viscosity, making 0.1wt% the optimum concentration. Contrastingly, the maximum viscosity reduction in the other bitumen samples necessitated a 0.5wt% concentration of either biochar or coke. As with AC, any concentration increase beyond the optimum had no impact on the final viscosity, rendering 0.5 wt% the optimal concentration for both biochar and coke.

Graphite, however, required a higher concentration - 1.0wt% - for maximum viscosity reduction, double that of biochar or coke, and ten times that of AC. The variation in optimum susceptor concentrations could be attributed to differing trace metal content within the carbon particles, impacting their catalytic and microwave absorption abilities, or to the surface area and pore volume associated with each particle, affecting the susceptors' surface properties and microwave radiation absorption abilities. These aspects will be further explored in subsequent sections of this chapter.

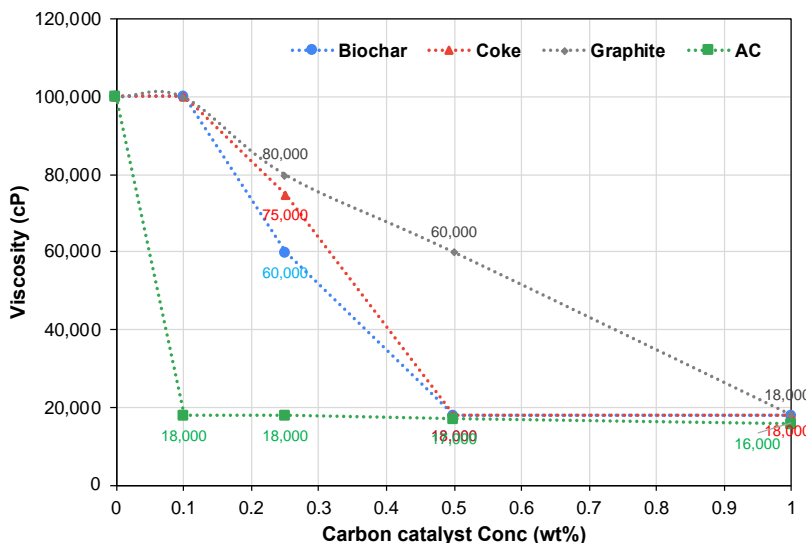


Figure 7.4: The effect of carbon susceptor concentrations on bitumen's viscosity after microwaving at 150°C for 10 minutes.

The Effect of Carbon Susceptors on Bitumen's SARA Fractions

The SARA (Saturates, Aromatics, Resins, Asphaltenes) composition of both the original bitumen sample and the upgraded samples, post 10 minutes of microwave heating at 150°C, are presented in Table 7.1. Only the optimum concentrations of each of the four susceptors (0.1wt% AC, 0.5wt% biochar, 0.5wt% coke, and 1.0 wt% graphite), required to achieve maximum viscosity reduction, were considered. Notably, these optimum concentrations offered almost equivalent heating rates of 21°C/min for the bitumen samples.

A consistent observation across the upgraded samples was a substantial increase in the saturate fraction, which increased from the original 18.5% to around 30% within a brief span of 10 minutes of microwave exposure. This remarkable transformation underscores the susceptibility of resin and asphaltene constituents, which, being rich in S, N, and O elements, are the most common polar compounds, to microwave radiation, crucial in facilitating electromagnetic field heating [168]. Interestingly, the asphaltene content experienced a marginal decrease, attributed to a limited extent of cracking reactions probably due to the limited reaction time. On the other hand, the resin and aromatic fractions displayed significant reductions, indicative of substantial cracking into smaller, saturated molecules during the microwave heating process. For instance, in the AC sample, the aromatic and resin content were reduced by about 7.5wt% and 9.7wt%, respectively. These findings align with studies such as Zhang et al.'s [184], which reported that out of the SARA fractions, resins and aromatics had the most significant impact on the dielectric loss factor in heavy oils, while saturates and asphaltenes had a minor impact. Contrary to previous beliefs, asphaltenes, despite being a primary polar component, were found to have a minor contribution to the dielectric loss. This behavior can be attributed to the low molecular mobility of the molecules, inhibiting their response to the electromagnetic field at microwave frequencies.

In terms of carbon susceptors, the 0.1wt% Activated Carbon (AC) sample demonstrated the greatest increase in saturates (from 18.5wt% to 31.2wt%) alongside the most significant reduction in viscosity (from 300,000cP to 18,000cP) when compared with the other 3 susceptors. At the same time, there was a slight reduction in aromatics, with resins and asphaltenes witnessing larger decreases. This highlights AC's efficiency, owing to its superior surface area and porosity, in absorbing microwaves and promoting the thermal cracking of heavier fractions into lighter ones. From a density perspective, all upgraded samples recorded a drop from the original 1020 Kg/m³

to 1000 Kg/m³, indicative of successful thermal cracking of heavier fractions, consequently reducing the overall weight of the bitumen. When compared with conventional upgrading methods, microwave upgrading with carbon susceptors appears to exhibit superior control over the hydrocarbon composition of the bitumen. Traditional methods such as coking or hydroprocessing typically necessitate higher temperatures and pressures and are associated with substantial energy consumption and greenhouse gas emissions. Furthermore, these methods may yield a higher proportion of undesired products like coke or gas. Conversely, microwave upgrading seems to augment the desirable saturates fraction and substantially curb the bitumen's viscosity, resulting in a more efficient and environmentally benign upgrading process.

Table 7.1: SARA composition of oil samples before and after 10 min microwave heating at 150°C.

Oil Samples	Hydrocarbon Composition (wt%)				Density (Kg/m ³)	Viscosity (cP)
	Saturates	Aromatics	Resins	Asphaltenes		
Original Bitumen	18.5	28.9	30.6	19.8	1020	300,000
Bitumen with 0.1wt% AC	31.2	27.3	21.0	18.5	1000	18,000
Bitumen with 0.5wt% Biochar	30.6	25.7	22.6	19.1	1000	18,400
Bitumen with 0.5wt% Coke	30.8	25.1	23.0	19.1	1000	18,600
Bitumen with 1wt% Graphite	28.8	26.4	23.4	19.4	1000	19,000

*Note: When bitumen samples are analyzed using clay column chromatography to determine their group composition, the sum of the percentages of the light and heavy components does not equal 100% since some nonhydrocarbon reserves remain in the column. The total mass of all the recovered fractions is equal to 97.68% (which still satisfies the ASTM-2007 [193] requirement of being > 97%).

The Role of Carbon Susceptors on Desulfurization of Bitumen

Table 7.2 outlines the sulfur content of bitumen samples, which were subjected to microwave heating at 150°C for 10 minutes with the aid of four carbon susceptors at their optimum concentrations. The results indicate a substantial reduction in sulfur content, by a factor of 21-24%, across all upgraded samples. Notably, the sample containing 0.1wt% activated carbon (AC) facilitated the greatest sulfur reduction compared to the other carbon susceptors.

This significant reduction can be attributed to the occurrence of cracking reactions in or near the hot-spots created by the carbon susceptors during microwave heating. The presence of these hot-spots increases the likelihood of heavier components, typically rich in sulfur, undergoing cracking. This process can break the C-S bonds, allowing for the release of sulfur in the form of H₂S, which results in lower sulfur content.

The varying desulfurization rates among different carbon susceptors are likely related to their individual properties. Specifically, AC, even at a lower concentration, proved the most efficient, possibly due to its high surface area and porosity, enhancing microwave absorption and interaction with sulfur compounds. Conversely, despite a higher concentration, graphite achieved slightly lower desulfurization, potentially due to its lower porosity and surface area. Biochar and coke exhibited intermediate performance, likely due to properties falling between those of AC and graphite. These findings underscore the role of carbon susceptors in enhancing microwave-induced desulfurization in bitumen. Nonetheless, a more in-depth investigation is necessary to understand the influence of carbon susceptors' surface properties on microwave absorption, a topic that will be further investigated in the subsequent section.

Table 7.2: The sulfur content of microwaved bitumen measured by XRF.

Sample	Sulfur Content (wt%)	Desulfurization (%)
Original bitumen	4.67	-
Upgraded with 0.1wt%AC	3.54	24.2
Upgraded with 0.5wt% Biochar	3.63	22.3
Upgraded with 0.5wt% Coke	3.66	21.6
Upgraded with 1.0wt% Graphite	3.58	23.3

7.3.2 Surface Properties of Carbon Susceptors and their Effect on Microwave Absorption

Effect of Trace Metal Content

The disparity in heating rates among different carbon susceptors was initially explored through a leaching process aimed at demineralizing carbon particles of any trace metal components. The procedure adopted was similar to that outlined in reference [194]. This involved submerging 20

grams of activated carbon in 500 mL of 0.1 mol/L HCl, ensuring even dissolution through gentle stirring, and allowing it to rest for 2 hours at 20°C. The resulting solution was then filtered, with the carbon residue thoroughly rinsed with distilled water until neutralization. The leached carbon powder, nearly pure at 99.99% carbon and less than 0.01% trace elements, was dried in an oven at 120°C to eliminate any residual moisture.

When the leached AC was incorporated into bitumen for microwave heating, both heating rate and viscosity values were measured. The findings revealed no discernible difference between leached and un-leached AC samples in terms of heating rates or viscosity reduction across different concentrations. A detailed analysis of this part can be found in Appendix D. Based on these observations, it was concluded that trace metal content in the carbon susceptors does not influence either the catalytic effect or microwave absorption abilities. Therefore, the variation in heating rates might primarily be attributed to a different surface property. This important discovery directs the path for future investigations.

Impact of Surface Area and Porosity

Investigations from several studies on porous carbon materials suggest that such structures, by providing alternative pathways for incident waves, can enhance electromagnetic wave absorption [195]. The porous nature of these materials enables multiple instances of absorption and scattering of electromagnetic waves, subsequently converting them into heat. This process enhances the dielectric loss factor of the absorbing material, a parameter signifying the material's efficiency in converting radiation into heat. Increased pore volume decreases effective permittivity and enhances connectivity with free space. Such properties allow electromagnetic waves to penetrate porous absorbers more efficiently and remain trapped for extended periods. Given these considerations, this study targeted the surface area and porosity of carbon susceptors. All four were analyzed using the BET method, with the summarized results presented in Table 7.3.

The activated carbon demonstrated significantly higher surface area and pore volume compared to the other carbon susceptors, explaining why a mere 0.1% AC was needed to achieve the maximum thermal conversion and viscosity reduction of bitumen. Conversely, higher amounts were necessary with biochar, coke, and graphite.

Table 7.3: BET results of the four carbon susceptors.

Susceptor	Multi-point BET specific surface area (m ² /g)	Total Pore volume (cm ³ /g)	Average Pore size (nm)
Activated Carbon	415.46	1.290	6.22
Biochar	12.01	0.023	6.50
Coke	11.39	0.038	6.72
Graphite	4.16	0.008	3.98
Activated Biochar	561.3	2.860	6.55

To further substantiate the proposed relationship between surface area and porosity to microwave absorption, the initially used biochar was further activated using KOH, enhancing its surface area and porosity beyond the activated carbon. This activated biochar was then blended with bitumen at various concentrations for microwave absorption testing. The performance of the activated biochar surpassed that of activated carbon, achieving a heating rate of 20.8°C/min and maximum viscosity reduction at just 0.05wt%. This result suggests the new optimal concentration of activated biochar is 0.05wt%, half that of AC. Conclusively, this investigation affirms the direct correlation between the surface area and porosity of carbon susceptors to their microwave absorption and heating rate. Further exploration was conducted to corroborate the established correlation between the surface area of carbon particles and their microwave absorption capabilities. Each type of carbon particle was placed individually in a quartz tube and directly subjected to microwave radiation without a solvent. This experiment aimed to expose potential differences in microwave absorption properties among the carbon susceptors and to compare hotspot temperatures with the previously measured bulk temperatures of the bitumen mixture. The outcomes of this investigation are consolidated in Table 7.4.

Table 7.4: The maximum temperature reached by carbon susceptors via direct microwave heating.

Microwaving Time (sec)	Particle Temperature (°C)				
	Activated Carbon	Biochar	Coke	Graphite	Activated Biochar
10	125	100	108	82	135
20	260	220	240	165	283
30	375	345	350	225	398
60	750	700	715	420	800

The achieved maximum temperatures underscore the assertion that carbon particles with larger surface areas and greater porosities exhibit enhanced microwave absorbance. One theory postulates that chars or cokes, due to their abundant delocalized electrons forming graphitic structures, possess superior microwave absorption qualities [196]. Furthermore, the presence of micropores within the carbon particles can make the susceptor an effective medium for microwave absorption, enhancing impedance matching and controlling effective permittivity. This theory finds support from Neji et al. [197], who demonstrated that the porous structure of the susceptor particle facilitates high impedance matching and subsequent attenuation of microwave radiation.

This investigation also highlights the significant discrepancy between local and bulk temperatures. With just 60 seconds of microwave heating, the temperature of activated carbon and activated biochar can reach 750°C and 800°C, respectively - high enough to fracture nearly all hydrocarbon bonds within the bitumen mixture. However, within the larger fluid body, heat is quickly dissipated from these localized hotspots, resulting in considerably lower overall bulk temperatures. Therefore, only bitumen fractions close to these hotspots undergo high-temperature exposure and consequent cracking.

7.3.3 Evaluation of Microwave Irradiation Operational Parameters on Upgrading Bitumen

Effect of Microwave Irradiation Time

In this investigation, the effect of varying irradiation times on the characteristics and quality of the upgraded oil was evaluated. The activated carbon (AC), given its superior surface area and porosity and hence better microwave absorbing abilities as established in prior sections, was selected as the

best carbon-based susceptor for the subsequent investigation. A concentration of 0.1wt% AC was identified as the optimum concentration, capable of inducing maximum viscosity reduction. This concentration was maintained, while other operational parameters underwent alteration. Firstly, the impact of microwaving duration was tested over a range of 0-20 minutes, while maintaining a reaction temperature of 150°C, which had been previously identified as the minimum to induce significant changes in bitumen properties. Figure 7.5 depicts the correlation between viscosity and SARA compositional changes concerning microwaving time. An irradiation duration of 10 minutes resulted in a dramatic viscosity reduction from 100,000 cP to 18,000 cP, translating to an 82% decrease. Extending the microwaving time by an additional 5 minutes (totaling 15 minutes) incrementally enhanced viscosity reduction, reaching a new viscosity of 15,000 cP and an overall reduction of 85%. Further extending the microwaving time to 20 minutes resulted in a viscosity of 13,000 cP and a maximum reduction of 87%. This data suggests the majority of thermal cracking reactions transpire within the initial 10 minutes of microwave irradiation, with any extension beyond this duration offering negligible improvements as viscosity values plateau.

Similarly, analysis of SARA fractions within the same microwaving times reveals a pattern. Within the initial 10-minute reaction window, the maximum reduction in resins and aromatics and the maximum increase in saturates by 72% were observed. Further extension of microwave irradiation time beyond this resulted in marginal improvements in hydrocarbon fractions until they plateaued at 20 minutes. The asphaltene fraction exhibited a minor decrease in the first 10 minutes, then remained constant, showing no further changes.

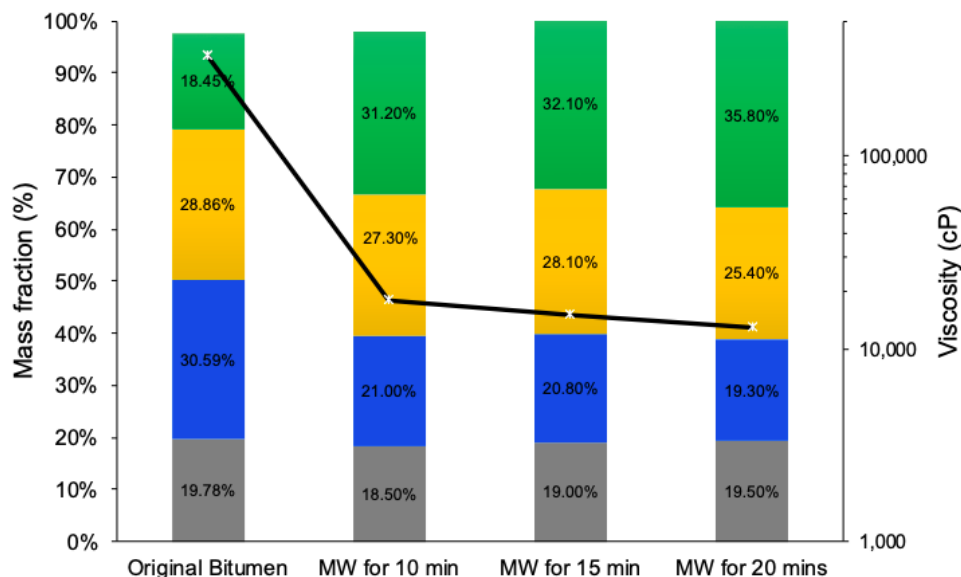


Figure 7.5: The effect of microwave irradiation time at the fixed temperature of 150°C on the viscosity reduction and SARA components of upgraded oil with 0.1wt% AC.

Effect of Maximum Microwaving Temperature

In this phase of the investigation, the impact of different maximum microwave temperatures on the upgraded oil was evaluated. The maximum reaction temperature was varied within the range of 150-200°C, while the reaction time was fixed at 10 minutes. Figure 7.6 illustrates the viscosity and SARA compositional changes in relation to microwave temperature. Findings indicate that a reaction temperature of 150°C facilitated a reduction in bitumen viscosity from 300,000 cP to 18,000 cP, signifying a 94% decrease. Increasing the maximum reaction temperature to 180°C further reduced viscosity to 14,500 cP, marking a 95.2% reduction. Finally, pushing the microwaving temperature to 200°C led to a viscosity of 11,000 cP, equating to a final viscosity reduction of approximately 96%.

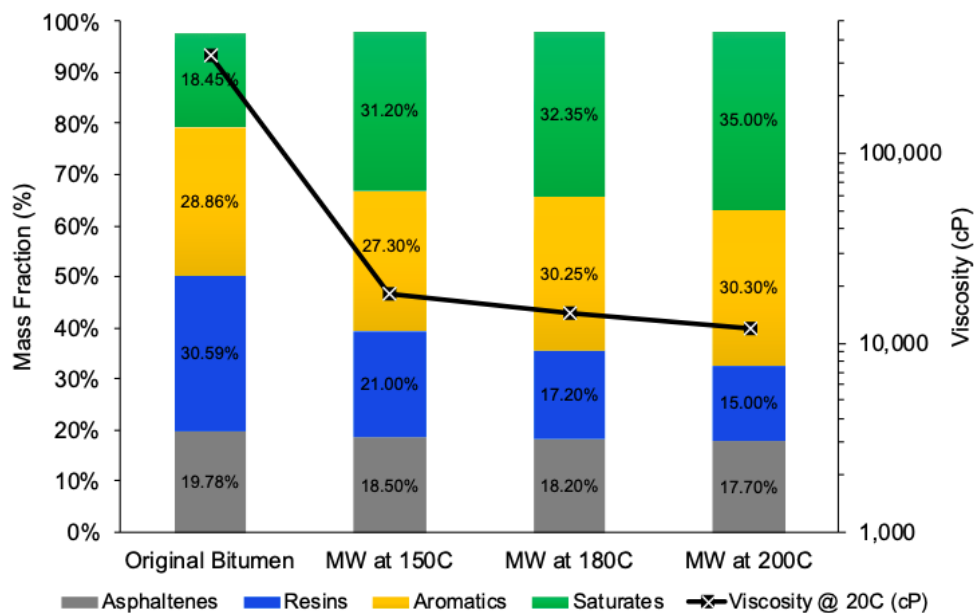


Figure 7.6: The effect of microwave (MW) reaction temperature at the fixed time of 10 mins on the viscosity reduction and SARA components of upgraded oil with 0.1wt% AC.

Subsequently, the combined effect of varying both the maximum microwaving temperature and the heating time. Parameters adjusted were the temperature, within the range of 150-200°C, and the reaction time, from 0-20 minutes. Figure 7.7 encapsulates viscosity changes as a function of both microwave temperature and time. It shows the maximum viscosity reduction occurring in the first 5 minutes of microwave heating at all tested temperatures. This is then followed by a deceleration in the reduction rate over the next 15 minutes. Optimal viscosity reduction was achieved under any one of the following conditions: microwaving at 200°C for 10 minutes, at 180°C for 15 minutes, or at 150°C for 20 minutes. Any increase beyond these parameters did not significantly alter the viscosity of bitumen or the compositional structure of the oil samples' hydrocarbon fractions.

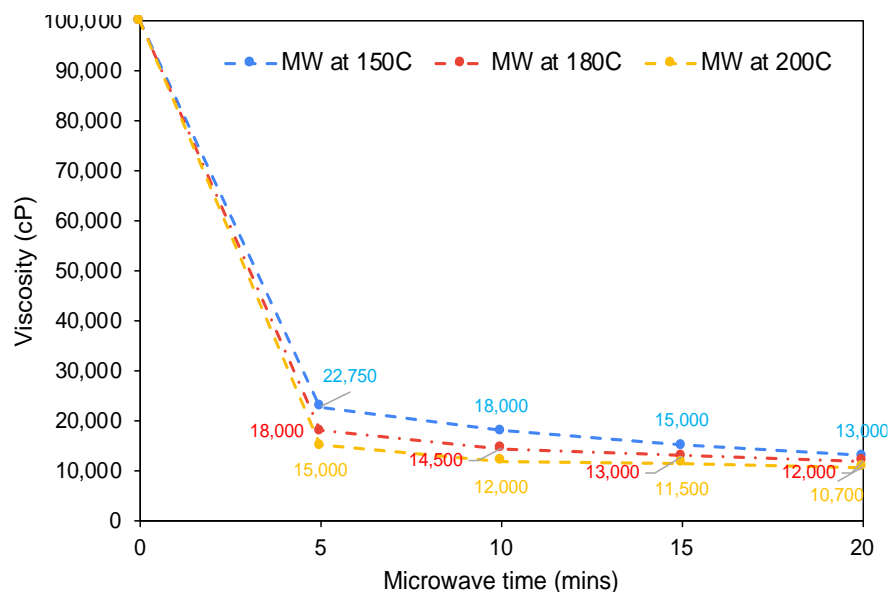


Figure 7.7: Summary of the combined effect of microwave reaction time and temperature on the viscosity reduction of upgraded oil with 0.1wt% AC.

Furthermore, the sulfur content was assessed in bitumen samples microwaved at varying temperatures and times, using XRF, with an error bar of (+/-0.01%). Table 7.5 summarizes the average sulfur results. Most tested microwaving conditions exhibited a similar effect on bitumen desulphurization, with minor improvement as either temperature or time increased. The maximum sulfur reduction was reported after microwaving bitumen at the highest irradiation of 200°C for 20 minutes, achieving a 5% sulfur reduction and reaching a minimum content of 4.45wt%.

Table 7.5: Sulfur content of upgraded oil at various microwave temperatures and times.

		Sulfur Content (wt%)		
		Maximum Microwaving Temperature		
		150°C	180°C	200°C
Microwaving Time	10 min	4.54	4.52	4.51
	20 min	4.50	4.47	4.45

Impact of the Stirring Rate

In this section, the effect of stirring rate on both the heating progression and the extent of cracking reactions was explored. The visibility of hot-spots within the light-colored PTFE reactor provided real-time observations during microwave irradiation at different stirring rates, as depicted in Figure 7.8. Without stirring (0 rpm) or at slow stirring (100 rpm), the formation of orange-colored hot-spots was conspicuous. However, a surge in the stirring rate gradually diminished both the number and intensity of these hot-spots, which were rendered undetectable at a rapid stirring rate of 600 rpm. The emergence of such hot-spots is due to microwave radiation reflection off the surface of activated carbon within the oil, a phenomenon also observed in Horikoshi et al.'s study [167]. The temperature of these hot-spots can reach an impressive 900°C, as noted in certain studies [167].

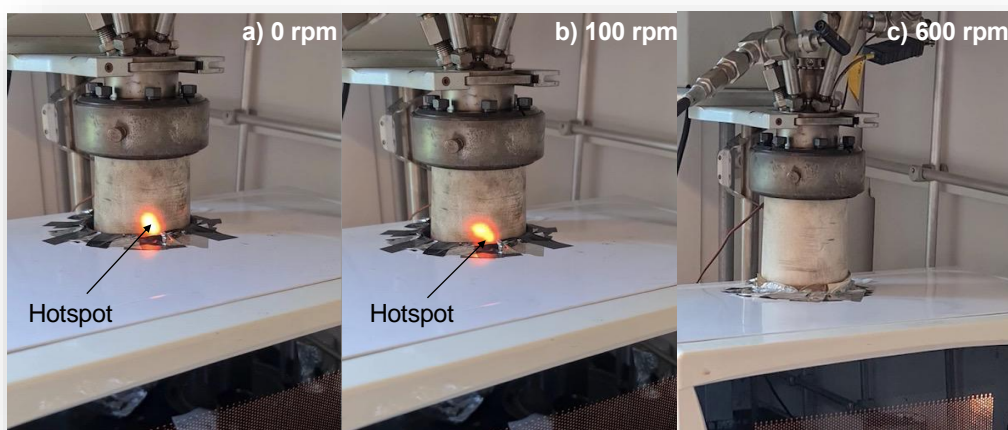


Figure 7.8: Real-time illustration of the hot-spots at various stirring rates a) at 0 rpm, b) at 100 rpm, and c) at 600 rpm.

The stirring rate's impact on the heating progression of bitumen samples is illustrated in Figure 7.9. An increased stirring rate resulted in a slower heating progression. While the heating rate remained relatively constant within the slow to medium stirring speeds (100-300 rpm), it experienced a significant drop when the stirring rate exceeded 300 rpm, bottoming at a heating rate of 10°C/min at 600 rpm. Rapid rotation probably limits the opportunity for microwave radiation to engage with the carbon surface, reducing absorption and reflection, and leading to a longer heating period.

However, stirring also facilitates a more uniform temperature profile within the bulk fluid and increases the likelihood of carbon particles interacting with bitumen's heavier fractions. Therefore, a slow stirring rate within 100-300 rpm is recommended, as employed in this study's experimental runs. Importantly, irrespective of the heating or stirring rates, the final viscosity remained consistent, suggesting that the carbon susceptor's absorption capacity was adequate for inducing the cracking reactions. As a consequence, the stirring rate appears to affect the rate of reaction rather than the extent of the reaction, providing the sample receives sufficient heating.

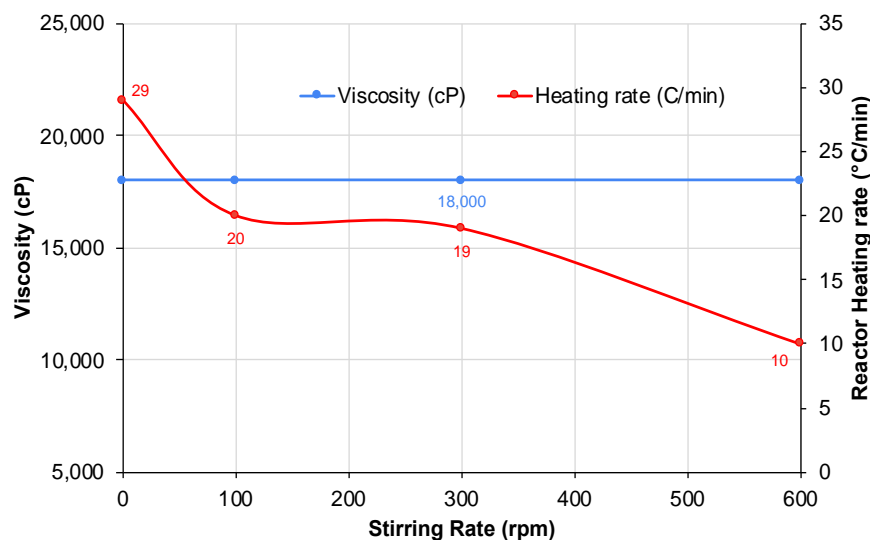


Figure 7.9: The effect of the stirring rate on the viscosity and heating rates.

7.3.4 Discussion of the key results

This chapter provides critical insights into microwave-assisted bitumen upgrading leveraging carbon-based particles as microwave susceptors. Key observations encompass the relationship between the characteristics of carbon susceptors and microwave absorbance, the effect of microwave irradiation parameters on upgraded oil, and the stirring rate's influence on the process. Activated carbon proved to be the most efficient susceptor owing to its superior surface area and porosity. Furthermore, microwave duration and temperature emerged as critical factors in decreasing bitumen's viscosity, with the majority of thermal cracking reactions occurring within the initial 10 minutes of microwave exposure. Additionally, the stirring rate was found to significantly influence the heating rate – a rise in the stirring rate resulted in a decrease in the heating rate. However, this did not affect the extent of the reaction, implying only the reaction rate was influenced.

Despite the advantages of incorporating carbon particles in the bitumen microwave partial upgrading process, this does introduce some potential operational challenges. Mainly among these is the possible build-up of carbon particles in the refineries' processing equipment, which could hinder operational efficiency or even cause equipment damage. Therefore, several preventative measures can be implemented, such as post-processing separation methods to extract carbon particles from the upgraded oil. Techniques like centrifugation, filtration, or sedimentation can be employed based on the carbon materials' particle size and characteristics. Given that the carbon susceptors' particle size usually falls within the micron or millimeter range, their separation should be manageable. An innovative approach involving the use of magnetic carbon susceptors could further simplify the separation process. Applying a magnetic field could allow for easy separation of these susceptors from the oil, mitigating risks linked to particle accumulation.

The transformation in bitumen properties through microwave upgrading hinges on several mechanisms, mainly the thermal and chemical influences of microwave irradiation, and the role of carbon susceptors employed in the process. Microwave irradiation is known to trigger certain chemical reactions, including the catalytic cleavage of C-S and C-C bonds which were witnessed as the sulfur content and the viscosity of bitumen were reduced on average by 24% and 94% respectively. Furthermore, carbon susceptors, characterized by their larger surface area and porosity, can absorb more microwaves, generating localized hot-spots within the bitumen, resulting in more efficient hydrocarbon cracking. The greater surface area also presents more sites for catalysis. Furthermore, to visualize the significance of employing microwave radiation as a partial upgrading technique. The Walther equations, as utilized by Arno de Klerk in [22], were used to accurately calculate the diluent volume required for the partially upgraded bitumen post-microwave treatment. The equations are mentioned below and are employed to meet target pipeline specifications of 350 cSt and 940 kg/m³:

$$\log(\log(v_m + 0.7)) = w_1 * \log(\log(v_1 + 0.7)) + w_2 * \log(\log(v_2 + 0.7)) \dots (\text{Eq. 7.1})$$

$$\rho_m = \left[\frac{w_1}{\rho_1} + \frac{w_2}{\rho_2} \right]^{-1} \dots \dots \dots (\text{Eq. 7.2})$$

Here, v_1 is the viscosity of the upgraded bitumen, v_2 is the viscosity of the diluent, w_1 and w_2 are the weight fractions of bitumen and diluent respectively, v_m is the viscosity of the mixture (bitumen

+ diluent), and ρ_m is the density of the mixture. It should be noted that the density of the diluent is assumed to be 642 kg/m^3 , and its dynamic viscosity is taken to be 0.5 cP at 25°C , equivalent to 0.8 cSt (kinematic viscosity). Assuming light naphtha as the main diluent with the density and viscosity values mentioned above, the calculations revealed a significant reduction in the required diluent volume, from the initial 30% to just 20%, post microwave treatment. This requirement can reduce the oil's viscosity and density from $10,000 \text{ cSt}$ and 1000 kg/m^3 post microwave irradiation to approximately 350 cSt and 940 kg/m^3 as per the pipeline specifications. This significant saving, marking a 10% decrease, was achieved merely by subjecting bitumen to microwave radiation for 20 minutes at 200°C . These findings highlight the efficiency of microwave radiation as a means to enhance bitumen's viscosity and density properties, ultimately leading to a more efficient and cost-effective use of diluents in the bitumen upgrading process.

In addition to the technical advancements demonstrated in this chapter, a preliminary analysis was made, and it suggests that the microwave-assisted bitumen upgrading process could offer significant cost and environmental benefits compared to traditional thermal cracking methods like visbreaking. The microwave irradiation technique, particularly with activated carbon as a susceptor, shows potential for higher energy efficiency and reduced operational costs due to lower energy consumption and shorter processing times, given that the initial capital costs of both processes is assumed to be the same. Additionally, the quality and yield of the upgraded bitumen could potentially enhance its market value, especially considering the significant viscosity reduction and improved SARA fractions. From an environmental standpoint, microwave irradiation is considered to be a greener alternative, primarily due to its lower greenhouse gas emissions. This is attributed to the process's energy efficiency and the potential for cleaner energy sources. Furthermore, the method might produce fewer or less harmful byproducts, contributing to a reduced environmental footprint. While these observations are based on theoretical considerations and necessitate further empirical validation, they underscore the potential of microwave irradiation as a more sustainable and cost-effective approach to bitumen partial upgrading. Therefore, detailed empirical studies or pilot-scale operations would still be necessary to provide concrete data and validate these assumptions.

Finally, while this study has provided significant insights into microwave-assisted bitumen upgrading, it also opens several avenues for future research. Paramount among these is the

exploration of scalability and industrial applicability of this method. Further studies are essential to assess the operational efficiency and economic viability of scaling up the microwave irradiation process for industrial-scale applications. Additionally, there is a need for long-term performance and reliability studies to evaluate the durability of the equipment and the consistency of upgraded bitumen quality over extended periods. Environmental impact assessments are also crucial, particularly focusing on greenhouse gas emissions and energy consumption, to comprehensively validate the environmental benefits of this technology.

7.4 Conclusion

The investigation carried out in this chapter has thoroughly examined the effect of microwave irradiation, supplemented by various carbon susceptors, on the partial upgrading of bitumen. The findings indicate that microwave irradiation of bitumen delivers a slow heating rate with negligible impact on viscosity reduction. However, when supplemented with 0.1wt% activated carbon, a brief 10-minute microwave treatment effectively raises the oil's bulk temperature to 200°C at a rate of 20.8°C/min, resulting in over a 90% decrease in bitumen viscosity. Extending the microwave exposure to 20 minutes at 150°C with 0.1wt% activated carbon induces additional cracking reactions, resulting in a further 40% reduction in viscosity. Furthermore, increasing the maximum microwave temperature from 150°C to 200°C with activated carbon stimulates additional cracking within the resin and aromatic fractions, achieving a maximum viscosity reduction. In addition to that, it was shown that the addition of just 0.1wt% of activated carbon within the bitumen blend was able to absorb the microwave radiation, creating hotspots that trigger the thermal cracking of highly polar resins and aromatics fractions into less polar, lighter saturates, with a liquid yield of over 97%. The superior microwave absorption capabilities of carbon susceptors with larger surface areas and higher porosity were also observed. Surprisingly, increasing the stirring rate during microwave irradiation resulted in a slower heating rate and faster cooling of the reaction mixture, with no significant impact on viscosity changes or the extent of the reaction. Thus, the study's results suggest that activated carbon particles can serve as an effective additive for microwave partial upgrading. This approach can achieve a reduction in bitumen viscosity of up to 96%, at considerably lower temperatures and reaction times, with less GHG emissions and overall lower operational costs compared to conventional upgrading methods.

Chapter 8 – Comparative Analysis, Conclusion, and Recommendations

8 Comparison of the Partial Upgrading Techniques

The objective of this section is to evaluate and compare the effectiveness, economic implications, and environmental sustainability of the various partial upgrading techniques outlined in the previous chapters. This assessment considers methods ranging from conventional thermal cracking at 400°C without any catalysts or additives to more innovative approaches such as the thermal cracking with surfactants as was discussed in chapter 4, Fe-based nanocatalysts (with and without hydrogen gas) as was discussed in chapter 5, Fe₃O₄ coated cenospheres (with and without hydrogen donors) as was discussed in chapter 6, microwave upgrading as was discussed in chapter 7, and finally delayed coking, and solvent deasphalting which will serve as benchmarks with their results primarily derived from existing literature.

The effectiveness of these bitumen upgrading techniques is evaluated by their impact on three key aspects: viscosity reduction, quality of the liquid product as indicated by SARA analysis, and their liquid (oil) yield, which reflect the severity and efficiency of the process. A detailed summary of these results is provided in Table 8.1.

Table 8.1: Comparison between all the partial upgrading techniques discussed against the conventional techniques.

Property	Un- Upgraded	Thermal cracking	With surfactant	With Fe ₃ O ₄ Nano	With Fe ₃ O ₄ plus H ₂	With Fe- Ceno plus H donor	Microwave upgrading	Delayed Coking	Solvent Deasphalting
Yield (wt%)									
Gas	0	5.2	5.8	6.0	6.0	6.0	2.0	3.1	0.0
Liquid	100	94.8	93.2	85.2	85.8	85.3	98.0	71.6	81.4
Coke	0	0	0	7	6.8	6.8	0	25	19
Physical Properties									
Viscosity (cP)	300,000	1700	1300	340	220	32	10,000	350	5000
Density (kg/m ³)	1020	980	980	975	975	937	1000	889	964
TAN (mg KOH/mg)	4.32	2.41	2.40	2.44	2.05	2.06	4.02	N/A	N/A
Sulfur Content (wt%)	4.67	3.54	3.54	3.21	3.23	3.43	4.54	2.40	3.90
HDS (%)	0	24.20	24.20	31.30	30.80	26.60	2.80	48.60	16.50
SARA fractions (wt%)									
Saturates	18.5	19.7	21.60	23.4	23.4	23.6	31.0	-	-
Aromatics	28.9	53.4	55.20	40.9	40.9	43.7	21.3	-	-
Resins	30.6	10.5	6.70	26.0	26.0	25.0	20.9	-	-
Asphaltenes	19.8	13.4	16.50	6.7	6.7	5.7	23.8	-	-
Dilution requirement to meet pipeline Viscosity									
Diluent content (wt%)	21	8.6	7.5	0	0	0	14	0	9.1
Diluent content (vol%)	30	13	11	0	0	0	20	0	14
Diluted oil Viscosity (cSt)	350	350	350	349	226	34	350	394	5,187

a) Viscosity reduction

Viscosity reduction is a pivotal measure of success in bitumen upgrading, primarily because it directly impacts the economic and logistical aspects of pipeline transportability. Unprocessed Athabasca Bitumen, with an original viscosity of 300,000 cP, poses significant challenges for transportation. Among the techniques evaluated, thermal cracking, both with and without surfactants, showed substantial viscosity reductions. The addition of surfactants was slightly more effective, reducing the viscosity to about 1300 cP, compared to 1700 cP achieved by thermal cracking alone. Despite these reductions, both values are substantially above the pipeline

specification of 350 cP, indicating that while effective, thermal cracking without additional processes is insufficient for meeting transport requirements.

The catalytic upgrading using Fe_3O_4 coated cenospheres with hydrogen donors achieved the most significant reduction, lowering the viscosity to only 32 cP. This far exceeds the pipeline specifications and demonstrates the potential of catalytic methods enhanced by hydrogen donors in drastically reducing bitumen viscosity. This method not only meets but significantly surpasses the necessary specifications, suggesting a highly effective upgrading strategy that could potentially lower energy costs associated with pumping and transportation. Similarly, the use of Fe_3O_4 nanocatalysts also effectively reduced the viscosity to levels within the acceptable range for pipeline transportation—340 cP without hydrogen and 220 cP with hydrogen. These results underscore the effectiveness of Fe-based nanocatalysts in improving the flow properties of bitumen, making it suitable for pipeline transportation.

Microwave upgrading, while not reaching the lows seen with some catalytic methods, still managed to significantly reduce viscosity to 10,000 cP under relatively mild operating conditions of 200°C and 20 minutes, without the use of catalysts. Although this level of viscosity reduction does not meet pipeline specifications, the significant reduction achieved under such gentle conditions highlights the potential of microwave technology as a complementary or standalone method in situations where mild upgrading is required.

Each of these methods has its strengths and limitations. Techniques involving catalysts, particularly those utilizing Fe_3O_4 with hydrogen donors, are highly effective but may involve higher costs and complexity. On the other hand, methods like microwave upgrading offer simplicity and potential cost savings, though they may require further enhancement or combination with other techniques to meet stringent pipeline standards.

b) SARA analysis

The SARA analysis serves as an important tool for understanding the impact of different upgrading techniques on bitumen composition, directly affecting the quality of the liquid product. This analysis reveals how each method alters the molecular structure of bitumen, which in turn influences both the chemical properties and commercial value of the outputs.

The introduction of surfactants in the upgrading process leads to a moderate increase in saturates from 18.5% to 21.6% and a decrease in asphaltenes from 19.8% to 16.5%. This change suggests a mild but beneficial modification towards lighter and less complex molecular structures, enhancing the fluidity and potentially reducing the propensity for pipeline fouling.

On the other hand, the introduction of the Fe_3O_4 nanocatalysts, both with and without hydrogen, results in a notable increase in saturates to 23.4% and a significant reduction in asphaltenes to 6.7%. These results indicate more profound structural changes within the bitumen, pushing the composition towards lighter and more stable hydrocarbon fractions, which are more desirable for pipeline transport and further refining processes. It is also worth to mention that microwave upgrading almost doubles the saturate content to 31% while significantly reducing aromatics to 21.3%. This significant shift suggests a transformation towards lighter and potentially more valuable hydrocarbon fractions under relatively mild operational conditions compared to traditional thermal and catalytic upgrading techniques.

c) Liquid Yield

The analysis of gas, liquid, and coke production is essential for understanding the thermal severity and operational efficiency of various upgrading processes. These metrics not only affect the yield but also have implications for environmental impact and economic viability.

Most methods involving thermal and catalytic processes, such as those using Fe_3O_4 nanocatalysts, typically yield a liquid product fraction of about 85%, with associated gas fractions of around 6% and coke fractions of 7%. These values indicate a relatively efficient conversion of feedstock to liquid product, although the generation of coke and gas signifies substantial molecular breakdown. In contrast, microwave upgrading shows a distinct advantage in terms of byproduct minimization, producing a much lower gas fraction of 2% and no coke formation. This method not only maintains a high liquid yield of over 90% but also emphasizes its potential for cleaner and more energy-efficient upgrading processes. On the other hand, a conventional method such as delayed coking leads to the highest coke production at 25%, which reflects its inefficiency and high operational challenges. Approximately one-fourth of the feedstock is converted into coke, a solid byproduct, resulting in only about 70% liquid yield. This high level of solid byproduct generation underscores the environmental and economic drawbacks of this technique.

Environmental Analysis

Evaluating the environmental impact of bitumen upgrading techniques is essential for advancing sustainable development within the industry. This analysis delves into the sustainability aspects of each method by examining energy consumption, emissions, waste generation, and potential environmental risks associated with these processes. Such evaluation is critical to ascertain the environmental friendliness and overall sustainability of these technological approaches.

Traditional upgrading methods such as delayed coking and visbreaking are notable for their high energy demands. These processes operate at elevated temperatures and for extended durations, leading to significant carbon emissions. In contrast, more innovative methods like microwave upgrading operate at considerably lower temperatures (200°C compared to approximately 400°C for traditional methods) and shorter reaction times, which can substantially reduce both energy use and thermal emissions. The environmental advantage of microwave upgrading significantly hinges on the energy source; if powered by renewable energy sources such as wind or solar, the carbon footprint could be dramatically reduced. Similarly, catalytic upgrading with Fe_3O_4 , especially when integrated with a H donor solution, offers a reduction in energy consumption as it facilitates reactions at lower temperatures.

Certain upgrading processes, particularly delayed coking, generate substantial amounts of solid byproducts like coke. These byproducts present not only disposal challenges but also potential environmental hazards if not managed correctly. Coke can be used as fuel in some industrial scenarios; however, if not burned under controlled conditions, it could contribute to air pollution. Additionally, the use of chemical additives and catalysts such as Fe_3O_4 in other upgrading techniques involves the production and disposal of chemicals that might have adverse environmental effects. Proper lifecycle management of these chemicals is essential to prevent environmental contamination, encompassing safe production, responsible usage, and proper disposal techniques.

Reducing or eliminating the need for diluents through certain upgrading techniques not only provides economic advantages but also significantly lessens the environmental impact associated with their production, transportation, and handling. Techniques that achieve pipeline-ready viscosity without the use of diluents—such as some catalytic and microwave methods—preferably

minimize ecological footprints. Moreover, the environmental impact of catalyst-based methods can be mitigated if the catalysts are reusable. Reducing the frequency of catalyst production through reusability lessens resource consumption and waste generation. Developing and implementing methods for catalyst recovery and recycling is crucial for enhancing the sustainability of these processes.

8.2 Best Practices and Recommendations

From the insights gained through the comparative analysis presented in this thesis, we can derive several best practices and recommendations for advancing bitumen upgrading technologies:

a) Adopt and Optimize Low-Energy Techniques

Technologies such as microwave upgrading demonstrate substantial advantages in terms of energy efficiency and effectiveness in reducing viscosity. These techniques should not only be further explored but also optimized for greater efficiency. Integrating renewable energy sources into these processes could significantly enhance their sustainability profiles, making them more aligned with global environmental goals.

b) Develop Reusable and Efficient Catalyst Systems

The employment of catalysts like Fe_3O_4 or Fe-based catalysts, which can be reused or easily regenerated, presents a significant opportunity to reduce both operational costs and environmental impacts. It is crucial to focus research efforts on improving the durability and reusability of these catalysts. Enhancing these aspects can lead to more sustainable and economically viable upgrading processes.

c) Reduce Dependence on Diluents

Prioritizing techniques that achieve acceptable viscosities without the use of diluents is essential. Reducing reliance on these substances not only decreases costs associated with their procurement and handling but also minimizes the environmental footprint of the upgrading process. Techniques that eliminate the need for diluents offer a dual benefit of economic savings and environmental conservation.

d) Standardize and Scale Up Promising Technologies

Promising upgrading techniques should transition from laboratory settings to pilot-scale implementations. This scale-up is vital for gathering data on operational challenges and real-world efficacy, which are crucial for refining the technology and assessing its commercial viability. Scaling up also provides insights into potential scalability issues and helps in developing solutions to address them.

Future Research Directions

To continue advancing in bitumen upgrading technologies, future research should focus on several pivotal areas:

Lifecycle Analysis (LCA): Conducting comprehensive studies on the lifecycle impacts of new upgrading technologies is essential. These studies should encompass the entire environmental footprint from manufacture to disposal, providing a full spectrum of data to assess sustainability.

Hybrid Techniques: Exploring hybrid approaches that combine the strengths of various upgrading methods could lead to innovative solutions. These hybrid techniques have the potential to optimize both economic and environmental outcomes, offering a balanced approach to bitumen upgrading.

Process Integration: Integrating new bitumen partial upgrading processes with existing refinery operations could significantly enhance overall efficiency. Research in this area should examine how such integrations can be implemented effectively without compromising the performance of each process.

Advanced Material Science: Developing new materials for catalysts and susceptors that are more effective, cost-efficient, and environmentally benign could revolutionize bitumen upgrading techniques. There is also a considerable potential in exploring biobased and recycled materials, which could further reduce the environmental impact of these processes.

Refinement of ANN Models: Further refinement of Artificial Neural Network (ANN) and other AI/ML models for better prediction and process control is crucial. Enhancing these models can

lead to more precise control over the upgrading processes, optimizing both their economic efficiency and environmental compliance.

8.3 Thesis Overall Conclusions

This thesis provides a comprehensive evaluation of advanced bitumen upgrading technologies, examining their effectiveness, sustainability, and economic viability within the Canadian oil sands industry. The initial chapters (2 and 3) offered a foundational overview, analyzing existing upgrading methods such as thermal cracking, hydrocracking, and catalytic cracking. These evaluations underscore the delicate balance required between environmental sustainability and economic feasibility, which is especially significant in optimizing such a crucial energy resource. Traditional thermal cracking methods like visbreaking, while effective in achieving high liquid yields, necessitate significant diluent usage, thereby impacting their environmental viability.

In a novel approach detailed in Chapter 4, the systematic investigation into the addition of ionic surfactants to bitumen before thermal partial upgrading was explored. The study revealed that adding just 0.25wt% of the cationic surfactant “DTAB” at upgrading temperatures ranging from 360-400°C resulted in viscosity reductions of 62%, 53%, and 27% respectively, compared to untreated samples. This indicates that DTAB promotes enhanced cracking reactions, facilitating the breakdown of heavier hydrocarbon fractions into lighter ones, thus improving the efficiency and environmental footprint of the upgrading process.

Although the addition of these surfactants enhanced the upgrading process, they did not fully meet pipeline specifications. Consequently, Chapter 5 focused on the impact of Fe-based catalysts on the partial upgrading of bitumen. It was discovered that catalysts such as FeS, FeO, and Fe₃O₄, particularly in their lower valency states, were instrumental in transforming heavier fractions into lighter ones, enhancing the quality and rheological properties of the upgraded oil. An optimal catalyst concentration of 0.5wt% was identified, with Fe₃O₄ nanoparticles significantly reducing the heavy vacuum residue fraction, which in turn resulted in an upgraded oil with a viscosity of only 340 cP, thus satisfying the pipeline specifications while eliminating the need for diluents.

Although the viscosity targets were achieved, other important properties such as density and olefin content were not met with the sole use of Fe₃O₄. Therefore, the exploration of iron-coated

cenospheres (Fe-Ceno) as a catalyst in Chapter 6 introduced a more environmentally sustainable method that significantly enhanced the quality of the upgraded oil. The Fe_3O_4 coating improved the catalyst's hydrogenation capabilities and enabled magnetic retrieval, facilitating catalyst recovery and reuse. Furthermore, the use of Fe-Ceno catalysts was supplemented with various organic liquid hydrogen donors, which resulted in the reduction of olefin content to below 1 wt% and improved oil product stability, aligning successfully with stringent pipeline specifications.

Finally, Chapter 7 investigated the use of microwave irradiation with carbon susceptors for the partial upgrading of bitumen. This method demonstrated remarkable effectiveness, particularly when 0.1wt% activated carbon was used. A 10-minute microwave treatment at 200°C achieved over a 90% decrease in viscosity. Additionally, this approach facilitated further cracking of resin and aromatic fractions, enhancing the lighter saturate content with a liquid yield surpassing 97%. This heating method was explored as an alternative to traditional heating techniques to spark interest in integrating renewable energy resources that can power microwave systems.

8.4 Significance and Novelty of this Research

The research presented in this thesis represents a significant advancement in the field of bitumen upgrading, addressing several critical knowledge gaps in the existing literature and introducing novel approaches to enhance the efficiency and selectivity of the upgrading process.

Firstly, the research breaks new ground by investigating the largely unexplored area of asphaltene cracking behavior in the presence of surfactants during high-temperature thermal upgrading. Focusing on the novel application of surfactants between 360-400°C, this study is the first to assess their effectiveness in bitumen partial upgrading rather than in-situ bitumen extraction. By examining the relationship between surfactant charge, concentration, and their impact on asphaltene structure and dispersion, the findings offer valuable insights that could significantly enhance the efficiency of bitumen upgrading processes and advance our understanding of asphaltene chemistry under extreme conditions.

Secondly, this research significantly advances the understanding of the role of iron-based catalysts in bitumen upgrading processes. Through a comprehensive investigation of Fe oxidation state, particle size, and concentration, the study sheds light on how these factors influence catalytic

performance. Beyond examining these parameters, it also delves into the reaction mechanisms and kinetics, providing essential insights for developing more efficient and selective iron-based catalysts. The novel findings pave the way for creating tailored catalysts that could lead to more sustainable and cost-effective bitumen upgrading processes, with broad implications for industrial applications.

Thirdly, this research introduces a novel and cost-effective catalyst for bitumen partial upgrading in the form of Fe_3O_4 coated cenospheres. The developed dual-function catalyst not only enhance reaction efficiency but also support diverse catalytic species, representing a new frontier in upgrading technology. Additionally, the study pioneers the use of Artificial Neural Networks (ANN) to predict the outcomes of upgrading experiments, significantly improving predictive accuracy. Together, the introduction of Fe_3O_4 coated cenospheres and the application of ANN offer scalable, cost-efficient solutions that remarkably advance the performance and understanding of bitumen upgrading processes.

Finally, this research makes a significant contribution to the field of bitumen upgrading by systematically addressing gaps in the application of microwave energy, particularly in the context of different carbon susceptors. By exploring the impact of key parameters such as microwaving time, operating temperature, carbon additive concentration, and agitation rate, the microwave study provides valuable insights into optimizing the microwave-assisted upgrading process. The findings not only enhance our understanding of how microwave energy can be effectively utilized but also lay the groundwork for future studies and potential industrial applications aimed at reducing energy consumption and improving process efficiency in bitumen upgrading.

References

- [1] I. Faergestad, “The Defining Series: Heavy Oil,” **2016**.
- [2] B. Israel, J. Gorski, and N. Lothian, *The Oilsands in a Carbonconstrained Canada : The Collision Course Between Overall Emissions and National Climate Commitments*, no. February. **2020**.
- [3] S. Yasemi, Y. Khalili, A. Sanati, and M. Bagheri, “Carbon Capture and Storage: Application in the Oil and Gas Industry,” *Sustain.*, vol. 15, no. 19, **2023**.
- [4] Alberta Energy, “Oil Sands: Facts and Statistics,” *Government of Alberta*, **2015**. Accessed on Jan 2022. Available: <http://www.energy.alberta.ca/oilsands/791.asp>.
- [5] Alberta Energy Outlook, “Alberta energy outlook,” 2020. Accessed on Jan 2022
- [6] International Energy Agency, “International Energy Agency (IEA) World Energy Outlook 2022,” <https://www.iea.org/reports/world-energy-outlook-2022/executive-summary>, p. 524, **2022**.
- [7] A. Shah, R. Fishwick, J. Wood, G. Leeke, S. Rigby, and M. Greaves, “A review of novel techniques for heavy oil and bitumen extraction and upgrading,” *Energy Environ. Sci.*, vol. 3, no. 6, pp. 700–714, **2010**.
- [8] AER, “Alberta Energy Outlook 2023,” **2023**. Accessed on Jan 2024.
- [9] Fatih Birol, “IEA (2019), World Energy Outlook 2019, IEA, Paris,” **2019**.
- [10] S. H. Ng *et al.*, “Preliminary Assessment of a Strategy for Processing Oil Sands Bitumen to Reduce Carbon Footprint,” *Energy and Fuels*, vol. 35, no. 11, pp. 9489–9496, **2021**.
- [11] P. He *et al.*, “Catalytic bitumen partial upgrading over Ag-Ga/ZSM-5 under methane environment,” *Fuel Process. Technol.*, vol. 156, pp. 290–297, **2017**.
- [12] A. Zachariah and A. De Klerk, “Partial Upgrading of Bitumen: Impact of Solvent Deasphalting and Visbreaking Sequence,” *Energy and Fuels*, vol. 31, no. 9, pp. 9374–9380, **2017**.
- [13] M. R. Gray, “Fundamentals of Partial Upgrading of Bitumen,” *Energy and Fuels*, vol. 33, no. 8, pp. 6843–6856, **2019**.
- [14] L. M. Yañez Jaramillo and A. De Klerk, “Partial Upgrading of Bitumen by Thermal Conversion at 150-300 °c,” *Energy and Fuels*, vol. 32, no. 3, pp. 3299–3311, **2018**.
- [15] J. Keesom, W.; Gieseman, “Bitumen Partial Upgrading,” *Whitepaper AM0401A; Alberta Innov. Calgary, AB*, **2018**.
- [16] J. Winter, V. Goodday, and G. K. Fellows, “Enabling Partial Upgrading In Alberta: A Review Of The Regulatory Framework And Opportunities For Improvement,” vol. 12, no. December, pp. 0–47, **2019**.
- [17] S. Badoga, P. Misra, G. Kamath, Y. Zheng, and A. K. Dalai, “Hydrotreatment followed by oxidative desulfurization and denitrogenation to attain low sulphur and nitrogen bitumen derived gas oils,” *Catalysts*, vol. 8, no. 12, pp. 1–19, **2018**.
- [18] S. Sharifvaghefi, B. Yang, and Y. Zheng, “New insights on the role of H₂S and sulfur

- vacancies on dibenzothiophene hydrodesulfurization over MoS₂ edges,” *Appl. Catal. A Gen.*, vol. 566, no. April, pp. 164–173, **2018**.
- [19] Government of Alberta, “Capping oil sands emissions,” *Government of Alberta*, **2015**. Available: <http://alberta.ca/climate/oilsands-emissions.cfm>. Accessed on Jan 2022.
- [20] J. Gieseman and W. Keesom, “Bitumen Partial Upgrading 2018 Whitepaper AM0401A,” no. March, p. 9, **2018**.
- [21] J. Zhou, Pg. Paolo Bomben, Pc. Murray Gray, and F. Bryan Helfenbaum, “Bitumen Beyond Combustion White Paper,” no. November, **2021**.
- [22] M. A. Al Bari *et al.*, “Economic and environmental assessment of asphaltene-derived carbon fiber production,” *Green Chem.*, vol. 25, no. 16, pp. 6446–6458, **2023**.
- [23] J. Zhou, Pg. Paolo Bomben, Pc. Murray Gray, and F. Bryan Helfenbaum, “Bitumen Beyond Combustion White Paper,” no. November, p. 36, **2021**.
- [24] A. De Klerk, “Unconventional Oil: Oilsands,” *Futur. energy (third Ed.)*, pp. 49–65, **2020**.
- [25] A. de Klerk, “Processing Unconventional Oil: Partial Upgrading of Oilsands Bitumen,” *Energy and Fuels*, vol. 35, no. 18, pp. 14343–14360, **2021**.
- [26] J. G. Speight, “A Review of: ‘The Chemistry of Alberta Oil Sands Bitumens and Heavy Oils,’” *Energy Sources*, vol. 27, no. 8, pp. 780–780, **2005**.
- [27] Arno de Klerk, Murray R.Gray, Nestor Zerpa, *Chapter 5 - Unconventional Oil and Gas: Oilsands*. **2014**.
- [28] S. Fakher, M. Ahdaya, M. Elturki, and A. Imqam, “Critical review of asphaltene properties and factors impacting its stability in crude oil,” *J. Pet. Explor. Prod. Technol.*, vol. 10, no. 3, pp. 1183–1200, **2020**.
- [29] P. G. Redelius, “The structure of asphaltenes in bitumen,” *Road Mater. Pavement Des.*, vol. 7, no. 2006, pp. 143–162, **2006**.
- [30] S. Rudyk, “Relationships between SARA fractions of conventional oil, heavy oil, natural bitumen, and residues,” *Fuel*, vol. 216, no. November 2017, pp. 330–340, **2018**.
- [31] Q. Liu, R. Fang, J. Wu, W. Cha, and P. Liu, “Effect of SARA fractions on the physical, structural and dynamic properties of bitumen using molecular dynamics simulation,” *Constr. Build. Mater.*, vol. 392, no. June, p. 132097, **2023**.
- [32] EIA, “US: Energy Information Administration,” **2013**. Accessed on Jan 2022.
- [33] Alberta Energy Regulator, “Alberta Energy Outlook, ST98-Executive Summary 2023,” p. 16, **2023**.
- [34] J. Keesom, W.; Gieseman, “Bitumen Partial Upgrading,” *Whitepaper AM0401A; Alberta Innov. Calgary, AB*, **2018**.
- [35] Oil sands magazine, “Bitumen Upgraders,” **2020**. Accessed on Jan 2022. Available: <https://www.oilsandsmagazine.com/projects/bitumen-upgraders>.
- [36] M. R. G. and N. Z. Arno de Klerk, “Unconventional Oil and Gas: Oilsands,” *Futur. energy (Second Ed.)*, pp. 95–116, **2014**.

- [37] T. Kaminski and M. M. Husein, "Partial upgrading of Athabasca bitumen using thermal cracking," *Catalysts*, vol. 9, no. 5, **2019**.
- [38] Murray R. Gray, "Upgrading Oilsands Bitumen and Heavy Oil," *Edmont. Univ. Alberta Press*, p. 496, **2015**.
- [39] B. Engineering, "Modeling Mild Thermal Cracking of Heavy Crude Oil and Bitumen with VLE Calculations André Guerra," **2018**.
- [40] A. Zachariah, L. Wang, S. Yang, V. Prasad, and A. De Klerk, "Suppression of coke formation during bitumen pyrolysis," *Energy and Fuels*, vol. 27, no. 6, pp. 3061–3070, **2013**.
- [41] A. de Klerk, "Thermal conversion modeling of visbreaking at temperatures below 400 °C," *Energy and Fuels*, vol. 34, no. 12, pp. 15285–15298, **2020**.
- [42] E. Fumoto, Y. Sugimoto, S. Sato, and T. Takanohashi, "Catalytic cracking of heavy oil with iron oxide-based catalysts using hydrogen and oxygen species from steam," *J. Japan Pet. Inst.*, vol. 58, no. 5, pp. 329–335, **2015**.
- [43] Y. Zhao, F. Wei, and D. Li, "Kinetics of the thermal cracking, thermal hydrocracking and catalytic hydrocracking of asphaltene," *Shiyou Xuebao, Shiyou Jiagong/Acta Pet. Sin. (Petroleum Process. Sect.)*, vol. 27, no. 5, pp. 753–759, **2011**.
- [44] O. Alade *et al.*, "Kinetic and thermodynamic modeling of thermal decomposition of bitumen under high pressure enhanced with simulated annealing and artificial intelligence," *Can. J. Chem. Eng.*, vol. 100, no. 6, pp. 1126–1140, **2022**.
- [45] J. Castillo and A. De Klerk, "Visbreaking of Deasphalted Oil from Bitumen at 280-400 °C," *Energy and Fuels*, vol. 33, no. 1, pp. 159–175, **2019**.
- [46] E. Rogel, C. Ovalles, and M. Moir, "Asphaltene chemical characterization as a function of solubility: Effects on stability and aggregation," *Energy and Fuels*, vol. 26, no. 5, pp. 2655–2662, **2012**.
- [47] J. G. Speight, *Heavy oil recovery and upgrading*. **2019**.
- [48] U.S. Energy Information Administration, "Coking is a refinery process that produces 19% of finished petroleum product exports," <https://www.eia.gov/todayinenergy/detail.php?id=9731>, **2013**. Accessed on Jan 2022. Available: <https://www.eia.gov/todayinenergy/detail.php?id=9731>.
- [49] P. P. Dik *et al.*, "Hydrocracking of vacuum gas oil over NiMo/zeolite-Al₂O₃: Influence of zeolite properties," *Fuel*, vol. 237, no. October **2018**, pp. 178–190, 2019.
- [50] K. Clark, P.D., Clarke, R.A., Hyne, J.B., Lesage, "Studies on the chemical reactions of heavy oils under steam stimulation condition," *AOSTRA J Res*, vol. 6, no. 1, pp. 29–39, **1990**.
- [51] S. K. Maity, J. Ancheyta, and G. Marroquín, "Catalytic aquathermolysis used for viscosity reduction of heavy crude oils: A review," *Energy and Fuels*, vol. 24, no. 5, pp. 2809–2816, **2010**.
- [52] H. F. Fan, Y. J. Liu, and L. G. Zhong, "Studies on the synergetic effects of mineral and steam on the composition changes of heavy oils," *Energy and Fuels*, vol. 15, no. 6, pp.

- 1475–1479, **2001**.
- [53] M. K. Abdrabou, X. Han, Y. Zeng, and Y. Zheng, “Optimization of iron-based catalyst for partial upgrading of Athabasca Bitumen : The role of Fe oxidation state, particle size, and concentration,” *Fuel*, vol. 357, no. PB, p. 129941, **2024**.
- [54] F. Zhao, Y. Liu, N. Lu, T. Xu, G. Zhu, and K. Wang, “A review on upgrading and viscosity reduction of heavy oil and bitumen by underground catalytic cracking,” *Energy Reports*, vol. 7, pp. 4249–4272, **2021**.
- [55] X. ZHAO, X. TAN, and Y. LIU, “Behaviors of oil-soluble catalyst for aquathermolysis of heavy oil,” *Ind. Catal.*, vol. 11, p. 11, **2008**.
- [56] Y. Chen, Y. Wang, C. Wu, and F. Xia, “Laboratory experiments and field tests of an amphiphilic metallic chelate for catalytic aquathermolysis of heavy oil,” *Energy and Fuels*, vol. 22, no. 3, pp. 1502–1508, **2008**.
- [57] J. Li, Y. Chen, C. Zhou, H. Liu, and X. Zhang, “Influences on the Aquathermolysis of Heavy Oil Catalyzed by Two Catalysts with Different Ligands,” *Pet. Sci. Technol.*, vol. 33, no. 11, pp. 1246–1252, **2015**.
- [58] M. Farahani *et al.*, “In Situ Burning of Crude Oils Using Iron Oxide Nanoparticles as Additives,” *SSRN Electron. J.*, vol. 330, no. July, p. 125568, **2022**.
- [59] E. Fumoto, “Upgrading of Heavy Oil with Steam Using Iron Oxide-based Catalyst,” *J. Japan Pet. Inst.*, vol. 61, no. 6, pp. 323–331, **2018**.
- [60] V. R. Choudhary, K. C. Mondal, and S. A. R. Mulla, “Simultaneous conversion of methane and methanol into gasoline over bifunctional Ga-, Zn-, In-, and/or Mo-modified ZSM-5 zeolites,” *Angew. Chemie - Int. Ed.*, vol. 44, no. 28, pp. 4381–4385, **2005**.
- [61] S. Zhang, D. Liu, W. Deng, and G. Que, “A review of slurry-phase hydrocracking heavy oil technology,” *Energy and Fuels*, vol. 21, no. 6, pp. 3057–3062, **2007**.
- [62] F. A. Aliev *et al.*, “In-situ heavy oil aquathermolysis in the presence of nanodispersed catalysts based on transition metals,” *Processes*, vol. 9, no. 1, pp. 1–22, **2021**.
- [63] F. Zhao, T. Xu, G. Zhu, K. Wang, X. Xu, and L. Liu, “A review on the role of hydrogen donors in upgrading heavy oil and bitumen,” *Sustain. Energy Fuels*, vol. 6, no. 8, pp. 1866–1890, **2022**.
- [64] T. M. Ignasiak and O. P. Strausz, “Reaction of Athabasca asphaltene with tetralin,” *Fuel*, vol. 57, no. 10, pp. 617–621, **1978**.
- [65] C. Vallejos, T. Vasquez, and C. Ovalles, “Downhole upgrading of extra-heavy crude oil using hydrogen donor and methane under steam injection conditions,” *Am. Chem. Soc. Div. Pet. Chem. Prepr.*, vol. 45, no. 4, pp. 591–594, **2000**.
- [66] A. Hart, M. Adam, J. P. Robinson, S. P. Rigby, and J. Wood, “Tetralin and decalin H-donor effect on catalytic upgrading of heavy oil inductively heated with steel balls,” *Catalysts*, vol. 10, no. 4, **2020**.
- [67] L. O. Alemán-Vázquez, J. L. Cano-Domínguez, and J. L. García-Gutiérrez, “Effect of tetralin, decalin and naphthalene as hydrogen donors in the upgrading of heavy oils,” *Procedia Eng.*, vol. 42, no. August, pp. 532–539, **2012**.

- [68] A. de Klerk, Y. Kim, D. Leistenschneider, and W. Chen, "Rigorous deasphalting, autoxidation, and bromination pretreatment methods for oilsands bitumen derived asphaltenes to improve carbon fiber production," *Energy and Fuels*, vol. 35, no. 21, pp. 17463–17478, **2021**.
- [69] D. P. Mohapatra and D. M. Kirpalani, "Bitumen heavy oil upgrading by cavitation processing: effect on asphaltene separation, rheology, and metal content," *Appl. Petrochemical Res.*, vol. 6, no. 2, pp. 107–115, **2016**.
- [70] O. P. Stebeleva and A. V. Minakov, "Application of Cavitation in Oil Processing: An Overview of Mechanisms and Results of Treatment," *ACS Omega*, vol. 6, no. 47, pp. 31411–31420, **2021**.
- [71] B. Avvaru, N. Venkateswaran, P. Uppara, S. B. Iyengar, and S. S. Katti, "Current knowledge and potential applications of cavitation technologies for the petroleum industry," *Ultrason. Sonochem.*, vol. 42, pp. 493–507, **2018**.
- [72] S. E. Taylor, "Interfacial chemistry in steam-based thermal recovery of oil sands bitumen with emphasis on steam-assisted gravity drainage and the role of chemical additives," *Colloids and Interfaces*, vol. 2, no. 2, pp. 1–26, **2018**.
- [73] M. Ahmadi and Z. Chen, "Molecular interactions between asphaltene and surfactants in a hydrocarbon solvent: Application to asphaltene dispersion," *Symmetry (Basel)*, vol. 12, no. 11, pp. 1–18, **2020**.
- [74] M. K. Abdrabou, X. Han, Y. Zheng, Y. Zeng, and S. Rohani, "The effect of cationic surfactants on bitumen's viscosity and asphaltene nanostructure under thermal partial upgrading," *Energy Sci. Eng.*, no. February, pp. 2540–2560, **2022**.
- [75] S. Mutyala, C. Fairbridge, J. R. J. Paré, J. M. R. Bélanger, S. Ng, and R. Hawkins, "Microwave applications to oil sands and petroleum: A review," *Fuel Process. Technol.*, vol. 91, no. 2, pp. 127–135, **2010**.
- [76] Z. Nasri, "Upgrading vacuum distillation residue of oil refinery using microwave irradiation," *Chem. Eng. Process. - Process Intensif.*, vol. 146, no. September, p. 107675, **2019**.
- [77] M. K. Abdrabou, X. Han, Y. Zeng, and Y. Zheng, "Harnessing the Power of Microwave Irradiation: A Novel Approach to Bitumen Partial Upgrading," *Molecules*, vol. 28, no. 23, **2023**.
- [78] A. Bera, J. Agarwal, M. Shah, S. Shah, and R. K. Vij, "Recent advances in ionic liquids as alternative to surfactants/chemicals for application in upstream oil industry," *J. Ind. Eng. Chem.*, vol. 82, pp. 17–30, **2020**.
- [79] A. M. Atta, A. O. Ezzat, M. M. Abdullah, and A. I. Hashem, "Effect of Different Families of Hydrophobic Anions of Imidazolium Ionic Liquids on Asphaltene Dispersants in Heavy Crude Oil," *Energy and Fuels*, vol. 31, no. 8, pp. 8045–8053, **2017**.
- [80] M. Boukherissa, F. Mutelet, A. Modarressi, A. Dicko, D. Dafri, and M. Rogalski, "Ionic liquids as dispersants of petroleum asphaltenes," *Energy and Fuels*, vol. 23, no. 5, pp. 2557–2564, **2009**.
- [81] C. Zheng, M. Brunner, H. Li, D. Zhang, and R. Atkin, "Dissolution and suspension of

- asphaltenes with ionic liquids,” *Fuel*, vol. 238, pp. 129–138, **2019**.
- [82] A. S. Ogunlaja, E. Hosten, and Z. R. Tshentu, “Dispersion of asphaltenes in petroleum with ionic liquids: Evaluation of molecular interactions in the binary mixture,” *Ind. Eng. Chem. Res.*, vol. 53, no. 48, pp. 18390–18401, **2014**.
- [83] M. I. H. Soiket, A. O. Oni, E. D. Gemechu, and A. Kumar, “Life cycle assessment of greenhouse gas emissions of upgrading and refining bitumen from the solvent extraction process,” *Appl. Energy*, vol. 240, no. October 2018, pp. 236–250, **2019**.
- [84] M. Baritto, A. O. Oni, and A. Kumar, “The development of a techno-economic model for the assessment of asphaltene-based carbon fiber production,” *J. Clean. Prod.*, vol. 428, no. September, p. 139489, **2023**.
- [85] J. Charry-Sanchez, A. Betancourt-Torcat, and A. Almansoori, “Environmental and Economics Trade-Offs for the Optimal Design of a Bitumen Upgrading Plant,” *Ind. Eng. Chem. Res.*, vol. 55, no. 46, pp. 11996–12013, **2016**.
- [86] C.E.R. Institute, “Refining Bitumen : Costs, Benefits and Analysis,” no. 145, **2014**.
- [87] Oil Price.com, “Oil Price Charts,” **2024**. Accessed on Jan 2024.
- [88] New Look at Heavy, “Heavy Oil Upgrading White Paper Vhtl : a New Look At Heavy Oil,” no. December, **2018**.
- [89] Bayshore Petroleum Corp., “Bayshore Petroleum Initiates Bitumen Upgrading Program Using Catalyst-Based Technology.” Accessed on Jan 2022. Available: <https://www.globenewswire.com/en/news-release/2015/07/28/997567/0/en/Bayshore-Petroleum-Initiates-Bitumen-Upgrading-Program-Using-Catalyst-Based-Technology.html>.
- [90] J. Jia, “HDR Diluent Reduction,” *Alberta Innov.*, **2019**.
- [91] M. Energy, “MEG Phase 1A: MDRU + SDA Program Report,” vol. 6, no. December, p. 128, **2013**.
- [92] G. Hayes, “Value creation,” *Cleanroom Technology*, **2004**. Available: <http://www.vctek.com/>.
- [93] F. Systems, “JetShear Technology Platform,” *Fractal Systems*, **2016**. Available: https://www.fractalsys.com/jetshear_technologies/.
- [94] S. Saad *et al.*, “Transformation of petroleum asphaltenes to carbon fibers,” *Carbon N. Y.*, vol. 190, pp. 92–103, **2022**.
- [95] H. Bisheh and Y. Abdin, “Carbon Fibers: From PAN to Asphaltene Precursors; A State-of-Art Review,” *C-Journal Carbon Res.*, vol. 9, no. 1, **2023**.
- [96] P. Zuo *et al.*, “Asphaltene thermal treatment and optimization of oxidation conditions of low-cost asphaltene-derived carbon fibers,” *J. Ind. Eng. Chem.*, vol. 104, pp. 427–436, **2021**.
- [97] M. L. Chacón-Patiño *et al.*, “Chemistry and Properties of Carbon Fiber Feedstocks from Bitumen Asphaltenes,” *Energy and Fuels*, vol. 37, no. 7, pp. 5341–5360, **2023**.
- [98] M. Baritto, A. O. Oni, and A. Kumar, “Estimation of life cycle greenhouse gas emissions

- of asphaltene-based carbon fibers derived from oil sands bitumen,” *Sustain. Mater. Technol.*, vol. 36, no. April 2022, p. e00627, **2023**.
- [99] A. Li *et al.*, “Electrospun Green Fibers from Alberta Oilsands Asphaltenes,” *Energy and Fuels*, vol. 37, no. 18, pp. 13645–13657, **2023**.
- [100] C. Devon, “Bitumen beyond combustion (BBC) and valorization,” **2021**. [Online]. Available: <https://natural-resources.canada.ca/energy/energy-offices-and-labs/canmetenergy/devon-ab-research-centre/bitumen-beyond-combustion-bbc-and-valorization/23380>.
- [101] A. Demirbas, A. Bafail, and A. S. Nizami, “Heavy oil upgrading: Unlocking the future fuel supply,” *Pet. Sci. Technol.*, vol. 34, no. 4, pp. 303–308, **2016**.
- [102] and G. K. F. J. Winter, V. Goodday, “Enabling Partial Upgrading In Alberta: A Review Of The Regulatory Framework And Opportunities For Improvement,” *SPP Res. Pap.*, vol. 12, no. 42, **2019**.
- [103] F. J. Ortega, F. J. Navarro, and M. García-Morales, “Dodecylbenzenesulfonic Acid as a Bitumen Modifier: A Novel Approach to Enhance Rheological Properties of Bitumen,” *Energy and Fuels*, vol. 31, no. 5, pp. 5003–5010, **2017**.
- [104] E. H. Kwon, K. S. Go, N. S. Nho, and K. H. Kim, “Effect of Alkyl Chain Length of Ionic Surfactants on Selective Removal of Asphaltene from Oil Sand Bitumen,” *Energy and Fuels*, vol. 32, no. 9, pp. 9304–9313, **2018**.
- [105] D. Ramimoghadam, M. Z. Bin Hussein, and Y. H. Taufiq-Yap, “The effect of sodium dodecyl sulfate (SDS) and cetyltrimethylammonium bromide (CTAB) on the properties of ZnO synthesized by hydrothermal method,” *Int. J. Mol. Sci.*, vol. 13, no. 10, pp. 13275–13293, **2012**.
- [106] G. Qian *et al.*, “Industrially Promising Nanowire Heterostructure Catalyst for Enhancing Overall Water Splitting at Large Current Density,” *ACS Sustain. Chem. Eng.*, vol. 8, no. 32, pp. 12063–12071, **2020**.
- [107] R. Kumari, A. Kakati, R. Nagarajan, and J. S. Sangwai, “Synergistic effect of mixed anionic and cationic surfactant systems on the interfacial tension of crude oil-water and enhanced oil recovery,” *J. Dispers. Sci. Technol.*, vol. 40, no. 7, pp. 969–981, **2019**.
- [108] A. Telmadarreie and J. J. Trivedi, “New insight on carbonate-heavy-oil recovery: Pore-scale mechanisms of post-solvent carbon dioxide foam/polymer-enhanced-foam flooding,” *SPE J.*, vol. 21, no. 5, pp. 1655–1668, **2016**.
- [109] Z. Derikvand, A. Rezaei, R. Parsaei, M. Riazi, and F. Torabi, “A mechanistic experimental study on the combined effect of Mg^{2+} , Ca^{2+} , and SO_4^{2-} ions and a cationic surfactant in improving the surface properties of oil/water/rock system,” *Colloids Surfaces A Physicochem. Eng. Asp.*, vol. 587, **2020**.
- [110] T. F. Yen, “Upgrading through cavitation and surfactant,” *World Pet. Congr. Proc.*, vol. 1997-Octob, no. 17, pp. 933–935, **1997**.
- [111] H. Hou, H. He, and Y. Wang, “Effects of SDS on the activity and conformation of protein tyrosine phosphatase from thermus thermophilus HB27,” *Sci. Rep.*, vol. 10, no. 1, p. 3195, **2020**.

- [112] M. Ahmadi and Z. Chen, "Insight into the Interfacial Behavior of Surfactants and Asphaltenes: Molecular Dynamics Simulation Study," *Energy and Fuels*, vol. 34, no. 11, pp. 13536–13551, **2020**.
- [113] A. Y. León, A. Guzmán M, H. Picón, D. Laverde C, and D. Molina V, "Reactivity of Vacuum Residues by Thermogravimetric Analysis and Nuclear Magnetic Resonance Spectroscopy," *Energy and Fuels*, vol. 34, no. 8, pp. 9231–9242, **2020**.
- [114] J. P. Elder, "Reconciliation of Arrhenius and iso-conversional analysis kinetics parameters of non-isothermal data," *Thermochim. Acta*, vol. 272, pp. 41–48, Jan. **1996**.
- [115] H. M. S. Lababidi, H. M. Sabti, and F. S. Alhumaidan, "Changes in asphaltenes during thermal cracking of residual oils," *Fuel*, vol. 117, no. PART A, pp. 59–67, **2014**.
- [116] M. K. Abdrabou, P. P. Morajkar, G. D. J. Guerrero Peña, A. Raj, M. Elkadi, and A. V. Salkar, "Effect of 5-membered bicyclic hydrocarbon additives on nanostructural disorder and oxidative reactivity of diffusion flame-generated diesel soot," *Fuel*, vol. 275, **2020**.
- [117] F. S. Alhumaidan, A. Hauser, M. S. Rana, H. M. S. Lababidi, and M. Behbehani, "Changes in asphaltene structure during thermal cracking of residual oils: XRD study," *Fuel*, vol. 150, pp. 558–564, **2015**.
- [118] A. Peraza, M. Sánchez, and F. Ruetze, "Modeling free-radical reactions, produced by hydrocarbon cracking, with asphaltenes," *Energy and Fuels*, vol. 24, no. 7, pp. 3990–3997, **2010**.
- [119] L. L. Zhang, G. H. Yang, J. Q. Wang, Y. Li, L. Li, and C. H. Yang, "Study on the polarity, solubility, and stacking characteristics of asphaltenes," *Fuel*, vol. 128, pp. 366–372, **2014**.
- [120] K. Yehliu, R. L. Vander Wal, and A. L. Boehman, "Development of an HRTEM image analysis method to quantify carbon nanostructure," *Combust. Flame*, vol. 158, no. 9, pp. 1837–1851, **2011**.
- [121] L. Lam, S.-. Lee, and C. Y. Suen, "Thinning methodologies-a comprehensive survey," *IEEE Trans. Pattern Anal. Mach. Intell.*, vol. 14, no. 9, pp. 869–885, **1992**.
- [122] K. Yehliu, R. L. Vander Wal, O. Armas, and A. L. Boehman, "Impact of fuel formulation on the nanostructure and reactivity of diesel soot," *Combust. Flame*, vol. 159, no. 12, pp. 3597–3606, **2012**.
- [123] Y. Li *et al.*, "A review of in situ upgrading technology for heavy crude oil," *Petroleum*, vol. 7, no. 2, pp. 117–122, **2021**.
- [124] J. G. Speight, "Visbreaking: A technology of the past and the future," *Sci. Iran.*, vol. 19, no. 3, pp. 569–573, **2012**.
- [125] D. Davudov and R. G. Moghanloo, "A systematic comparison of various upgrading techniques for heavy oil," *J. Pet. Sci. Eng.*, vol. 156, no. June, pp. 623–632, 2017.
- [126] A. Hart, M. Greaves, and J. Wood, "A comparative study of fixed-bed and dispersed catalytic upgrading of heavy crude oil using-CAPRI," *Chem. Eng. J.*, vol. 282, pp. 213–223, **2015**.
- [127] T. A. Al-Attas *et al.*, "Recent Advances in Heavy Oil Upgrading Using Dispersed

- Catalysts,” *Energy and Fuels*, vol. 33, no. 9, pp. 7917–7949, **2019**.
- [128] C. Li, W. Huang, C. Zhou, and Y. Chen, “Advances on the transition-metal based catalysts for aquathermolysis upgrading of heavy crude oil,” *Fuel*, vol. 257, no. March, p. 115779, **2019**.
- [129] N. N. Nassar, A. Hassan, and P. Pereira-Almao, “Application of nanotechnology for heavy oil upgrading: Catalytic steam gasification/cracking of asphaltenes,” *Energy and Fuels*, vol. 25, no. 4, pp. 1566–1570, **2011**.
- [130] A. Lakhova *et al.*, “Aquathermolysis of heavy oil using nano oxides of metals,” *J. Pet. Sci. Eng.*, vol. 153, no. February, pp. 385–390, **2017**.
- [131] J. Liu, Y. Song, X. Guo, C. Song, and X. Guo, “Recent advances in application of iron-based catalysts for CO_x hydrogenation to value-added hydrocarbons,” *Chinese J. Catal.*, vol. 43, no. 3, pp. 731–754, **2022**.
- [132] M. A. Suwaid *et al.*, “In-situ catalytic upgrading of heavy oil using oil-soluble transition metal-based catalysts,” *Fuel*, vol. 281, no. June, p. 118753, **2020**.
- [133] P. Sirikulbodee, T. Ratana, T. Sornchamni, M. Phongaksorn, and S. Tungkamani, “Catalytic performance of Iron-based catalyst in Fischer-Tropsch synthesis using CO₂ containing syngas,” *Energy Procedia*, vol. 138, pp. 998–1003, **2017**.
- [134] A. A. A., “Laboratory investigation of nanoscale dispersed catalyst for inhibition coke formation and upgrading of heavy oil during THAI process,” *Univ. Birmingham.*, no. September, **2015**.
- [135] Y. H. Shokrlu and T. Babadagli, “Viscosity reduction of heavy oil/bitumen using micro- and nano-metal particles during aqueous and non-aqueous thermal applications,” *J. Pet. Sci. Eng.*, vol. 119, pp. 210–220, **2014**.
- [136] I. I. Mukhamatdinov, A. R. Khaidarova, R. D. Zaripova, R. E. Mukhamatdinova, S. A. Sitnov, and A. V. Vakhin, “The composition and structure of ultra-dispersed mixed oxide (ii, iii) particles and their influence on in-situ conversion of heavy oil,” *Catalysts*, vol. 10, no. 1, **2020**.
- [137] A. O. Alabi and A. S. Sambo, “Comparative bio-energy potential of De-oiled coconut pulp and Coconut shell: Insights from physicochemical characterization, pyrolysis kinetics and thermodynamic studies,” *Fuel Process. Technol.*, vol. 243, p. 107658, **2023**.
- [138] X. Huang, H. Yin, H. Zhang, N. Mei, and L. Mu, “Pyrolysis characteristics, gas products, volatiles, and thermo-kinetics of industrial lignin via TG/DTG-FTIR/MS and in-situ Py-PI-TOF/MS,” *Energy*, vol. 259, no. August, p. 125062, **2022**.
- [139] J. Li *et al.*, “Effect of alkalis on iron-based Fischer-Tropsch synthesis catalysts: Alkali-FeO_x interaction, reduction, and catalytic performance,” *Appl. Catal. A Gen.*, vol. 528, pp. 131–141, **2016**.
- [140] R. Guzmán, J. Ancheyta, F. Trejo, and S. Rodríguez, “Methods for determining asphaltene stability in crude oils,” *Fuel*, vol. 188, pp. 530–543, **2017**.
- [141] M. V. K. Kök, M. A. Varfolomeev, and D. K. Nurgaliev, “Crude oil characterization using TGA-DTA, TGA-FTIR and TGA-MS techniques,” *J. Pet. Sci. Eng.*, vol. 154, no.

- December 2016, pp. 537–542, **2017**.
- [142] Z. Wang, Q. Wang, C. Jia, and J. Bai, “Thermal evolution of chemical structure and mechanism of oil sands bitumen,” *Energy*, vol. 244, p. 123190, **2022**.
- [143] T. Wang, J. Wang, W. Yang, and D. Yang, “Quantification of low-temperature oxidation of light oil and its SAR fractions with TG-DSC and TG-FTIR analysis,” *Energy Sci. Eng.*, vol. 8, no. 2, pp. 376–391, **2020**.
- [144] E. Esmailnezhad, M. Karimian, and H. J. Choi, “Synthesis and thermal analysis of hydrophobic iron oxide nanoparticles for improving in-situ combustion efficiency of heavy oils,” *J. Ind. Eng. Chem.*, vol. 71, pp. 402–409, **2019**.
- [145] K. Miura and T. Maki, “A simple method for estimating $f(E)$ and $k_0(E)$ in the distributed activation energy model,” *Energy and Fuels*, vol. 12, no. 5, pp. 864–869, 1998.
- [146] S. Vyazovkin *et al.*, “ICTAC Kinetics Committee recommendations for collecting experimental thermal analysis data for kinetic computations,” *Thermochim. Acta*, vol. 590, pp. 1–23, **2014**.
- [147] A. Al-Marshed, A. Hart, G. Leeke, M. Greaves, and J. Wood, “Effectiveness of Different Transition Metal Dispersed Catalysts for In Situ Heavy Oil Upgrading,” *Ind. Eng. Chem. Res.*, vol. 54, no. 43, pp. 10645–10655, **2015**.
- [148] X. Li, P. Chi, X. Guo, and Q. Sun, “Effects of asphaltene concentration and asphaltene agglomeration on viscosity,” *Fuel*, vol. 255, no. June, p. 115825, **2019**.
- [149] O. Morelos-Santos *et al.*, “A novel direct method in one-step for catalytic heavy crude oil upgrading using iron oxide nanoparticles,” *Catal. Today*, vol. 392–393, pp. 60–71, **2022**.
- [150] A. Al-Marshed, A. Hart, G. Leeke, M. Greaves, and J. Wood, “Optimization of Heavy Oil Upgrading Using Dispersed Nanoparticulate Iron Oxide as a Catalyst,” *Energy and Fuels*, vol. 29, no. 10, pp. 6306–6316, **2015**.
- [151] X. Qu *et al.*, “Catalytic aquathermolysis of Mackay River bitumen with different types of Mo-based catalysts,” *Fuel*, vol. 326, no. July, p. 125134, **2022**.
- [152] M. Salehzadeh, T. Kaminski, and M. M. Husein, “An optimized thermal cracking approach for onsite upgrading of bitumen,” *Fuel*, vol. 307, no. August 2021, p. 121885, **2022**.
- [153] N. Al O, C. Al, and O. C. Heated, “Naphthalene to Explore Heavy Oil Upgrading Using,” *Catalyst*, pp. 1–18, **2020**.
- [154] A. Hart, C. Lewis, T. White, M. Greaves, and J. Wood, “Effect of cyclohexane as hydrogen-donor in ultradispersed catalytic upgrading of heavy oil,” *Fuel Process. Technol.*, vol. 138, pp. 724–733, **2015**.
- [155] B. A. Peprah, “Iron Hydrogenation,” **2023**.
- [156] N. Ranjbar and C. Kuenzel, “Cenospheres: A review,” *Fuel*, vol. 207, pp. 1–12, **2017**.
- [157] V. S. Chandane, A. P. Rathod, K. L. Wasewar, and S. S. Sonawane, “Efficient cenosphere supported catalyst for the esterification of n-octanol with acetic acid,” *Comptes Rendus Chim.*, vol. 20, no. 8, pp. 818–826, **2017**.

- [158] B. Samojeden, J. Drużkowska, D. Duraczyńska, M. Poddębniak, and M. Motak, "Use of iron and copper-promoted cenospheres as catalysts in the selective catalytic reduction of nitrogen(II) oxide with ammonia," *Przem. Chem.*, vol. 98, no. 4, pp. 541–545, **2019**.
- [159] J. Zhang, B. Wang, H. Cui, C. Li, J. Zhai, and Q. Li, "Synthesis of CeO₂/fly ash cenospheres composites as novel photocatalysts by modified pyrolysis process," *J. Rare Earths*, vol. 32, no. 12, pp. 1120–1125, **2014**.
- [160] B. Samojeden *et al.*, "Novel nickel- and magnesium-modified cenospheres as catalysts for dry reforming of methane at moderate temperatures," *Catalysts*, vol. 9, no. 12, **2019**.
- [161] A. Macchi, P. Plouffe, G. S. Patience, and D. M. Roberge, "Experimental methods in chemical engineering: Micro-reactors," *Can. J. Chem. Eng.*, vol. 97, no. 10, pp. 2578–2587, **2019**.
- [162] J. Zhan, H. Zhang, and G. Zhu, "Magnetic photocatalysts of cenospheres coated with Fe₃O₄/TiO₂ core/shell nanoparticles decorated with Ag nanoparticles," *Ceram. Int.*, vol. 40, no. 6, pp. 8547–8559, **2014**.
- [163] S. Horikoshi, M. Kamata, T. Mitani, and N. Serpone, "Control of microwave-generated hot spots. 6. Generation of hot spots in dispersed catalyst particulates and factors that affect catalyzed organic syntheses in heterogeneous media," *Ind. Eng. Chem. Res.*, vol. 53, no. 39, pp. 14941–14947, **2014**.
- [164] J. Taheri-Shakib, A. Shekarifard, and H. Naderi, "Experimental investigation of comparing electromagnetic and conventional heating effects on the unconventional oil (heavy oil) properties: Based on heating time and upgrading," *Fuel*, vol. 228, no. March, pp. 243–253, **2018**.
- [165] A. D8253-21, "Standard Test Method for Determination of the Asphaltene Solvency Properties of Bitumen, Crude Oil, Condensate and/or Related Products to calculate Stability, Compatibility for Blending, Fouling, and Processibility (Manual Micros)."
- [166] L. Y. Yu, Z. X. Huang, and M. X. Shi, "Synthesis and characterization of silica by sol-gel method," *Adv. Mater. Res.*, vol. 1030–1032, pp. 189–192, **2014**.
- [167] B. Hariyanto, D. A. P. Wardani, N. Kurniawati, N. P. Har, N. Darmawan, and Irzaman, "X-ray peak profile analysis of silica by Williamson–Hall and size-strain plot methods," *J. Phys. Conf. Ser.*, vol. 2019, no. 1, **2021**.
- [168] A. A. Mohammed, Z. T. Khodair, and A. A. Khadom, "Preparation and investigation of the structural properties of α -Al₂O₃ nanoparticles using the sol-gel method," *Chem. Data Collect.*, vol. 29, **2020**.
- [169] J. Jing, J. Li, J. Feng, W. Li, and W. W. Yu, "Photodegradation of quinoline in water over magnetically separable Fe₃O₄/TiO₂ composite photocatalysts," *Chem. Eng. J.*, vol. 219, pp. 355–360, **2013**.
- [170] F. S. AlHumaidan, A. Hauser, M. S. Rana, and H. M. S. Lababidi, "NMR Characterization of Asphaltene Derived from Residual Oils and Their Thermal Decomposition," *Energy and Fuels*, vol. 31, no. 4, pp. 3812–3820, **2017**.
- [171] S. M. Elahi, C. E. Scott, Z. Chen, and P. Pereira-Almao, "In-situ upgrading and enhanced recovery of heavy oil from carbonate reservoirs using nano-catalysts: Upgrading reactions

- analysis,” *Fuel*, vol. 252, pp. 262–271, **2019**.
- [172] S. Alkhalidi and M. M. Husein, “Hydrocracking of heavy oil by means of in situ prepared ultradispersed nickel nanocatalyst,” *Energy and Fuels*, vol. 28, no. 1, pp. 643–649, **2014**.
- [173] I. Higuerey, M. Orea, and P. Pereira, “Estimation of visbroken and selective catalytic steam cracked product stability using iatroskan TLC-FID,” *ACS Div. Fuel Chem. Prepr.*, vol. 47, no. 2, pp. 656–658, **2002**.
- [174] S. I. Andersen and J. G. Speight, “Thermodynamic models for asphaltene solubility and precipitation,” *J. Pet. Sci. Eng.*, vol. 22, no. 1–3, pp. 53–66, **1999**.
- [175] E. Rogel, M. Roye, J. Vien, and T. Miao, “Characterization of asphaltene fractions: Distribution, chemical characteristics, and solubility behavior,” *Energy and Fuels*, vol. 29, no. 4, pp. 2143–2152, **2015**.
- [176] A. Navlani, A. Fandango, and I. Idris, *Python Data Analysis : Perform Data Collection, Data Processing, Wrangling, Visualization, and Model Building Using Python*. **2021**.
- [177] R. Ssebadduka, N. N. H. Le, R. Nguete, O. Alade, and Y. Sugai, “Artificial neural network model prediction of bitumen/light oil mixture viscosity under reservoir temperature and pressure conditions as a superior alternative to empirical models,” *Energies*, vol. 14, no. 24, **2021**.
- [178] L. Hanyong, C. Kexin, J. Ling, W. Leilei, and Y. Bo, “Experimental study on the viscosity reduction of heavy oil with nano-catalyst by microwave heating under low reaction temperature,” *J. Pet. Sci. Eng.*, vol. 170, no. June, pp. 374–382, **2018**.
- [179] H. Shang *et al.*, “Effect of microwave irradiation on the viscosity of crude oil: A view at the molecular level,” *Fuel Process. Technol.*, vol. 170, no. pp. 44–52, **2018**.
- [180] Y. Zhang, M. Adam, A. Hart, J. Wood, S. P. Rigby, and J. P. Robinson, “Impact of Oil Composition on Microwave Heating Behavior of Heavy Oils,” *Energy and Fuels*, vol. 32, no. 2, pp. 1592–1599, **2018**.
- [181] A. Punase and B. Hascakir, “Stability determination of asphaltenes through dielectric constant measurements of polar oil fractions,” *Energy and Fuels*, vol. 31, no. 1, pp. 65–72, **2017**.
- [182] H. Liao, M. Morte, and B. Hascakir, “Effect of crude oil composition on microwave absorption of heavy oils,” *SPE West. Reg. Meet. Proc.*, vol. 2019, 2019.
- [183] M. Alshaikh, G. Huff, and B. Hascakir, “An Innovative Dielectric Constant Measurement Method to Determine the Ideal Surfactant Candidate to Enhance Heavy Oil Recovery,” **2018**.
- [184] K. Li, B. Hou, L. Wang, and Y. Cui, “Application of carbon nanocatalysts in upgrading heavy crude oil assisted with microwave heating,” *Nano Lett.*, vol. 14, no. 6, pp. 3002–3008, **2014**.
- [185] Z. Yu, “Research on absorbing performance of activated carbon,” *IOP Conf. Ser. Mater. Sci. Eng.*, vol. 563, no. 2, **2019**.
- [186] N. Horikoshi, S., & Serpone, *Microwaves in Catalysis: Methodology and Applications*, vol. 2015, no. 12. John Wiley & Sons., **2015**.

- [187] B. Materials, “Standard Test Method for Viscosity Determination of Asphalt at Elevated Temperatures Using a Rotational Viscometer 1,” **2014**.
- [188] D4294-16, “Sulfur in Petroleum and Petroleum Products by Energy Dispersive X-ray Fluorescence Spectrometry,” *ASTM Int.*, vol. 11, no. October, pp. 6–7, **1995**.
- [189] A. Drews, “Standard Test Method for Characteristic Groups in Rubber Extender and Processing Oils and Other Petroleum-Derived Oils by the Clay-Gel Absorption Chromatographic Method,” **2008**.
- [190] L. Li *et al.*, “Performance of bio-char and energy analysis on CH₄ combined reforming by CO₂ and H₂O into syngas production with assistance of microwave,” *Fuel*, vol. 215, pp. 655–664, **2018**.
- [191] J. B. Cheng, H. G. Shi, M. Cao, T. Wang, H. B. Zhao, and Y. Z. Wang, “Porous carbon materials for microwave absorption,” *Mater. Adv.*, vol. 1, no. 8, pp. 2631–2645, **2020**.
- [192] J. A. Menéndez *et al.*, “Microwave heating processes involving carbon materials,” *Fuel Process. Technol.*, vol. 91, no. 1, pp. 1–8, **2010**.
- [193] A. H. Alshareef, “Asphaltenes: Definition, Properties, and Reactions of Model Compounds,” *Energy and Fuels*, vol. 34, no. 1, pp. 16–30, **2020**.

Appendices

Appendix A

A-1: Detailed Sample processing method:

Experimental Setup for the bitumen upgrading reactor:

Apparatus: Parr Bench Top Reactor

Location: Thompson Engineering Building
417, Western University

Sample: Oil sand bitumen

Temperature range: 360-400°C

Pressure range: 0-200 psi

Reaction Time: 2 hours

Number of Experiments: 4 runs per condition

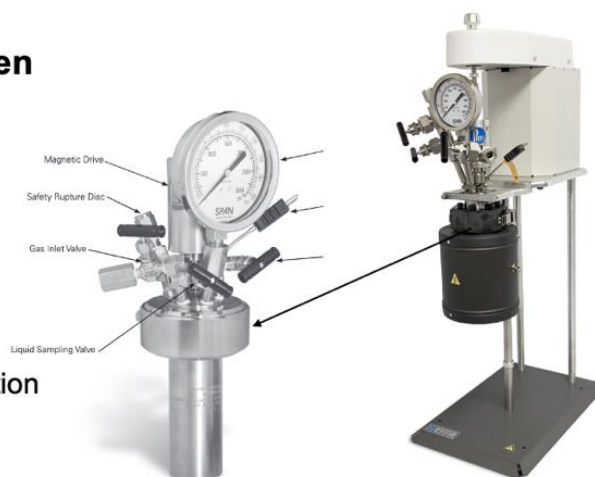


Figure 10A: Experimental setup for the upgrading reactor.

1. Each bitumen sample was preheated using hot water until it became flowable (oil temperature should be about 80°C); then about 60 g of bitumen was added to the autoclave (Parr Bench Top Reactor of series 4590 as shown in Figure 1 above).
2. The reactor was charged with N₂ gas at 1 bar so that the reaction takes place in an inert environment.
3. The reactor was heated from room temperature to the required temperature at a stirring rate of 300 rpm, and the reactor pressure and temperature were recorded as a function of heating time.
4. After that, the reactor temperature was maintained for 2 hours.
5. The gas products and liquid products (after condensation) were collected every 60 mins. Therefore, two sets of gas and liquid products were collected during each thermal cracking reaction, and one set of gas and liquid products is collected after reaction and condensation.
6. After the reaction completion, the reactor was cooled down with water to room temperature, and the cooling time was recorded as well as the reactor pressure versus reactor temperature.
7. The reactor lid was opened, and all the weights of liquid and solid products were recorded.
8. The reaction was repeated 3 more times; as a result, 4 sets of data were collected in total.

9. After each run, the upgraded bitumen was removed from the autoclave and its physical properties such as viscosity, density, and asphaltene content were measured.
10. Later, the asphaltene fraction (insoluble in *n*-pentane) was extracted from the treated bitumen and subjected to detailed characterization tests.

A-2: Detailed SARA procedure:

The Saturates, Aromatics, Resins, and Asphaltenes (SARA) fractions of oil sand bitumen.

I. Separation of Asphaltenes

- 1) 10±0.5 g bitumen sample is weighted in a pre-weighed 250-mL conical flask, and 100 mL *n*-pentane is added and is well-mixed with bitumen sample. (5 mins)
- 2) Warm the liquid mixture on the heat plate for a few seconds with intermittent swirling.
- 3) Allow the mixture to stand about 30 min at room temperature. (30 mins)
- 4) Using a 500-mL suction filter to filter the sample. Rinse the conical flask and stirring rod with 60-mL *n*-pentane, and then pour the rinse through the paper filter. (30 mins)
- 5) Put the pre-weighed filter paper and residue (asphaltene) in oven overnight in 70°C, after that the weight of residue/asphaltene (W_1) is recorded.
- 6) Transfer the solution after filtration to a beaker and evaporate the *n*-pentane in a water bath with the temperature of 45°C on the hot plate.
- 7) Record the weight of solution (W_2) until the weight loss between the weighs is less than 10 mg and check the weight of Asphaltenes (W_1) with the weight of Asphaltenes by difference ($10 - W_2$).
- 8) The solution (W_2) contains the Saturates, Resins, and Aromatics components, and the concentration of each component is determined as following.

II. Separation of Saturates

- 9) Prepare the Clay-Gel Percolating Column: (a) in the upper section, clay adsorbent of 100 g is added; (b) in the lower section, silica gel of 200 g plus clay of 50 g on top of the silica gel are added.
- 10) Place a piece of glass wool over the top surface of clay in the upper section to prevent the agitation of the clay while charging the solvents.
- 11) The solution (W_2) is charged with 25 mL *n*-pentane solvent and is well-mixed to ensure a uniform and stable solution.
- 12) Charge the Clay-Gel Percolating Column with 25 mL *n*-pentane and allow to percolate into the clay, and then add the diluted solution to the column.

- 13) Wash the sample beaker with n-pentane and add the washings to the column.
- 14) Charge n-pentane to the column and maintain a head level of 20 mm well above the top of the upper column.
- 15) Collect 280 ± 10 mL of the first n-pentane effluent from the bottom of Clay-Gel Percolating Column in a 500-mL pre-weighed beaker.
- 16) The n-pentane solvent in 500-mL pre-weighed beaker is evaporated at 45°C in a water bath, and the weight of Saturates (W3) is obtained by the difference method.

III. Separation of Resins

- 17) Disconnect the two columns and allow the lower column to drain into a receiver. Continue washing the upper clay section with n-pentane.
- 18) Maintain a moderate liquid head level above the clay during the washing and adjust n-pentane additions so that the level is about 25 mm when 150 mL have been collected in the receiver, and this n-pentane effluent is part of Aromatics component.
- 19) Discontinue additions at this point and allow the liquid to essentially drain from the clay column.
- 20) After n-pentane effluent has essentially drained from the column, charge a 50 to 50 volume mixture of toluene–acetone solution.
- 21) Collect 250 mL of the toluene-acetone (plus n-pentane) effluent from the bottom of clay column.
- 22) The solvent toluene-acetone (plus n-pentane) is evaporated at 110°C on a heat plate, and the weight of Resins (W4) is obtained by the difference method.

IV. Separation of Aromatics

- 23) The gel column (lower section) is placed in the extraction apparatus. Toluene (200 ± 10 mL) is added into a 500-mL flask and refluxed at such a rate of 10 ± 2 mL/min for 2 h.
- 24) At the end of this time, the valve of extraction apparatus is opened, and the toluene removed into a waste solvent receiver to a volume of approximately 50-mL in the flask. The solution remaining is then combined with the n-pentane effluent from step 18 for the recovery of aromatics.
- 25) The solvent toluene is evaporated at 110°C , and the weight of Aromatics (W5) is obtained.

A-3: Additional Results for un-upgraded Bitumen:

1. The Saturates, Aromatics, Resins, and Asphaltenes (SARA) fractions of oil sand bitumen.

Table 1A. SARA analysis result of oil sand bitumen.

No.	Type	Weight /g	Ratio /%
1	Saturates	1.853	18.45
2	Aromatics	2.898	28.86
3	Resins	3.072	30.59
4	Asphaltenes	1.986	19.78

Note: total mass of all the recovered fraction is equal to 97.68% (ASTM-2007 > 97%).

2. The Thermogravimetric Analysis (TGA) analysis of oil sand bitumen.

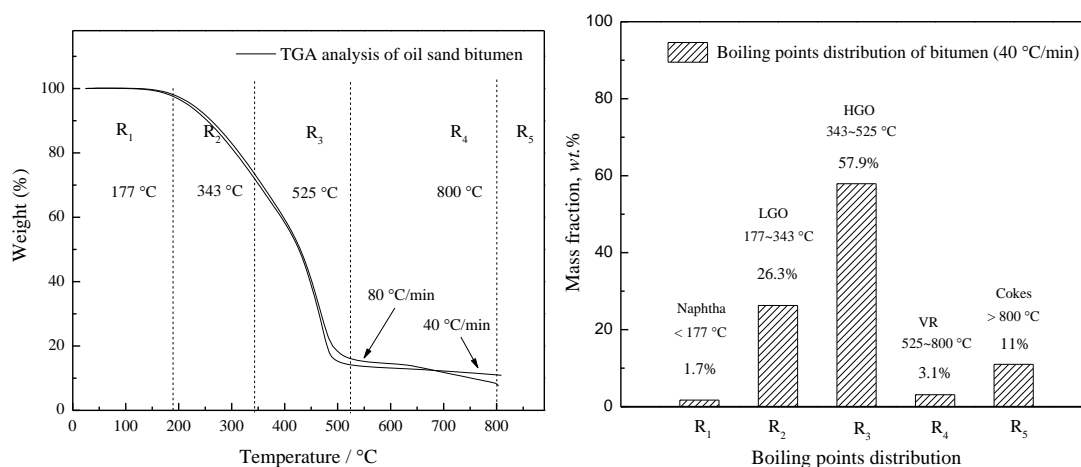


Figure 2A. The TGA curve and boiling points distribution of oil sand bitumen at 40 and 80 °C/min.

3. The Differential Scanning Calorimeter (DSC) analysis of oil sand bitumen.

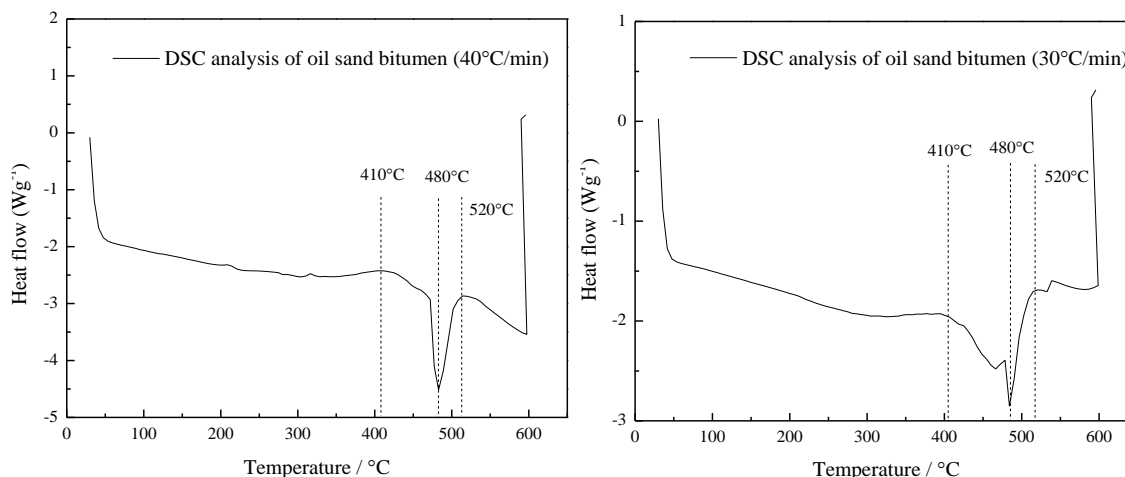


Figure 3A. The DSC curves of oil sand bitumen at 30 and 40 °C/min. (Note: the onset and optimal temperatures for thermal cracking of oil sand bitumen are 410 °C and 480 °C, respectively.)

A-4: Initial Results for thermal upgrading at 440 °C

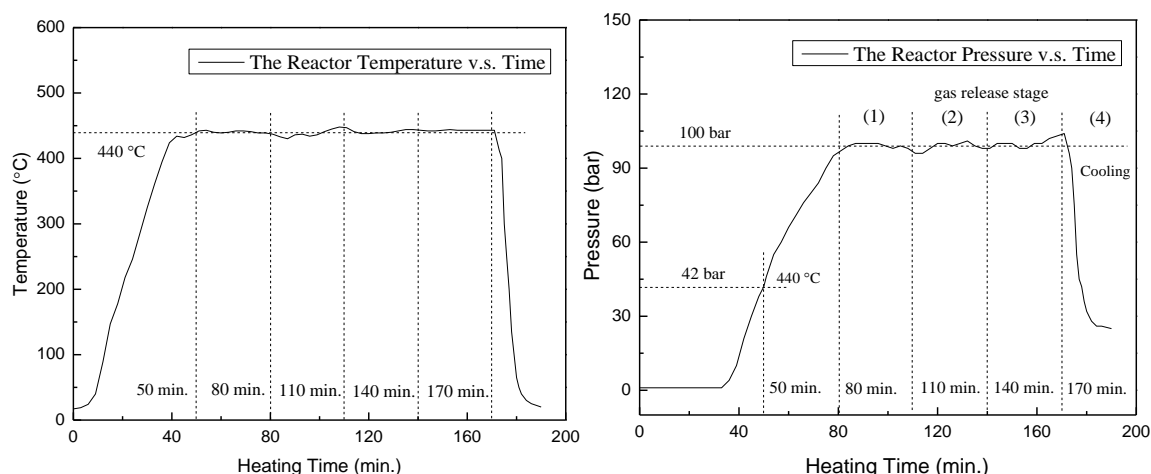


Figure 4A. The reactor temperature and pressure as a function of heating time.

Table 2A. The mass balance of bitumen thermal cracking at 440 °C.

No.	Feed bitumen (g)	Gas product(g)*	Liquid product (g)	Coke (g)	Total mass (g)	Liquid yield (%)	Mass balance
Test 1	151.6	35.6	55.7	56.8	148.1	36.7%	97.7%
Test 2	150.5	35.7	52.7	58.2	146.6	35.0%	97.4%
Test 3	150.2	37.3	51.3	59.0	147.6	34.1%	98.2%

* Note: gas weight = gas molecular mass × gas volume/gas molar volume, and the gas molecular mass is obtained by GC analysis.

Table 3A. The boiling point distribution of oil sand bitumen and oil products at 440 °C

Boiling Points	Oil Sand Bitumen (%)	Oil Product at 440 C-Test 1	Oil Product at 440 C-Test 2	Oil Product at 440 C-Test 3
Naphtha (< 177 °C)	1.7	51.5	43.9	50.1
LGO (177 - 343 °C)	26.3	45.9	49.6	46.3
HGO (343 - 524 °C)	57.9	1.1	3.0	1.7
VR (524 - 800 °C)	3.1	1.4	3.3	1.4
Cokes (> 800 °C)	11	0.1	0.2	0.5

A-5: Additional Results for thermal upgrading at 400 °C

Table 6A. The mass balance of bitumen thermal cracking at 400 °C

No.	Feed bitumen (g)	Gas product(g)*	Liquid product (g)	Coke (g)	Total mass (g)	Liquid yield (%)	Mass balance
Test 1	151.85	7.12	139.73	0	146.85	92.1%	96.7%
Test 2	152.95	7.53	139.84	0	147.37	91.4%	96.4%
Test 3	152.50	8.35	139.14	0	147.49	91.3%	96.7%
Test 4	153.75	7.13	141.16	0	148.29	91.8%	96.4%

* Note: gas weight = gas molecular mass × gas volume/gas molar volume, and the gas molecular mass is obtained by GC analysis.

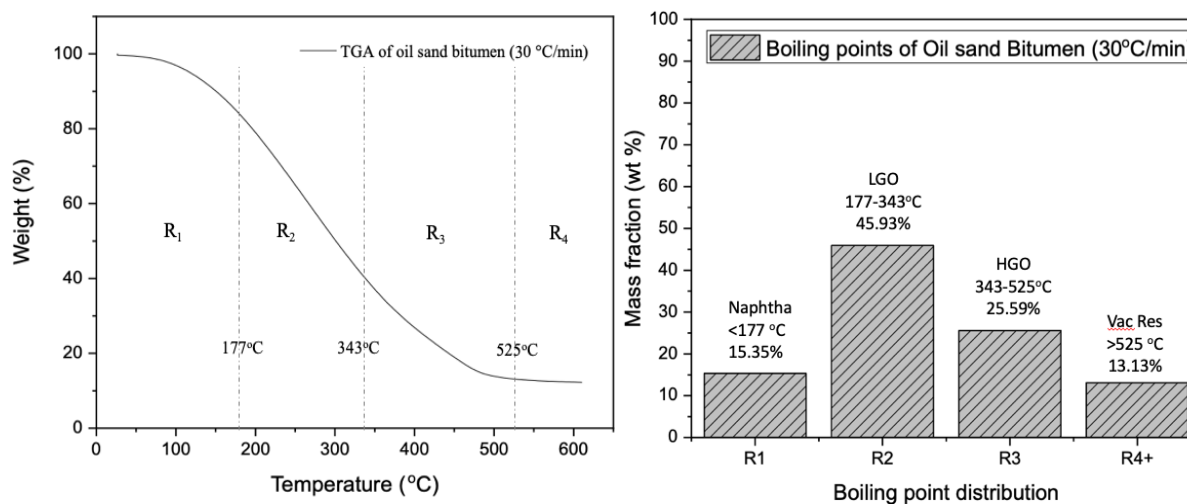


Figure 5A. The TGA curve and boiling points distribution of oil sand bitumen at 400 °C.

A-6: Additional Results for thermal upgrading at 360 °C

Table 7A. The mass balance of bitumen thermal cracking at 360 °C

No.	Feed bitumen (g)	Gas product(g)*	Liquid product (g)	Coke (g)	Total mass (g)	Liquid yield (%)	Mass balance
Test 1	151.49	1.12	150.2	0	151.3	99.14%	99.8%
Test 2	150.21	1.13	149.03	0	150.16	99.2%	99.9%
Test 3	151.37	1.11	150.06	0	148.29	99.13%	99.8%
Test 4	149.5	1.12	147.73	0	148.85	98.8%	99.56%

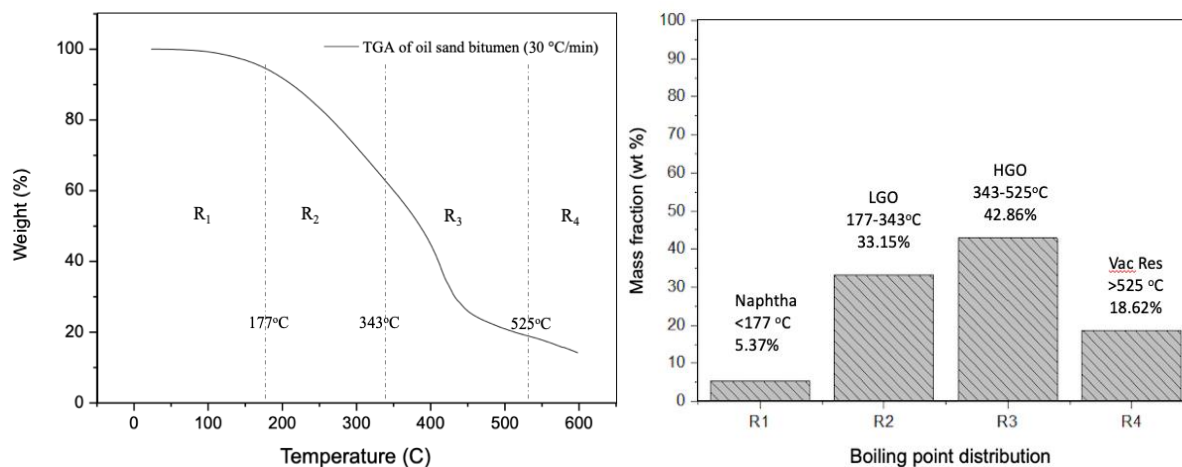


Figure 6A. The TGA curve and boiling points distribution of bitumen at 360°C at 30°C/min.

Table 8S. SARA analysis on thermally cracked products at various reaction times.

No.	Type	Bitumen (%)	360°C (%)		400°C (%)	
			1 h	2h	1h	2h
1	Saturates	18.45	20.25	20.10	19.50	19.66
2	Aromatics	28.86	39.28	39.17	53.06	53.44
3	Resins	30.59	22.45	22.23	10.50	10.45
4	Asphaltenes	19.78	15.02	15.50	14.00	13.40

A-7: Additional TGA results for surfactants:

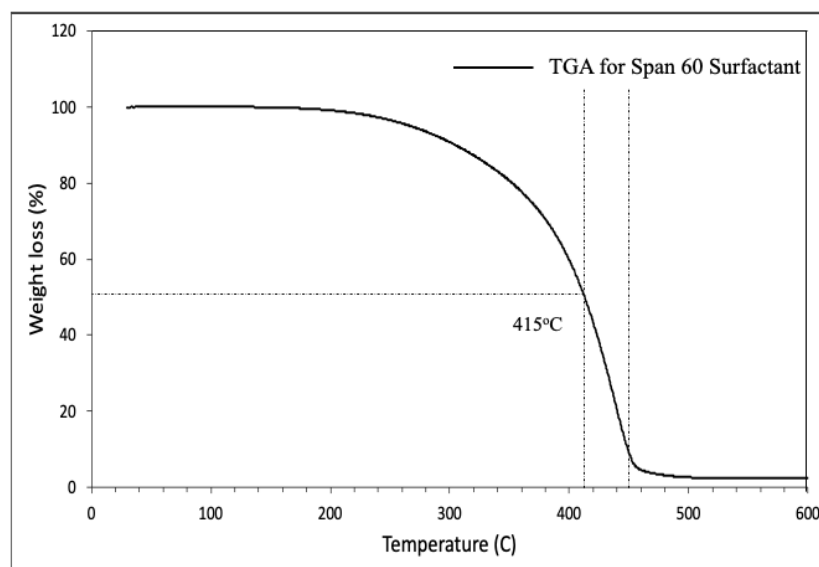


Figure 7A. The TGA curve for the degradation of Span 60 at 30°C/min.

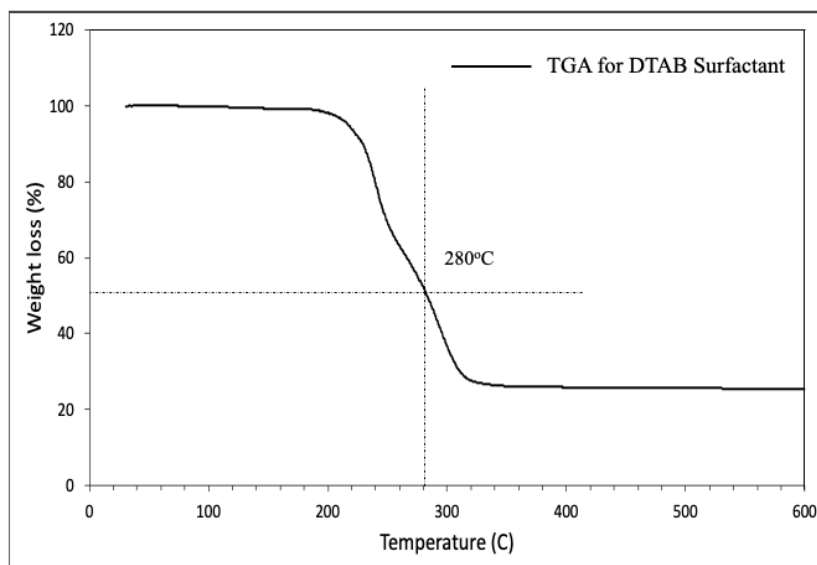


Figure 8A. The TGA curve for the degradation of DTAB at 30°C/min.

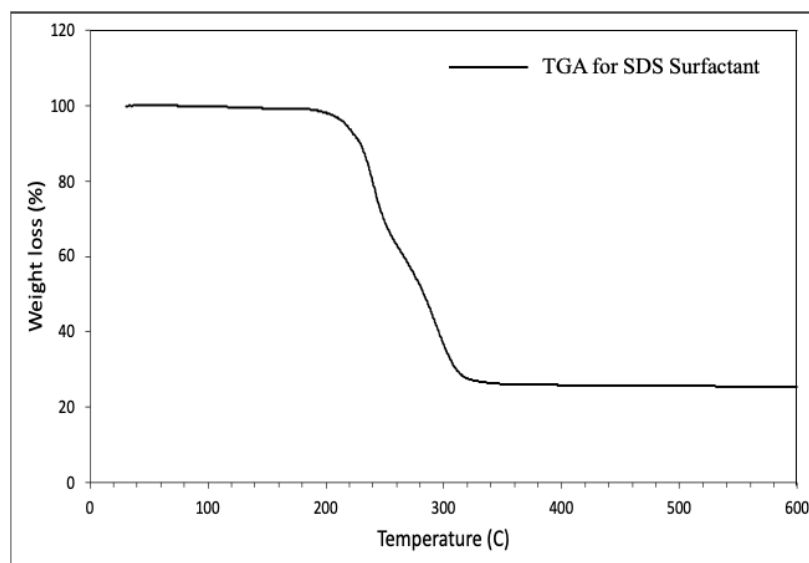
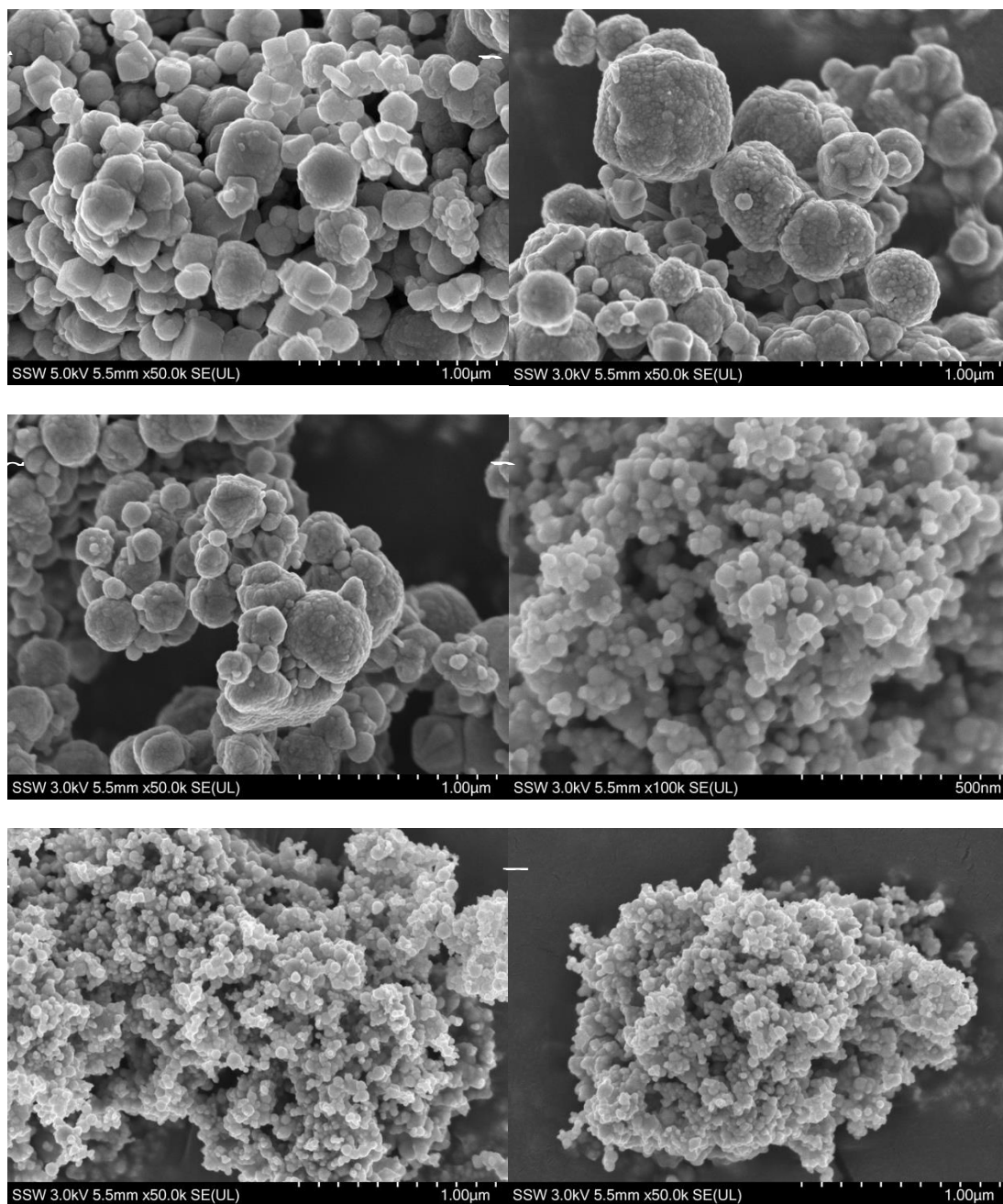


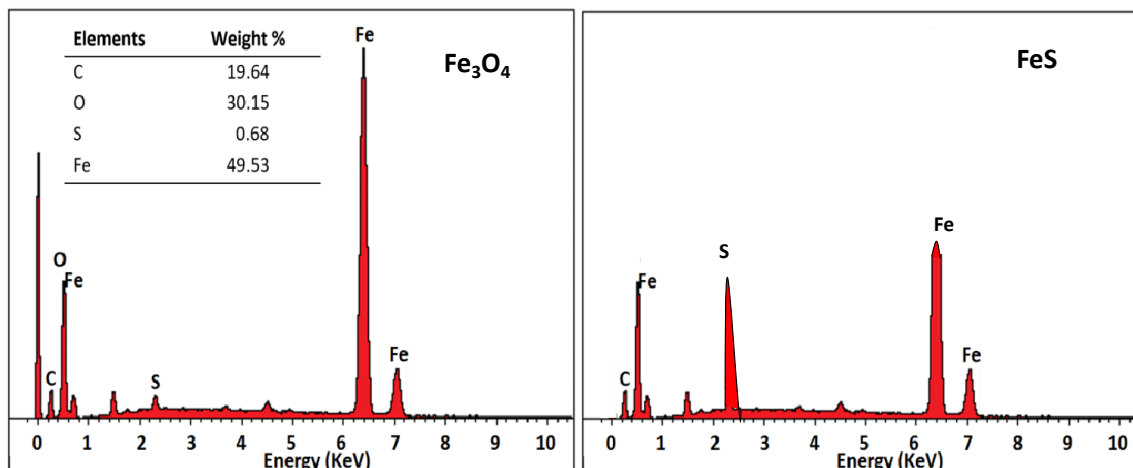
Figure 9A. The TGA curve for the degradation of SDS at 30°C/min.

Appendix B

B-1: Additional SEM images of the Fe_3O_4 nanocatalysts:



B-2: EDX results for the Fe₃O₄ and FeS catalysts:



Appendix C

C-1: Detailed methodology used for coating the cenospheres:

The Fe₃O₄ nanoparticles were coated onto the cenosphere surface using a precipitation method as mentioned by Zhan et al. in [20].

1. Solution Preparation:

- Dissolve 5.4 g of ferric chloride hexahydrate (FeCl₃·6H₂O) and 5.56 g of iron sulfate heptahydrate (FeSO₄·7H₂O) in 200 ml of deionized water to prepare a solution with 0.1 M concentration for each iron ion while maintaining the 1:1 molar ratio for Fe²⁺ to Fe³⁺.
- Stir the solution vigorously at 30°C to ensure complete dissolution of the precursors.

2. Cenosphere Addition:

- 6 g of cenospheres were etched in 150 ml of 1% HF solution at 40 °C for 10 min, followed by being washed with the anhydrous ethanol solution for 10 min, and then were completely washed with deionized water, and finally dried at 110 °C in an oven for 12 h.
- Add the cenospheres to the iron solution while continuing to stir. It is important that the cenospheres are properly etched (treated to increase their surface roughness) beforehand to ensure good adhesion of the nanoparticles.

3. Precipitation Process:

- Add aqueous ammonia (28 wt%) dropwise to the mixture to initiate the precipitation of Fe₃O₄. Continue stirring at 500 rpm.

- Adjust the pH to 9 and maintain it, watching for the color change from pink to brown, and then to black, which indicates the formation of Fe₃O₄ nanoparticles.
- Once the desired pH is stable and the color change indicates the completion of the reaction, continue stirring for an additional 2 hours to ensure completion.

4. Washing and Drying:

- Wash the coated cenospheres with acetone, ethanol, and deionized water, each for 15 minutes, to remove any impurities and by-products.
- Filter the cenospheres from the washing solution.
- Dry the coated cenospheres in a vacuum oven at 60°C for 12 hours to remove all moisture.

C-2: Detailed methodology used for P-value calculations:

1) Calculation of the Dilution Number (D):

$$D = 100 \times \left(\frac{\text{Oil mass}}{\text{Oil density} \times (\text{Hep}_{\text{tot}} + \text{Tol}_{\text{tot}})} \right)$$

Where, Oil mass: The weight of the oil sample in (g).

Oil density: The density of the oil sample in (g/mL).

Hep_{tot}: The total volume of heptane used in (mL).

Tol_{tot}: The total volume of toluene used in (mL).

2) Calculation of the Flocculation Ratio (FR):

$$FR = 100 \times \left(\frac{\text{Tol}_{\text{tot}}}{\text{Hep}_{\text{tot}} + \text{Tol}_{\text{tot}}} \right)$$

FR against D for different sample masses were plotted and the best fit line was drawn. The y-intercept of this line is the FR_{max}, which represents the maximum flocculation ratio. The x-intercept from the plot is the Critical Dilution Ratio (D_{crit}). This is the point at which asphaltenes start to precipitate out of the solution.

$$D_{\text{crit}} = \frac{-b}{m}$$

3) Calculating the Peptizing Power (Po):

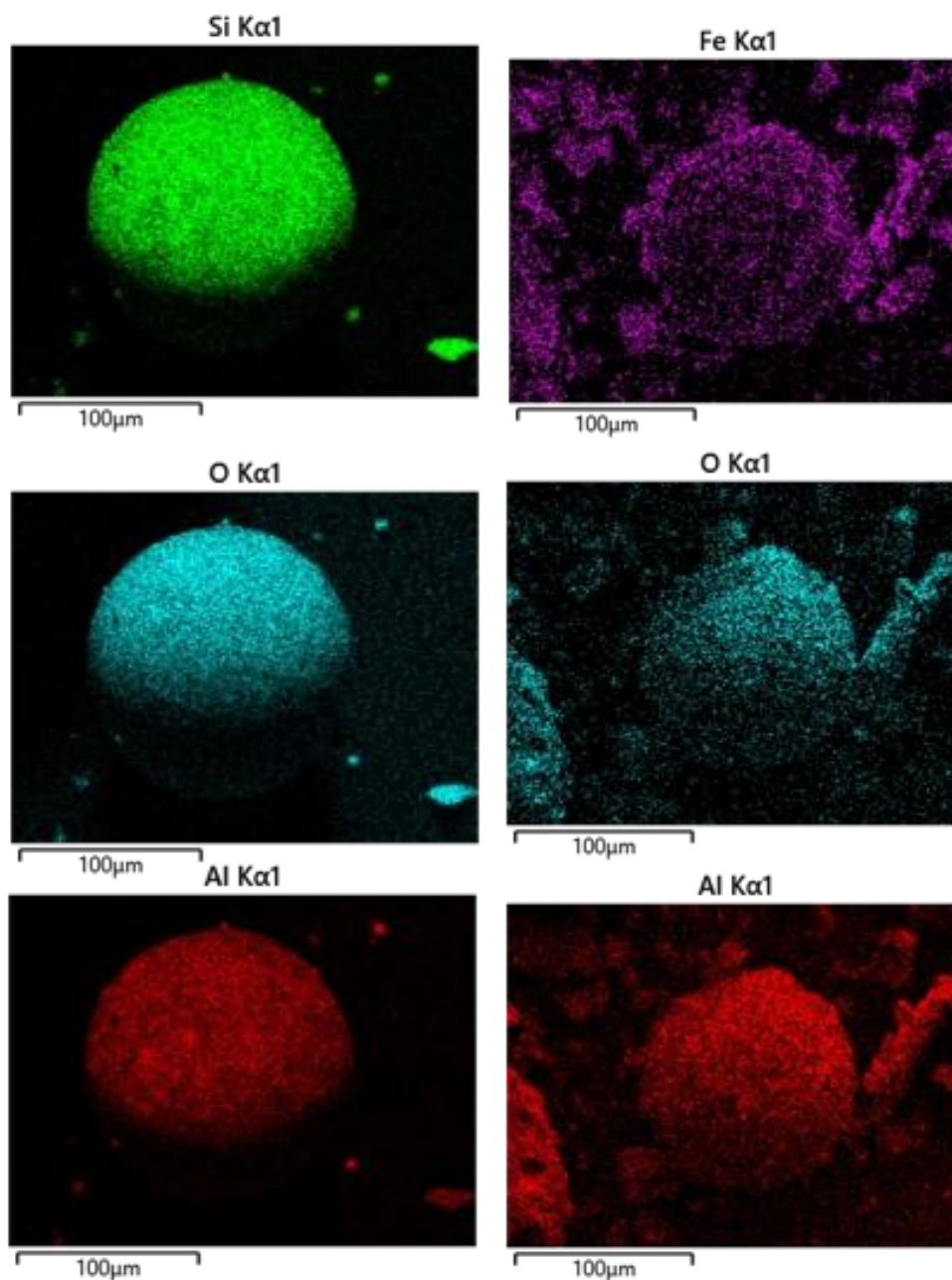
$$Po = FR_{\text{max}} \times \left(1 + \frac{100}{D_{\text{crit}}} \right)$$

Finally, the stability index, or P-value is calculated by dividing the Peptizing Power by the maximum flocculation ratio:

$$\text{P-Value} = \frac{Po}{FR_{max}}$$

To ensure validity, the process involves confirming that the R-squared value of the linear regression is above 0.99, indicating a strong correlation. If the R-squared value is below this, it suggests there may be an error with the data, and the experiment should be repeated.

C-3: Additional SEM/EDS images for the coated cenospheres:



Appendix D

D-1: BET plots for the carbon susceptor used for microwave absorption:

1. Activated Carbon (AC):

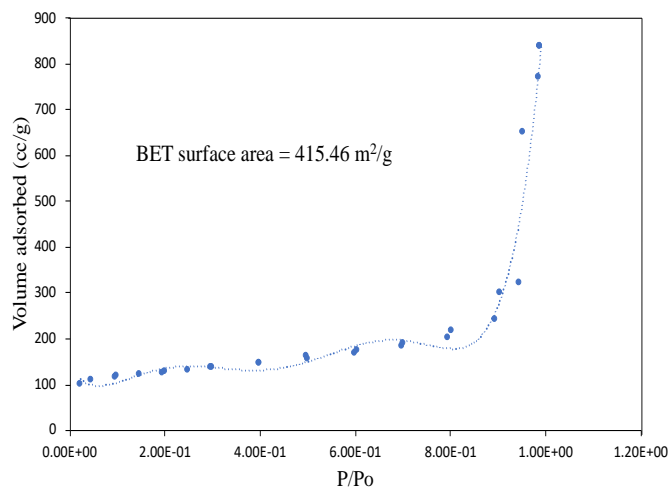


Figure 1D. t-Plot Method Micropore Analysis for activated carbon particles.

2. Biochar:

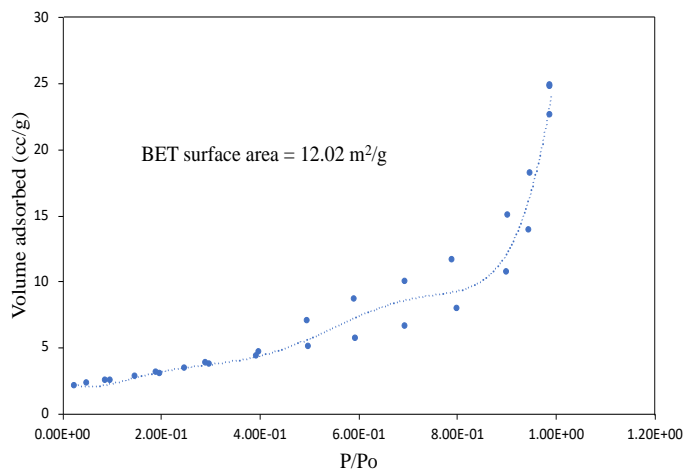


Figure 2D. t-Plot Method Micropore Analysis for Biochar particles.

3. Coke:

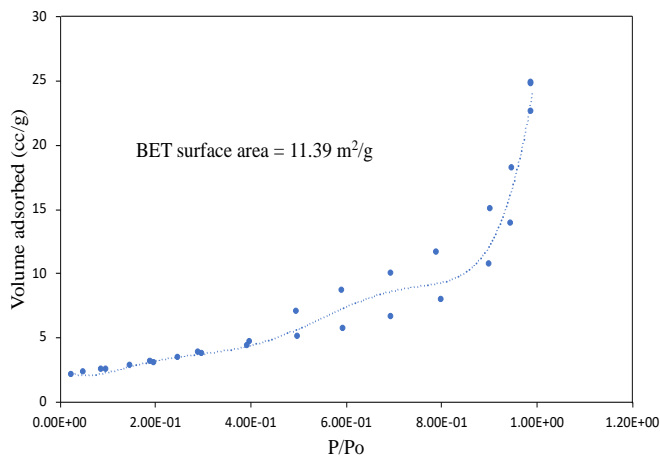


Figure 3D. t-Plot Method Micropore Analysis for Coke particles.

4. Graphite

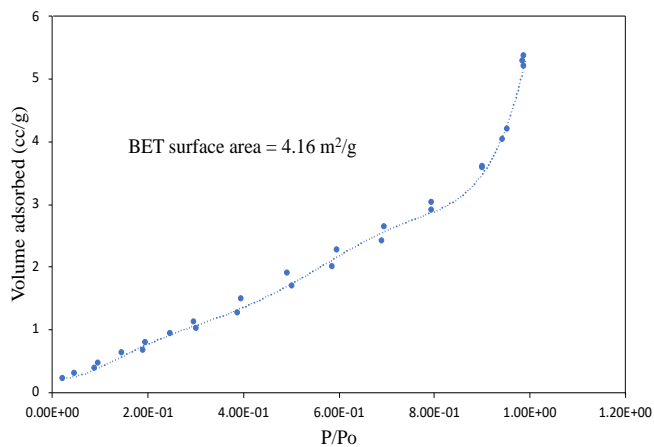


Figure 4D. t-Plot Method Micropore Analysis for Graphite particles.

5. Activated Biochar

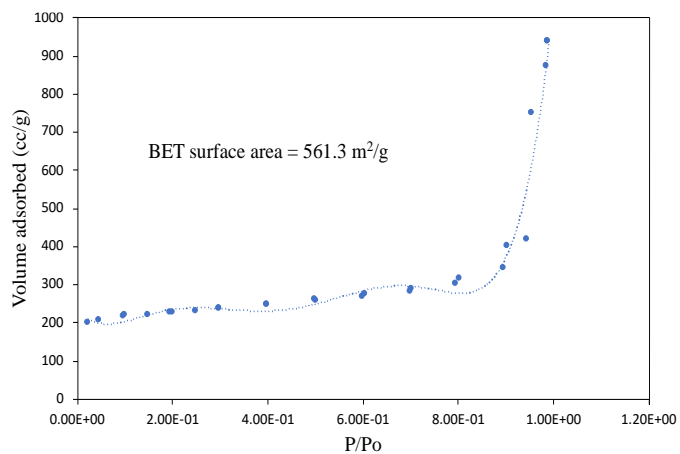


Figure 5D. t-Plot Method Micropore Analysis for Activated biochar particles.

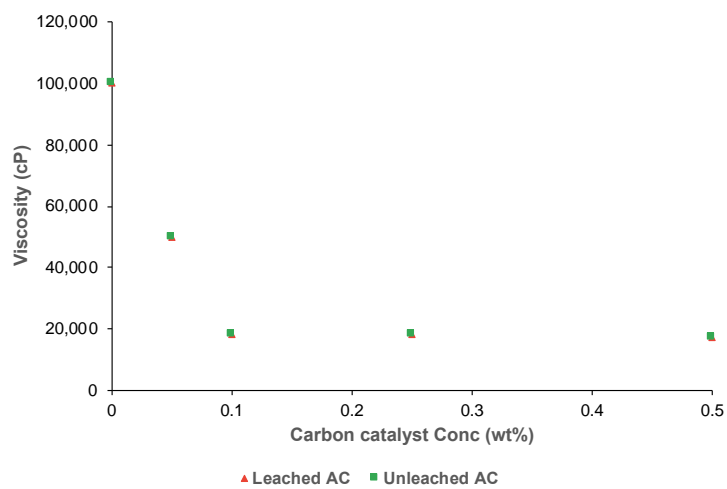
D-2: Results for leached Activated carbon as a microwave susceptor:

Figure 6D. The effect of leached AC on bitumen viscosity reduction at 150°C.

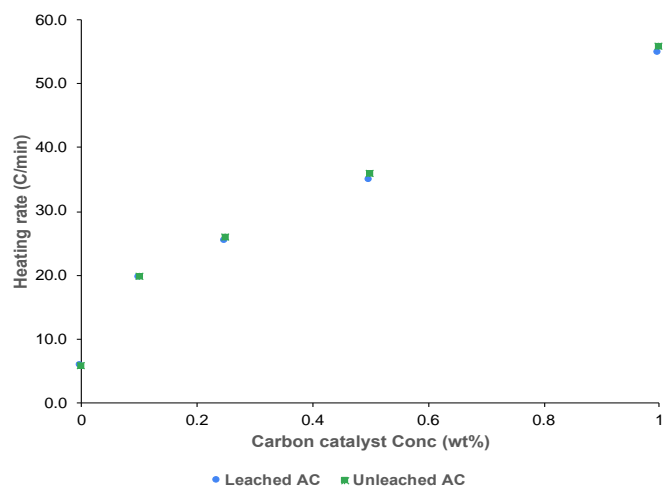


Figure 7D. The effect of leached AC on microwave heating rates.

Appendix E: Asphaltene Chemistry, Structure, and Reactions

Asphaltenes are a complex and poorly defined fraction of petroleum, characterized by their solubility in aromatic solvents and insolubility in normal alkanes. Structurally, asphaltenes are composed of highly aromatic and polar molecules, including a wide array of heteroatoms such as nitrogen, sulfur, oxygen, and metals like nickel and vanadium. These molecules are known for their high molecular weight and strong tendency to self-associate, leading to the formation of aggregates and eventual precipitation under certain conditions. The molecular structure of asphaltenes has been a topic of extensive research and debate, with two primary structural models emerging: the "archipelago" model, consisting of alkyl-bridged aromatic clusters, and the "island" model, which features condensed polycyclic aromatic cores with peripheral alkyl chains as shown in Figures 1E-A and B. Recent studies, including those utilizing advanced techniques like atomic force microscopy (AFM), have revealed that asphaltenes likely consist of a continuum of these structural motifs, with considerable molecular diversity [193].

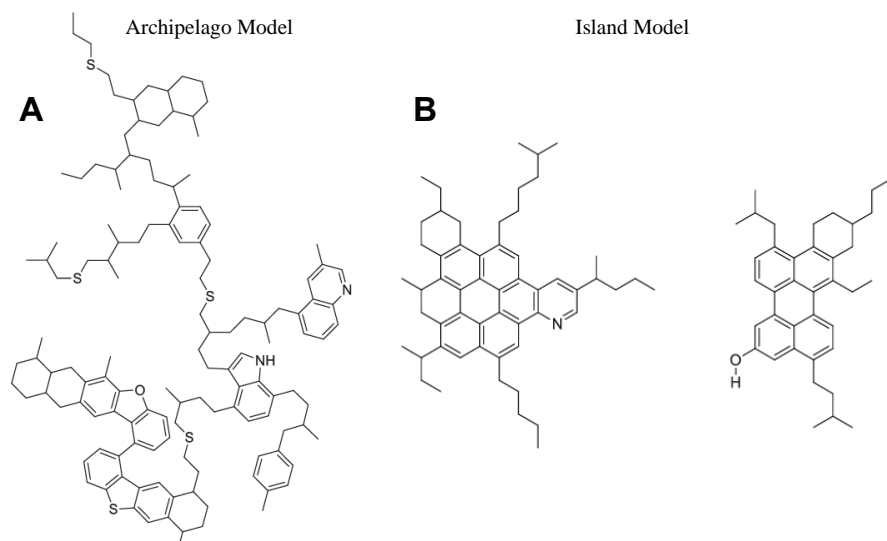


Figure 1E: Representative asphaltene structures following A) the archipelago model and B) the island model, adapted from Sheremata et al.[105].

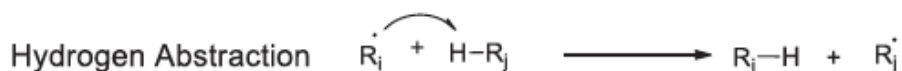
The thermal conversion of asphaltenes involves a series of complex chemical reactions driven by high temperatures, typically above 350°C. The process is initiated by the thermal cracking of asphaltene molecules, which possess high aromaticity and large, complex structures. This cracking process primarily occurs through homolysis, where chemical bonds within asphaltene molecules

break to form highly reactive free radicals. These radicals then participate in a series of chain reactions that propagate the cracking process. A key aspect of these reactions is the classic Rice-Herzfeld mechanism, which describes important propagation steps for radicals. These include β -scission, hydrogen abstraction, and hydrogen shuttling (or donor-acceptor reactions) in aromatic groups. β -scission, in particular, involves the breaking of aliphatic radical bonds, leading to the formation of an olefin and another radical. The most abundant products in these cracking reactions typically arise from the most energetically stable radicals. The olefins formed through β -scission can further participate in chain reactions, such as hydrogenation or radical-addition reactions, occurring in the liquid phase or under high-pressure gaseous conditions.

Mechanisms of Key Propagation Reactions

1. Hydrogen Abstraction

Description: In hydrogen abstraction, a free radical extracts a hydrogen atom from a donor molecule, creating a new radical in the process. This reaction is crucial in radical chain reactions because it helps propagate the chain by transferring the radical from one molecule to another.

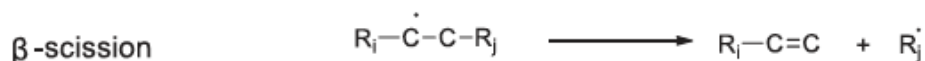


- **R***: Represents a free radical.
- **RH**: Represents a hydrogen donor molecule.
- **R-H**: Represents the product formed after hydrogen abstraction.

Explanation: The free radical R^* abstracts a hydrogen atom from the molecule RH , leading to the formation of a stable molecule R-H and a new radical R^* . This new radical can further participate in subsequent reactions, continuing the chain reaction.

2. β -Scission

Description: β -Scission occurs when a radical located at a carbon atom undergoes cleavage at the β -position, resulting in the formation of a new radical and an unsaturated molecule, typically an olefin.

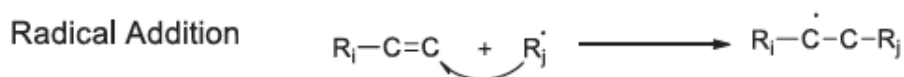


- $\mathbf{R_i-C-C-R_j}$: The starting radical, where \mathbf{R} and $\mathbf{R'}$ are alkyl groups.
- $\mathbf{R_j\cdot}$: The new radical formed after β -scission.
- $\mathbf{R_i-C=C}$: The resulting olefin.

Explanation: In β -scission, the bond between the β -carbon (second carbon away from the radical site) and the adjacent atom breaks, resulting in the formation of a new radical and an olefin. This reaction is critical in the thermal cracking process, contributing to the production of smaller hydrocarbon molecules.

3. Radical Addition

Description: In radical addition, a free radical adds to an unsaturated bond, such as a double bond in an alkene, resulting in the formation of a new radical. This reaction is crucial in the polymerization of monomers and in the formation of larger molecules during thermal cracking.



- $\mathbf{R^*j}$: Represents the free radical.
- $\mathbf{R_i-C=C}$: Represents an ethylene molecule (an example of an unsaturated bond).
- $\mathbf{R_i-C-C-R_j}$: Represents the new radical formed after the addition.

Explanation: The free radical $\mathbf{R^*}$ adds to the double bond of an alkene (in this case, ethylene), resulting in the formation of a new radical. This reaction is fundamental in radical polymerization processes and contributes to the growth of molecular chains.

The reaction pathways during thermal conversion are influenced by several factors, including the nature of the chemical bonds, the presence of heteroatoms, and the molecular structure of the asphaltenes. Aromatic rings, which are prevalent in asphaltenes, are particularly resistant to thermal cracking due to their resonance stabilization, requiring higher temperatures for effective breakdown. In addition to cracking, addition reactions play a significant role, especially in the liquid phase, where they contribute to the formation of larger, more complex molecules, ultimately leading to coke formation. This duality in the reaction pathways—where smaller molecules are produced alongside larger ones—can be effectively incorporated into simple kinetic models that describe the overall process.

Curriculum Vitae

Name: Moataz Abdrabou

Post-secondary Education and Degrees: American University of Sharjah
Sharjah, United Arab Emirates
2011-2015 B.Sc. in Chemical Engineering

Khalifa University
Abu Dhabi, United Arab Emirates
2018-2020 M.Sc. in Chemical Engineering

The University of Western Ontario
London, Ontario, Canada
2020-2024 Ph.D. in Chemical and Biochemical Engineering

Honours and Awards: AUS Chancellor Cup and Gold medal -2015
Sheikh Khalifa Presidential Award - 2014

Postgraduate Master's degree Scholarship Tier I
2018-2019, 2019-2020

Ontario Graduate Scholarship
2021-2022, 2022-2023, 2023-2024

Related Work Experience Graduate Teaching Assistant
Khalifa University
2018-2020

Graduate Teaching Assistant
The University of Western Ontario
2020-2024

Publications:

- 1) **M. K. Abdrabou**, X. Han, Y. Zheng, Y. Zeng, "Optimization of iron-based catalyst for partial upgrading of Athabasca Bitumen: The role of Fe oxidation state, particle size, and concentration", *Fuel*, vol. 357, Feb. **2024**.
- 2) **M. K. Abdrabou**, X. Han, Y. Zheng, Y. Zeng, "Harnessing the Power of Microwave Irradiation: A Novel Approach to Bitumen Partial Upgrading," *Molecules*, 28, 7769, **2023**.
- 3) **M. K. Abdrabou**, X. Han, Y. Zheng, Y. Zeng, and S. Rohani, "The effect of cationic surfactants on bitumen's viscosity and asphaltene nanostructure under thermal partial upgrading," *Energy Sci. Eng.*, Volume 10, issue 7, pp. 2540–2560, **2022**.
- 4) Farahani, M., **Abdrabou, M.**, Zhang, H., Zhu, J., Wang, F., Lee, K., & Zheng, Y. "In Situ Burning of Crude Oils Using Iron Oxide Nanoparticles as Additives." *Fuel*, vol. 330, Dec. **2022**.